Structural and Biochemical Investigation of the Regulation of Rab11a by the Guanine Nucleotide Exchange Factors SH3BP5 and TRAPPII

by

Meredith L Jenkins
B.Sc. (Hons) Microbiology, University of Victoria, 2015

A Thesis Submitted in Partial Fulfillment
of the Requirements for the Degree of

MASTER OF SCIENCE

in the Department of Biochemistry and Microbiology

Supervisory Committee

Structural and Biochemical Investigation of the Regulation of Rab11a by the Guanine Nucleotide Exchange Factors SH3BP5 and TRAPPII

by

Meredith L Jenkins
B.Sc. (Hons) Microbiology, University of Victoria, 2015

Supervisory Committee

Dr. John E Burke, Supervisor
Department of Biochemistry and Microbiology

Dr. Alisdair Boraston, Departmental Member
Department of Biochemistry and Microbiology

Dr. Robert Chow, Outside Member
Department of Biology

Abstract

Rab11 is a critical GTPase involved in the regulation of membrane trafficking in the endocytic pathway, and it's misregulation is involved in a variety of human diseases including Huntington's disease and Alzheimer's disease. Additionally, de novo mutations (DNMs) of Rab11 have been identified in patients with developmental disorders, and interestingly several parasites, viruses, and bacteria can subvert membrane trafficking through Rab11 positive vesicles to allow for replication and evasion from the immune system. Although Rab11 is one of the best characterized Rab GTPases, hindering the capability to completely understand Rab11 regulation and its role in human disease is the lack of detail describing how Rab11 proteins are activated by their cognate guanine nucleotide exchange factors (GEFs). This thesis is therefore focused on revealing the molecular mechanisms of the GEFs responsible for the activation of Rab11: SH3BP5 and TRAPPII. To investigate the recently discovered GEF SH3BP5, we solved the 3.1Å structure of Rab11 bound to SH3BP5 and revealed a coiled coil architecture of SH3BP5 that mediates exchange through a unique Rab-GEF interaction. The structure revealed a unique rearrangement of the switch-I region of Rab11 compared to other solved Rab-GEF structures, with a constrained conformation when bound to SH3BP5. Mutational analysis of switch-I revealed the molecular determinants that allow for Rab11 selectivity over evolutionarily similar Rab GTPases, and GEF deficient mutants of SH3BP5 show greatly decreased Rab11 activation in cellular assays of active Rab11. To interrogate the highly controversial GEF TRAPPII, we recombinantly expressed and purified the 9 subunit, 427 kDa complex in *Spodoptera frugiperda 9*(Sf9) cells. We found that the TRAPPII complex is a GEF for both Rab1 and Rab11, and we discovered novel activity for another Rab GTPase. To interrogate the role of these GEFs in human disease, we used HDX-MS and nucleotide exchange assays to show that some DNMs destabilize Rab11 either through a complete or partial disruption of nucleotide binding. Importantly, we discovered that one of these DNMs, K13N, completely prevented SH3BP5 and TRAPPII mediated

nucleotide exchange, revealing a putative mechanism of disease. Overall the work completed in this thesis leads to a greater understanding of the molecular mechanisms underlying the activation of Rab11 by its cognate GEFs.

Table of Contents

List of Tables

List of Figures

Acknowledgments

First, I would like to acknowledge that this research was supported by a graduate scholarship from Natural Sciences and Engineering Research Council of Canada (NSERC), a University of Victoria Fellowship, and generous donor awards including the Greig Cosier Memorial Scholarship, the Edythe Hembroff-Schleicher Scholarship, and the Eileen Ford Wood and Alexander James Wood Scholarship. I am very grateful for this financial support.

I would like to particularly thank Dr. John Burke for first taking me on first as a technician teaching me how to run the Mass Spec, and then as a graduate student teaching me the ins and outs of research, funding acquisition, and publishing. Your guidance over the last four years have helped me grow both as a scientist and a person, and I am forever grateful. I would also like to thank my committee members, Dr. Alisdair Boraston and Dr. Bob Chow for their insight over the last few years, and who's advice during meetings has greatly improved the work in this thesis. I would also like to thank Dr. Martin Boulanger for his help in solving the structure of SH3BP5, I am very grateful for your help. I'd also like to acknowledge our collaborators Dr. Jean Piero Margaria and Dr. Emilio Hirsch from the University of Turin. Your work on the cellular Rab11 activation studies helped immensely, and I am grateful for the opportunity to have worked with you both.

I would of course like to thank my lab mates: Jordan, Jacob, Manoj, Gill, Braden, Emily, Kaelin, Noah, Reece (the list goes on and on). You all made working in the lab so much fun, and I am very happy to have been able to work with you all. I would like to especially thank Jordan for her dedication to the project during her honors degree, you helped make working on this project so much more fun and I wish you the best of luck in med school. Thank you to the shop guys Scott, Steve, and Ryan, you all helped make sure things were running smoothly, and made the scary broken mass spec moments less scary (and I appreciate that a lot). I feel like there are so many people in the department that have helped me over the years. You know who you are, thank you!

Dedication

I would like to dedicate this thesis to all of the people who have helped me get where I am. To my family, I love you all, and thank you so much for supporting me throughout my undergraduate degree and throughout my pursuit of a Master of Science degree. I'm not sure I could have done this without all your consistent votes of confidence. To my friends, thank you for keeping me sane over the last few years, and for always being there for me. In particular, thank you to Laura for always being game to go have a blast at music bingo after a long day in the lab, to Miles and Kristen for always being up for a board game night, to the rad crew for some amazing New Year's parties and skiing trips, and to Danielle for always having my back no matter what. A massive thank you to Keegan for putting up with me while I stressed out about work, and for patiently listening to my practice talks. You are my rock (along with Tiegan and Bisou, of course). Finally, I would like to dedicate this thesis to my Nana. I know how proud you would have been to see me handing in my MSc Thesis, and I know you are looking down and smiling.

List of Abbreviations

Abbreviation	Expanded word
Sf9	*Spodoptera frugiperda 9*
AA	Amino acid
AD	Alzheimer's disease
Arf	ADP-ribosylation factor
Bacmid	Bacterial artificial chromosome containing the baculovirus genome
BME	beta mercaptoethanol
C.elegans	*Caenorhabditis elegans*
CNS	Central nervous system
Cryo EM	Cryogenic electron microscopy
DEE	developmental and epileptic encephalopathies
DENN	differentially expressed in neoplastic versus normal cells
DNA	Deoxyribonucleic acid
DNM's	de novo mutations
D. melanogaster	*Drosophila melanogaster*
ER	Endoplasmic reticulum
EVI5	Ecotropic viral integration site 5
FBS	Feotal Bovine Serum
GAP	GTPase activating protein
GDI	GDP dissociation inhibitor
GDP	Guanosine diphosphate
GEF	Guanine nucleotide exchange factor
GF	Gel Filtration
GFB	Gel Filtration Buffer
GPCR	G protein coupled receptor
GTP	Guanosine triphosphate
HD	Huntington disease
HDX-MS	Hydrogen Deuterium Exchange
Huntington	HTT
HVT	Hypervariable Tail
kDa	Kilo Dalton
LECA	Last evolutionarily conserved ancestor
Lip-TEV	tobacco etch virus protease with a lipoyl tag
MADD	MAPK-activating protein containing a death domain
MS	Mass spectrometry
MS/MS	Tandem mass spectrometry
Ni-NTA	Nickel nitrilotriacetic acid
PBS	Phosphate-buffered saline
PC	Phosphatidylcholine
PCR	Poymerase chain reaction
PDB	Protein data bank

Abbreviation	Expanded word
PE	Phosphatidylethanolamine
PHYRE2	Protein Homology/analogY Recognition Engine V 2.0
PI	Phosphatidylinositol
PI3P	Phosphoinositide 3-phosphate
PI4P	Phosphoinositide 4-phosphate
PM	Plasma membrane
PS	Phosphatidylserine
Rab	Ras-related in brain
Rabex-5	Rabaptin-5-associated exchange factor for Rab5
RabGGTase	Rab geranylgeranyltransferase
Rabin	Rab-3A-interacting protein
Rac	Ras-related C3 botulinum toxin substrate
Ran	RAs-related Nuclear protein
Ras	Rat Sarcoma
RE	Recycing endosome
REP	Rab escort protein
Rho	Ras homologous
Rin	Ras And Rab Interactor 1
SDS-PAGE	Sodium dodecyl sulfate polyacrylamide gel electrophoresis
SEDT	Spondyloepiphyseal dysplasia tarda
SH3BP5	SH3 binding protein 5
SNARE	Soluble NSF attachment protein receptor
Strep	Streptavidin
TBC	Tre-2/Bub2/Cdc16
TCEP	Tris(2-carboxyethyl)phosphine
TEV	tobacco etch virus protease
TRAPP	transport protein particle
WT	Wildtype
Ypt	Yeast protein transport

Thesis Format and Manuscript Claims

This thesis is presented in the format of a manuscript. The first chapter provides a general background and introduces the rationale for the thesis and outlines thesis objectives. Chapters two and three are written in a manuscript style and contain an Abstract, Introduction, Materials and Methods, Results, and Discussion. The last chapter provides an overall conclusion, discussion of the significance or the work, and a future directions section.

Chapter Two adapted from: Jenkins ML, Margaria JP, Stariha JTB, Hoffmann RM, McPhail JA, Hamelin DJ, Boulanger MJ, Hirsch E, Burke JE. 2018. Structural determinants of Rab11 activation by the guanine nucleotide exchange factor SH3BP5. Nat Commun 9:3772.

Chapter 1 – Introduction

1.1 Overview

Survival of all eukaryotic cells depends on a highly regulated and organized flow of membrane traffic. Intricate systems mediate the correct delivery of intracellular cargos to specific cellular locations, and disruptions in the functioning of these systems plays key roles in many human diseases, emphasizing the need for proper regulation. One of the major protein families regulating membrane trafficking are the Rab GTPases. Rab11 is one of the best characterized Rabs, and plays key roles in regulating trafficking of recycling endosomes(1). Thus, Rab11 signaling plays fundamental roles in cilliogenesis(2), cytokinesis(3), and endosomal recycling(4), and it's dysfunction has been implicated in neurodegenerative diseases including Huntington's disease(5).

Active Rab11 regulates membrane trafficking by recruiting effector proteins to specific cellular locations. As with all GTPases, Rab11 cycles between a GTP bound "active" state and a GDP bound "inactive state", and the interconversion between the states is mediated by guanine exchange factors (GEFs) and GTPase activating proteins (GAPs). The type of bound nucleotide dictates function; therefore, it is important to fully characterize the proteins regulating the Rab GTP/GDP cycle. In the past decade, considerable research has gone into discovering which GEFs are responsible for the regulation of Rab11. The TRAPP complex has been shown to have GEF activity on Rab11, however its role is still controversial. Only recently SH3BP5 was shown to be a novel GEF for Rab11(6), however despite this finding, the mechanism of SH3BP5 activation of Rab11 is unknown as it does not contain any previously characterized GEF domains. This thesis is focused on the investigation of these two GEFs using a variety of biochemical assays to determine their mechanisms of action and their specificity. These studies will help to define the molecular mechanisms of Rab11 regulation by its cognate GEFs and will expand our understanding of how Rab11 mediates membrane trafficking.

1.2 Rab Small GTPases

Small GTPases are important proteins that regulate a myriad of cellular functions. These critical proteins have been very well characterized over the last few decades, however some questions remain unanswered. This section of the thesis will generically introduce the evolution of small GTPases, with a focus on Rab GTPases. The structural conservation of Rabs, and their ability to act as molecular switches will then be introduced. Finally, the critical proteins regulating Rab activation, Guanine nucleotide exchange factors (GEFs) and GTPase activating proteins (GAPs), will be introduced and their generic enzymatic mechanisms described.

1.2.1 The Evolution of Rab GTPases

GTP binding proteins (G proteins) are involved in a variety of biological processes and span many different families including the heterotrimeric G proteins, translation factors, and Ras-like small GTPases, which were first identified in the 60's from the Harvey and Kirsten sarcoma virus, and later classified as the Ras superfamily. The Ras superfamily of GTPases contains five sub-families within the superfamily called Ras, Rho/Rac, Rab, Arf and Ran(7). This thesis is focused on the Rab GTPases, which are key regulators of membrane trafficking pathways crucial for proper cellular function. All eukaryotic cells contain a variety of intracellular compartments separated by membranes, and thus they possess a highly regulated system for directing membrane cargo to the proper cellular location. One of the key determinants of membrane trafficking is the regulation of Rab GTPases(8–11). Rab proteins mediate exchange of specific protein and lipid cargos between distinct intracellular organelles, through selective binding and recruitment of Rab binding proteins.

In the last evolutionarily conserved ancestor (LECA) there are 20 Rab GTPases forming 6 groups(12). Although a majority of these ancient Rabs have been conserved throughout evolution, there has been a large expansion in the Rab family in higher organisms. It is thought that this

expansion allowed for increased complexity of membrane trafficking systems, leading to increased complexity of organisms. Studies on Rabs have provided insights into the evolution of the eukaryotic endomembrane system, and it is now known that Rabs participate in central nervous system (CNS) development(13), polarized neurite growth(14), endocytosis and axonal retrograde transport(15), and synaptic vesicle exocytosis(16).

In humans, Rab proteins show a remarkable diversity, with over 66 identified members(12). Different Rab GTPases are generally localized in different cellular compartments to carry out diverse biological processes through a shared general mechanism. A figure depicting the evolution of Rab GTPases from the LECA to humans is depicted in Figure 1.1.

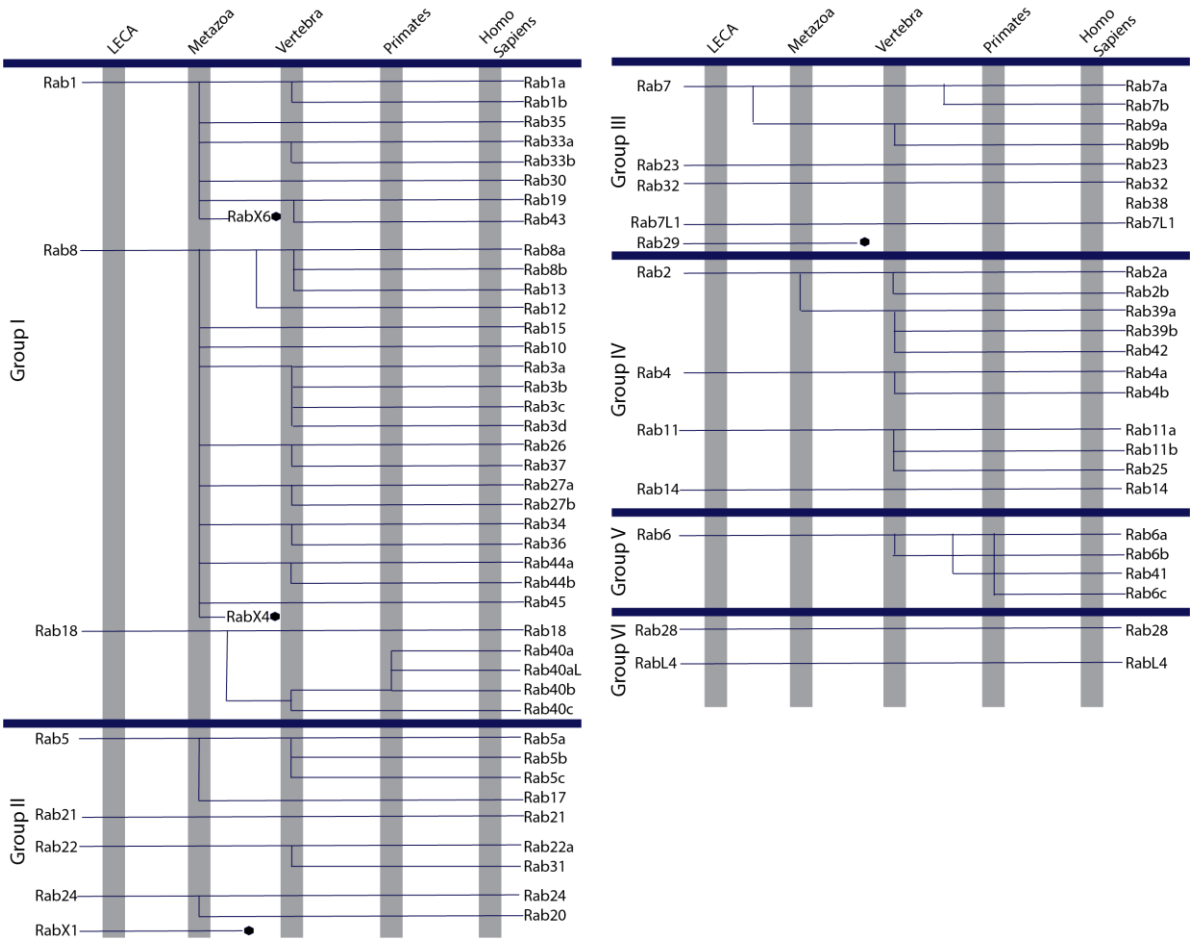

Figure 1.1. Evolution of Rab small GTPases. This figure was adapted from Tobias H Klöpper *et al.*, 2012, BMC Biology(12).

1.2.2 The Small GTPase Molecular Switch

Several Rab GTPases structures have been solved, and alignment of primary and tertiary structures shows a high level of conservation. The GTP binding domain is made up of five conserved motifs(G1-G5), which all play important roles in nucleotide and effector binding. Rab GTPases also contain two regions known as the switch I and the switch II, which allow for effector recognition and binding. These regions are far more variable in sequence than the G1-G5 and are essential in determining effector specificity. The third important region in Rab GTPases is the c-terminal hypervariable tail (HVT). This region, as its name suggests, is highly variable and is a key differentiating feature between members of the Rab GTPase family. A representative structure of Rab is depicted in figure 1.2 below.

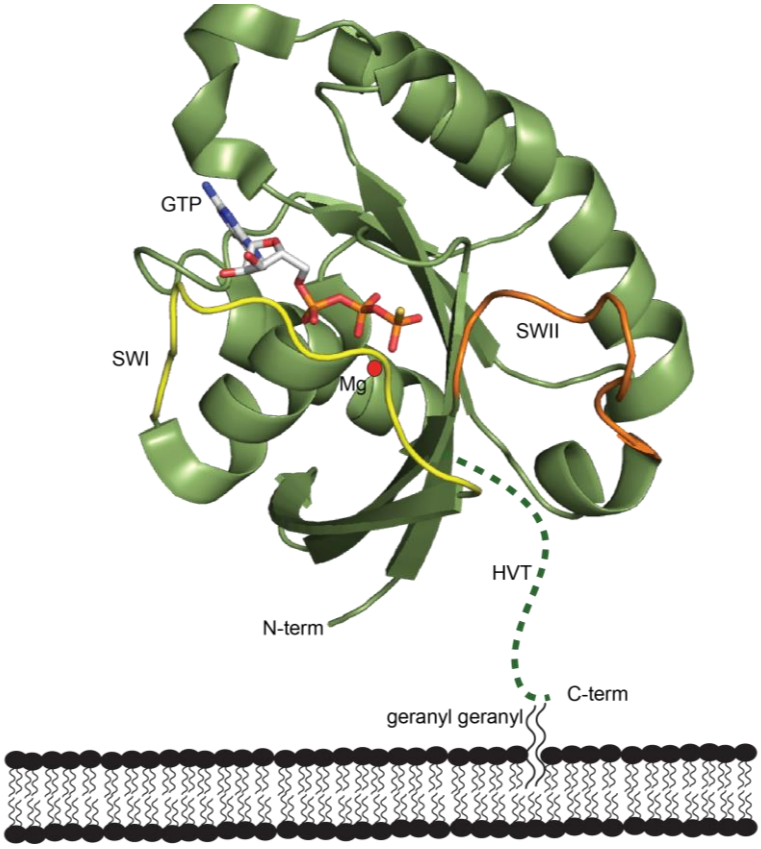

Figure 1.2. Rab GTPase structure. This is the structure of Rab11 bound to GTPγS(1OIW). The Switch I (SWI) region is colored yellow, while the Switch II (SWII) region is colored orange. The dotted line represents the hypervariable tail (HVT) domain, which is not present in the structure.

Generically, for Rab GTPases to be able to associate with membranes, they must first be prenylated at one, or most often two, c-terminal cysteine residues (Figure 1.2). For this to occur, newly synthesized Rab proteins first bind a Rab escort protein (REP), which then allows for prenylation by Rab geranylgeranyltransferase (RabGGTase). After geranylgeryanylation, Rabs are delivered to target membranes and are activated by guanine nucleotide exchange factors (GEFs) to allow for bound GDP to be replaced with GTP, which is at a 10-fold higher cellular abundance than GDP (17). Once inserted into the membrane, Rabs can be removed by guanine nucleotide dissociation inhibitors (GDIs), which bind and solubilize the prenyl groups to allow the protein to exist in cytosolic space. It is unclear exactly what factors bring soluble prenylated Rabs in REP or GDI complexes to their target membrane. It has been proposed that localization of Rabs is dependent on the location of GEFs(18), while others have postulated that localization is due to other membrane binders such as GDI displacement factor(GDF) which interact with the Rab and the GDI to only allow insertion at specific membrane compartments(19). It was originally thought that the HVT domain allowed for Rab proteins to associate with specific target membranes(20), however the specific association with different membrane compartments is much more complex and probably involves interactions with a combination of specific GEFs, GDIs, GDFs, effectors, as well as interactions of the HVT with the membrane(21).

Rab GTPases act as molecular switches, and cycle between a GDP-bound ‘off’ state and a GTP-bound ‘on’ state(22). These nucleotides induce different switch conformations and control binding to downstream effector proteins. Once delivered to a membrane, Rabs interact with GEFs which catalyze the release of GDP and allow for binding of GTP. At this stage, the GTPase is considered “active”, and can interact with downstream effector proteins. Rab effectors in general are proteins that interact with the GTP bound form of the GTPase. These effectors may be adaptors, tethers, motors, fusion regulators, kinases, phosphatases, membrane regulators, or Rab regulators such as GAPs. Specific effectors are described in greater detail in section 1.3.2.

Rabs intrinsically have GTPase activity, however the rate of hydrolysis can be enhanced by GTPase activating proteins (GAPs). Once hydrolyzed, the Rab GTPase can be removed from the membrane by GDIs, or the cycle can be restarted by another GEF. The molecular mechanisms by which these GEFs and GAPs act on their cognate Rab is described in greater detail in section 1.2.3. A schematic depicting the cycle is shown in Figure 1.3.

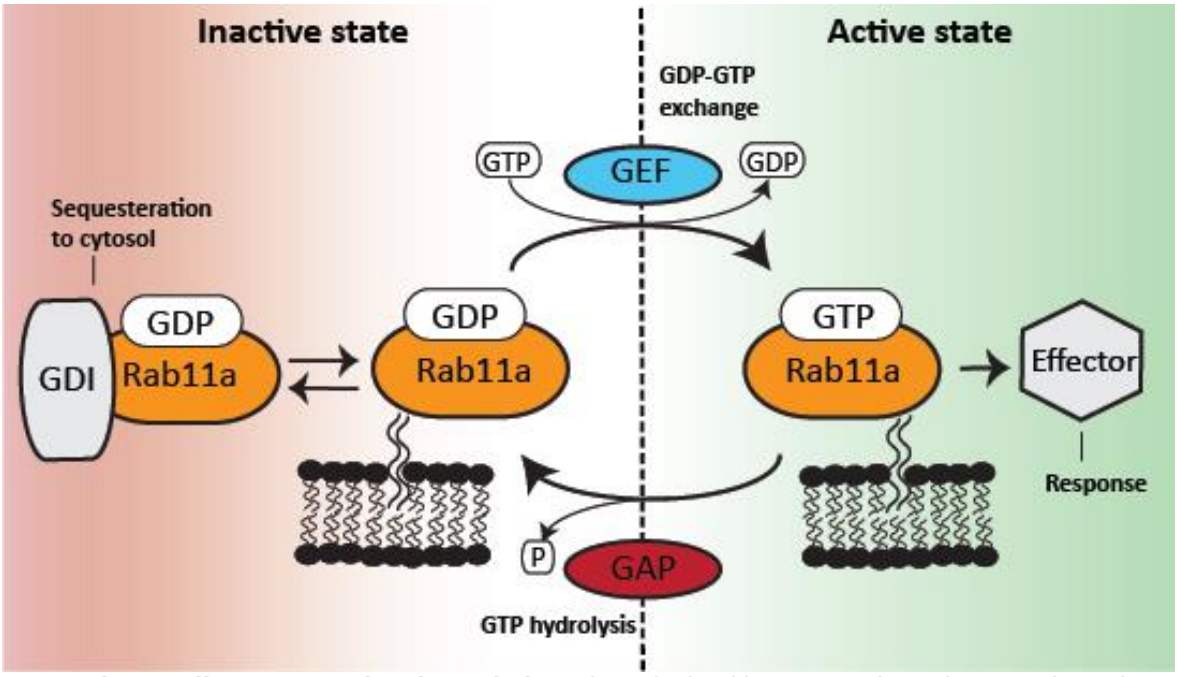

Figure 1.3 The Small GTPase molecular switch. Rabs exist in either a GDP bound or GTP bound state, and GEFs and GAPs act as master regulators of this cycle. Figure adapted from Stenmark and Olkkonen, 2001, Genome Biol (23).

1.2.3 GEFs and GAPs of Rab GTPases

The association of Rab-binding partners depends on the nucleotide state, with most Rab effectors binding the GTP-bound active conformation. The intrinsic rates of conversion between the two states are slow and therefore Rabs require regulatory proteins to control their spatiotemporal activation and inactivation. The nucleotide state is regulated through the coordinated interplay of activating guanine nucleotide exchange factors (GEFs) and inactivating GTPase activating proteins (GAPs), with an additional level of control mediated by guanine nucleotide dissociation inhibitory proteins (GDIs)(24–27). GEFs are often recognized as master

regulators of Rab signalling, as they are primarily responsible for deciding the spatial and temporal activation of Rabs.

Several Rab GEFs have been identified, with a majority being members of the Vps9 and DENN families. A summary of these different GEF domains is shown in Figure 1.4. As of mid 2019, there have been 133 GEF:Small GTPase complex structures that have been solved and deposited in the PDB(28). These structures comparing GEF:GTPase and apo GTPase have all increased our understanding of the mechanisms GEFs use to allow for nucleotide displacement. Generally, all GEFs employ a similar mechanism of action. First, they form a low-affinity complex with the switch regions of nucleotide bound Rab. This low affinity interaction becomes stronger as the switches are structurally rearanged away from the nucleotide and magnesium binding pocket. This movement reduces the affinity of the GDP for the pocket, allowing for its release(29). The displacement of nucleotide can also be achived by certain GEFs through the insertion of a glutamic acid finger which destabilizes binding of the terminal phosphate of GDP to the nucleotide binding pocket, facilitating release(30). Other GEFs insert residues into the interswitch region, inhibiting the coordination of Mg^{2+} which destabilizes nucleotide binding(31). In all cases, the release of nucleotide allows for the GDP to be replaced with the 10-fold more abundant nucleotide GTP, leading to release from the GEF and activation of the small GTPase (17).

As is in every biological system, once a signal is turned on there is always a mechanism for the signal to be turned off. Most small GTPases have low intrinsic rates of nucleotide hydrolysis, with the half life of the GTP active state ranging from minutes to hours(25). For hydrolysis to occur in a physiologically meaningful timeframe, the process is enhanced by GTPase activating proteins (GAPs) (25, 32–34). The Rab GAPs consist primarily of one family, the TBC(Tre-2/Bub2/Cdc16) domain GAPs, which were first described in the 1990s, and all function by a similar mechanism of insertion of a catalytic glutamine which induces a rapid conformational change. During this conformational change, a arginine is recruited to the active site, leading to hydrolysis of the

phosphate group(35). It should be noted however that GAPs are thought to be less important than GEFs in general, as many Rabs do hydrolyze GTP at a physiologically relevant rate intrinsically(36).

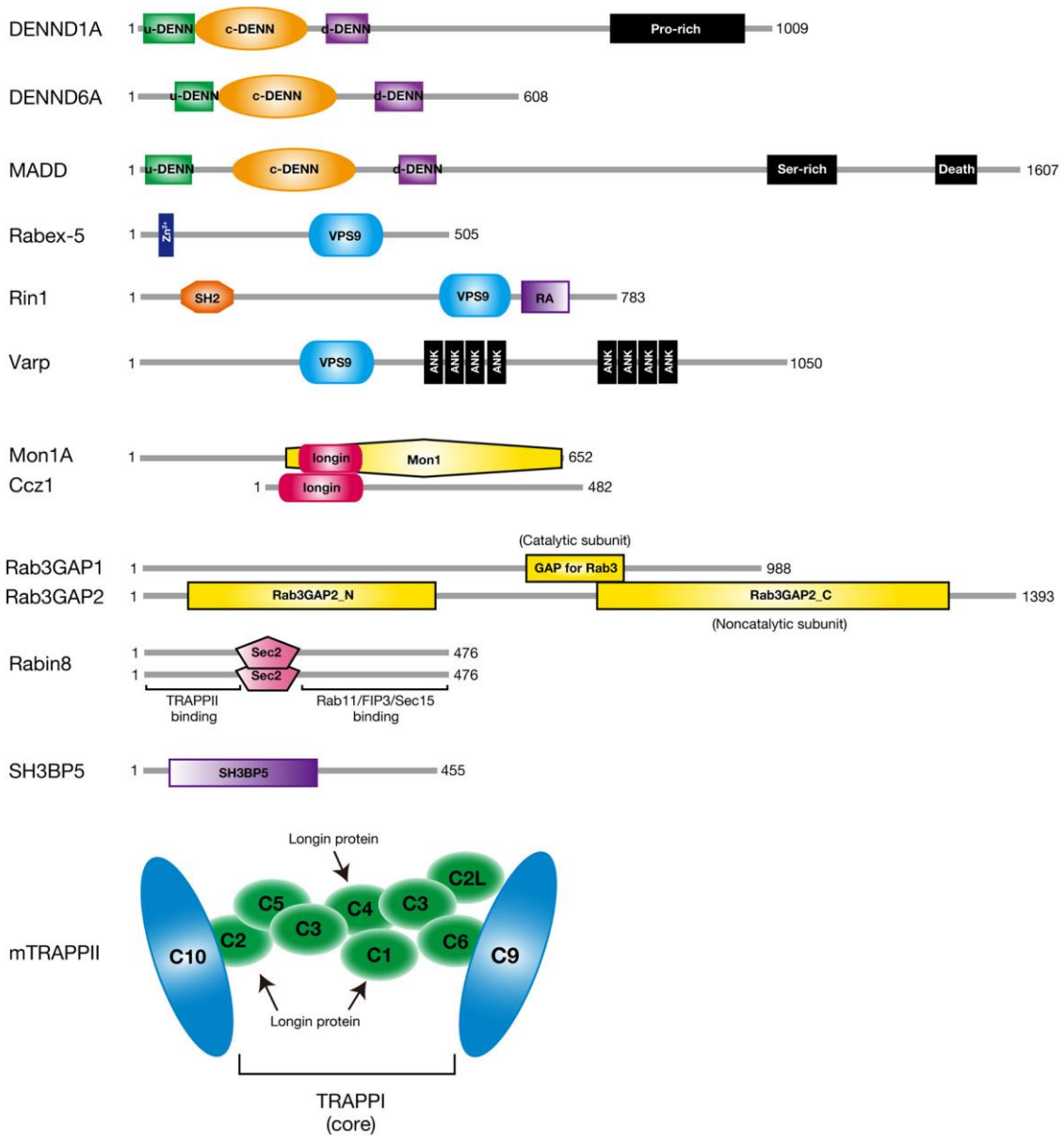

Figure 1.4. Representative human GEF protein domain organization. This figure was generated by Ishida *et al.*, Cell Structure and Function, 2016(34). Permission was obtained for reuse, and is shown in Appendix A

GEFs and GAPs must be tightly regulated to turn different Rabs off or on in different membrane compartments at different times. This process is often refered to as a Rab cascade, where Rab recruitment and activation is tightly linked with the susequent inactivation of previous Rabs(37). In order for this process to work, Rabs work in a highly organized fasion, where an activated Rab can recruit a GEF for the Rab of the next trafficking step(38). This process can also be linked with a GAP for the previous Rab, turning off this transport step and allowing for a new Rab to take over the trafficking. In a sense, these cascades are key in maintaining the identity of distinct cellular compartments by correctly positioning specific Rabs in the appropriate compartments. These processes have been described in yeast and humans, and are critically important for the regulation of membrane trafficking(39, 40).

1.3. The small GTPase Rab11

This section will introduce the small GTPase Rab11, the research focus of this thesis. It will establish Rab11's role in membrane trafficking, and the different Rab11 family members in humans. The different effectors of Rab11 will then be discussed, followed by an introduction to the roles of Rab11 in human disease.

1.3.1 Rab11 family members and their functions

Among the best studied Rab GTPases is Rab11, a critical GTPase that primarily regulates the recycling of endocytosed proteins, and are therefore master regulators of the surface expression of receptors(41). They are mostly localized at the trans-golgi network, post-Golgi vesicles, and the recycling endosome, where they facilitate cytokinesis(42), ciliogenesis(2), oogenesis(43), and neuritogenesis(44). Furthermore, Rab11-positive vesicles have also been identified as precursors for autophagosome assembly(45), which is one of the initiating steps of

autophagy. Each of these fundamental biological processes are regulated by Rab11 through the recruitment of Rab11 effector proteins.

Rab11 is conserved back to the LECA and is critical for normal development, as knockout of Rab11a in mice has been found to be embryonic lethal(46). Yeast has two Rab11 genes (Ypt31/32) whereas in humans there are three Rab11 isoforms: Rab11A, Rab11B, and Rab25 (also known as Rab11C). Rab11a is by far the best characterized of the Rab11 family members and is ubiquitously expressed, while Rab11b is specifically expressed in the heart, testis, and brain, and Rab25 is expressed in the gastrointestinal mucosa, kidney, and lung(47–49). Rab11a and Rab11b share 89% amino acid sequence identity, differing only in the c-terminal hypervariable region, while there is only a 62% identity between Rab11a and Rab25. An alignment of these family members is shown in figure 1.5, with structural domains annotated from the structure of Rab11a bound to GDP (PDB:1OIV)(50).

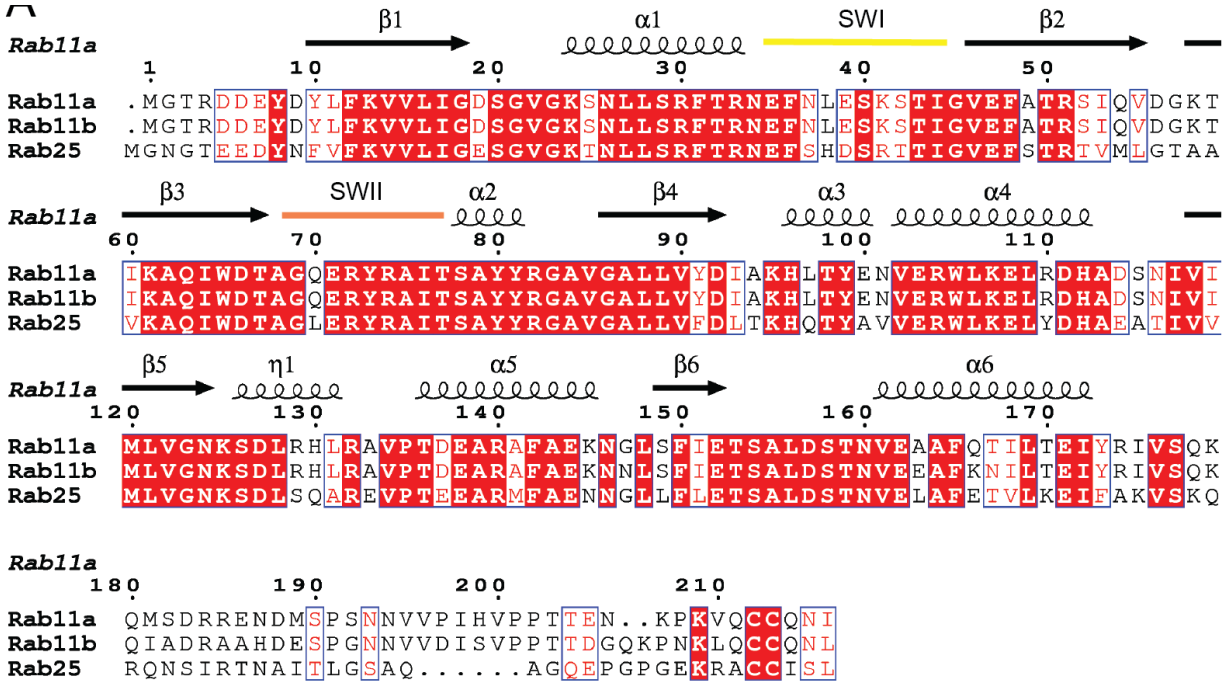

Figure 1.5 Alignment of Rab11 family members Rab11a, Rab11b and Rab25. Alignment generated using Clustal W and ESPript 3.0(51).

Intriguingly, Rab25 contains a Leucine instead of a Glutamine at the 70th residue, and a threonine instead of a serine at the 25th residue. Often a mutation of Q70L is used to mimic an "active, on" GTP bound state in other small GTPases, while a mutation of S25N is used to mimic an "inactive, off" state in cellular studies. It is thought that the Q70L mutation does not allow for normal hydrolysis of GTP, making this mutation extremely useful in cell studies to keep the GTPase in a constant active state. On the other hand, the S25N mutation prevents GTP binding, preventing the protein from being activated (52). Intriguingly, some research has shown that Q70L does not alter intrinsic or GAP stimulated GTPase activity in Rab11 (53), so it is unclear if the substitution of these residues in Rab25 alter its activity.

1.3.2 Effectors and Regulators of Rab11

Multiple studies on Rab11 have uncovered numerous effector proteins, with the most well characterized including PI4KIIIB(54), MyosinV(55), and the 5 members of the Rab11-family interacting proteins (Rab11-FIPs)(56). Although most of these effectors exclusively bind the switch regions of GTP-bound Rab11, PI4KIIIB has been shown to bind a unique interface, allowing for ternary complex formation with FIP3(54). Rabin8 has also been shown to bind at this unique interface, forming a ternary complex with FIP3 during cilliogenesis(57).

As Rab11 is so critical to membrane trafficking, there has been a considerable effort to understand the GEFs and GAPs regulating its activation. In 2007, EVI5 was identified as both an effector and a GAP for Rab11(58, 59). Biochemical reconstitution of the large macromolecular TRAPPII complex with Rab11 in both yeast (*Saccharomyces cerevisiae*) and fruit flies (*Drosophila melanogaster*) has revealed clear GEF activity towards both Rab1 (yeast Ypt1) and Rab11 (yeast Ypt31/32)(60, 61), although its role has remained controversial. The *Drosophila* DENN protein Crag was also identified as a GEF towards both Rab10 and Rab11, although the GEF activity towards Rab11 was much weaker than Rab10(62). Neither of these GEFs is selective for Rab11, with both Rab10 and Rab1 having a different spatial organization compared to Rab11, implying

the existence of other more specific Rab11 GEFs. The first insight into Rab11-specific GEF proteins came with the discovery of the protein REI-1 and its homolog REI-2 in *C. elegans*, with loss of both leading to defects in cytokinesis(6). These enzymes are found only in metazoans, and knockouts of the REI-1 ortholog in *D. melongaster* (parcas) are viable but have defects in oogenesis and muscle development(63–65). Intriguingly, knockouts of either TRAPPII or Parcas are viable in Drosophila but the double knockout is embryonic lethal, suggesting the shared GEF activity for Rab11 is partially redundant(60). Although two GEFs have been identified for Rab11, their molecular mechanisms of activity and specificity remain unclear.

1.3.3 Rab11 related human diseases

The regulation of Rab11 is tightly regulated to ensure that cargo is transported to the correct location at the correct time. The recycling pathway that Rab11 regulates is critically important for neurodevelopment, and thus misregulation of Rab11 can manifest as diseases associated with this process. The most prominent diseases involving defective Rab11 regulation include Huntington Disease(5, 66, 67), Alzheimer's Disease(68, 69), Cancer(70), and neurodevelopmental disorders(71, 72). Furthermore, many intracellular pathogens, including viruses(73), bacteria(74), and parasites(75) subvert membrane trafficking by targeting Rab11 positive vesicles to allow for their invasion and replication. The current understanding of the role of Rab11 in human disease and disorders is summarized below.

In Huntington Disease (HD), impairment of Rab11 activation has been shown to lead to defective formation of recycling vesicles (5, 66, 67). So far, studies have showed that Huntington (HTT) protein can activate Rab11, and that mutant HTT protein leads to a reduction of Rab11 membrane localization and activation. It is becoming apparent that HTT is capable of interacting with the GEF responsible for Rab11 activation, although it is still not clear which GEF it interacts with, or if it works further upstream of this activation pathway(76). Rab11 is also implicated with the development of Alzheimer's Disease (AD). The hallmarks of AD are Aβ-amyloid-containing

neuritic plaques, and phosphorylated Tau-containing neurofibrillary tangles(77). Erroneous regulation of endocytic pathways has been implicated in the appearance of these hallmarks with Rab11 being major regulator of Aβ production(68, 69).

Overexpression of Rab25 has been linked to poor prognosis in ovarian cancer, with stapled peptide inhibitors of Rab25-effector binding inhibiting migration and proliferation of cancer cells(78, 79). Further, high expression levels of Rab25 has been shown to contribute to prostate cancer recurrence(80), and is also implicated in gastric cancer(81), cervical cancer(82), bladder cancer(83) and other epithelial cell cancers.

Both Rab11A and Rab11B are mutated in developmental disorders, with putative inactivating Rab11A or Rab11B mutations leading to intellectual disability and brain malformation (71, 72). Rab11 point mutations have been identified in patients with developmental and epileptic encephalopathies. These mutations were first discovered in parent-child exome sequencing studies, where it was found that cases of DEE were often linked to de novo mutations (DNMs). Regions both inside and outside of the nucleotide sensitive switch regions were identified, indicating they all may result in the same phenotype by different mechanisms. Some of these mutations, such as R82C are localized in the SWII region of Rab11, and could thus be expected to alter binding to effector proteins(71). Other mutations such as V22M and A68T are localized near the GTP/GDP binding pocket, and it is thought that they likely cause altered GDP/GTP binding, and may induce aberrant GEF binding leading to protein mislocalization(72). There are also mutations such as K13N, K24R, and S154L that are not predicted to alter nucleotide-binding dynamics and are not in the switch regions, so it is unclear on how they contribute to developmental encephalopathies(71). A summary of these mutations, and the subfamily member in which they were first identified, is shown in table 1.1 below.

Table 1.1 Rab11 single point mutations involved in disease

Subamily	Mutation	Role	Reference
Rab11a	K13N	DNM that does not affect any of the switch domains of RAB11A, unclear on how it results in developmental encephalopathies	(71)
Rab11a	K24R	Predicted-damaging DNM	(71)
Rab11a	R82C	The highly conserved Arg82 residue is located in the nucleotide-sensitive switch domain II of RAB11A and is involved in binding to the RAB11A effector FIP3	(71)
Rab11a	S154L	Does not affect any of the switch domains of RAB11A, unclear on how this DNM results in developmental encephalopathies	(71)
Rab11b	V22M, A68T	Dominant DNMs that lead to a neurodevelopmental syndrome. Likely causes altered GDP/GTP binding, and induces GEF binding and subsequent protein mislocalization.	(72)

1.4 Research objectives

Rab11 is a critical GTPase involved in membrane trafficking in the endocytic pathway, and it's misregulation is involved in a variety of human diseases including Huntington's disease, Alzheimer's disease, and developmental disorders. Hindering the capability to fully understand Rab11 regulation and its role in human disease is the lack of molecular detail describing how Rab11 proteins are activated by their cognate GEFs. The goal of this thesis is to interrogate the molecular mechanisms of the GEFs responsible for the activation of Rab11. Specifically, the aim is to structurally and biochemically characterize both SH3BP5 and TRAPPII, the GEFs that putatively regulate Rab11. The specificity of both TRAPPII and SH3BP5 have thus far been poorly characterized, and it is therefore a goal to characterize the specificity of these proteins. The interrogation of each of these GEFs is split into two thesis objectives, which are expanded on further below.

1.4.1 Thesis Objective #1: Determine if SH3BP5 is a specific GEF for Rab11, and determine its molecular mechanism of activation

The overall goal of objective 1 of this thesis is to reveal the molecular architecture of SH3BP5 in order to decipher the mechanism of Rab11 GEF activation. Further aims are to determine if SH3BP5 is a specific GEF for Rab11, and if so, determine what the mechanism of specificity is. With this information, the role of clinically relevant Rab11 mutations can be interrogated.

1.4.2 Thesis Objective #2: Characterize the specificity of the TRAPPII Complex, and investigate several different 'Trappopathies' to better understand their mechanisms of disease

The overall goal of this objective is to interrogate the specificity of the human TRAPPII complex, in order to clarify if it truly is a bona fide GEF for Rab11. Goals are to clone, purify, and express the 427kDa, 9 subunit complex, and use biochemical assays to determine its specificity. Further aims include determining if different clinically relevant TRAPPII mutants (Trappopathies) cause disease through a Rab11 binding mechanism and determining what the influence of TRAPPII is on clinically relevant Rab11 mutations.

Overall, this research will advance our understanding of the regulation of the critically important GTPase Rab11. Thesis objective 1 has recently been published in Nature Communications and is presented as Chapter 2 of the thesis. It is therefore presented as a manuscript, with a general introduction, materials and methods, results and a discussion. Thesis objective 2 is in preparation for a manuscript and is presented in Chapter 3 of the thesis. It will also be presented with a general introduction, materials and methods, results, and discussion. Finally, an overall summary of the major findings is summarized in Chapter 4.

Chapter 2 - Structural determinants of Rab11 activation by the guanine nucleotide exchange factor SH3BP5

Meredith L Jenkins[1], Jean Piero Margaria[2], Jordan TB Stariha[1], Reece M Hoffmann[1], Jacob A McPhail[1], David J Hamelin[1], Martin J Boulanger[1], Emilio Hirsch[2], John E Burke[1]

1. Department of Biochemistry and Microbiology, University of Victoria, Victoria, BC, Canada

2. Department of Molecular Biotechnology and Health Sciences, University of Turin, Torino, Italy

Adapted from: Jenkins ML, Margaria JP, Stariha JTB, Hoffmann RM, McPhail JA, Hamelin DJ, Boulanger MJ, Hirsch E, Burke JE. 2018. Structural determinants of Rab11 activation by the guanine nucleotide exchange factor SH3BP5. Nat Commun 9:3772.

Contributions: JEB and **MLJ** designed all biophysical/biochemical experiments. **MLJ** carried out protein cloning/expression/purification, with assistance from JTBS, and RMH. **MLJ** and JTBS carried out all biochemical studies. **MLJ** and JTBS generated all crystals. JEB, **MLJ**, JTBS, and JAM screened and collected diffraction data. JEB and MJB carried out crystallographic data analysis. **MLJ** carried out HDX-MS experiments with assistance from DJH and JTBS. JPM and EH designed and carried out all cellular Rab11 activation assays. **MLJ** and JEB wrote the manuscript, with input from all authors.

* At the time of this study, I was training JTBS in her undergraduate honours degree, and thus she assisted with many of the experiments. I trained DJH how to utilize the mass spectrometer, so he assisted by learning to run samples and perform data analysis.

2.1 Abstract

The GTPase Rab11 plays key roles in receptor recycling, oogenesis, autophagosome formation, and ciliogenesis. However, investigating Rab11 regulation has been hindered by limited molecular detail describing activation by cognate guanine nucleotide exchange factors (GEFs). Here we present the structure of Rab11 bound to the GEF SH3BP5, along with detailed characterisation of Rab-GEF specificity. The structure of SH3BP5 reveals a coiled coil architecture that mediates exchange through a unique Rab-GEF interaction. The structure reveals a striking rearrangement of the switch-I region of Rab11 compared to solved Rab-GEF structures, with a constrained conformation when bound to SH3BP5. Mutation of switch-I reveals the molecular determinants that allow for Rab11 selectivity over evolutionarily similar Rab GTPases present on Rab11 positive organelles. GEF deficient mutants of SH3BP5 show greatly decreased Rab11 activation in cellular assays of active Rab11. Overall, our results reveal unique molecular insight into Rab11 regulation, and how Rab-GEF specificity is achieved.

2.2 Introduction

Critical to almost all aspects of membrane trafficking and cellular signaling is the ability to properly traffic membrane cargoes. Cells possess a highly regulated system for directing membrane cargo to the proper cellular location, with one of the key determinants being the regulation of Rab (Ras related proteins in brain) GTPases(8–11). Among the best studied Rab GTPases are members of the Rab11 subfamily, which in humans comprised three isoforms (Rab11A, Rab11B, and Rab25 [also known as Rab11C]). The Rab11 proteins are master regulators of the surface expression of receptors(41). They are primarily localized at the trans-Golgi network, post-Golgi vesicles, and the recycling endosome, and they facilitate cytokinesis(42), ciliogenesis(2), oogenesis(43), and neuritogenesis(44). Both Rab11A and

Rab11B are mutated in developmental disorders, with putative inactivating Rab11A or Rab11B mutations leading to intellectual disability and brain malformation.

Hindering the capability to fully understand Rab11 regulation is the lack of molecular detail describing how Rab11 proteins are activated by their cognate GEFs. Biochemical reconstitution of the large macromolecular TRAPPII complex with their cognate Rab11 homologs in both yeast (Saccharomyces cerevisiae) and fruit flies (Drosophila melanogaster) revealed clear GEF activity toward both Rab1 (yeast Ypt1) and Rab11 (yeast Ypt31/32)(60, 61). The Drosophila DENN protein Crag was also identified as a GEF toward both Rab10 and Rab11(62). Neither of these GEFs is selective for Rab11, with both Rab10 and Rab1 having a different spatial organization compared with Rab11, implying the existence of other more specific Rab11 GEFs.

The first insight into potentially Rab11-specific GEF proteins was the discovery of the protein REI-1 and its homolog REI-2 in Caenorhabditis elegans, with loss of both leading to defects in cytokinesis(6). These enzymes are found only in metazoans, and knockouts of the REI-1 ortholog in Drosophila (parcas, also known as poirot) are viable, but have defects in oogenesis, and muscle development(63–65). Intriguingly, knockouts of either TRAPPII or parcas are viable in Drosophila, but the double knockout is embryonic lethal, suggesting the shared GEF activity for Rab11 is partially redundant(60). The mammalian ortholog of REI-1, SH3 binding protein 5 (SH3BP5) also has GEF activity towards Rab11, and was shown to be selective for Rab11 over Rab5(6). In addition, mammals contain a SH3BP5 homolog, SH3BP5L, that has not yet been tested for Rab11 GEF activity. The role of SH3BP5 in development and signaling is complicated by its additional capability to directly regulate Bruton tyrosine kinase (BTK) signaling through binding to the BTK SH3 domain(84), as well as to inhibit JNK signaling through engagement of the disordered C-terminus of SH3BP5(85, 86).

The fundamental molecular mechanism by which Rab11 proteins can be activated by their cognate GEFs has remained unclear. To decipher the mechanism of SH3BP5 GEF activity we

have determined the structure of the GEF domain of SH3BP5 bound to nucleotide-free Rab11A. Detailed biochemical studies reveal that SH3BP5 is highly selective for Rab11 isoforms, with no activity towards any of the most evolutionarily similar Rab GTPases. A subset of clinical Rab11 mutations found in developmental disorders were found to disrupt SH3BP5 mediated nucleotide exchange, providing a possible mechanism of disease. Detailed mutational analysis of both Rab11 and SH3BP5 reveals the molecular basis for Rab selectivity, as well as allowing for the design of GEF deficient SH3BP5 mutants. These SH3BP5 mutants were tested using a cellular Rab11 FRET sensor and show significantly decreased Rab11 activation. Overall, our study thus reveals insight into Rab11 regulation and defines how Rab11-GEF selectivity is achieved.

2.3 Materials and Methods

2.3.1 Plasmids and antibodies

The full length SH3BP5 gene was provided by MGC (DanaFarber HsCD00326538) pDONR223-SH3BP5(31-455) was a gift from William Hahn & David Root (Addgene plasmid # 23579). Rab25(HsCD00327861) SH3BP5L (HsCD00323009, Rab8a(HsCD00044586), Rab4b(HsCD00296539), Rab2a(HsCD00383517), Rab14(HsCD00322387), and Rab12(HsCD00297182) were purchased from the Dana Farber Plasmid Repository. Genes were subcloned into vectors containing a N-terminal GST-tag, and in some cases a C-terminal His-tag by Gibson assembly. Rab11 and SH3BP5 substitution mutations were generated using site-directed mutagenesis according to published protocols, and C-terminal and N-terminal residues of SH3BP5 were removed using Gibson ligation independent assembly(87). The following antibodies were used in this study: rabbit anti-SH3BP5 (SIGMA, HPA057988, IF 1:50), anti-rabbit IgG Alexa fluor 568 (Thermo-fisher, A-11036, IF 1:1000).

2.3.2 Bioinformatics

Sequences were aligned using Clustal Omega Multiple Sequence Alignment, and the aligned sequences were subsequently analyzed by ESPript 3.0 to visualize conserved regions. The protein interaction interfaces from the asymmetric unit was examined using the PDBePISA (Proteins, Interfaces, Structures and Assemblies) server(88). The SH3BP5 structure was compared to similar PDB structures using the DALI server(89). The surface potential map was generated using the APBS server(90).

2.3.3 Protein expression

Constructs of SH3BP5 and Rab11 were all expressed in BL21 C41 *E.coli.* Rab11 was induced with 0.5mM IPTG and grown at 37°C for 4h. Rab25 was expressed in Rosetta cells, induced with 0.1mM IPTG and grown overnight at 23°C. SH3BP5 and the remaining Rab proteins were induced with 0.1mM IPTG and grown overnight at 23°C. SeMet Rab11 and SH3BP5 were expressed in B834 *E.coli* in minimal media with SeMet (Molecular Dimensions), induced with 0.1mM IPTG, and grown overnight at 23°C. Pellets were washed with ice-cold phosphate-buffered saline (PBS), flash frozen in liquid nitrogen, and stored at -80°C until use.

2.3.4 Protein purification

Cell pellets were lysed by sonication for 5 minutes in lysis buffer (20mM Tris pH 8.0, 100mM NaCl, 5% (v/v) glycerol, 2mM ß–mercaptoethanol (BME), and protease inhibitors (Millipore Protease Inhibitor Cocktail Set III, Animal-Free)). Triton X-100 was added to 0.1% v/v, and the solution was centrifuged for 45 minutes at 20,000 x g at 1°C. Supernatant was loaded onto a 5ml GSTrap 4B column (GE) in a superloop for 2 hours and the column was washed in Buffer A (20mM Tris pH 8.0, 100mM NaCl, 5% (v/v) glycerol, 2mM BME) to remove non-specifically bound proteins. The GST-tag was cleaved by adding Buffer A containing 10mM BME and TEV protease to the column and incubating overnight at 4°C. Cleaved protein was eluted with Buffer A. Protein was further purified by separating on a 5ml HiTrap Q column with a gradient of Buffer A and Buffer

B (20mM Tris pH 8.0, 1M NaCl, 5% (v/v) glycerol, 2mM BME). Protein was pooled and concentrated using Amicon 30K concentrator and size exclusion chromatography (SEC) was performed using a Superdex 200 increase 10/300 or Superdex 75 10/300 column equilibrated in SEC Buffer (20mM HEPES pH 7.5, 500mM NaCl, 0.5mM TCEP). Rab proteins not used for crystallography were purified using SEC Buffer 2 (20mM HEPES pH 7.5, 150mM NaCl, 1mM $MgCl_2$ and 0.5mM TCEP). Fractions containing protein of interest were pooled, concentrated, flash frozen in liquid nitrogen and stored at -80°C.

Protein for crystallization was generated through mixing the SH3BP5 truncations and Rab11(Q70L) described above at an equimolar amount. The protein mixture was incubated for 5 min at 4°C. EDTA (pH 7.5) was added to a final concentration of 20 mM and the solution was left to incubate for 1 hr at 4°C. The protein complex was centrifuged for 3 min at 21130 x g and loaded onto a Superdex 200 10/300 column to separate the complex from free nucleotide. Fractions containing protein of interest were pooled, concentrated, flash frozen in liquid nitrogen and stored at -80°C.

2.3.5 Lipid vesicle preparation

Nickelated lipid vesicles were made to mimic the composition of the Golgi organelle [15% phospatidylethanolamine (egg yolk PE, Sigma), 20% phosphatidylinositol (soybean PI from Avanti), 10% phosphatidylserine (bovine brain PS, Sigma), 45% phosphatidylcholine (egg yolk PC Sigma), and 10% DGS-NTA(Ni) (18:1 DGSNTA(Ni), Avanti)]. All other vesicle compositions are described in Appendix C. Phosphatidylinositol-3-phosphate (PI3P) and L-α-phosphatidylinositol-4-phosphate (PI4P) were obtained from Avanti. Vesicles were prepared by combining liquid chloroform stocks together at appropriate concentrations and evaporating away the chloroform with nitrogen gas. The resulting lipid film layer was desiccated for 20 min before being resuspended in lipid buffer (20mM HEPES (pH 7.5) and 100mM KCl) to a concentration of 2.0 mg/mL or 1mg/ml. The lipid solution was vortexed for 5 min, bath sonicated for 10 min, and

flash frozen in liquid nitrogen. Vesicles were then subjected to three freeze thaw cycles using a warm water bath. Vesicles were extruded 11 times through a 100-nm NanoSizer Liposome Extruder (T&T Scientific) or a 400- nm NanoSizer Liposome Extruder (T&T Scientific) and stored at -80°C.

2.3.6 In-vitro GEF Assay

C-terminally His-tagged Rab11 was purified as described above. Rab11 was preloaded for the assay by adding EDTA to a final concentration of 5 mM and incubating for 30 mins prior to adding 5-fold excess of Mant-GDP (ThermoFisher Scientific). Magnesium chloride was added to 10mM to terminate the loading process and the solution was incubated for 30 min at 25°C. Size exclusion chromatography was performed using a Superdex 75 10/300 column in SEC Buffer 2 (20mM HEPES pH 7.5, 150mM NaCl, and 1mM $MgCl_2$, 0.5mM TCEP) to remove any unbound nucleotide. Fractions containing Mant-GDP loaded Rab11 were pooled, concentrated, flash frozen in liquid nitrogen, and stored at -80°C. Reactions were conducted in 10µl volumes with a final concentration of 4µM Mant-GDP loaded Rab11, 100uM GTPγS and SH3BP5(9nM-1µM) or SH3BP5L. Rab11 and membrane (0.2mg/ml-0.4mg/ml, see Appendix C) were aliquoted into a 384-well, black, low-volume plate (Corning 3676). To start the reaction, SH3BP5 and GTPγS were added simultaneously to the wells and a SpectraMax® M5 Multi-Mode Microplate Reader was used to measure the fluorescent signal for 1hr (Excitation λ = 366nm; Emission λ = 443nm). Data was analyzed using GraphPad Prism 7 Software, and k_{cat}/K_m analysis was carried out according to the protocol of(91). In brief, GEF curves were fit to a non-linear dissociate one phase exponential decay using the formula $I(t)=(I_0-I_\infty)*\exp(-k_{obs}*) + I_\infty$ (GraphPad Software), where I(t) is the emission intensity as a function of time, and I_0 and I_∞ are the emission intensities at t=o and t=∞. The catalytic efficiency k_{cat}/K_m was obtained by a slope of a linear least squares fit to $k_{obs}=k_{cat}/K_m*[GEF]+ k_{intr}$, where k_{intr} is the rate constant in the absence of GEF.

2.3.7 Crystallography

Crystallization trials of the SH3BP5-Rab11 complex were set using a Crystal Gryphon liquid handling robot (Art Robbins Instruments) in 96-well Intelli-Plates using sitting drops at 18°C. Initial hits were obtained in the Index HT crystallization kit (Hampton Research), and refinement plates for Index HT condition F11 (25% (w/v) PEG-3350, 200 mM sodium chloride, 100 mM Bis Tris pH 6.5) were set. The best crystals of the optimized SH3BP5 construct with Rab11A were obtained in 2 μL hanging drops, with a reservoir solution of 23% (w/v) PEG-3350, 200 mM sodium chloride, 100 m*M* Bis Tris pH 6.5, with a ratio of 4:1 protein / reservoir. Crystals were frozen in liquid nitrogen using cryo buffer [24% PEG-3350 (w/v), 200 mM sodium chloride, 100 mM Bis Tris pH 6.5, 15% (v/v) ethylene glycol]. SeMet containing crystals were obtained in 1.6 µL hanging drops with a reservoir solution of 14% (w/v) PEG-3350, 200mM NaBr, 100mM Bis-Tris pH 5.5, and 5% Tacsimate pH 6.0 at a ratio of 4:1 protein to reservoir. Crystals were frozen in liquid nitrogen using cryo buffer 2 [20% (w/v) PEG-3350, 150mM NaCl, 50mM NaBr, 100mM Bis-Tris pH 5.5, 5% Tacsimate pH 6.0, and 15% (v/v) ethylene glycol].

Diffraction data were collected at 100 K at beamline 08ID-1 of the Canadian Macromolecular Crystallography Facility (Canadian Light Source, CLS). Native data was collected at a wavelength of 0.97949 Ã, and SeMet data was collected at 0.97895 Ã. Data were integrated using XDS(92) and scaled with AIMLESS(93). Datasets were collected for both native SH3BP5 (1-265) / Rab11 (1-213) and SeMet incorporated SH3BP5 (1-265) / Rab11 (1-213). Full crystal collection details are shown in Table 1. Initial phases were determined by single-wavelength anomalous dispersion at the selenium peak energy with initial phases, density modification and automated model building carried out using CRANK (version 2.0)(94). This allowed for an initial model of SH3BP5 to be built, and the location of Rab11 was identified in the asymmetric unit through molecular replacement using PHASER(95), with the structure of GDP bound Rab11 used as the search model with both switch I and switch II removed(50). The final model of SH3BP5-Rab11 complex

was built using iterative model building, including manual rebuilding of the Rab11 switches in COOT(96) and refinement using phenix.refine(97) to a R_{work} = 23.54 and R_{free} = 27.80. Ramachandran statistics for final model - favoured 96.6%, outliers 0.51%. Full crystallographic statistics are shown in Table 1.

2.3.8 Identification of Disordered Regions in SH3BP5 using HDX-MS

HDX reactions were conducted in 50µl reaction volumes with a final concentration of 0.2µM SH3BP5(1-455) per sample. Exchange was carried out in triplicate for a single time point (3s at 1 ºC) and all steps were carried out in a 4ºC cold room. Hydrogen deuterium exchange was initiated by the addition of 48µl of D_2O buffer solution (10mM HEPES pH 7.5, 50mM NaCl, 97% D_2O) to the protein solution, to give a final concentration of 93% D_2O. Exchange was terminated by the addition of acidic quench buffer at a final concentration 0.6M guanidine-HCl and 0.9% formic acid. Samples were immediately frozen in liquid nitrogen at -80°C.

2.3.9 Mapping changes in Rab11 mutants using HDX-MS

All clinically relevant Rab11 mutants were purified identically to WT Rab11. HDX reactions were conducted in 50µl reaction volumes with a final concentration of 0.5µM Rab11(WT, V22M, K24R or S154L) per sample. Exchange was carried out in triplicate for two time points: 3s at 1 ºC, and 300s at 18 ºC. Hydrogen deuterium exchange was initiated by the addition of 49µl of D_2O buffer solution (10mM HEPES (pH 7.5), 50mM NaCl, 97% D_2O) to the protein solution, to give a final concentration of 95% D_2O. Exchange was terminated by the addition of acidic quench buffer at a final concentration 0.6M guanidine-HCl and 0.9% formic acid. Samples were immediately frozen in liquid nitrogen at -80°C.

2.3.10 Mapping of the SH3BP5-Rab11 Binding Interface using HDX-MS

HDX reactions were conducted in 20µl reaction volumes with a final concentration of 1.0µM Rab11(Q70L), and 1.0µM SH3BP5(31-455) per sample. Exchange was carried out in triplicate for four time points (3s at 1 ºC and 3s, 30s and 300s at room temperature). Prior to the addition of

D_2O, both proteins were incubated on ice in the presence of 20µM EDTA for 1hr to facilitate release of nucleotide. Hydrogen deuterium exchange was initiated by the addition of 17.5µl of D_2O buffer solution (10mM HEPES pH 7.5, 500mM NaCl, 97% D_2O) to 2.5µl of the protein solutions, to give a final concentration of 78% D_2O. Exchange was terminated by the addition of acidic quench buffer at a final concentration 0.6M guanidine-HCl and 0.9% formic acid. Samples were immediately frozen in liquid nitrogen at -80°C.

2.3.11 Investigating the role of membrane using HDX-MS

HDX reactions were conducted in 20µl reaction volumes with a final concentration of 0.4 µM C-terminally His-tagged Rab11A (1-211), 0.4 µM SH3BP5 (31-455) and 0.2 mg/mL nickelated lipid vesicles [15% PE, 20% PI, 10% PS, 45% PC, and 10% DGS-NTA(Ni)] per sample. Exchange was carried out in triplicate for four time points (3s, 30s, 300s, 3000s) at room temperature. Prior to the addition of D_2O, 1µl of 20µM Rab11 and 2µl of 2 mg/mL membrane (or membrane buffer) were left to incubate for 30 seconds. One microliter of 20µM SH3BP5 was then added and incubated a further 30 seconds prior to the initiation of hydrogen deuterium exchange by the addition of 16µl of D_2O buffer solution (10mM HEPES pH 7.5, 200mM NaCl, 97% D_2O) to the samples to give a final concentration of 77% D_2O. Exchange was terminated by the addition of acidic quench buffer giving a final concentration 0.6M guanidine-HCl and 0.9% formic acid. Samples were immediately frozen in liquid nitrogen at -80°C.

2.3.12 Mutational analysis of SH3BP5 using HDX-MS

HDX reactions were conducted in 50µl reaction volumes with a final concentration of 0.6µM SH3BP5(WT) or 0.6µM SH3BP5(LNQ52AAA), or 0.6µM SH3BP5(LE250AK) per sample. Exchange was carried out in triplicate for two time points (3s, 300s at 18ºC). Hydrogen deuterium exchange was initiated by the addition of 48.5µl of D_2O buffer solution (10mM HEPES pH 7.5, 200mM NaCl, 97% D_2O) to the samples to give a final concentration of 94% D_2O. Exchange was

terminated by the addition of acidic quench buffer giving a final concentration 0.6M guanidine-HCl and 0.9% formic acid. Samples were immediately frozen in liquid nitrogen at -80°C.

2.3.13 HDX-MS data Analysis

Protein samples were rapidly thawed and injected onto an ultra-performance liquid chromatography (UPLC) system kept in a cold box at 2ºC. The protein was run over two immobilized pepsin columns (Applied Biosystems; Porosyme 2-3131-00) and the peptides were collected onto a VanGuard Precolumn trap (Waters). The trap was eluted in line with an ACQUITY 1.7um particle, 100 x 1mm2 C18 UPLC column (Waters), using a gradient of 5%-36% B (Buffer A 0.1% formic acid, Buffer B 100% acetonitrile) over 16 min. Mass spectrometry experiments were performed on an Impact QTOF (Bruker), and peptide identification was done by running tandem mass spectrometry (MS/MS) experiments run in data-dependent acquisition mode. The resulting MS/MS datasets were analyzed using PEAKS7 (PEAKS), and a false discovery rate was set at 1% using a database of purified proteins and known contaminants. HDExaminer Software (Sierra Analytics) was used to automatically calculate the level of deuterium incorporation into each peptide. All peptides were manually inspected for correct charge state and presence of overlapping peptides. Deuteration levels were calculated using the centroid of the experimental isotope clusters. Fully deuterated samples were generated by incubating SH3BP5 with 3M guanidine for 30 minutes prior to the addition of D_2O. The protein was exchanged for 1 hour on ice before adding quench buffer. This fully deuterated sample allows for the control of peptide back exchange levels during digestion and separation. Differences in exchange were in a peptide were considered significant if they met all three of the following criteria: >5% change in exchange, >0.5 Da difference in exchange, and a p value <0.01 using a two tailed student t-test. Samples were only compared within a single experiment and were never compared to experiments completed at a different time with a different final D_2O level.

2.3.14 Rab11 activated sensor cellular experiments

$2*10^5$ HEK 293Tcells (ATCC, CRL-11268) were plated in a 6-well plate and Lipofectamine 2000 (Invitrogen) was used for transfection. Less than 500 ng of DNA were transfected in every condition. After 36 hours of transfection, lysis was performed in lysis buffer (50mM Tris-HCl, pH 7.4, 1% Tritorn X-100, 10mM $MgCl_2$, 100mM NaCl, proteinase inhibitors) and lysate was measured in a fluorometer cuvette. The Fluoromax-4 Horiba fluorometer was used to perform the measure. Laser excitation at 433 nm was used and the emission spectrum from 450 to 550 nm was recorded. A second measurement was made by directly exciting YFP at 505 nm and measuring its emission at 525 nm, to normalize for biosensor concentration. Co-localization analysis was performed using ImageJ JACOP plugin. Pearson's coefficient of correlation was calculated using Costes' automatic threshold.

2.3.15 Quantification of Rab11 activity in COS-7 cells

The sensitized FRET and CFP images acquired from transfected COS-7 cells (ATCC, CRL-165), were smoothed using Gaussian blur and background subtraction was performed according to previous published protocol(98). Afterwards, FRET activity ratio was computed by dividing sensitized FRET pixels by the CFP pixels, excluding saturated signals.

2.3.16 Statistical analysis

Six independent experiments (n) were performed for microscopy-based experiments, and statistical significance were obtained. Means ± SEM were used to present values. *P* values were calculated using one-way ANOVA followed by Bonferroni's multiple comparison posttest (GraphPad Software). The following legends are used for statistical significance: $*P < 0.05$, $**P < 0.01$, and $***P < 0.005$. For all GEF and HDX-MS assays experiments were carried out in triplicate, and means ± SD are shown. Statistical analysis between conditions was performed using a two-tailed student t-test, with p-values shown the same as described for cellular experiments.

2.3.17 Data accessibility

The structure factors and coordinates for the structure of Rab11A bound to SH3BP5 have been deposited in the protein databank with the accession code 6DJL. The mass spectrometry proteomics data have been deposited to the ProteomeXchange Consortium via the PRIDE(99) partner repository with the dataset identifier PXD010586. The processed HDX-MS data is provided in Appendix J-M.

2.4 Results

2.4.1 Biochemical characterization of SH3BP5 GEF activity

SH3BP5 was previously demonstrated to act as a GEF for Rab11(6), and this activity was strongly dependent on the membrane presentation of Rab11. To examine the specificity of GEF activity for Rab11 family members, GEF assays were carried out on the Rab11 isoforms Rab11A and Rab25 loaded with the fluorescent GDP analog 3-(N-methyl-anthraniloyl)-2-deoxy-GDP (Mant-GDP) and nucleotide exchange was determined as a function of SH3BP5 concentration. Rab11 proteins were generated with a C-terminal His-tag which allows for localization on NiNTA containing membranes (Fig. 2.1a). Domain schematics of all purified protein constructs generated in this study are shown in Appendix B.

The catalytic efficiency of SH3BP5 GEF activity (k_{cat}/K_m) was highest for Rab11A, ~$3.5x10^4$ $M^{-1}s^{-1}$, with slightly lower values for Rab25 (11c) at ~$1.8x10^4$ $M^{-1}s^{-1}$ (Fig. 2.1b). SH3BP5L GEF activity was even higher, with values of ~$8.1x10^4$ $M^{-1}s^{-1}$ against Rab11A. Measurements of SH3BP5 Rab GEF activity were characterized both in solution, and in a membrane reconstituted system where Rab isoforms were attached to NiNTA containing membrane using a C-terminal His-tag, similar to previous Rab11 GEF studies on the *Drosophila* and yeast variants of the TRAPPII complex(60, 61). SH3BP5 GEF activity showed only a weak dependence on Rab11A

being present on a lipid membrane, with a ~2 fold higher rate on a membrane compared to free in solution, consistent with biochemical studies performed on the *Drosophila* homolog parcas(60).

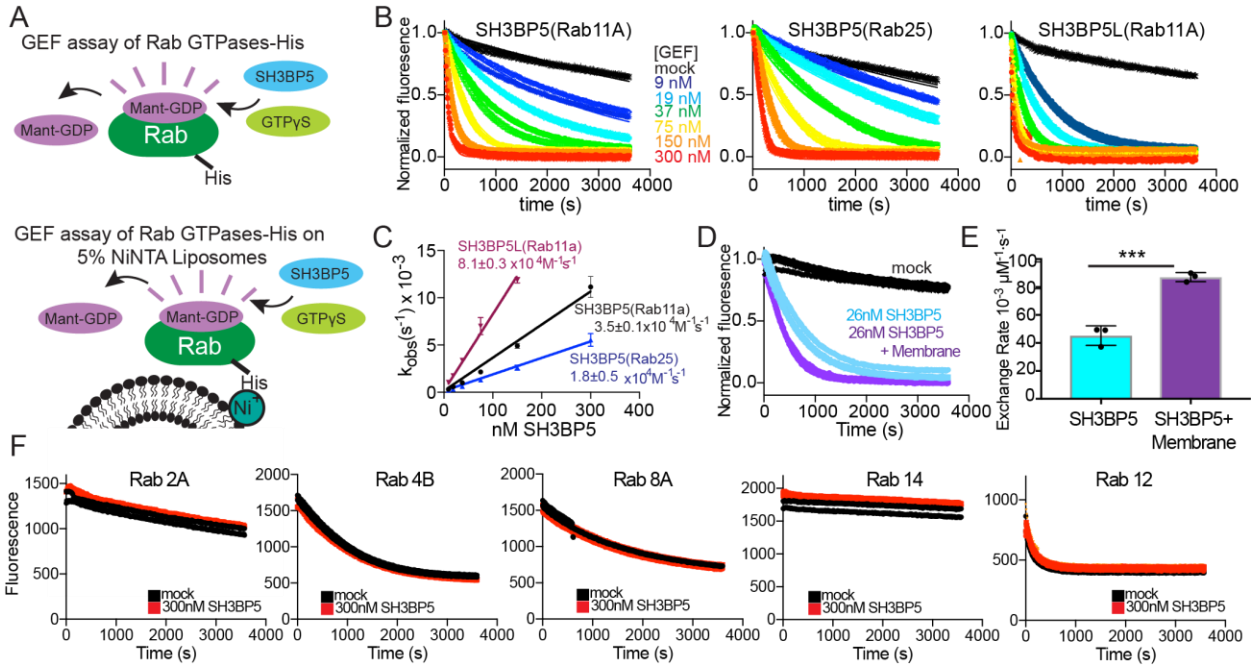

Figure 2.1. *In vitro* GEF assays reveal that SH3BP5 is a potent and selective GEF for Rab11.

(A)Schematic of GEF activation assays using fluorescent analog Mant-GDP in the presence and absence of NiNTA-containing lipid vesicles. (B) *In vitro* GEF assay of SH3BP5 (1–455) on Rab11A and Rab25, and SH3BP5L (1–393) on Rab11A. Nucleotide exchange was monitored by measuring the fluorescent signal during the SH3BP5(1–455) (9 nM-300 nM) catalyzed release of Mant-GDP from 4 μM of Rab11a-His6 in the presence of 100 μM GTPγS. Each concentration was conducted in triplicate. (C) Calculation of kcat/Km values for nucleotide exchange rates of Rab11A (SH3BP5 and SH3BP5L) and Rab25 (SH3BP5) according to the protocol of Delprato *et al.* (91). (D) *In vitro* GEF assay of SH3BP5 on Rab11A in the presence and absence of 100 nm extruded liposomes at 0.2 mg/ml (10% DGS-NTA(Ni), 10% PS, 15% PE, 20% PI, 45% PC). Nucleotide exchange was monitored by measuring the fluorescent signal during the SH3BP5 (1–455) (26 nM)-catalyzed release of Mant-GDP from 4 μM of Rab11A-His6 in the presence of 100 μM GTPγS. e Bar graph representing the difference in GEF activity in the presence and absence of Ni-NTA membranes. (F) *In vitro* GEF assays of SH3BP5 against a panel of evolutionarily related Rab GTPases loaded with Mant-GDP at a final concentration of 300 nM SH3BP5 and 4 μM Rab GTPase. For all panels, error bars represent SD (n = 3), with p-values generated using a two-tailed Student's t-test (***p < 0.005)

Previously Rab11 activation has been associated with the generation of different phosphoinositides, including PI3P and PI4P(100–102). To test this biochemically, GEF assays were carried out on vesicles of both different size (100 nm and 400 nm) and different membrane composition including variations of surface charge and phosphoinositide (PS, PI, PI3P, and PI4P)

composition (Appendix C). There was no difference in membrane stimulated GEF activity across all membranes tested (Appendix 2b). Rab GEF mediated nucleotide exchange has also been previously shown to have a strong dependence on dominant active switch II mutants(103) (Q70L in Rab11). However, GEF assays on Q70L Rab11A showed a slightly elevated GEF-mediated nucleotide exchange rate for Q70L compared to WT Rab11A (Appendix C). The dominant negative mutant of Rab11A (S25N) caused rapid release of Mant-GDP even in the absence of SH3BP5 (Appendix C).

SH3BP5 has been found to be selective for Rab11 over Rab5(6). However, these GTPases are highly evolutionarily distinct. To define the selectivity of SH3BP5 for Rab11, we characterized the GEF activity of SH3BP5 towards the most evolutionarily similar Rab GTPases (Rab2A, Rab4B, Rab14, and Rab12)(12) as well as Rab8, which is activated downstream of a Rab11 dependent Rab cascade(2). SH3BP5 showed no detectable Rab GEF activity for any of these Rab GTPases at up to 300 nM concentration of GEF, revealing that SH3BP5 is both a highly potent and highly selective Rab11 GEF (Fig. 2.1f).

2.4.2 Structure and dynamics of the Rab11A-SH3BP5 complex

To define the dynamics of the full length SH3BP5 protein, we used hydrogen deuterium exchange mass spectrometry (HDX-MS). HDX-MS measures the exchange rate of amide hydrogens with solvent, and as the main determinant of exchange is the stability of secondary structure, it is an excellent probe of secondary structure dynamics(104). HDX experiments with extremely short exposures of D_2O can be used to identify disordered regions within proteins(105). We carried out HDX experiments with a short pulse of deuterium exposure (3 s at 1°C) for the full length SH3BP5, with both the N-terminus and C-terminus of SH3BP5 having >50% deuterium incorporation, indicating limited secondary structure (Appendix D). HDX-MS results were used to generate a crystal construct of SH3BP5, with all of the C-terminal disordered region removed

(SH3BP5 1-265). GEF assays carried out using either full length SH3BP5, a N-terminally truncated (31-455) version, and the 1-265 crystal construct revealed no difference in SH3BP5 mediated Rab11A nucleotide exchange, suggesting that the disordered N and C-termini have no effect on Rab11 binding or SH3BP5 GEF activity (Appendix D c, d). The complex of the crystal construct of SH3BP5 (1-265) and Rab11A Q70L was able to be purified to homogeneity and eluted as a 1:1 complex on gel filtration (Appendix D e, f).

To understand the molecular basis of how SH3BP5 mediates Rab11A nucleotide exchange, we determined the structure of the N-terminal GEF domain of SH3BP5 bound to full length Q70L Rab11A to a final resolution of 3.1 Å. The Q70L construct of Rab11 was used for structural studies as the marginally increased GEF rate for Q70L vs WT suggested Q70L might form a slightly more stable complex with SH3BP5. Initial phases were generated by SeMet single wavelength anomalous diffraction of 3.3 Å and extended to 3.1 Å using native data (Fig. 2.2, details on unit cell data collection and refinement details are in Appendix E and Table 2.1). The structure is composed of four complexes of SH3BP5-Rab11A per asymmetric unit, with each of the copies in the asymmetric unit sharing an overall similar architecture. The following structural analysis refers to the complex of SH3BP5 chain E and Rab11A chain F, as this complex showed the best-defined electron density. The GEF domain of SH3BP5 is composed of a coiled coil that is kinked to form an overall v-shape. The v is composed of four long alpha helices (α1-α4), with a small helix connecting helices α2 α3. This connecting region between helix α2 α3 shows the highest degree of conformational flexibility between copies in the asymmetric unit (Appendix E). The putative SH3 binding site for BTK is located at the turn from helix α3 to α4 (84). However, this region shares no similarity to any previously identified SH3 binding site. A surface potential map of SH3BP5 reveals limited highly charged regions, with one basic stretch located at the base of the v shape (Appendix E). There also are no putative amphipathic helices in SH3BP5 that would potentially mediate membrane binding. The N-terminal GEF domain of SH3BP5 was previously predicted to

share homology to F-bar domains(6). However, bioinformatic analysis using the DALI server revealed that the closest structural homologs are the cell invasion protein SipB (PDB: 3tul), the stalk region of dynein (PDB: 5ayh), and the bacterial chaperone prefoldin (PDB: 1fxk). The highest similarity to the α1/α4 Rab11 binding coiled coil is the archaeal chaperone prefoldin(106). The characteristic v-shape of SH3BP5, however, is unique among solved coiled coil proteins.

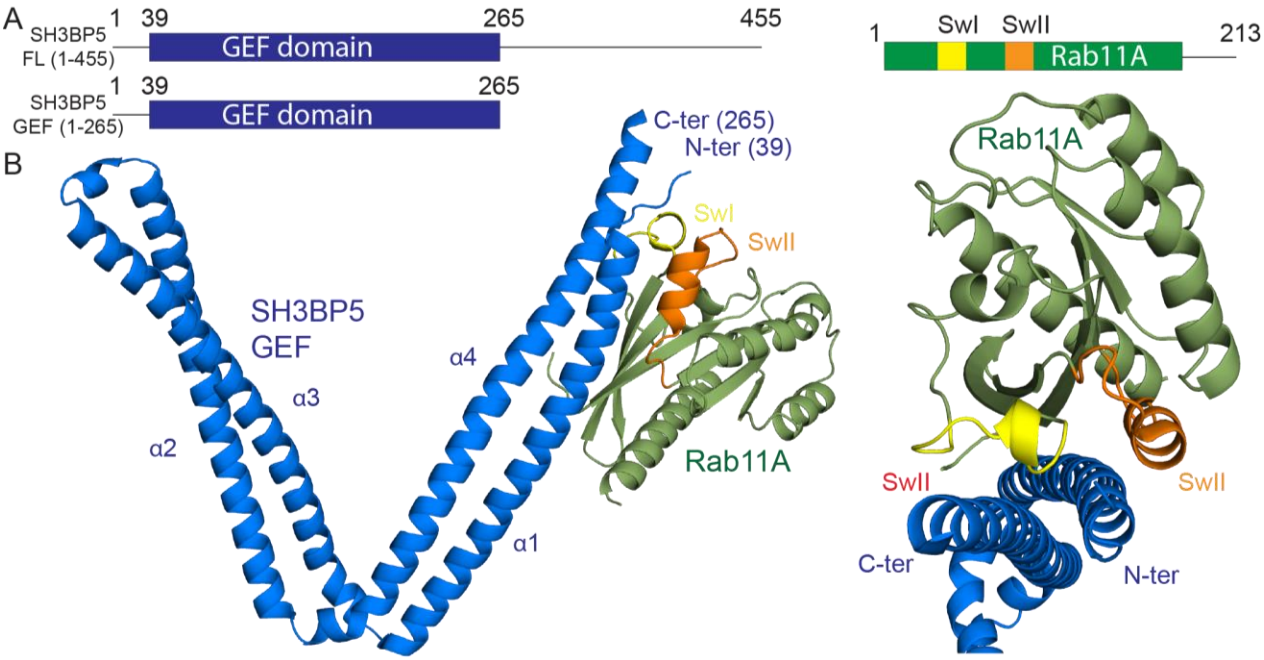

Figure 2.2. Structure of SH3BP5 in complex with Nucleotide-free Rab11.

A) Schematic of full-length SH3BP5(1–455), the crystal construct of SH3BP5 (1–265) and Rab11A with switch I (SwI) and switch II (SwII) regions annotated. B) The structure of the GEF domain of SH3BP5 with nucleotide-free Rab11 solved to 3.1 Å resolution. The GEF domain of SH3BP5 is composed of a v-shaped coiled coil with four long α-helices annotated on the figure. The switch regions of Rab11 are colored yellow (Switch I (SwI)) and orange (switch II (swII)), with the SwI situated between helix α1 and α4 of SH3BP5

Table 2.1. Data Collection and Refinement Statistics.

	SH3BP5-Rab11 native	SH3BP5-Rab11 SeMet (peak)
Data collection		
Space group	I222	I222
Cell dimensions		
a, *b*, *c* (Å)	114.85, 197.04, 304.71	114.13, 197.18, 304.20
α, *β*, *γ* (°)	90, 90, 90	90, 90, 90
Resolution (Å)	49.26–3.10 (3.21–3.10)[a]	49.39–3.25 (3.36–3.25)
R_{merge}	0.1363 (2.189)	0.156 (2.214)
$I / \sigma I$	8.26 (0.75)	13.68 (1.35)
Completeness (%)	99.74 (99.79)	99.88 (99.72)
Redundancy	4.9 (5.1)	13.2 (13.0)
Refinement		
Resolution (Å)	49.26–3.1 (3.21– 3.1)	
No. reflections	62,902 (6236)	
R_{work} / R_{free}	23.5/27.8	
No. atoms		
Protein	12,888	
Ligand/ion	0	
Water	0	
B-factors		
Protein	132.44	
Ligand/ion		
Water		
R.m.s. deviations		
Bond lengths (Å)	0.003	
Bond angles (°)	0.55	
[a]Values in parentheses are for highest-resolution shell.		
Number of crystals used for structure = 1		

Nucleotide-free Rab11A was bound to the GEF domain of SH3BP5 at one end of the v at a surface composed of the N-terminus of helix α1 and the C-terminus of helix α4 of the coiled coil. The SH3BP5-Rab11 interface is composed of a large extended, primarily hydrophobic interface (~1250 Å^2) (Fig. 2.3a). The Rab11 binding surface of SH3BP5 is composed of residues 39-67 and residues 240-262. The contact residues at this interface are highly conserved both in SH3BP5 and SH3BP5L, as well as the parcas and REI-1/2 homologs in both *Drosophila* and *C. elegans,* respectively (Fig. 2.3b). The SH3BP5 binding surface of Rab11 is composed of residues spanning

the N-terminus (residues 6-13), residues in and near switch I (residues 35-48), the inter-switch region 58-65, residues in and near switch II (72-85), and the C-terminus (180-181). Rab11 packs along the center of the coiled coil of SH3BP5, with the main binding interface composed of a contiguous hydrophobic surface of Rab11 residues including Y8, L10 and Y11 at the N-terminus, F36 and I44 in switch I, Y73 and I76 in switch II, and the hydrophobic triad (F48, W65, Y80), which plays a conserved role in interacting with Rab effectors (107) (Fig. 2.3c).

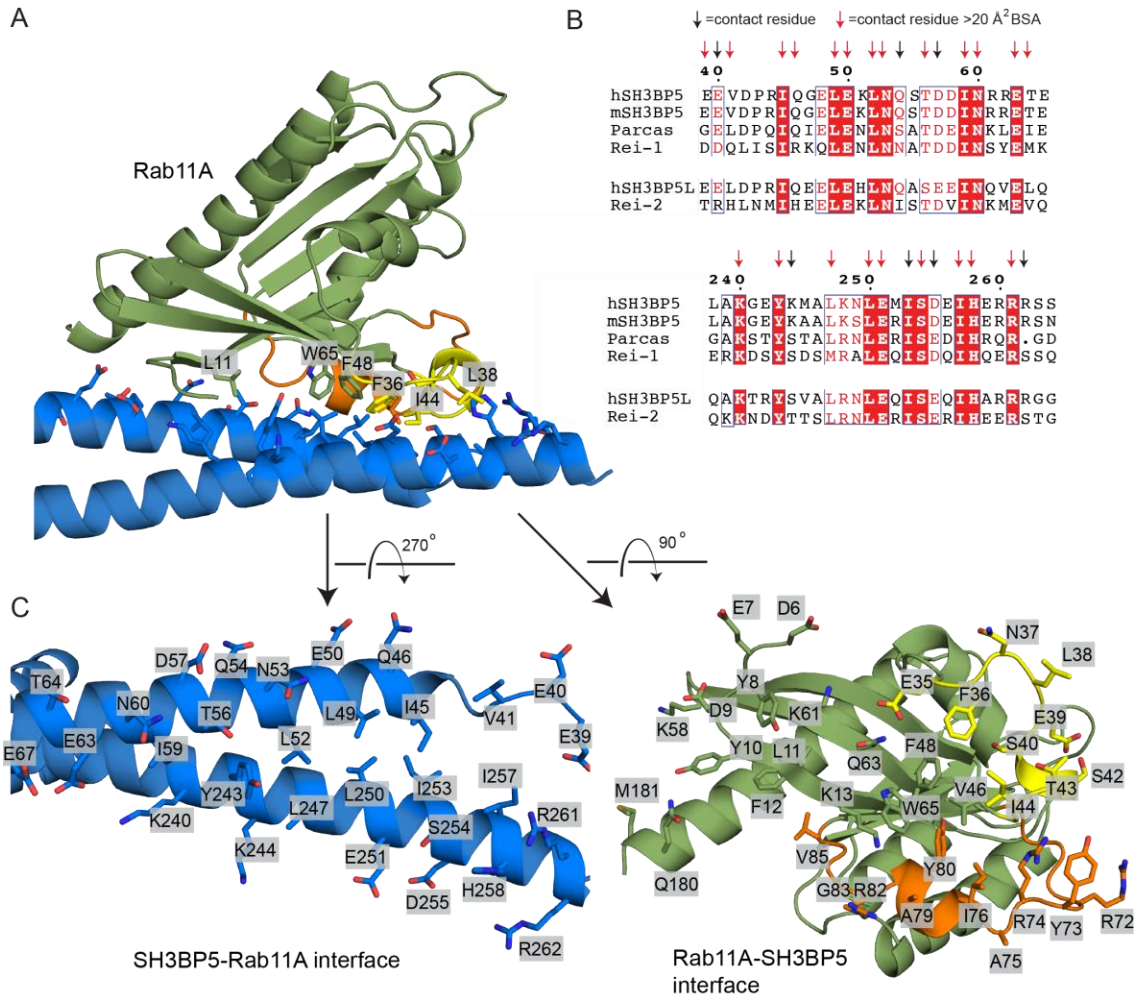

Figure 2.3. Rab11A SH3BP5 interface.

(A) Zoom in on the binding interface of Rab11 and SH3BP5. Key Rab11 residues forming important interactions at the interface are labeled. (B) Alignment of the Rab11-binding site on both helix α1 and α4 of SH3BP5 and SH3BP5L along with paralogs from M. musculus (mSH3BP5), D. melanogaster (parcas), and C. elegans (REI-1/REI-2), with contact residues indicated by arrows. Red arrows indicate greater than 20 Å2 of buried surface area (BSA). (C) All interacting residues from both SH3BP5 and Rab11 are shown in stick representation and labeled, with the structures rotated and the interacting partner removed to allow for visualization. SwI and SwII are colored according to Fig. 2.2

HDX-MS experiments were carried out to both verify the crystallographic complex as well as define how SH3BP5 works on a membrane surface. HDX-MS experiments revealed differences in exchange for Rab11A Q70L when bound to a N-terminally truncated SH3BP5 (31-455), with decreased HDX at the SH3BP5 interface (Appendix Fa-c), verifying the crystallographic interface in solution. Increased exchange was observed surrounding the Rab11 nucleotide-binding pocket, and this likely corresponds to loss of nucleotide upon SH3BP5 binding. HDX-MS experiments mapping out the Rab11 interface for the N-terminally truncated variant of SH3BP5 (31-455) were carried out with both soluble and membrane localized WT Rab11A (1-211, C-term his) to analyze conformational changes that may occur upon membrane binding. Decreases in exchange were observed for SH3BP5 at the crystallographic interface with Rab11A, with the only consequence of membrane being a larger decrease in exchange in Rab11A interfacial residues in SH3BP5 (Appendix F d-f), and no additional regions showing changes in H/D exchange. This potentially signifies a tighter interaction between SH3BP5 and Rab11A occurring on a membrane surface, which might possibly explain the limited selectivity of SH3BP5 for different membrane compositions (Appendix C).

2.4.3 Comparison to previously solved Rab-GEF complexes

Comparison of the structure of nucleotide-free Rab11A bound to SH3BP5 compared to Rab11A bound to either GDP or GTP reveals an extensive rearrangement of switch I(50), with only limited conformational changes in switch II (Fig. 2.4a +Appendix G). One of the minor conformational changes that occurs in switch II upon SH3BP5 binding is a reorientation of Y73, where the hydroxyl group is in position to cap the switch I helix (S40-G45). There were also conformational changes that occurred around the nucleotide binding pocket, including decreased secondary structure, although not to the same extent as seen in the Rab8:MSS4 GEF complex(108). HDX-MS studies of differences between nucleotide-bound Rab11 and SH3BP5-bound nucleotide-free Rab11 showed large increases in exchange in all regions of Rab11 around

the nucleotide binding pocket when bound to SH3BP5 (Appendix F a-c), further highlighting decreased stability of the nucleotide binding pocket.

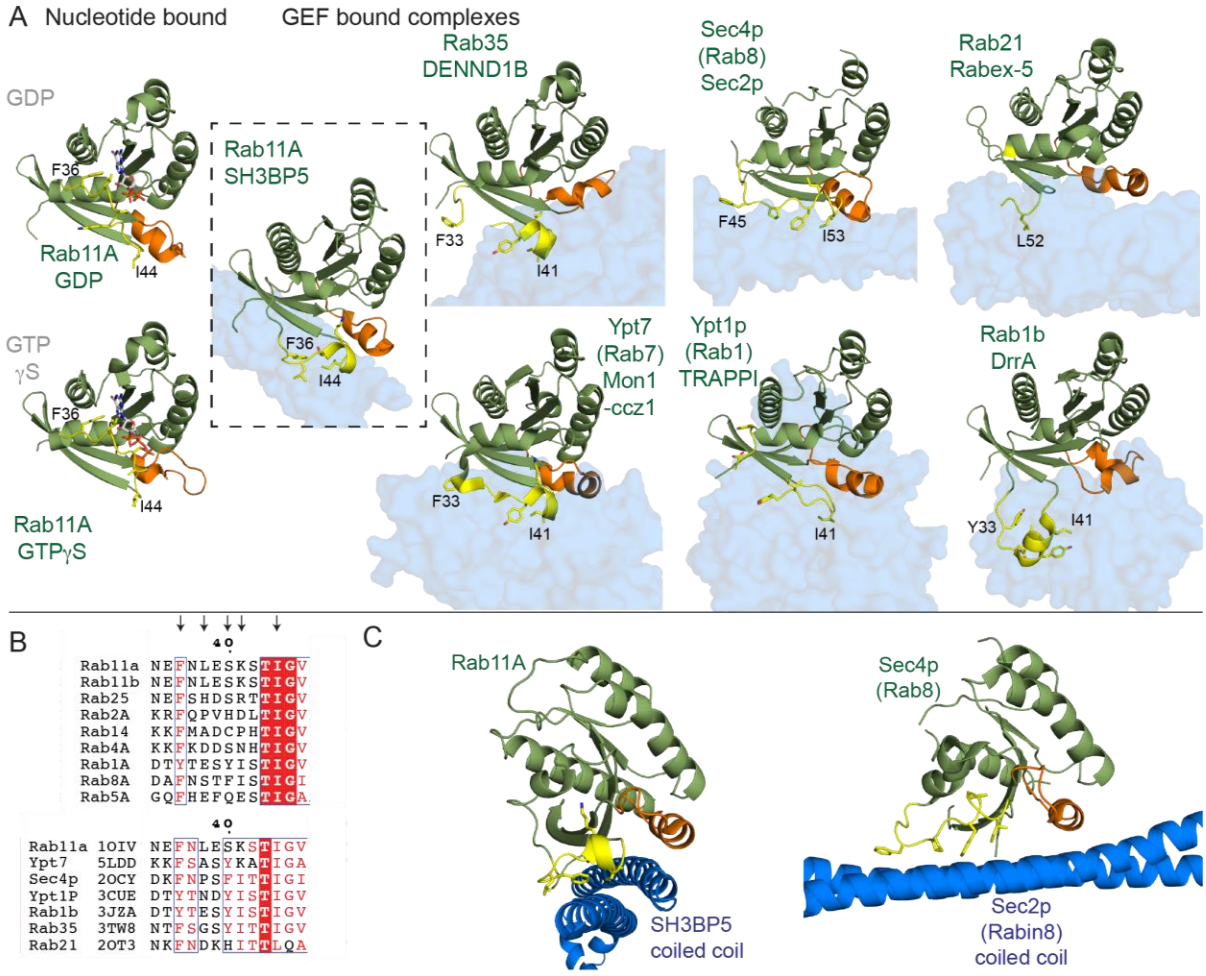

Figure 2.4. Unique switch orientations of Rab11-SH3BP5 compared to previously solved Rab-GEF structures.

A) Structures of nucleotide-bound Rab11 are compared to the GEF bound structures of Rab11-SH3BP5 (dotted box), Rab35-DENND1B(109), Ypt7-Mon1-Ccz1(110), Sec4p-Sec2p(111), Ypt1p-TRAPPI(112), Rab21-Rabex-5(113), and Rab1b-DrrA(114). The Rab GTPases are aligned to each other, with the GEF domain shown as a transparent surface. Switch I and II are colored according to Fig. 2.2, and the residues corresponding to F36 residue and I44 in Rab11 are labeled on all structures (the residue corresponding to F36 is disordered in the Ypt1p-TRAPPI complex, and in the Rab21-Rabex-5 structures). B) Alignment of the Switch I of Rab11 to a selection of closely related Rab isoforms and all previously solved Rab-GEF structures (PDB codes indicated). Switch I residues shown as sticks are highlighted by arrows. C) Alignment of the coiled coil GEF domains of SH3BP5 and Sec2P (Rabin8)(111). This reveals a completely orthogonal binding interface, with the two GEF coiled coils binding to their cognate Rab in a perpendicular orientation, revealing independent evolution of coiled coils as Rab-GEFs

The substantial conformational change of switch I upon SH3BP5 binding is present in all previously solved Rab-GEF structures, and is predicted to mediate nucleotide exchange through disrupting switch I nucleotide interactions. However, comparison of the conformational change in switch I reveals striking differences between previously solved Rab-GEF structures. The main difference is in the conformation of F36 and I44 in Rab11. These residues pack directly against each other, which requires a constrained conformation of switch I. This constrained orientation of the highly conserved F36 and I44 residues (Fig. 2.4a,b) is unique compared to previously solved Rab-GEF structures. There are a number of similarities with previously solved GEF structures, with a helix forming from S40 to G45 in switch I of Rab11, similar to DENND1B-Rab35(109) and Mon1-Ccz1-Ypt7(110) structures. Lysine 41 in Rab11 when bound to SH3BP5 is oriented towards the empty Mg^{2+} binding site, however, there was limited electron density around this residue, indicating that it is quite flexible (Appendix E). This same lysine residue in Ypt7 plays a key role in activation by Mon1-Ccz1(110), with the mechanism proposed to be mediated through disruption of the Mg^{2+} binding site.

Individual point mutations in Rab11A (K13N, K24R, R82C, S154L) and Rab11B (V22M, A68T) are found in developmental disorders that lead to intellectual disability(71, 72). Mapping these mutations onto the structures of nucleotide-bound Rab11, Rab11-GTPγS bound to the Rab11 effector FIP3, and SH3BP5-Rab11 revealed possible roles of these mutations in Rab11 regulation (Fig.2.5, Appendix H). The V22M and S154L would be expected to sterically disrupt nucleotide binding, and HDX-MS experiments of these mutants compared to WT Rab11 revealed large increases in exchange throughout the entire Rab protein (Appendix H), indicating that indeed these mutants are not able to bind nucleotide. No GEF assays were able to be carried out on these mutants, as they could not be loaded with Mant-GDP. K24R is part of the P-loop that coordinates the phosphate groups in bound nucleotide, and GEF assays revealed that this mutant had rapid nucleotide exchange even in the absence of SH3BP5 (Fig.2.5), indicating decreased

affinity for nucleotide. HDX-MS experiments on this mutant revealed increased exchange throughout the majority of Rab11, although not as large as changes seen for V22M and S154L (Appendix H). The A68T mutant is located at the beginning of switch II, with the Ala oriented towards the region of switch II that interacts with SH3BP5, and it only showed a modest effect in decreasing SH3BP5 mediated GEF activity. K13N and R82C are located directly at the Rab11-SH3BP5 interface, with R82 forming a salt bridge with E50 in SH3BP5, and K13 forming a polar bond with Q53 in SH3BP5. The K13 residue also forms pi-stacking interaction with the hydrophobic triad residue W65, which directly binds to SH3BP5. Mutation of K13N resulted in a >100-fold decrease in SH3BP5 mediated GEF activity, with R82 only partially decreasing SH3BP5 GEF activity (Fig.2.5). However, these mutations are unlikely to modify only GEF activity, as the R82 residue also forms a salt bridge with E747 in FIP3(115).

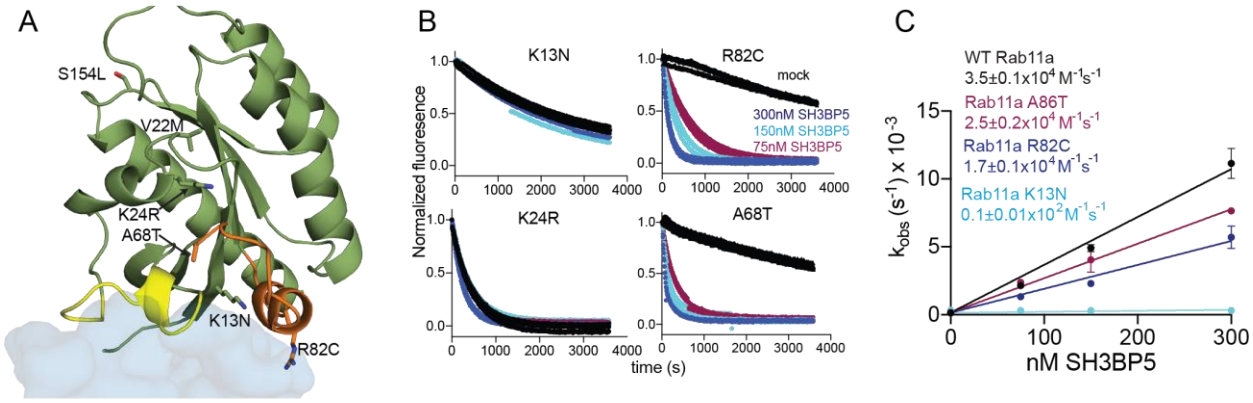

Figure 2.5. Clinically relevant Rab11 mutations disrupt nucleotide-binding or alter SH3BP5 GEF activity.

A) Point mutations found in developmental disorders mapped on the structure of Rab11 bound to SH3BP5. B) *In vitro* GEF assay of SH3BP5 on clinical Rab11 mutations. Nucleotide exchange was monitored by measuring the fluorescent signal during the SH3BP5 (1–455) (300 nM, 150 nM, or 75 nM) catalyzed release of Mant-GDP from 4 μM of the indicated Rab in the presence of 100 μM GTPγS. Fluorescent measurements were completed every 11 s for a total of 60 min (Excitation λ = 366 nm; Emission λ = 443 nm). C) Nucleotide exchange rates of Rab11A mutants plotted as a function of SH3BP5 concentration. The kcat/Km values for all Rab11A mutations were calculated from the slope. Error bars represent SD (n = 3)

The discovery that the SH3BP5 coiled coil acts as a GEF suggested that it may act similarly to the previously structurally characterized coiled coil Sec2p GEF Sec4p (Rab8 and Rabin8 in humans)(111, 116). Surprisingly the SH3BP5 coiled coil is perpendicular to the Sec2p coiled coil (Fig. 2.4C), and the two Rab GEFs interact with completely divergent binding surfaces on their cognate Rabs. Intriguingly, this suggests independent evolution of coiled coils to act as GEFs towards Rab GTPases.

2.4.4 Defining the molecular basis of SH3BP5 Rab11 selectivity

To further understand how SH3BP5 is able to achieve selectivity for Rab11 over evolutionarily similar Rab GTPases, we carried out site directed mutagenesis of switch I residues in Rab11. We tested the role of F36 and I44 residues, with mutation of these residues to Alanine leading to almost completely abrogated SH3BP5 mediated GEF activity (Fig. 2.6a-c). Mutations in switch I that mimic residues found in Rab2A (L38P), Rab8 (S40F), and Rab14 (K41P) were also found to decrease GEF activity greater than 100-fold, with limited effect on intrinsic nucleotide exchange (Fig. 2.6a,b). These residues would all be predicted to disrupt the constrained conformation of F36 and I44 relative to each other, leading to disruption of the contiguous hydrophobic surface required for interaction with SH3BP5. Mutation of these residues to Ala, also greatly decreased GEF activity. In Ypt7, the yeast homolog of Rab7, K41 plays a key role in mediating GEF activity through insertion into the Mg^{2+} binding site. To determine if this was conserved in Rab11, we tested GEF activity of a K41A Rab11 mutant. This led to a relatively minor ~3 fold decrease in GEF activity, compared to the previously reported 10 fold decrease in GEF activity for Mon1-Ccz1 on the K38A mutant of Ypt7(110). This suggests that the role of this lysine residue in inserting into the Mg^{2+} binding site is less important in SH3BP5 mediated GEF activity on Rab11 compared to Mon1-Ccz1 mediated GEF activity towards Ypt7.

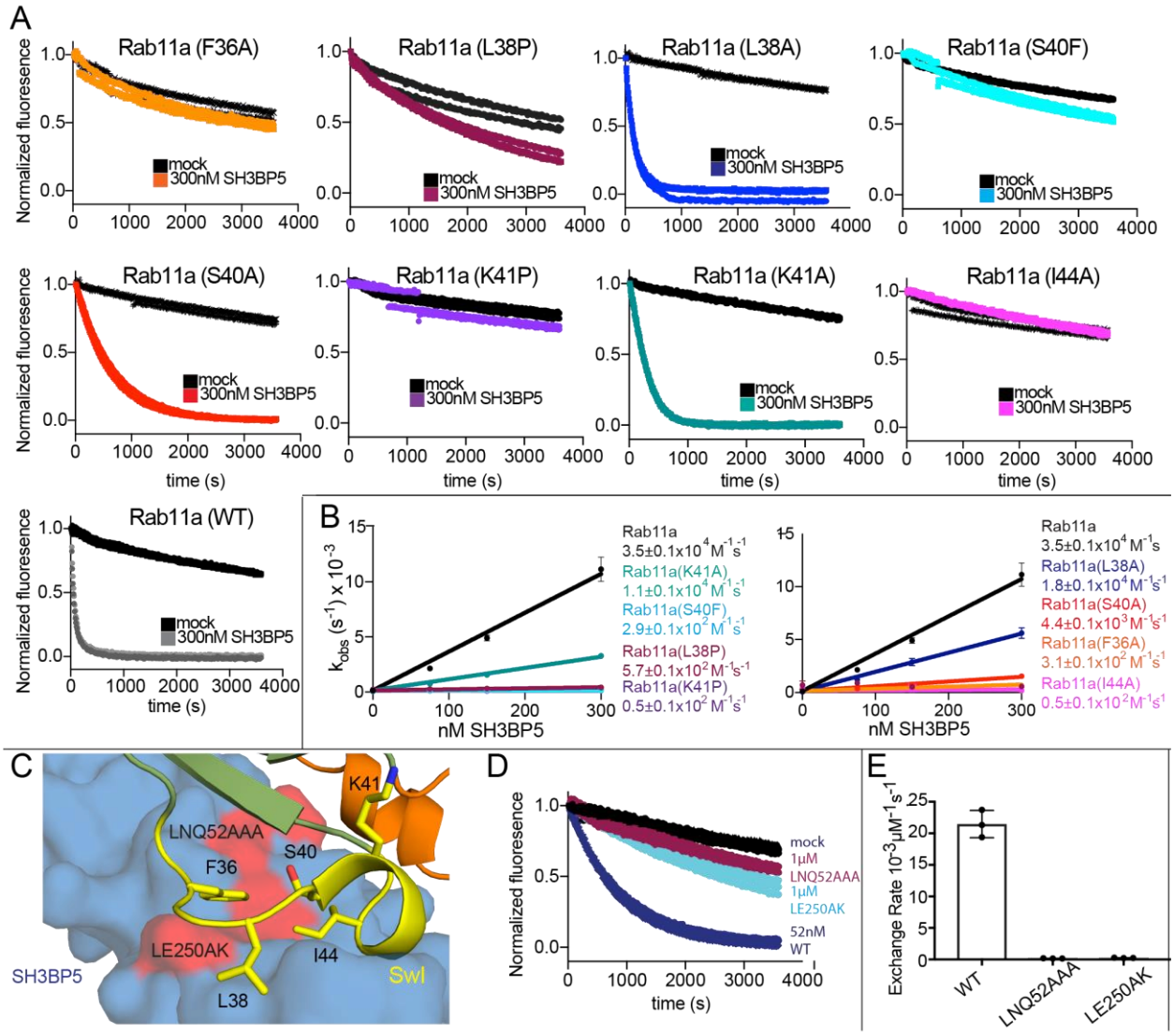

Figure 2.6. Molecular basis of SH3BP5 specificity and generation of GEF-deficient mutants.

A) *In vitro* GEF assay of SH3BP5 on Switch I Rab11 mutations. Nucleotide exchange was monitored by measuring the fluorescent signal during the SH3BP5 (1–455) (300 nM) catalyzed release of Mant-GDP from 4 μM of the indicated Rab in the presence of 100 μM GTPγS. Fluorescent measurements were completed every 11 s for a total of 60 min (Excitation λ = 366 nm; Emission λ = 443 nm). Two GEF curves are shown for each condition. B) Nucleotide exchange rates of Rab11A mutants plotted as a function of SH3BP5 concentration. The kcat/Km values for all switch I Rab11A mutations were calculated from the slope. All points have error bars, some are smaller than the size of the point. C) Zoomed in view of the binding interface of SH3BP5 and Rab11. Key Rab11 residues involved in the interface with SH3BP5 are shown as sticks and labeled on the structure. Regions in SH3BP5 critical for GEF activity (LNQ52, LE250) are highlighted in red. D) GEF assay of WT SH3BP5 (52 nM) and GEF-deficient mutants SH3BP5 (LNQ52AAA) and SH3BP5(LE250AK) (1000 nM), in the presence of the same concentrations of Rab11A and GTPγS as described in a. Two GEF curves are shown for each condition. E) Quantification of Rab11 GEF activity for WT SH3BP5 and GEF-deficient mutations. For all panels error bars represent SD (n = 3)

2.4.5 Generation of SH3BP5 GEF deficient mutations

Critical to understanding the role of SH3BP5 is to define differences between its BTK/JNK regulatory roles and Rab11 regulatory roles, which requires the generation of point mutations that disrupt only specific SH3BP5 functions. From examining the structure of SH3BP5 bound to Rab11 and sequence conservation throughout evolution, we separately mutated Rab11 contact interfaces in helix α1 (LNQ52AAA) and α4 (LE250AK) of SH3BP5. To ensure the protein was properly folded we used HDX-MS to test conformational dynamics. Both mutants showed increased exchange only at the Rab11 interface, with no global changes in deuterium incorporation (Appendix H), suggesting these mutants remain properly folded. Both mutants led to a >100 fold decrease in GEF activity compared to WT SH3BP5 (Fig 2.6 d,e).

To study activation of Rab11 in a cellular context we used a recently developed Rab11 activation sensor (AS-Rab11)(100). AS-Rab11 is composed of the Rab binding domain (RBD) of FIP3, monomeric yellow fluorescent protein (mcpVenus), a proteinase K-sensitive linker, a monomeric cyan fluorescent protein (mECFP) and human Rab11A (Fig. 2.7a). The RBD of FIP3 is specific to GTP bound Rab11, with the consequence being that in the absence of active Rab11 there is low FRET, and upon Rab11 activation the FRET signal increases. This was verified using AS-Rab11 mutants, both active Rab11 (AS-Rab11 Q70L) and inactive Rab11 (AS-Rab11 S25N), with increased FRET levels for Q70L, and decreased FRET for S25N (Appendix I).

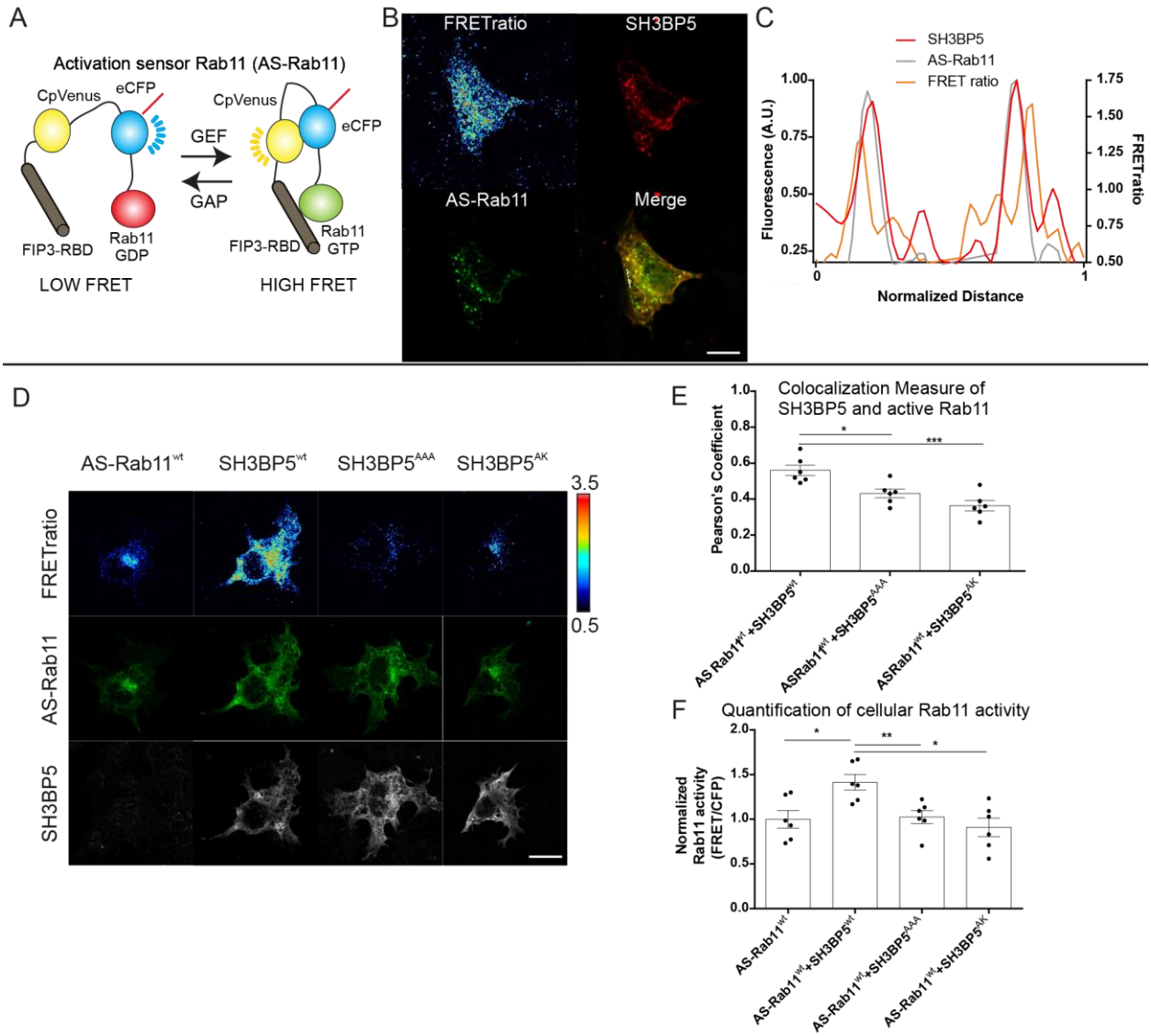

Figure 2.7. Cellular assays of Rab11 activation.

A) Schematic of activation sensor Rab11 (AS-Rab11)(100). Upon activation by GEF proteins, GTP-loaded Rab11 will bind to FIP3 inducing FRET between the two fluorescent proteins. B) Immunofluorescence localization of FLAG-tagged SH3BP5 and the AS-Rab11 sensor, along with the FRET ratio, measuring active Rab11. Scale bar, 10 µm. C) Representative line intensity profile of AS-Rab11, SH3BP5, and the active pool of Rab11 (FRET ratio). D) FRET ratio and localization of AS-Rab11 alone or with SH3BP5wt, as well as the two GEF-deficient mutations (LNQ52AAA and LE250AK). Right side bar represents upper and lower limits of the FRET/CFP ratio. Scale bar, 10 µm. E) Quantification of colocalization of SH3BP5 and active Rab11 (FRET ratio). F) Quantification of Rab11 activity in COS-7 cells transfected with AS-Rab11 alone or in concomitance with SH3BP5wt, SH3BP5AK, or SH3BP5AAA. For all panels, error bars represent SEM (n = 6). Significance determined by one-way ANOVA (*p < 0.05, **p < 0.01, ***p < 0.005)

Immunofluorescence of FLAG tagged SH3BP5 revealed an intracellular membrane distribution (Fig.2.7b-d) similar to the AS-Rab11 sensor (Fig.2.7c). While $SH3BP5^{wt}$ showed an important colocalization with both total Rab11 and active Rab11(Fig.2.7d,e, Appendix I), the two GEF mutants $SH3BP5^{AAA}$ and $SH3BP5^{AK}$ displayed lower colocalization with active Rab11(Fig. 7d,e). Accordingly, transfection of SH3BP5 led to increased Rab11 activation, which was not observed with transfection of the GEF deficient mutants, confirming that these mutations disrupt Rab11 activation by SH3BP5 in living cells and cell lysates (Fig. 2.7f, Appendix I).

2.5 Discussion

Rab11 GTPases are essential mediators of numerous membrane trafficking processes and are especially important in controlling receptor recycling. Most Rab11 dependent processes have been studied through the use of dominant active (Q70L) and dominant inactive (S25N) mutants. These mutations can lead to misleading results, since many Rab GTPases are activated by GEFs through direct interactions with the catalytic Gln residue (103), leading to impaired activation for GTPase deficient mutants. Complicating the ability to fully probe Rab11 and its role in both fundamental biological processes and disease has been the lack of molecular detail for the coordinated action of Rab11 GEFs and GAPs. Multiple Rab11 GAPs have been identified, including the proteins TBC1D11(117), TBC1D15(118), and EVI5(58, 59). Similarly, multiple Rab11 GEFs have been characterized, with the yeast and *Drosophila* TRAPPII complex activating both Rab1 and Rab11(60, 61), and the *Drosophila* DENN family protein Crag being identified as a weak activator of Rab11, with a much higher activity towards Rab10(62). SH3BP5, which is conserved in *C. elegans*, is a potent Rab11 GEF(6), and knockout of the *Drosophila* homolog parcas leads to defects in oogenesis(63). Intriguingly, it has been shown that Rab11 plays a key role in oogenesis, through mediating asymmetric cell division(43), revealing a potential role of SH3BP5 in Rab11 regulation.

The structure of SH3BP5 bound to Rab11 reveals that the extended coiled coil of the GEF domain forms an extended predominantly hydrophobic interface with Rab11. The catalytic efficiency of SH3BP5L (~8.1x10^4 $M^{-1}s^{-1}$) and SH3BP5 (~3.5x10^4 $M^{-1}s^{-1}$) is comparable to previously determined Rab GEFs, including the Mon1-Ccz1 complex (~2.1 × 10^4 M^{-1} s^{-1})(110), DENND1 (~2.9 × 10^4 M^{-1} s^{-1})(109), and the TRAPP complex (~1.6 × 10^4 M^{-1} s^{-1})(112). There was a slight activation of SH3BP5 when Rab11 was presented on a membrane surface, with no strong dependency on surface charge, or phosphoinositide content. Rab11 activation has been found to be associated with different phosphoinositide species, including PI4P during cytokinesis(102), and PI3P in ciliogenesis(101). One of the main ways that Rab proteins are localized is through targeting of GEFs to specific intracellular membranes, and further experiments will be needed to define if SH3BP5 is involved in phosphoinositide dependent activation, potentially through localization to specific phosphoinositide containing organelles by protein binding partners.

Active Rab11 mediates its roles in membrane trafficking through recruiting a number of protein binding partners, including motor protein complexes, and the exocyst complex(1). Rab11 is also unique among Rab GTPases in that it can interact with the protein binding partners PI4KB(54) and Rabin8(57) through a unique interface directly over the nucleotide binding pocket, which allows for the formation of tertiary complexes with Rab11 effectors. PI4KB can bind GDP bound Rab11(105), suggesting there might be a role in GEF presentation. However, the structure of Rab11 bound to SH3BP5 precludes formation of a ternary complex with PI4KB.

The structure of SH3BP5 bound to Rab11 reveals the mechanism for how SH3BP5 binding leads to nucleotide exchange and Rab11 specificity (Fig. 2.8). Switch I residues plays a key role in stabilizing bound nucleotide, with F36 and L38 forming a hydrophobic cap over the guanine ring in both GDP and GTP bound structures(50). In the SH3BP5 bound complex there is a substantial conformational change in switch I of Rab11 compared to nucleotide-bound states, which leads to disruption of switch I nucleotide contacts and allows for release of bound

nucleotide. Specifically, F36 and L38 undergo an extensive rearrangement to interact with SH3BP5, and this disrupts their ability to interact with bound nucleotide. Mutation of either F36 or L38 to alanine surprisingly does not lead to a large increase in the intrinsic exchange rate, as seen for the corresponding F33 in Ypt7 (equivalent to F36 in Rab11)(110), however, mutation of F36 to alanine prevents SH3BP5 mediated nucleotide exchange. The disruption of the interaction of the aromatic residue located in SwI with nucleotide plays a key role in nucleotide exchange in TRAPP(112) and DENND1(109), and this is conserved in SH3BP5. The large conformational change in switch I is characteristic of previously solved Rab-GEF structures(108–112, 114, 116). The SH3BP5 coiled coil that interacts with Rab11 shares the closest structural homology to the coiled coil archaeal chaperone prefoldin(106), and this ability to stabilize partially unfolded proteins reveals a potential evolutionary path to stabilizing the partially unfolded Rab11 nucleotide-free state.

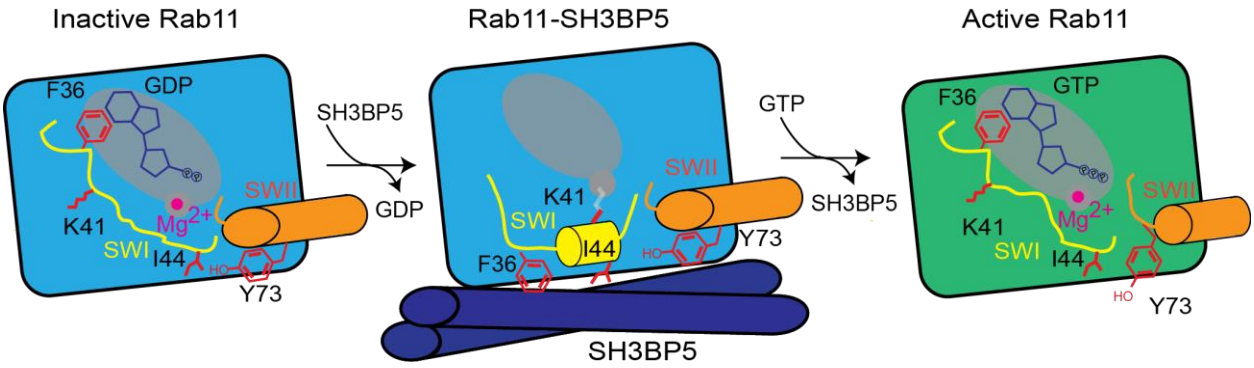

Figure 2.8. Model of Rab11 activation by SH3BP5.

In the GDP-bound state switch I (SWI) directly interacts with bound nucleotide, with F36 having a key role in stabilizing this interaction. Upon SH3BP5 binding, switch I undergoes a large conformational rearrangement, with F36 and I44 forming hydrophobic contacts with SH3BP5, leading to exposure of the nucleotide-binding pocket. F36 and I44 are in a highly constrained orientation and require the interspersing residues to allow for formation of this interface. Similar to the Ypt7 GEF Mon1-ccz1(110) the K41 residue projects into the Mg2+-binding pocket. The lack of clear electron density around K41 is indicated by being colored in gray, to indicate ambiguity in its exact positioning. There are limited conformational changes in switch II upon SH3BP5 binding, with the hydroxyl from Y73 in position to cap the switch I helix. Upon SH3BP5 disengagement, Mg2+ and GTP can enter the nucleotide-binding pocket, with active Rab11 able to bind and recruit downstream effectors

SH3BP5 is highly selective for Rab11, and this is likely driven through a highly constrained conformation of the hydrophobic residues F36 and I44 in switch I. This makes Rab11 extremely sensitive to mutation of switch I residues between F36 and I44, which prevent this constrained F36-I44 orientation. The K41 in switch I projects into the Mg^{2+} binding pocket, similar to seen in the Ypt7-Mon1-Ccz1 complex(110). However, mutation of this residue in Rab11 leads to only a minor decrease in GEF efficiency, with this suggesting it does not play as critical a role as for Ypt7-Mon1-Ccz1. Rab11A and Rab11B are mutated in developmental disorders(71, 72), leading to encephalopathies and co-occurrence of seizures and intellectual disability. The V22M, S154L, and K24R all destabilized Rab11, either through a complete (V22M, S154L) or partial (K24R) disruption of nucleotide binding. K13N almost completely prevented SH3BP5 mediated nucleotide exchange, with R82C and A68T both leading to slightly decreased rates. This reveals that clinically relevant Rab11 mutations disrupt SH3BP5 mediated exchange.

The use of a genetically encoded Rab11 FRET sensor(100) revealed that transfection of SH3BP5 leads to a significant increase in Rab11 activation, with no increase seen with SH3BP5 GEF deficient mutations. Fluorescently labelled SH3BP5 and AS-Rab11 co-localize, with SH3BP5 primarily localizing to intracellular membranes. Among the key unanswered questions are the mechanisms by which SH3BP5 is localized to specific intracellular membranes, and whether SH3BP5 is required for activation of a specific Rab11 pool. As SH3BP5 plays key roles in regulation of the signaling kinases BTK and JNK through a non GEF mediated process, the molecular details presented here provide an approach to define the roles of SH3BP5 in Rab11 dependent processes. Misregulation of Rab11 isoforms is a key driver in oncogenesis (Rab25) and developmental diseases (Rab11A, Rab11B) and our work reveals insight into how Rab11 can be activated. Moreover, our results not only reveal the specifics of Rab11-GEF activation, but also provide important insight into the mechanisms by which Rab GEFs achieve specificity.

Chapter 3: Determination of the GEF specificity of the human TRAPPII Complex and its role in health and disease

Meredith L Jenkins[1], Kaelin D Fleming*[1], Emily M Martin*[1], Jordan T.B Stariha[1], John E Burke[1]

1. Department of Biochemistry and Microbiology, University of Victoria, Victoria, BC, Canada

* These authors contributed equally

Contributions: JEB and **MLJ** designed all biophysical/biochemical experiments. **MLJ** cloned the TRAPPII complex. **MLJ** carried out protein expression/purification, with assistance from EMM and JTBS. **MLJ** carried out all biochemical studies, with assistance from EMM. **MLJ** and KDF carried out HDX-MS experiments. **MLJ** wrote the manuscript. This manuscript is in preparation for submission.

* At the time of this study, I was training EMM in her undergraduate honours degree, and thus she assisted with some of the experiments.

3.1 Abstract

The TRAPPII complex is a guanine nucleotide exchange factor (GEF) for both Rab1 and Rab11, however the basis for specificity towards these GTPases in metazoans has yet to be determined. Here we present detailed characterisation of Rab-GEF specificity of the human TRAPPII complex and show that TRAPPII has novel GEF activity against Rab43. We use hydrogen deuterium exchange mass spectrometry (HDX-MS) to map the binding site of each of these GTPases with TRAPPII and show that they all interact at the same interface. Furthermore, using guanine nucleotide exchange assays, we reveal a reduced dependence on membrane for activation of the human TRAPPII complex compared to the yeast TRAPPII counterpart, and assays conducted on clinical mutants of both Rab11 and TRAPPII reveal insight into their putative disease mechanisms. Overall, our results show that Rab43 is a novel binding partner of TRAPPII and reveal the molecular interface of TRAPPII-Rab binding.

3.2 Introduction

The transport protein particle (TRAPP) complex was first discovered in 1998 in yeast cells and has been shown to play critical roles in ER to Golgi membrane trafficking(119). Since its discovery, it has become one of the best characterized multi subunit tethering complexes, and it has been shown that the complex not only works as a tether, but also as a guanine nucleotide exchange factor (GEF) for the Rab GTPase Ypt1 (Yeast Rab1), otherwise known as Rab1(120, 121). Importantly, an emerging set of disorders have recently been linked to mutations in TRAPP genes that have since been named TRAPPopathies(122). Disorders associated with these mutations include Spondyloepiphyseal dysplasia tarda (SEDT), neurodevelopmental delay(123, 124), microcephaly(125–127), epilepsy(124, 128), and severe intellectual disability(129, 130).

The TRAPP complex is predicted to exist in a variety of forms, including TRAPPI, TRAPPII, TRAPPIII, and more recently TRAPPIV(131). The yeast TRAPPI complex consists of seven different proteins (Bet5p, Bet3p, Trs20p, Trs23p, Trs31p, Trs33p, and Trs85p), which have all been conserved throughout evolution. For convenience, the rest of this paper will refer to each of the yeast subunits using their mammalian names (see Appendix O for details). Four of these subunits form the conserved core (TRAPPC1, TRAPPC3, TRAPPC4 and TRAPPC5), and are sufficient for GEF activity on Rab1(132). The structure of the yeast TRAPPI core bound to Rab1 has been solved by X-Ray crystallography, and this structure has provided insight into the overall assembly of the core and how the catalytic GEF site interacts with Rab1 (112). Cryo-EM has since been used to interrogate the structure of yeast TRAPPII, and has shown that the complex forms a large three-layered diamond shape (133). This research by Yip *et al*. showed that the complex has clear two-fold symmetry, indicating that it forms a dimer. Their studies also used antibody-labeling experiments to demonstrate that TRAPPC10 possibly directly interacts with TRAPPC2, and TRAPPC9 interacts with TRAPPC6 and TRAPPC3. However, other groups have proposed that TRAPPC2 acts as an adaptor and binds TRAPPC9, which in turn binds TRAPPC10(134). No

high-resolution structural information yet exists for the TRAPPII specific subunits TRAPPC9 and TRAPPC10, and thus is still unclear as to where these proteins interact with the rest of the TRAPP complex.

The TRAPPII complex has been proposed to act as a GEF for Rab11, however this has remained a controversial subject for several years(133, 135). GST pulldowns using the yeast TRAPPII with Rab1 and Rab11 showed that TRAPPII only bound Rab1(133), while other experiments showed clear GEF activity against Rab11(135). Only recently has the TRAPPII complex been shown to truly be a potent activator of Rab11 in both drosophila and yeast (60, 61). In yeast, TRAPPII activates Rab GTPases in a membrane dependent manner(61). To interrogate the mechanisms of specificity and membrane dependence, Thomas *et al*. developed a new assay for interrogating GEF-GTPase interactions in yeast, and found that the Rab hypervariable domain is responsible for conferring substrate specificity of the TRAPPII and TRAPPIII complexes(136). The hypervariable tail is longer in Rab11 than Rab1, and Thomas *et al.* proposed that the TRAPPII specific subunits TRAPPC9 and TRAPPC10 keep the TRAPPII core further away from the membrane surface than TRAPPIII, altering the accessibility to the active GEF core(136). Intriguingly, there seems to be less membrane dependence for GEF activity in metazoan TRAPPII than in yeast, so it is unclear whether a system like this is in place in the higher eukaryotes(60). Furthermore, the vertebrate TRAPPII specific subunit TRAPPC10 has been postulated to contain a longin domain, which may act as a GEF for Rab11(137). It is currently unclear if this domain is capable of binding small GTPases, or if it contains any catalytic activity.

So far there have been no detailed investigations on the Rab GTPase specificity of the TRAPPII complex, or on the mechanisms through which specificity is achieved in metazoans. To decipher the specificity of the human TRAPPII complex, we sampled 14 different human Rab GTPases that were closely related phylogenetically to (or localized to the same subcellular compartments of) Rab1 and Rab11. Detailed biochemical studies reveal that TRAPPII has activity

against Rab1 and Rab11, as well as Rab43, with no activity towards other evolutionarily similar Rab GTPases. Using hydrogen deuterium exchange mass spectrometry, we also show that each of these GTPases binds at the same site on TRAPPII. A subset of clinical Rab11 mutations observed in developmental disorders were found to disrupt TRAPPII mediated nucleotide exchange, providing possible mechanisms of disease. Further, a subset of clinical TRAPP mutations were found to disrupt complex formation or alter GEF activity, providing insight into their mechanisms of disease.

3.3 Materials and Methods

3.3.1 Plasmids and antibodies

The full-length human TRAPP genes, TRAPPC1(HsCD00337916), TRAPPC2L (HsCD00340414), TRAPPC10 (HsCD00341380) were purchased from the Dana Farber Plasmid Repository. The full-length human TRAPP genes, TRAPPC2 (HsCD00040385), TRAPPC6a (HsCD00674667), TRAPPC4 (HsCD00396892), TRAPPC5 (HsCD00398807) TRAPPC6b (HsCD00352944) and TRAPPC9(HsCD00820727) were purchased from the DNASU. The full length human TRAPPC3 gene (Plasmid #34711) was purchased from the AddGene. Genes were subcloned into pLIB vectors, and in the case of TRAPPC3 a TEV cleavable c-term 2x strep tag was added while a c-term 6x his tag was added to the c-term of TRAPPC10. Genes were subsequently amplified following the biGBac protocol to generate 3 plasmids, each containing 4-5 TRAPP genes. (138). The protocol for gene assembly is shown in figure Appendix Q. The full length human Rab genes, Rab1(49467), Rab3a(49542), Rab6a(49469), Rab18(49550) and Rab33(49551) were purchased from AddGene. Rab35(HsCD00327461), Rab39(00335627) and Rab43(HsCD00334332) were purchased from Dana Farber Plasmid Repository. Genes were subcloned into pOPTGcH vectors for expression with an n-terminal cleavable GST tag and a non-cleavable c-terminal his tag.

3.3.2 Bioinformatics

Human and yeast sequences were aligned using Clustal Omega Multiple Sequence Alignment, and the aligned sequences were subsequently analyzed by ESPript 3.0 to visualize conserved regions.

3.3.3 Protein expression

All TRAPPII complexes were similarly expressed as previously described (139). To express TRAPPII complexes, an optimized ratio of baculovirus was used to co-infect *Spodoptera frugiperda* (Sf9) cells between 1-2×10^6 cells/mL. Co-infections were harvested at 66-hours and washed with ice-cold PBS before snap-freezing in liquid nitrogen. Rab constructs were all expressed in BL21 C41 *E.coli,* induced with 0.5mM IPTG and grown at 37°C for 4hrs. Pellets were washed with ice-cold phosphate-buffered saline (PBS), flash frozen in liquid nitrogen, and stored at -80°C until use.

3.3.4 Protein purification

TRAPPII cell pellets were lysed by sonication for 1.5 minutes in lysis buffer (20mM Tris pH 8.0, 100mM NaCl, 5% (v/v) glycerol, 2mM ß–mercaptoethanol (BME), and protease inhibitors (Millipore Protease Inhibitor Cocktail Set III, Animal-Free)). Triton X-100 was added to 0.1% v/v, and the solution was centrifuged for 45 minutes at 20,000 x g at 1°C. The supernatant was then loaded onto a 5 mL HisTrap™ FF column (GE Healthcare) that had been equilibrated in NiNTA A buffer (20 mM Tris pH8.0, 100 mM NaCl, 10 mM imidazole pH 8.0, 5% (v/v) glycerol, 2 mM bME). The column was washed with 20 mL of NiNTA buffer, 20 mL of 6% NiNTA B buffer (20 mM Tris pH 8.0, 100 mM NaCl, 200 mM imidazole pH 8.0, 5% (v/v) glycerol, 2 mM bME) before being eluted with 100% NiNTA B. The eluate was subsequently loaded on a 5ml Strep™ column and washed with 10ml SEC buffer (20mM HEPES pH 7.5, 150mM NaCl, 0.5mM TCEP). The Strep-tag was cleaved by adding SEC buffer containing 10mM BME and TEV protease to the column and incubating overnight at 4°C. Protein was pooled and concentrated using Amicon 50K

concentrator and size exclusion chromatography (SEC) was performed using a Superdex 200 increase 10/300 column equilibrated in SEC Buffer. Fractions containing protein of interest were pooled, concentrated, flash frozen in liquid nitrogen and stored at -80°C. For purification of Rabs, see chapter 2, method 2.2.4 protein purification.

3.3.5 Lipid vesicle preparation

Nickelated lipid vesicles were made with [20% phosphatidylserine (bovine brain PS, Sigma), 10% L-α-phosphatidylinositol-4-phosphate(PI4P, Avanti) 67.5% phosphatidylcholine (egg yolk PC Sigma), and 2.5% DGS-NTA(Ni) (18:1 DGSNTA(Ni), Avanti)]. Vesicles were prepared by combining liquid chloroform stocks together at appropriate concentrations and evaporating away the chloroform with nitrogen gas. The resulting lipid film layer was desiccated for 20 min before being resuspended in lipid buffer (20mM HEPES (pH 7.5) and 100mM KCl) to a concentration of 1mg/ml. The lipid solution was vortexed for 5 min, bath sonicated for 10 min, and flash frozen in liquid nitrogen. Vesicles were then subjected to three freeze thaw cycles using a warm water bath. Vesicles were extruded 11 times through a 100nM or 400- nm NanoSizer Liposome Extruder (T&T Scientific) and stored at -80°C.

3.3.6 In-vitro GEF assay

C-terminally His-tagged Rabs were purified and nucleotide loaded as described in chapter 2. Reactions were conducted in 10µl volumes with a final concentration of 4µM Mant-GDP loaded Rab, 100uM GTPγS and TRAPP (30nM-150nM). Rab and membrane (0.2mg/ml) was aliquoted into a 384-well, black, low-volume plate (Corning 3676). To start the reaction, TRAPPII and GTPγS were added simultaneously to the wells and a SpectraMax® M5 Multi-Mode Microplate Reader was used to measure the fluorescent signal for 1hr (Excitation λ = 366nm; Emission λ = 443nm). Data was analyzed using GraphPad Prism 7 Software, and k_{cat}/K_m analysis was carried out according to the protocol of(91).

3.3.7 Mapping of the TRAPPII-Rab Binding Interfaces using HDX-MS

HDX reactions were conducted in 20µl reaction volumes with a final concentration of 1uM Rab1, Rab11, or Rab43 and 350nM TRAPPII per sample. Exchange was carried out in triplicate for four time points (3s, 30s, 300s and 3000s at room temperature). Prior to the addition of D_2O, proteins were incubated on ice in the presence of 20mM EDTA for 30 minutes to facilitate release of nucleotide. Hydrogen deuterium exchange was initiated by the addition of 17µl of D_2O buffer solution (10mM HEPES pH 7.5, 50mM NaCl, 97% D_2O) to 3µl of the protein solutions, to give a final concentration of 85% D_2O. Exchange was terminated by the addition of acidic quench buffer at a final concentration 0.6M guanidine-HCl and 0.9% formic acid. Samples were immediately frozen in liquid nitrogen at -80°C.

3.3.8 HDX-MS data Analysis

Protein samples were rapidly thawed and injected onto an ultra-performance liquid chromatography (UPLC) system kept in a cold box at 2ºC. The protein was run over two immobilized pepsin columns (Applied Biosystems; Porosyme 2-3131-00) and the peptides were collected onto a VanGuard Precolumn trap (Waters). The trap was eluted in line with an ACQUITY 1.7um particle, 100 x 1mm2 C18 UPLC column (Waters), using a gradient of 5%-36% B (Buffer A 0.1% formic acid, Buffer B 100% acetonitrile) over 16 min. Mass spectrometry experiments were performed on an Impact QTOF (Bruker), and peptide identification was done by running tandem mass spectrometry (MS/MS) experiments run in data-dependent acquisition mode. The resulting MS/MS datasets were analyzed using PEAKS7 (PEAKS), and a false discovery rate was set at 1% using a database of purified proteins and known contaminants. HDExaminer Software (Sierra Analytics) was used to automatically calculate the level of deuterium incorporation into each peptide. All peptides were manually inspected for correct charge state and presence of overlapping peptides. Deuteration levels were calculated using the centroid of the experimental isotope clusters. Differences in exchange were in a peptide were considered significant if they

met all three of the following criteria: >4% change in exchange, >0.4 Da difference in exchange, and a p value <0.01 using a two tailed student t-test. Samples were only compared within a single experiment and were never compared to experiments completed at a different time with a different final D_2O level.

3.4 Results

3.4.1. Recombinant Purification of the TRAPP complex

To interrogate the specificity of the TRAPPII complex, we established a protocol to recombinantly express the human TRAPPII complex using the BigBac system(138) in Sf9 cells. Each of the nine genes were purchased, PCR amplified, and inserted into pLIB vectors. These genes were amplified using BigBac specific primers each with unique flanking sequences to allow for insertion of up to 5 genes into a single vector using Gibson Assembly, as described in Appendix Q and Figure 3.1. These vectors were subsequently used to express all nine TRAPPII genes at one time in Sf9 cells. The complex was next purified using tandem affinity purification, with a cleavable strep tag on the TRAPPC3 protein and a 6x his tag on the TRAPPC10 protein, similar to the purification strategy used by Riedel *et al.* (60). We found that the entire 9 subunit complex could be purified using this approach, and validated the presence of each gene using tandem MS. The complex was then purified further using size exclusion chromatography (SEC), resulting in a single peak, indicating it forms a stable complex (Fig 3.1B). The entire human TRAPPII complex has never been purified recombinantly, and these findings indicate that humans do not have more subunits than drosophila that are required for assembly. A summary of the purification strategy is depicted on the SDS page gel in figure 3.1C.

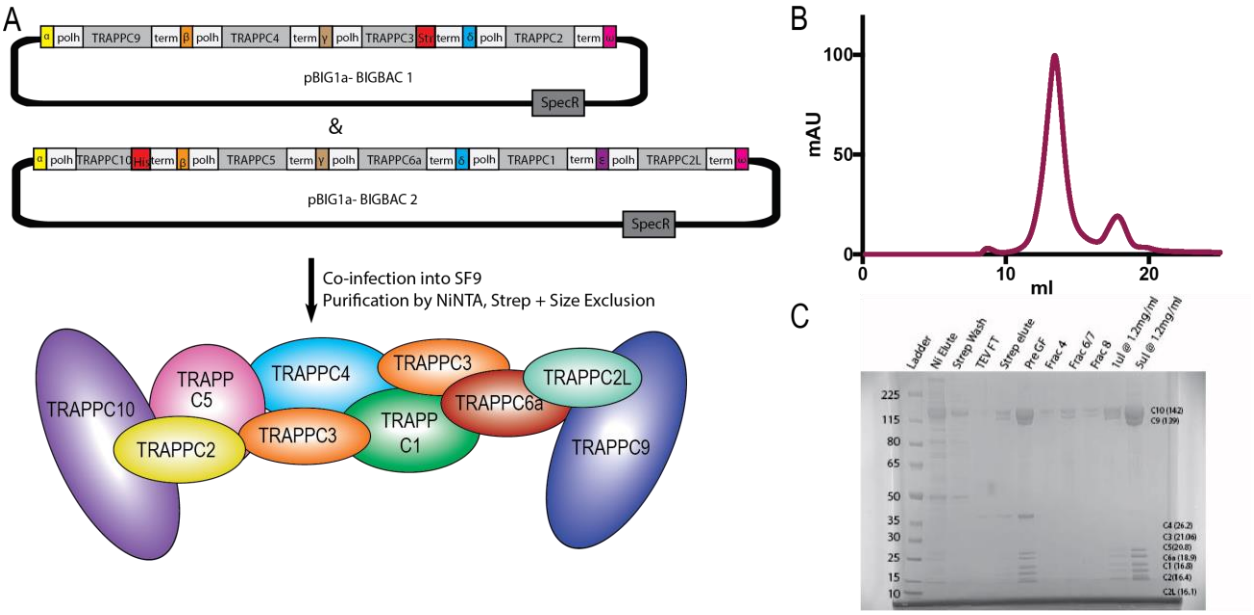

Figure 3.1. Purification of human TRAPPII complex .

(A) TRAPPII was expressed in Sf9 cells using a BigBac system, where all 9 genes were placed in 2 vectors. (B) All TRAPPII subunits purified in a single size exclusion chromatography peak. (C) SDS-PAGE gel showing the purification of TRAPPII. All 9 subunits were detected on the gel.

3.4.2 Determination of TRAPPII Rab Specificity

TRAPPII has been studied for years, yet a comprehensive study of its specificity has yet to have been completed. To examine the specificity of GEF activity, GEF assays were carried out on 14 of the most evolutionarily conserved Rabs related to Rab1 and Rab11, as well as Rabs localized in the same compartments as TRAPPII (Appendix P). Rates of exchange were determined by loading each GTPase with the fluorescent GDP analog 3-(N-methyl-anthraniloyl)-2-deoxy-GDP (Mant-GDP) and measuring the decrease in fluorescence as a function of TRAPPII concentration. Each small GTPase was generated with a C-terminal His-tag to allow for localization on NiNTA containing membranes. A schematic depicting the assay setup is shown In Figure 3.2a. GEF activity was observed for Rab1a and Rab11a as previously described, and interestingly we found novel GEF activity against Rab43, a relatively poorly characterized Rab GTPase (Fig 3.2b). Rab43 has been shown to be important for golgi maintenance, and plays a role in specifically modulating ER to Golgi transport of GPCRs(140–142). Interestingly, Haas *et*

al. suggest that Rab1 and Rab43 are solely required for the maintenance of the Golgi, while other Rabs are functionally redundant(142). The fact that TRAPPII can activate both of these Rab GTPases gives insight into the clear importance of the complex for golgi maintenance.

We detected no GEF activity against 13 other closely evolutionarily related small GTPases, including Rab25, commonly known as Rab11c. Rab25 and Rab11a are highly evolutionarily conserved, yet intriguingly we detected no GEF activity against this GTPase. This indicates a unique form of specificity detection, as we recently showed that the GEF SH3BP5 does not discriminate between Rab11a and Rab25(143). We also detected no GEF activity against Rab18, even though in recent years it has been proposed that the TRAPPII complex acts as a GEF against it in mammalian cells(144). However, it does not appear as though the TRAPPII complex is active on Rab18, as recently other groups have shown that recombinant purified TRAPPII complex does not have activity on this small GTPase (60).

Interestingly, we showed that Rab1 and Rab11 GEF rates are enhanced by the presence of membrane, while the rate of Rab43 exchange is not altered (Fig 3.2c). We detected an approximately 4-fold enhancement in GEF activity in the presence of lipid vesicles, in agreement with data generated from TRAPP in drosophila(60). As an important control, we engineered a TEV protease cleavage site to remove the c-terminal his tag of TRAPPC10 to ensure that it was not altering membrane enhancement, and we found that this tag did not alter GEF rate of the TRAPP complex in the presence of membrane (Appendix R).

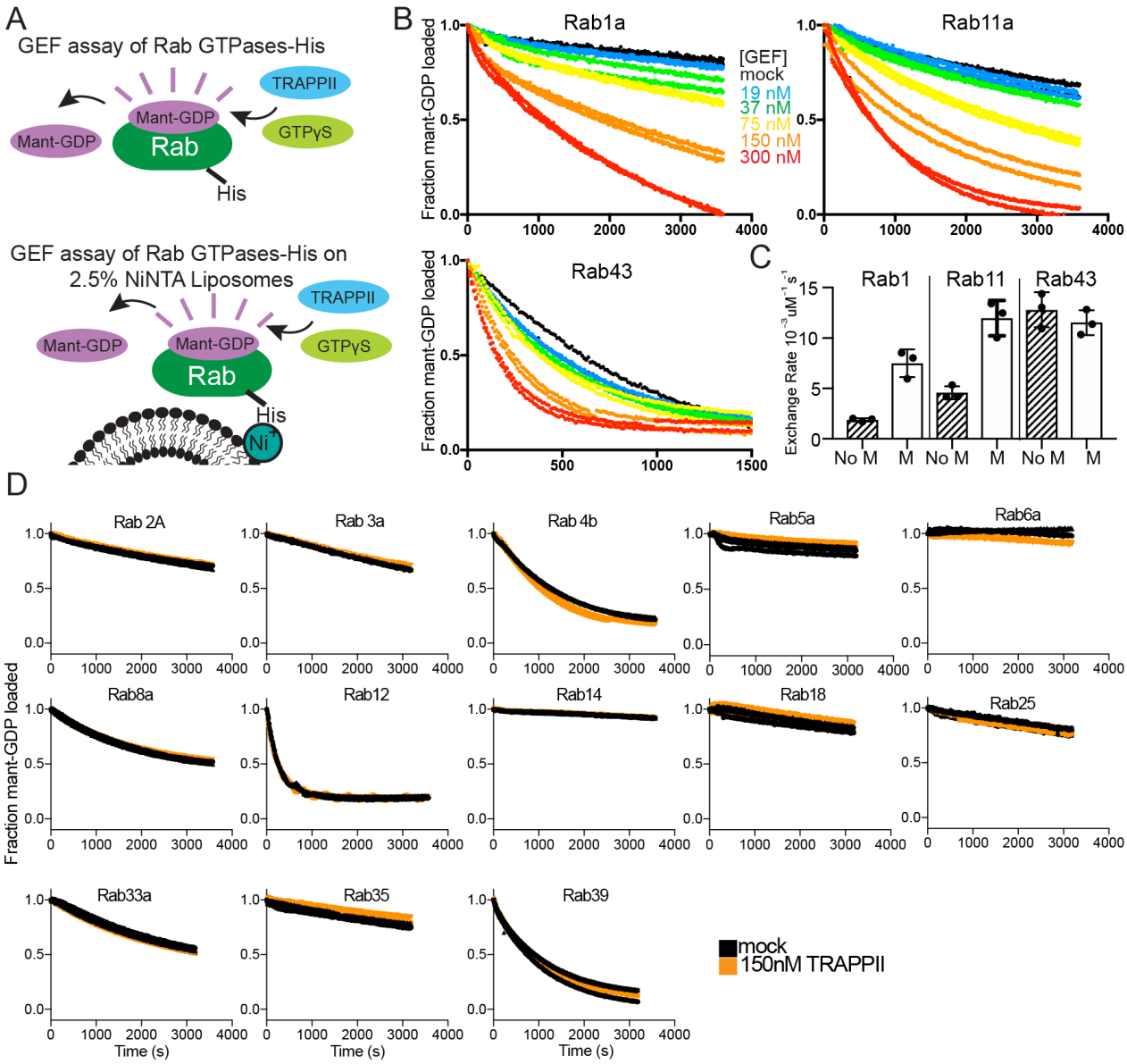

Figure 3.2 *In vitro* GEF assays reveal that TRAPPII is a potent GEF for Rab1, Rab11 and Rab43.

(A) Schematic of GEF activation assays using fluorescent analog Mant-GDP in the presence and absence of NiNTA-containing lipid vesicles. (B) *In vitro* GEF assay of TRAPPII on Rab1A, Rab11A and Rab43. Nucleotide exchange was monitored by measuring the fluorescent signal during the TRAPPII (19 nM-300 nM) catalyzed release of Mant-GDP from 4 μM of Rab-His6 in the presence of 100 μM GTPγS. Each concentration was conducted in duplicate. (C) Bar graph representing the difference in GEF activity in the presence and absence of 400 nm extruded liposomes at 0.2 mg/ml (67.5% PC, 20% PS, 10% PI(4)P, 2.5% DGS NTA). Nucleotide exchange was monitored by measuring the fluorescent signal during the TRAPPII (150 nM)-catalyzed release of Mant-GDP from 4 μM of Rab-His6 in the presence of 100 μM GTPγS. (D) *In vitro* GEF assays of TRAPPII against a panel of evolutionarily related Rab GTPases loaded with Mant-GDP at a final concentration of 150 nM TRAPPII and 4 μM Rab GTPase.

3.4.3 Hydrogen deuterium exchange mass spectrometry (HDX-MS) of TRAPPII and different Rab GTPases reveal the binding interface of TRAPPII and Rab11

The structure of the yeast TRAPPI core bound to Rab1 has been solved by x-ray crystallography and it has shown that TRAPPC4 makes up the primary binding interface(112). Since then, it has been proposed that the longin domain of TRAPPC10 could be the GEF for Rab11, to explain the differences in specificity of TRAPPII and TRAPPIII(137). To understand the molecular basis of how TRAPPII mediates Rab1, Rab11, and Rab43 nucleotide exchange, we used hydrogen deuterium exchange mass spectrometry (HDX-MS). We found that all three of these GTPases bound primarily to the TRAPPC4 component, as we saw decreases in exchange in β1, the loop between β4 and β5, and the loop between α2 and α3. It was previously known that TRAPPC4 made up the major binding interface of Rab1; however, this data clarifies which portions of TRAPPC4 are responsible for binding Rab1. It was previously unknown if Rab11 bound to the same site as Rab1, and here we show that they in fact do interact at a conserved binding interface. Interestingly, we found that Rab43 formed the tightest interaction, while also stabilizing regions of TRAPPC2L and TRAPPC5 (Fig 3.3).

The TRAPPC4 subunit has an additional PDZ-like (PDZL) domain which evolved in metazoans. PDZ domains typically act as signaling motifs that recognize short amino acid sequences, and are involved in the regulation of many biological processes(145). It could be thought that the addition of a new domain in the protein responsible for Rab binding could alter the Rab-TRAPPII binding interface, however our HDX data shows no evidence that the binding site of TRAPPII is significantly altered compared to the yeast TRAPPII complex. The PDZL domain of metazoans can be seen in Figure 3.4d.

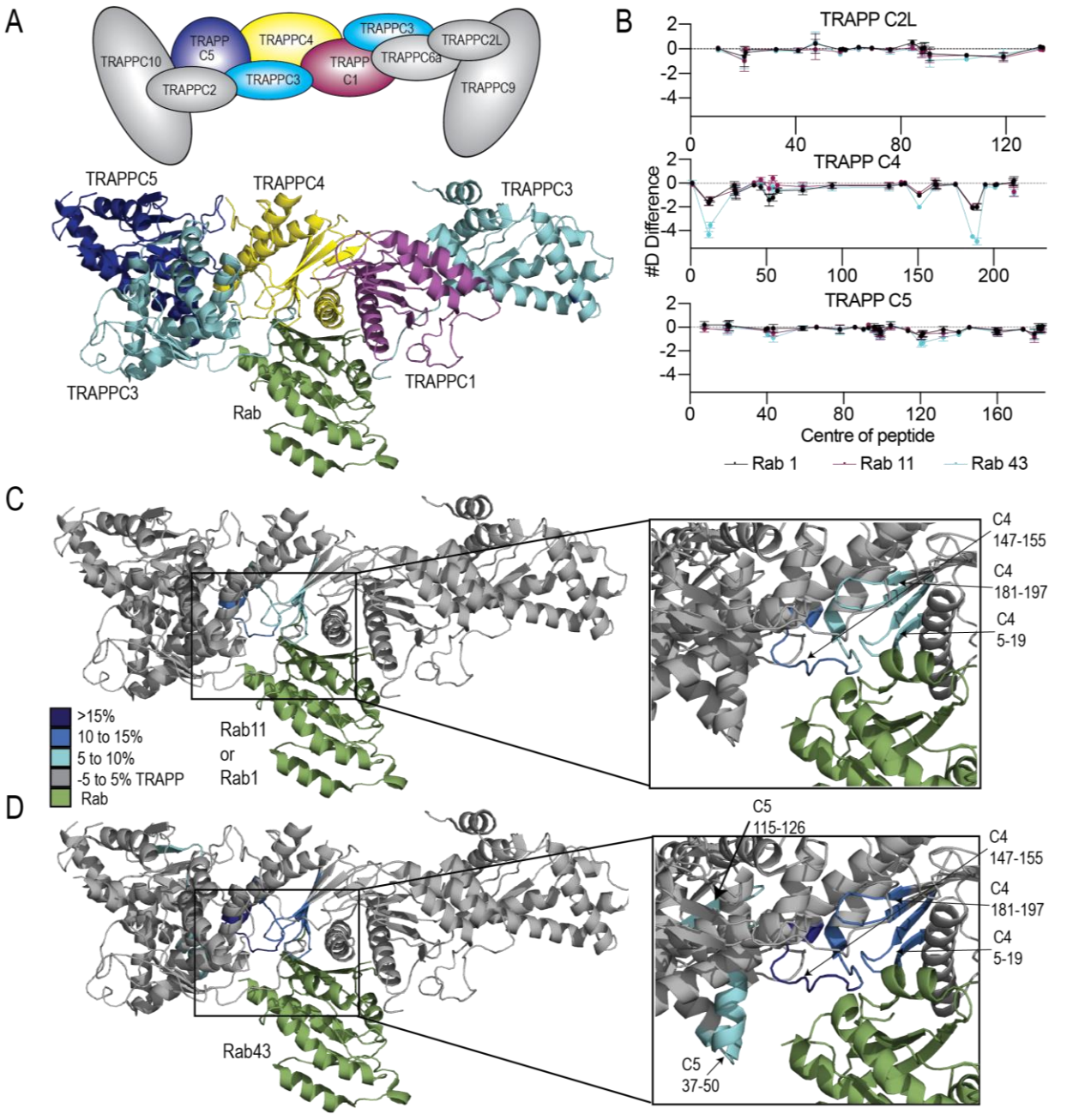

Figure 3.3 HDX-MS reveals the binding interface of Rab11, Rab1 and Rab43 with TRAPPII.

(A) Cartoon schematic depicting TRAPPII subunits. Colored subunits match the structure of TRAPPI-Ypt1 (3CUE), and show the general orientation that the data is presented in. (B) The number of deuteron difference for peptides analyzed over the entire deuterium exchange time course for Rab1, Rab11 or Rab43 in the presence of TRAPPII. Only subunits with significant differences are shown. Every point represents the central residue of an individual peptide. (C) Significant differences observed when Rab11 or Rab1 are incubated with TRAPPII are mapped on the structure of TRAPPI-Ypt1 (3CUE). Changes are mapped according to the legend. (D) Significant differences observed when Rab43 is incubated with TRAPPII are mapped on the structure of TRAPPI-Ypt1 (3CUE). Appendix S shows the difference maps of all the subunits, and Appendix T-W shows all peptides analyzed in the experiment, while Appendix X shows the alignment of human TRAPPC3 and TRAPPC5 with their yeast counterparts used to map on the structure.

We did not see any difference in exchange in TRAPPC10, which has the putative longin domain that was thought to act as a GEF for Rab11. It is intriguing that all of the Rabs bind at the same site, although this leaves ambiguity as to why the TRAPPII complex, but not the TRAPPIII complex, can act as a GEF for Rab11. Thomas *et al.* have recently proposed that the hypervariable tail(HVT) is responsible for Rab specificity through a steric gating mechanism in yeast (136). It is possible that specificity is also determined through the lengths of these HVTs in humans; however, we do measure activity of both Rab11 and Rab1 on a membrane surface (Fig 3.2).

HDX measurements on Rab11 in the presence and absence of TRAPPII showed an increase in exchange in the nucleotide binding pocket, and a decrease in exchange in switch I (data not shown). This type of exchange is expected for the loss of nucleotide, and mimics the exchange profile seen with the GEF SH3BP5(143). Overall our HDX-MS results reveal that the binding interface of Rab GTPases is conserved, and that specificity must be achieved by some other mechanism. The longin domain of TRAPPC10 shows no difference in exchange, and although this cannot completely rule out the site acting as a GEF, it does seem unlikely to interact with Rab1, Rab11 or Rab43. It is possible that TRAPPII is brought to different cellular locations where Rab1, Rab11 or Rab43 are already localized in order to ensure that each of these GTPases are only activated in certain cellular compartments.

3.4.4 Function of clinical mutations of TRAPPII and Rab11

Over the last few decades, mutations of TRAPP complex genes have been identified in patients with varying diseases and disorders. These mutations have since been classified as “trappopathies”, and include single point mutations, deletions, and insertions, found in several different components including TrappC2, TrappC2L, TrappC6a and TrappC9. Many of these trappopathies have no biochemical data, so we sought to determine if these mutations affect the GEF activity of TRAPPII against Rab11 *in vitro*. The subset of mutations investigated are depicted

in Figure 3.4a. TRAPPII clinical mutants were expressed in Sf9 cells, and the resulting complexes were subsequently purified, and point mutations were validated using tandem MS. We found that 6 of the 7 mutations still allowed for purification of all 9 TRAPPII subunits, while the mutation of TRAPPC2 D47Y resulted in poor purification. From the structure of TRAPPC2-TRAPPC5-TRAPPC3, it could be proposed that this mutation leads to a steric clash with residues of TRAPPC10 (Fig 3.4c). Because the TRAPPC10 subunit has the 6x his-tag, and is used for purification of the entire complex, reduction in this binding could result in poor purification. It has been shown that the TRAPPII specific subunits TRAPPC10 and TRAPPC9 are critical for Rab11 GEF activity, so this mutation would very likely alter GEF activation of Rab11 in living cells.

GEF assays were carried out on all of the TRAPPII mutants that could be purified. We found that the majority of these mutants did not alter the GEF rate of TRAPPII against Rab11, however, we saw an ~50% decrease in GEF activation by TRAPPC2 H80R, as shown in Figure 3.4b. This mutation is at the interface of TRAPPC2 and TRAPPC5 and could very feasibly alter the overall dynamics of the complex (Fig3.4c). This mutation was first identified by Lin *et al.* in 2008 as a novel missense mutation in a four-generation Chinese spondyloepiphyseal dysplasia tarda (SEDT) pedigree(146), and the decrease in GEF rate we show may account for some of the clinical phenotypes seen in affected patients. Clinical mutations in the TRAPPC9 subunit also resulted in small but significant decreases in GEF exchange rate, however without structural information on the complex it is unclear how they may alter the rate of exchange.

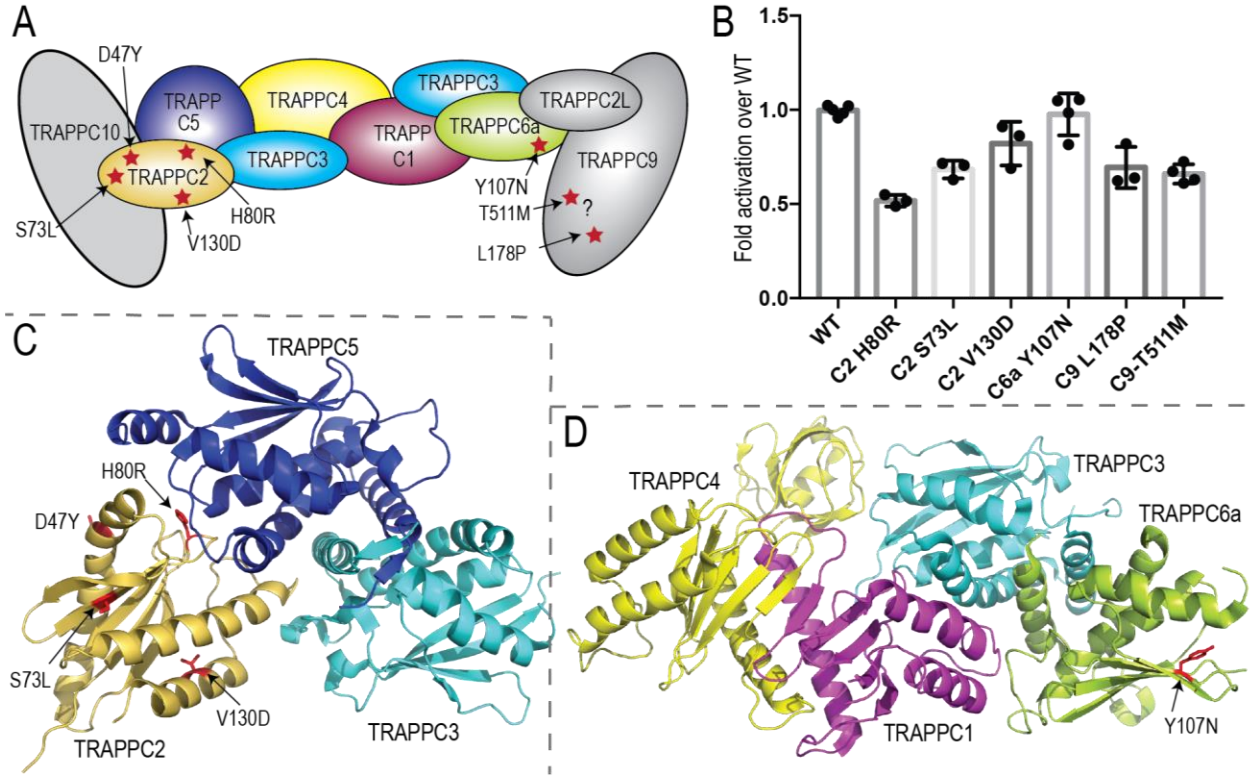

Figure 3.4. TRAPPII clinical mutants alter GEF exchange on Rab11.

(A) Cartoon schematic depicting the TRAPPII complex with clinical mutations noted as stars. Subunits that are colored have structural data accessible in the PDB. (B) Bar graph depicting the difference in GEF exchange of TRAPPII mutants normalized to wild type. (C) Point mutations are mapped on the structure of the *Danio rerio* and *Mus musculus* TRAPPC2-TRAPPC5-TRAPPC3 (2J3W) (132). (D) Point mutations are mapped on the structure of the Mus musculus/ Homo sapiens TRAPPC4-TRAPPC1-TRAPPC3-TRAPPC6 complex (2J3T)(132).

Individual point mutations in Rab11A (K13N, K24R, R82C, S154L) and Rab11B (V22M, A68T) are found in developmental disorders that lead to intellectual disability(71, 72). As we recently showed with the GEF SH3BP5, the A68T mutant only showed a modest effect in decreasing TRAPPII mediated GEF activity(143). The K13N and R82C were located directly at the Rab11-SH3BP5 interface, and with the lack of a structure of TRAPPII-Rab11 we did not know if they would also be at the binding interface. We show that these mutations inhibit TRAPPII mediated GEF activity to a similar level as SH3BP5, with K13N completely abolishing GEF activation, as shown in Figure 3.5.

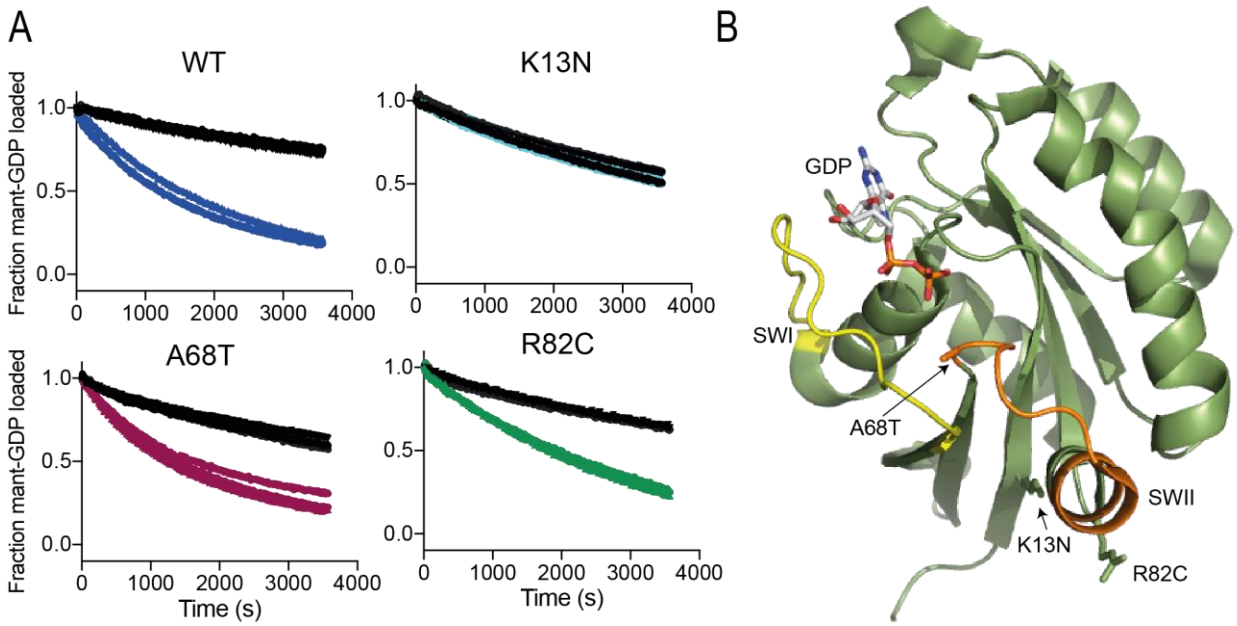

Figure 3.5. Rab11 clinical mutants alter GEF dynamics.
(A) *In vitro* GEF assay of TRAPPII on Rab11A WT, K13N, A68T or R82C. Nucleotide exchange was monitored by measuring the fluorescent signal during the TRAPPII (150 nM) catalyzed release of Mant-GDP from 4 μM of Rab11a-His6 in the presence of 100 μM GTPγS.(B) Point mutations found in developmental disorders mapped on the structure of Rab11 bound to GDP (1OIV).

3.5 Discussion

The TRAPP complex has become one of the best characterized multi subunit tethering complexes, yet its role as a GEF has been a controversial topic for many years. It is becoming more accepted that TRAPPII does have GEF activity against both Rab1 and Rab11, at least *in vitro*. The complex has generally been studied in yeast, and these studies have paved the way to understanding how the complex forms and interacts with Rab1. Despite this, it is still unclear where or how Rab11, a critical GTPase involved in mediating numerous membrane trafficking processes, interacts with TRAPPII. Furthermore, there have not yet been any detailed investigations on the Rab GTPase specificity of the TRAPPII complex.

Here we show that human TRAPPII is catalytically active against both Rab1 and Rab11, and we discover novel GEF activity against the small GTPase Rab43. Rab43 is a relatively poorly characterized GTPase that is involved in Golgi maintenance and ER-Golgi transport(140–142). It

is intriguing that TRAPPII is capable of regulating this trans Golgi localized Rab, and it opens many questions into what could drive the specificity of the complex during membrane trafficking processes. Generally, it is thought that Rab1 regulates the cis-golgi, while Rab43 regulates the trans-golgi(142). It could be possible that other membrane localized proteins are capable of recruiting the TRAPPII complex to each of these Rabs, although more research is required to answer these questions. Intriguingly, Rab43 has also recently been discovered to interact with Rab11a S25N in a screen capable of identifying effectors and regulators of small GTPases named MitoID, along with TRAPPII genes TRAPPC9 and TRAPPC10(147). Rabs have often been found to interact with GEFs of other Rabs as a form of recruitment and activation, often referred to as a Rab cascade. It could be possible that Rab43 is capable of recruiting the TRAPPII complex to Rab11, however it is unclear what the significance of this finding is at this time.

The TRAPPII complex has been studied for years, yet no comprehensive studies on its GEF specificity have yet to be conducted. We show that TRAPPII does have some selectivity, as it has no GEF activity against 13 closely evolutionarily related small GTPases, including Rab25, commonly known as Rab11c. Rab25 and Rab11a are highly evolutionarily conserved, yet intriguingly we detected no GEF activity against this GTPase. This indicates a unique form of specificity detection, as we recently showed that the GEF SH3BP5 does not discriminate between Rab11a and Rab25(143). Furthermore, a recent study published in EMBO J suggested that mammalian TRAPPII has GEF activity on Rab18(144), although with our recombinant purified complex we were unable to detect this Rab18 activity. Rab18 is evolutionarily conserved back to the LECA, and other groups have tried to detect this GEF activity in drosophila(60) and have also not been able to observe activity on this small GTPase. It is possible that there are other binding partners that have yet to be described which are required for the activation observed in the in vivo studies conducted by C.Li *et al*(144). The overall mechanism of specificity is still unclear; however,

these results should help advance our knowledge of how the TRAPPII complex can achieve specificity.

In agreement with data generated from TRAPPII in drosophila, we also showed that Rab1 and Rab11 GEF rates are enhanced by membranes, with an approximately 4-fold enhancement in the presence of lipid vesicles(60). It is quite puzzling that metazoan TRAPP complexes are only slightly enhanced by membranes, while yeast TRAPPII is essentially dependent on membrane for activation of Rab11(61). From structural information on the yeast TRAPPII complex, it does seem that the complex is capable of forming a dimer (133). Therefore, it could be possible that the active site for Rab binding is occluded in dimer form, and membrane is required to pull the complex apart. In preliminary negative stain experiments with the mammalian TRAPPII complex, we see no evidence of dimer formation (data not shown), and our size exclusion experiments are indicative of a monomeric state. Therefore, it is possible that this explains the difference in membrane requirement for activation in metazoans and humans, however more work is required to make any definitive claims on the subject.

It has been suggested that TRAPPII specific subunits contain GEF domains to explain the specificity of the TRAPPII complex for Rab11(137). To understand the molecular basis of how TRAPPII mediates Rab1, Rab11 and Rab43 nucleotide exchange, we used hydrogen deuterium exchange mass spectrometry (HDX-MS), and found that all three of these GTPases bind primarily to the catalytic TRAPPC4 subunit. Interestingly, we found that Rab43 formed the tightest interaction, and also stabilized regions of TRAPPC2L and TRAPPC5. All of our GTPases were treated with EDTA for half an hour prior to incubation with TRAPPII to prevent HDX observable nucleotide loss dynamics, however it is important to note that Rab43 had the highest rate of intrinsic nucleotide exchange. It is known that GEFs generally interact with nucleotide free forms of Rab GTPases with the highest affinity, so it is possible that TRAPPII does bind Rab43 with the

highest affinity, but our findings may be clouded by this fact. Therefore, more detailed studies on the affinities of TRAPPII for these small GTPases should be conducted.

Misregulation of Rab11 isoforms is a key driver in neurodegeneration and developmental diseases, and several mutations of *trapp* genes (known as TRAPPopathies) have also been linked to neurodevelopmental disorders. Here we show that mutations in Rab11 alter the ability of TRAPPII to catalyze nucleotide exchange in the same manner as with the GEF SH3BP5(143). Moreover, our results reveal that certain *trapp* gene mutations can reduce the GEF efficiency of TRAPPII for Rab11 and can lead to altered complex formation. It is possible that misregulation of TRAPPII is also linked to diseases such as Huntington's and Alzheimer's, however this link must be interrogated further. Overall these results will help medical researchers understand how clinical mutations lead to disease, and eventually could help patients living with diseases related to these de novo mutations.

Chapter 4: Conclusions and Future Directions

4.1 Conclusions

Rab11 is a critical GTPase involved in membrane trafficking in the endocytic pathway. Its misregulation is involved in a variety of human diseases including Huntington's disease and Alzheimer's disease, and mutations in Rab11 have been identified in patients with developmental disorders. Rab11 is conserved back to the LECA, and is arguably one of the best studied Rab GTPases, yet hindering the capability to fully understand Rab11 regulation and its role in disease is the lack of detail describing how Rab11 proteins are activated by their cognate GEFs. In recent years, two separate proteins have been identified as putative GEFs for Rab11: SH3BP5 and TRAPPII. This thesis was therefore focused on investigating both of these proteins to determine their molecular mechanisms of GEF activity and their mechanisms of specificity in order to better understand the regulation of the critical GTPase Rab11.

The first objective of this thesis was to understand the molecular architecture of SH3BP5 in order to decipher the mechanism of Rab11 GEF activation. In late 2015, Sakaguchi *et al*. described SH3BP5 as having GEF activity against Rab11 in *C.elegans*(6), and they showed that the loss of SH3BP5 impairs Rab11 targeting to the late Golgi, and delayed cytokinesis. This paper therefore revealed a novel GEF for Rab11, however it contained no conserved GEF domains, so it was unclear how it functions. To determine the molecular mechanism of GEF activity and the specificity of activation, we solved the 3.1 Å structure of SH3BP5 bound to Rab11. We found that it forms an extended coiled coil GEF domain, with comparable catalytic efficiency to previously determined Rab GEFs. The structure of SH3BP5 bound to Rab11, along with detailed mutagenesis, revealed the mechanism for how SH3BP5 binding leads to nucleotide exchange and Rab11 specificity. In brief, upon SH3BP5 binding, switch I undergoes a large conformational rearrangement, with F36 and I44 forming hydrophobic contacts with SH3BP5, leading to exposure of the nucleotide-binding pocket. F36 and I44 are in a highly constrained orientation and require

the interspersing residues to allow for formation of this interface, giving rise to the mechanism of specificity of SH3BP5. Since our work on SH3BP5 was published, Sakurako Goto-Ito *et al.* released a manuscript containing structures of both apo SH3BP5 and SH3BP5 bound to Rab11 that are nearly identical to our structure(148). Their work also validated our findings that SH3BP5 localizes to Rab11-positive recycling endosomes, and further clarified that SH3BP5L also localizes to these vesicles. These studies also showed that SH3BP5 does not localize to mitochondria, as previous studies have suggested(86). This may indicate that SH3BP5 is not a mitochondrial localized JNK scaffold, or that localization to the mitochondria only occurs under certain cellular stresses.

The second objective of this thesis was to characterize the GEF activity of the large TRAPPII complex. There has been controversy in the field whether TRAPPII is truly a GEF for Rab11. We found that recombinantly purified TRAPPII was a strong GEF for both Rab1 and Rab11, and we discovered novel activity against Rab43. Using HDX-MS, we revealed that all three of these GTPases bind to the same location on the TRAPPII complex, with Rab43 binding with the highest affinity. This provides strong evidence that the longin domain of TRAPPC10 is not responsible for the GEF activation of Rab11 as previously suggested(137).

Rab11 mutations have been identified in patients with developmental disorders and encephalopathies, and it is unclear how several of these mutations result in disease. Using HDX-MS and nucleotide exchange assays, we found that the V22M, S154L, and K24R mutations all destabilized Rab11, either through a complete (V22M, S154L) or partial (K24R) disruption of nucleotide binding. K13N almost completely prevented SH3BP5 and TRAPPII mediated nucleotide exchange, with R82C and A68T both leading to slightly decreased rates. This reveals that clinically relevant Rab11 mutations can disrupt GEF mediated exchange. Furthermore, we also found that TRAPPII mutations can alter the GEF rate of TRAPPII for Rab11, giving insight into their mechanisms of disease.

4.2 Future directions

Overall, this research advances our understanding of the regulation of Rab11. We now know that humans have three GEFs regulating its activation: SH3BP5, SH3BP5L and TRAPPII. Recent studies have shown that the knockout of Parcas (SH3BP5 in *drosophila*) along with mutation of TRAPPC9 is synthetically lethal in fruit flies(60). These GEFs have therefore been shown to act redundantly, and it is still unclear why metazoans have these redundant pathways. It will be interesting to see if these GEFs are capable of working in cell-specific or tissue-specific processes, and it is possible that these questions can begin to be answered with further detailed studies using the Rab11 FRET sensor used in this thesis(100).

Another key unanswered question is how SH3BP5 and TRAPPII are localized to specific intracellular membranes. Membranes contain a variety of different lipids and proteins that define their localization and function, and recently it was proposed that active Arf1 and anionic lipids can recruit TRAPPII to membranes in yeast (61), however no work has yet been done to validate this in metazoans. It is possible that localization is dependent on Rab-GDIs as previously suggested(19), or other membrane localized scaffolds that have yet to be described. Recently, experiments were conducted to identify Rab GTPase interactors by mitochondrial relocalization (147), therefore it is possible that the putative scaffold protein for Rab11 or its cognate GEFs has already been discovered, and more work could reveal the exact protein or proteins responsible. It is also still unclear how membrane enhances GEF activity of TRAPPII in humans. In yeast, a nice model of steric gating for TRAPPII has been described, whereby the length of the HVT dictates substrate specificity(136). However, membrane seems to play less of a role in activation for human TRAPPII than its yeast counterpart, with only a 4-fold enhancement of GEF activity in the presence of membrane, compared to a greater than 10-fold enhancement in yeast(61). Therefore, it is unclear if a mechanism like this is in place for metazoans, and further experiments are required to expand our knowledge on how membranes alter GEF activity.

Finally, the architecture of the human TRAPP complexes has yet to be determined. Although the cryo-EM structure of yeast TRAPPII has been solved, the resolution of the TRAPPC9 and TRAPPC10 subunits is relatively poor. Furthermore, the TRAPPC9 and TRAPPC10 subunits both have no homology to structurally characterized domains, and thus structure prediction and modelling software (such as PHYRE2) are unable to predict how these proteins are arranged. X-Ray Crystallography could help elucidate the structures of these TRAPPII specific proteins, to gain more insight into their functions. Cryo-EM technologies are advancing rapidly, and it is possible that the use of cryo-EM on the metazoan TRAPPII could result in a higher resolution structure that could give greater insight into how TRAPPC9 and TRAPPC10 subunits allow for Rab11 GEF activation. Finally, chemical crosslinking followed by mass spectrometry of TRAPPII could help reveal details on how the complex is arranged.

Bibliography

1. Welz, T., Wellbourne-Wood, J. & Kerkhoff, E. Orchestration of cell surface proteins by Rab11. Trends Cell Biol.24, 407–15 (2014).
2. Knödler A. 2010. Coordination of Rab8 and Rab11 in primary ciliogenesis. Proc Natl Acad Sci USA 107.
3. Yu X, Prekeris R, Gould GW. 2007. Role of endosomal Rab GTPases in cytokinesis. Eur J Cell Biol 86:25–35.
4. Takahashi S, Kubo K, Waguri S, Yabashi A, Shin H-W, Katoh Y, Nakayama K. 2012. Rab11 regulates exocytosis of recycling vesicles at the plasma membrane. J Cell Sci 125:4049–4057.
5. Steinert J, Campesan S, Richards P, Kyriacou C, Forsythe I, Giorgini F. 2012. Rab11 rescues synaptic dysfunction and behavioural deficits in a Drosophila model of Huntington's disease. Hum Mol Genet 13:2912–2922.
6. Sakaguchi A. 2015. REI-1 is a guanine nucleotide exchange factor regulating RAB-11 localization and function in C. elegans embryos. Dev Cell 35.
7. Kahn RA, Der CJ, Bokoch GM. 1992. The ras superfamily of GTP-binding proteins: guidelines on nomenclature. FASEB J 6:2512–2513.
8. Zhen Y, Stenmark H. 2015. Cellular functions of Rab GTPases at a glance. J Cell Sci 128.
9. Barr FA. 2013. Review series: Rab GTPases and membrane identity: causal or inconsequential? J Cell Biol 202.
10. Mizuno-Yamasaki E, Rivera-Molina F, Novick P. 2012. GTPase networks in membrane traffic. Annu Rev Biochem 81.
11. Stenmark H. 2009. Rab GTPases as coordinators of vesicle traffic. Nat Rev Mol Cell Biol 10.
12. Klöpper TH, Kienle N, Fasshauer D, Munro S. 2012. Untangling the evolution of Rab G proteins: implications of a comprehensive genomic analysis. BMC Biol 10.
13. Eggenschwiler JT, Espinoza E, Anderson KV. 2001. Rab23 is an essential negative regulator of the mouse Sonic hedgehog signalling pathway. Nature 412:194–198.

14. Di Giovanni S, Knights CD, Rao M, Yakovlev A, Beers J, Catania J, Avantaggiati ML, Faden AI. 2006. The tumor suppressor protein p53 is required for neurite outgrowth and axon regeneration. EMBO J 25:4084–4096.

15. Deinhardt K, Salinas S, Verastegui C, Watson R, Worth D, Hanrahan S, Bucci C, Schiavo G. 2006. Rab5 and Rab7 control endocytic sorting along the axonal retrograde transport pathway. Neuron 52:293–305.

16. Morciano M, Burré J, Corvey C, Karas M, Zimmermann H, Volknandt W. 2005. Immunoisolation of two synaptic vesicle pools from synaptosomes: a proteomics analysis. J Neurochem 95:1732–1745.

17. Traut TW. 1994. Physiological concentrations of purines and pyrimidines. Mol Cell Biochem 140:1–22.

18. Cabrera M, Ungermann C. 2013. Guanine nucleotide exchange factors (GEFs) have a critical but not exclusive role in organelle localization of Rab GTPases. J Biol Chem 288:28704–28712.

19. Pfeffer SR. 2005. A model for Rab GTPase localization. Biochem Soc Trans 33:627–630.

20. Chavrier P, Gorvel J-P, Stelzer E, Simons K, Gruenberg J, Zerial M. 1991. Hypervariable C-termmal domain of rab proteins acts as a targeting signal. Nature 353:769–772.

21. Li F, Yi L, Zhao L, Itzen A, Goody RS, Wu Y-W. 2014. The role of the hypervariable C-terminal domain in Rab GTPases membrane targeting. Proc Natl Acad Sci U S A 111:2572–2577.

22. Zerial M, McBride H. 2001. Rab proteins as membrane organizers. Nat Rev Mol Cell Biol 2:107–117.

23. Stenmark H, Olkkonen VM. 2001. The Rab GTPase family. Genome Biol 2:reviews3007.1-reviews3007.7.

24. Pylypenko O, Hammich H, Yu IM, Houdusse A. 2017. Rab GTPases and their interacting protein partners: Structural insights into Rab functional diversity. Small GTPases 113.

25. Müller MP, Goody RS. 2017. Molecular control of Rab activity by GEFs, GAPs and GDI. Small GTPases 13.

26. Novick P. 2016. Regulation of membrane traffic by Rab GEF and GAP cascades. Small GTPases 7.

27. Cherfils J, Zeghouf M. 2013. Regulation of small GTPases by GEFs, GAPs, and GDIs. Physiol Rev 93.

28. Toma-Fukai, Shimizu. 2019. Structural Insights into the Regulation Mechanism of Small GTPases by GEFs. Molecules 24:3308.

29. Bos JL, Rehmann H, Wittinghofer A. 2007. GEFs and GAPs: Critical Elements in the Control of Small G Proteins. Cell 129:865–877.

30. Renault L, Guibert B, Cherfils J. 2003. Structural snapshots of the mechanism and inhibition of a guanine nucleotide exchange factor. Nature 426:525–530.

31. Uejima T, Ihara K, Goh T, Ito E, Sunada M, Ueda T, Nakano A, Wakatsuki S. 2010. GDP-bound and Nucleotide-free Intermediates of the Guanine Nucleotide Exchange in the Rab5·Vps9 System. J Biol Chem 285:36689–36697.

32. Rensland H, Lautwein A, Wittinghofer A, Goody RS. 1991. Is there a rate-limiting step before GTP cleavage by H-ras p21? Biochemistry 30:11181–11185.

33. Simon I, Zerial M, Goody RS. 1996. Kinetics of Interaction of Rab5 and Rab7 with Nucleotides and Magnesium Ions. J Biol Chem 271:20470–20478.

34. Bergbrede T, Pylypenko O, Rak A, Alexandrov K. 2005. Structure of the extremely slow GTPase Rab6A in the GTP bound form at 1.8Å resolution. J Struct Biol 152:235–238.

35. Gavriljuk K, Gazdag E-M, Itzen A, Kötting C, Goody RS, Gerwert K. 2012. Catalytic mechanism of a mammalian Rab·RabGAP complex in atomic detail. Proc Natl Acad Sci 109:21348–21353.

36. Barr F, Lambright DG. 2010. Rab GEFs and GAPs. Curr Opin Cell Biol 22:461–470.

37. Rabs and their effectors: Achieving specificity in membrane traffic | PNAS.

38. Markgraf DF, Peplowska K, Ungermann C. 2007. Rab cascades and tethering factors in the endomembrane system. FEBS Lett 581:2125–2130.

39. Zhu S, Bhat S, Syan S, Kuchitsu Y, Fukuda M, Zurzolo C. 2018. Rab11a–Rab8a cascade regulates the formation of tunneling nanotubes through vesicle recycling. J Cell Sci 131:jcs215889.

40. Rivera-Molina FE, Novick PJ. 2009. A Rab GAP cascade defines the boundary between two Rab GTPases on the secretory pathway. Proc Natl Acad Sci U S A 106:14408–14413.

41. Kelly EE, Horgan CP, McCaffrey MW. 2012. Rab11 proteins in health and disease. Biochem Soc Trans 40.

42. Hobdy-Henderson KC, Hales CM, Lapierre LA, Cheney RE, Goldenring JR. 2003. Dynamics of the apical plasma membrane recycling system during cell division. Traffic 4.

43. Holubcová Z, Howard G, Schuh M. 2013. Vesicles modulate an actin network for asymmetric spindle positioning. Nat Cell Biol 15.

44. Shirane M, Nakayama KI. 2006. Protrudin induces neurite formation by directional membrane trafficking. Science 314.

45. Puri C. 2018. The RAB11A-positive compartment is a primary platform for autophagosome assembly mediated by WIPI2 recognition of PI3P-RAB11A. Dev Cell 45.

46. Sobajima T, Yoshimura S-I, Iwano T, Kunii M, Watanabe M, Atik N, Mushiake S, Morii E, Koyama Y, Miyoshi E, Harada A. 2014. Rab11a is required for apical protein localisation in the intestine. Biol Open 4:86–94.

47. Gromov PS, Celis JE, Hansen C, Tommerup N, Gromova I, Madsen P. 1998. Human rab11a: transcription, chromosome mapping and effect on the expression levels of host GTP-binding proteins1. FEBS Lett 429:359–364.

48. Goldenring JR, Shen KR, Vaughan HD, Modlin IM. 1993. Identification of a small GTP-binding protein, Rab25, expressed in the gastrointestinal mucosa, kidney, and lung. J Biol Chem 268:18419–18422.

49. Lai F, Stubbs L, Artzt K. 1994. Molecular Analysis of Mouse Rab11b: A New Type of Mammalian YPT/Rab Protein. Genomics 22:610–616.

50. Pasqualato S. 2004. The structural GDP/GTP cycle of Rab11 reveals a novel interface involved in the dynamics of recycling endosomes. J Biol Chem 279.

51. Robert X, Gouet P. 2014. Deciphering key features in protein structures with the new ENDscript server. Nucleic Acids Res 42:W320–W324.

52. Ren M, Xu G, Zeng J, De Lemos-Chiarandini C, Adesnik M, Sabatini DD. 1998. Hydrolysis of GTP on rab11 is required for the direct delivery of transferrin from the pericentriolar recycling compartment to the cell surface but not from sorting endosomes. Proc Natl Acad Sci 95:6187–6192.

53. Casanova JE, Wang X, Kumar R, Bhartur SG, Navarre J, Woodrum JE, Altschuler Y, Ray GS, Goldenring JR. 1999. Association of Rab25 and Rab11a with the Apical Recycling System of Polarized Madin–Darby Canine Kidney Cells. Mol Biol Cell 10:47–61.

54. Burke JE. 2014. Structures of PI4KIIIβ complexes show simultaneous recruitment of Rab11 and its effectors. Science 344.

55. Lindsay AJ, Jollivet F, Horgan CP, Khan AR, Raposo G, McCaffrey MW, Goud B. 2013. Identification and characterization of multiple novel Rab-myosin Va interactions. Mol Biol Cell 24:3420–3434.

56. Horgan CP, McCaffrey MW. 2009. The dynamic Rab11-FIPs. Biochem Soc Trans 37:1032–1036.

57. Vetter M, Stehle R, Basquin C, Lorentzen E. 2015. Structure of Rab11-FIP3-Rabin8 reveals simultaneous binding of FIP3 and Rabin8 effectors to Rab11. Nat Struct Mol Biol 22.

58. Dabbeekeh JTS, Faitar SL, Dufresne CP, Cowell JK. 2007. The EVI5 TBC domain provides the GTPase-activating protein motif for RAB11. Oncogene 26.

59. Westlake CJ. 2007. Identification of Rab11 as a small GTPase binding protein for the Evi5 oncogene. Proc Natl Acad Sci USA 104.

60. Riedel F, Galindo A, Muschalik N, Munro S. 2018. The two TRAPP complexes of metazoans have distinct roles and act on different Rab GTPases. J Cell Biol 217.

61. Thomas LL, Fromme JC. 2016. GTPase cross talk regulates TRAPPII activation of Rab11 homologues during vesicle biogenesis. J Cell Biol 215.

62. Xiong B. 2012. Crag is a GEF for Rab11 required for rhodopsin trafficking and maintenance of adult photoreceptor cells. PLoS Biol 10.

63. Beckett K, Baylies MK. 2006. Parcas, a regulator of non-receptor tyrosine kinase signaling, acts during anterior-posterior patterning and somatic muscle development in Drosophila melanogaster. Dev Biol 299.

64. Sinka R. 2002. poirot, a new regulatory gene of Drosophila oskar acts at the level of the short Oskar protein isoform. Development 129.

65. Artero R, Furlong EE, Beckett K, Scott MP, Baylies M. 2003. Notch and Ras signaling pathway effector genes expressed in fusion competent and founder cells during Drosophila myogenesis. Development 130.

66. Li X, Standley C, Sapp E, Valencia A, Qin Z-H, Kegel KB, Yoder J, Comer-Tierney LA, Esteves M, Chase K, Alexander J, Masso N, Sobin L, Bellve K, Tuft R, Lifshitz L, Fogarty K, Aronin N, DiFiglia M. 2009. Mutant Huntingtin Impairs Vesicle Formation from Recycling Endosomes by Interfering with Rab11 Activity. Mol Cell Biol 29:6106–6116.

67. Dendritic spine loss and neurodegeneration is rescued by Rab11 in models of Huntington's disease | Cell Death & Differentiation.

68. Udayar V, Buggia-Prévot V, Guerreiro RL, Siegel G, Rambabu N, Soohoo AL, Ponnusamy M, Siegenthaler B, Bali J, Guerreiro R, Brás J, Sassi C, Gibbs JR, Hernandez D, Lupton MK, Brown K, Morgan K, Powell J, Singleton A, Hardy J, Simons M, Ries J, Puthenveedu MA, Hardy J, Thinakaran G, Rajendran L. 2013. A Paired RNAi and RabGAP Overexpression Screen Identifies Rab11 as a Regulator of β-Amyloid Production. Cell Rep 5:1536–1551.

69. Buggia-Prévot V, Fernandez CG, Riordan S, Vetrivel KS, Roseman J, Waters J, Bindokas VP, Vassar R, Thinakaran G. 2014. Axonal BACE1 dynamics and targeting in hippocampal neurons: a role for Rab11 GTPase. Mol Neurodegener 9:1.

70. Mosesson Y, Mills GB, Yarden Y. 2008. Derailed endocytosis: an emerging feature of cancer. Nat Rev Cancer 8:835–850.

71. Hamdan FF. 2017. High rate of recurrent de novo mutations in developmental and epileptic encephalopathies. Am J Hum Genet 101.

72. Lamers IJC. 2017. Recurrent de novo mutations disturbing the GTP/GDP binding pocket of RAB11B cause intellectual disability and a distinctive brain phenotype. Am J Hum Genet 101.

73. Ilnytska O. 2013. Enteroviruses harness the cellular endocytic machinery to remodel the host cell cholesterol landscape for effective viral replication. Cell Host Microbe 14.

74. Mölleken K, Hegemann JH. 2017. Acquisition of Rab11 and Rab11-Fip2-A novel strategy for Chlamydia pneumoniae early survival. PLoS Pathog 13.

75. Romano JD. 2017. The parasite Toxoplasma sequesters diverse Rab host vesicles within an intravacuolar network. J Cell Biol 216.

76. Li X, Sapp E, Valencia A, Kegel KB, Qin Z-H, Alexander J, Masso N, Reeves PB, Ritch JJ, Zeitlin S, Aronin N, Difiglia M. 2008. A function of huntingtin in guanine nucleotide exchange on Rab11. Neuroreport 19:1643–1647.

77. Xu W, Fang F, Ding J, Wu C. 2018. Dysregulation of Rab5-mediated endocytic pathways in Alzheimer's disease. Traffic 19:253–262.

78. Mitra S. 2017. Stapled peptide inhibitors of RAB25 target context-specific phenotypes in cancer. Nat Commun 8.

79. Cheng KW. 2004. The RAB25 small GTPase determines aggressiveness of ovarian and breast cancers. Nat Med 10.

80. Hu C, Chen B, Zhou Y, Shan Y. 2017. High expression of Rab25 contributes to malignant phenotypes and biochemical recurrence in patients with prostate cancer after radical prostatectomy. Cancer Cell Int 17:45.

81. Cao C, Lu C, Xu J, Zhang J, Zhang J, Li M. 2013. Expression of Rab25 correlates with the invasion and metastasis of gastric cancer. Chin J Cancer Res 25:192–199.

82. Nikoshkov A, Broliden K, Attarha S, Sviatoha V, Hellström A-C, Mints M, Andersson S. 2015. Expression pattern of the PRDX2, RAB1A, RAB1B, RAB5A and RAB25 genes in normal and cancer cervical tissues. Int J Oncol 46:107–112.

83. Zhang J, Wei J, Lu J, Tong Z, Liao B, Yu B, Zheng F, Huang X, Chen Z, Fang Y, Li B, Chen W, Xie D, Luo J. 2013. Overexpression of Rab25 contributes to metastasis of bladder cancer through induction of epithelial–mesenchymal transition and activation of Akt/GSK-3β/Snail signaling. Carcinogenesis 34:2401–2408.

84. Yamadori T. 1999. Bruton's tyrosine kinase activity is negatively regulated by Sab, the Btk-SH3 domain-binding protein. Proc Natl Acad Sci USA 96.

85. Laughlin JD. 2012. Structural mechanisms of allostery and autoinhibition in JNK family kinases. Structure 20.

86. Wiltshire C, Matsushita M, Tsukada S, Gillespie DAF, May GHW. 2002. A new c-Jun N-terminal kinase (JNK)-interacting protein, Sab (SH3BP5), associates with mitochondria. Biochem J 367.

87. Gibson DG. 2009. Enzymatic assembly of DNA molecules up to several hundred kilobases. Nat Methods 6.

88. Krissinel E, Henrick K. 2007. Inference of macromolecular assemblies from crystalline state. J Mol Biol 372.

89. Holm L, Laakso LM. 2016. Dali server update. Nucleic Acids Res 44.

90. Jurrus E. 2018. Improvements to the APBS biomolecular solvation software suite. Protein Sci 27.

91. Delprato A, Merithew E, Lambright DG. 2004. Structure, exchange determinants, and family-wide rab specificity of the tandem helical bundle and Vps9 domains of Rabex-5. Cell 118.

92. Kabsch W. 2010. XDS. Acta Crystallogr Biol Crystallogr 66.

93. Evans PR, Murshudov GN. 2013. How good are my data and what is the resolution? Acta Crystallogr Biol Crystallogr 69.

94. Skubák P, Pannu NS. 2013. Automatic protein structure solution from weak X-ray data. Nat Commun 4.

95. McCoy AJ. 2007. Phaser crystallographic software. J Appl Crystallogr 40.

96. Emsley P, Cowtan K. 2004. Coot: model-building tools for molecular graphics. Acta Cryst 2004 60.

97. Afonine PV. 2012. Towards automated crystallographic structure refinement with phenix.refine. Acta Crystallogr Biol Crystallogr 68.

98. Broussard JA, Rappaz B, Webb DJ, Brown CM. 2013. Fluorescence resonance energy transfer microscopy as demonstrated by measuring the activation of the serine/threonine kinase Akt. Nat Protoc 8.

99. Vizcaíno JA. 2016. 2016 update of the PRIDE database and its related tools. Nucleic Acids Res 44.

100. Campa CC. 2018. Rab11 activity and PtdIns(3)P turnover removes recycling cargo from endosomes. Nat Chem Biol 14.

101. Franco I. 2014. PI3K class II α controls spatially restricted endosomal PtdIns3P and Rab11 activation to promote primary cilium function. Dev Cell 28.

102. Polevoy G. 2009. Dual roles for the Drosophila PI 4-kinase four wheel drive in localizing Rab11 during cytokinesis. J Cell Biol 187.

103. Langemeyer L. 2014. Diversity and plasticity in Rab GTPase nucleotide release mechanism has consequences for Rab activation and inactivation. eLife 3.

104. Masson GR, Jenkins ML, Burke JE. 2017. An overview of hydrogen deuterium exchange mass spectrometry (HDX-MS) in drug discovery. Expert Opin Drug Discov 12.

105. Fowler ML. 2016. Using hydrogen deuterium exchange mass spectrometry to engineer optimized constructs for crystallization of protein complexes: case study of PI4KIIIβ with Rab11. Protein Sci 25.

106. Siegert R, Leroux MR, Scheufler C, Hartl FU, Moarefi I. 2000. Structure of the molecular chaperone prefoldin: unique interaction of multiple coiled coil tentacles with unfolded proteins. Cell 103.

107. Merithew E. 2001. Structural plasticity of an invariant hydrophobic triad in the switch regions of Rab GTPases is a determinant of effector recognition. J Biol Chem 276.

108. Itzen A, Pylypenko O, Goody RS, Alexandrov K, Rak A. 2006. Nucleotide exchange via local protein unfolding--structure of Rab8 in complex with MSS4. EMBO J 25.

109. Wu X. 2011. Insights regarding guanine nucleotide exchange from the structure of a DENN-domain protein complexed with its Rab GTPase substrate. Proc Natl Acad Sci USA 108.

110. Kiontke S. 2017. Architecture and mechanism of the late endosomal Rab7-like Ypt7 guanine nucleotide exchange factor complex Mon1-Ccz1. Nat Commun 8.

111. Dong G, Medkova M, Novick P, Reinisch KM. 2007. A catalytic coiled coil: structural insights into the activation of the Rab GTPase Sec4p by Sec2p. Mol Cell 25.

112. Cai Y. 2008. The structural basis for activation of the Rab Ypt1p by the TRAPP membrane-tethering complexes. Cell 133.

113. Delprato A, Lambright DG. 2007. Structural basis for Rab GTPase activation by VPS9 domain exchange factors. Nat Struct Mol Biol 14.

114. Schoebel S, Oesterlin LK, Blankenfeldt W, Goody RS, Itzen A. 2009. RabGDI displacement by DrrA from Legionella is a consequence of its guanine nucleotide exchange activity. Mol Cell 36.

115. Eathiraj S, Mishra A, Prekeris R, Lambright DG. 2006. Structural basis for Rab11-mediated recruitment of FIP3 to recycling endosomes. J Mol Biol 364.

116. Sato Y, Fukai S, Ishitani R, Nureki O. 2007. Crystal structure of the Sec4p.Sec2p complex in the nucleotide exchanging intermediate state. Proc Natl Acad Sci USA 104.

117. Fuchs E. 2007. Specific Rab GTPase-activating proteins define the Shiga toxin and epidermal growth factor uptake pathways. J Cell Biol 177.

118. Zhang XM, Walsh B, Mitchell CA, Rowe T. 2005. TBC domain family, member 15 is a novel mammalian Rab GTPase-activating protein with substrate preference for Rab7. Biochem Biophys Res Commun 335.

119. Sacher M. 1998. TRAPP, a highly conserved novel complex on the cis-Golgi that mediates vesicle docking and fusion. EMBO J 17:2494–2503.

120. Jones S, Newman C, Liu F, Segev N. 2000. The TRAPP Complex Is a Nucleotide Exchanger for Ypt1 and Ypt31/32. Mol Biol Cell 11:4403–4411.

121. Wang W, Sacher M, Ferro-Novick S. 2000. Trapp Stimulates Guanine Nucleotide Exchange on Ypt1p. J Cell Biol 151:289–296.

122. Sacher M, Shahrzad N, Kamel H, Milev MP. 2019. TRAPPopathies: An emerging set of disorders linked to variations in the genes encoding transport protein particle (TRAPP)-associated proteins. Traffic 20:5–26.

123. Milev MP, Graziano C, Karall D, Kuper WFE, Al-Deri N, Cordelli DM, Haack TB, Danhauser K, Iuso A, Palombo F, Pippucci T, Prokisch H, Saint-Dic D, Seri M, Stanga D, Cenacchi G, Gassen KLI van, Zschocke J, Fauth C, Mayr JA, Sacher M, Hasselt PM van. 2018. Bi-allelic mutations in TRAPPC2L result in a neurodevelopmental disorder and have an impact on RAB11 in fibroblasts. J Med Genet 55:753–764.

124. Bögershausen N, Shahrzad N, Chong JX, von Kleist-Retzow J-C, Stanga D, Li Y, Bernier FP, Loucks CM, Wirth R, Puffenberger EG, Hegele RA, Schreml J, Lapointe G, Keupp K, Brett CL, Anderson R, Hahn A, Innes AM, Suchowersky O, Mets MB, Nürnberg G, McLeod DR, Thiele H, Waggoner D, Altmüller J, Boycott KM, Schoser B, Nürnberg P, Ober C, Heller R, Parboosingh JS, Wollnik B, Sacher M, Lamont RE. 2013. Recessive TRAPPC11 Mutations Cause a Disease Spectrum of Limb Girdle Muscular Dystrophy and Myopathy with Movement Disorder and Intellectual Disability. Am J Hum Genet 93:181–190.

125. Marin-Valencia I, Novarino G, Johansen A, Rosti B, Issa MY, Musaev D, Bhat G, Scott E, Silhavy JL, Stanley V, Rosti RO, Gleeson JW, Imam FB, Zaki MS, Gleeson JG. 2018. A homozygous founder mutation in TRAPPC6B associates with a neurodevelopmental

disorder characterised by microcephaly, epilepsy and autistic features. J Med Genet 55:48–54.

126. Mir A, Kaufman L, Noor A, Motazacker MM, Jamil T, Azam M, Kahrizi K, Rafiq MA, Weksberg R, Nasr T, Naeem F, Tzschach A, Kuss AW, Ishak GE, Doherty D, Ropers HH, Barkovich AJ, Najmabadi H, Ayub M, Vincent JB. 2009. Identification of Mutations in TRAPPC9, which Encodes the NIK- and IKK-β-Binding Protein, in Nonsyndromic Autosomal-Recessive Mental Retardation. Am J Hum Genet 85:909–915.

127. Mochida GH, Mahajnah M, Hill AD, Basel-Vanagaite L, Gleason D, Hill RS, Bodell A, Crosier M, Straussberg R, Walsh CA. 2009. A Truncating Mutation of TRAPPC9 Is Associated with Autosomal-Recessive Intellectual Disability and Postnatal Microcephaly. Am J Hum Genet 85:897–902.

128. Milev MP, Grout ME, Saint-Dic D, Cheng Y-HH, Glass IA, Hale CJ, Hanna DS, Dorschner MO, Prematilake K, Shaag A, Elpeleg O, Sacher M, Doherty D, Edvardson S. 2017. Mutations in TRAPPC12 Manifest in Progressive Childhood Encephalopathy and Golgi Dysfunction. Am J Hum Genet 101:291–299.

129. Abbasi AA, Blaesius K, Hu H, Latif Z, Picker-Minh S, Khan MN, Farooq S, Khan MA, Kaindl AM. 2017. Identification of a novel homozygous TRAPPC9 gene mutation causing non-syndromic intellectual disability, speech disorder, and secondary microcephaly. Am J Med Genet B Neuropsychiatr Genet 174:839–845.

130. Mortreux J, Busa T, Germain DP, Nadeau G, Puechberty J, Coubes C, Gatinois V, Cacciagli P, Duffourd Y, Pinard J-M, Tevissen H, Villard L, Sanlaville D, Philip N, Missirian C. 2018. The role of CNVs in the etiology of rare autosomal recessive disorders: the example of TRAPPC9 -associated intellectual disability. Eur J Hum Genet 26:143–148.

131. Lipatova Z, Majumdar U, Segev N. 2016. Trs33-Containing TRAPP IV: A Novel Autophagy-Specific Ypt1 GEF. Genetics 204:1117–1128.

132. Kim Y-G, Raunser S, Munger C, Wagner J, Song Y-L, Cygler M, Walz T, Oh B-H, Sacher M. 2006. The Architecture of the Multisubunit TRAPP I Complex Suggests a Model for Vesicle Tethering. Cell 127:817–830.

133. Yip CK, Berscheminski J, Walz T. 2010. Molecular architecture of the TRAPPII complex and implications for vesicle tethering. Nat Struct Mol Biol 17:1298–1304.

134. Zong M, Wu X, Chan CWL, Choi MY, Chan HC, Tanner JA, Yu S. 2011. The Adaptor Function of TRAPPC2 in Mammalian TRAPPs Explains TRAPPC2-Associated SEDT and TRAPPC9-Associated Congenital Intellectual Disability. PLoS ONE 6:e23350.

135. Morozova N, Liang Y, Tokarev AA, Chen SH, Cox R, Andrejic J, Lipatova Z, Sciorra VA, Emr SD, Segev N. 2006. TRAPPII subunits are required for the specificity switch of a Ypt–Rab GEF. Nat Cell Biol 8:1263–1269.

136. Thomas LL, van der Vegt SA, Fromme JC. 2019. A Steric Gating Mechanism Dictates the Substrate Specificity of a Rab-GEF. Dev Cell 48:100-114.e9.

137. Levine TP, Daniels RD, Wong LH, Gatta AT, Gerondopoulos A, Barr FA. 2013. Discovery of new Longin and Roadblock domains that form platforms for small GTPases in Ragulator and TRAPP-II. Small GTPases 4:62–69.

138. Weissmann F, Petzold G, VanderLinden R, Huis in ’t Veld PJ, Brown NG, Lampert F, Westermann S, Stark H, Schulman BA, Peters J-M. 2016. biGBac enables rapid gene assembly for the expression of large multisubunit protein complexes. Proc Natl Acad Sci 113:E2564–E2569.

139. Dornan GL, Siempelkamp BD, Jenkins ML, Vadas O, Lucas CL, Burke JE. 2017. Conformational disruption of PI3Kδ regulation by immunodeficiency mutations in PIK3CD and PIK3R1. Proc Natl Acad Sci 114:1982–1987.

140. Cox JV, Kansal R, Whitt MA. 2016. Rab43 regulates the sorting of a subset of membrane protein cargo through the medial Golgi. Mol Biol Cell 27:1834–1844.

141. Li C, Wei Z, Fan Y, Huang W, Su Y, Li H, Dong Z, Fukuda M, Khater M, Wu G. 2017. The GTPase Rab43 Controls the Anterograde ER-Golgi Trafficking and Sorting of GPCRs. Cell Rep 21:1089–1101.

142. Analysis of GTPase-activating proteins: Rab1 and Rab43 are key Rabs required to maintain a functional Golgi complex in human cells | Journal of Cell Science.

143. Jenkins ML, Margaria JP, Stariha JTB, Hoffmann RM, McPhail JA, Hamelin DJ, Boulanger MJ, Hirsch E, Burke JE. 2018. Structural determinants of Rab11 activation by the guanine nucleotide exchange factor SH3BP5. Nat Commun 9:3772.

144. Li C, Luo X, Zhao S, Siu GK, Liang Y, Chan HC, Satoh A, Yu SS. 2017. COPI–TRAPPII activates Rab18 and regulates its lipid droplet association. EMBO J 36:441–457.

145. Lee H-J, Zheng JJ. 2010. PDZ domains and their binding partners: structure, specificity, and modification 18.

146. Lin Y, Rao SQ, Yang Y. 2008. [A novel mutation in the SEDL gene leading to X-linked spondyloepiphyseal dysplasia tarda in a large Chinese pedigree]. Zhonghua Yi Xue Yi Chuan Xue Za Zhi Zhonghua Yixue Yichuanxue Zazhi Chin J Med Genet 25:150–153.

147. Gillingham AK, Bertram J, Begum F, Munro S. 2019. In vivo identification of GTPase interactors by mitochondrial relocalization and proximity biotinylation. eLife 8:e45916.

148. Goto-Ito S, Morooka N, Yamagata A, Sato Y, Sato K, Fukai S. 2019. Structural basis of guanine nucleotide exchange for Rab11 by SH3BP5. Life Sci Alliance 2:e201900297.

149. Thomas LL, Joiner AMN, Fromme JC. 2018. The TRAPPIII complex activates the GTPase Ypt1 (Rab1) in the secretory pathway. J Cell Biol 217:283–298.

150. Kakuta S, Yamamoto H, Negishi L, Kondo-Kakuta C, Hayashi N, Ohsumi Y. 2012. Atg9 Vesicles Recruit Vesicle-tethering Proteins Trs85 and Ypt1 to the Autophagosome Formation Site. J Biol Chem 287:44261–44269.

151. Westlake CJ, Baye LM, Nachury MV, Wright KJ, Ervin KE, Phu L, Chalouni C, Beck JS, Kirkpatrick DS, Slusarski DC, Sheffield VC, Scheller RH, Jackson PK. 2011. Primary cilia membrane assembly is initiated by Rab11 and transport protein particle II (TRAPPII) complex-dependent trafficking of Rabin8 to the centrosome. Proc Natl Acad Sci 108:2759–2764.

152. Shirahama-Noda K, Kira S, Yoshimori T, Noda T. 2013. TRAPPIII is responsible for vesicular transport from early endosomes to Golgi, facilitating Atg9 cycling in autophagy. J Cell Sci 126:4963–4973.

Appendix

Cell Structure and Function
Published by
Japan Society for Cell Biology
Shimodachiuri Ogawa Higashi, Kamigyo-ku, Kyoto 602-8048, JAPAN
TEL:81-75-415-3661 FAX:81-75-415-3662
E-mail: jscb@nacos.com

Dear Meredith Jenkins
JBurke Lab, University of Victoria
(mlj@uvic.ca)

September 19, 2019

Dear Meredith Jenkins

We are pleased to grant permission for the use of the following material:

Morié Ishida, Mai E. Oguchi, Mitsunori Fukuda
Multiple Types of Guanine Nucleotide Exchange Factors (GEFs) for Rab Small GTPases
Figure 3
Cell Structure and Function, 41(2): 61-79 (2016)

Sincerely yours,

Hiroshi Ohno
President
Japan Society for Cell Biology

Appendix A. Permission for reuse

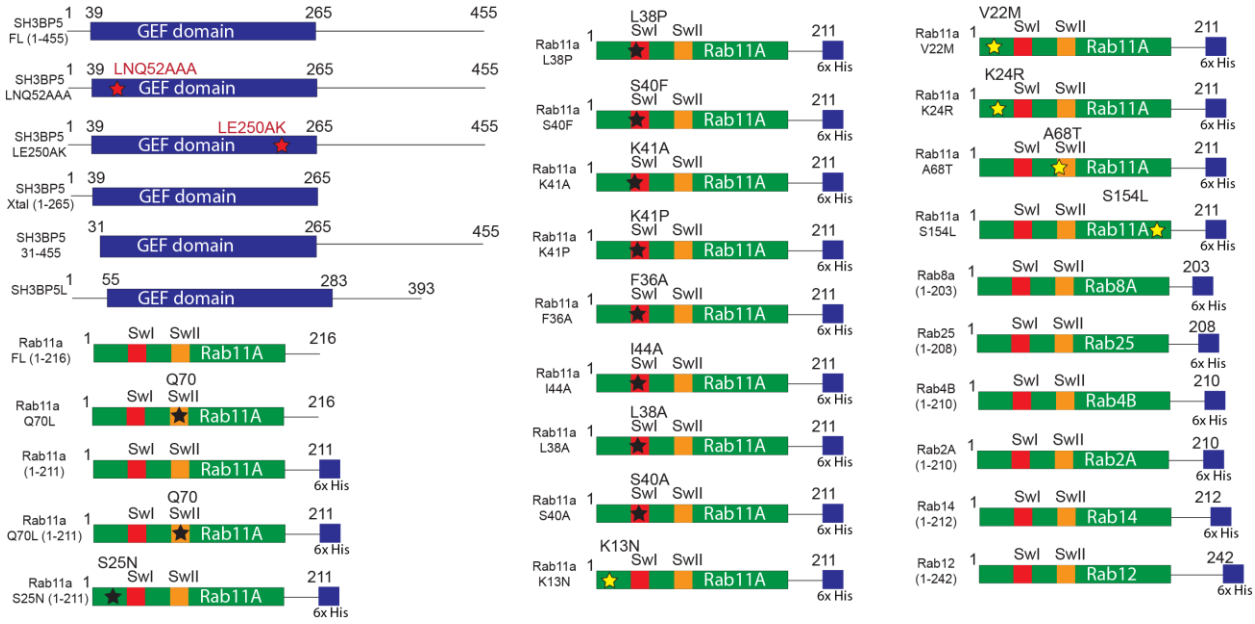

Appendix B. List of all purified SH3BP5 and Rab11 constructs. Domain representation of all constructs used in this paper is listed above. Clinically relevant mutations are highlighted with a yellow star.

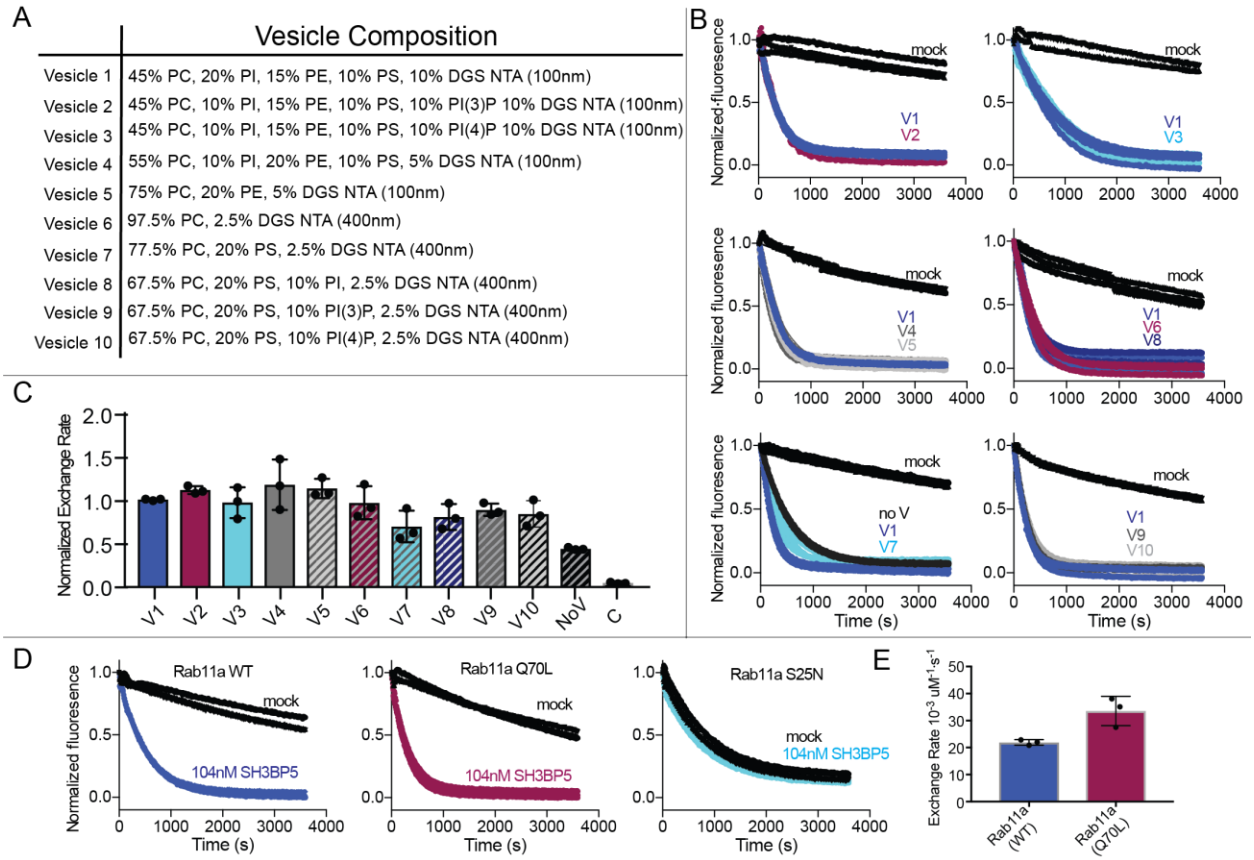

Appendix C. GEF assays of Rab11 in the presence of membrane. (A) Lipid compositions in the different membrane vesicles used in this experiment, different vesicles are abbreviated as V1, V2, etc. (B) *In vitro* GEF activity exhibited towards Rab11A in the presence and absence of membrane. Composition of vesicles does not affect GEF activity *in vitro*. Nucleotide exchange was monitored by measuring the fluorescent signal during the SH3BP5(1-455) (52nM) catalyzed release of Mant-GDP from 4μM of Rab11A-His6 in the presence of 100μM GTPγS. Membrane was present at a final concentration of 0.2mg/ml (V1, V2, V3, V4, V5) or 0.4mg/ml (V6, V7, V8, V9, V10). Fluorescent measurements were completed every 11 sec for a total of 60 min (Excitation λ = 366nm; Emission λ = 443nm). GEF activity was monitored in the presence of varying membrane. compositions, with total GEF activity normalised to the Rab11 GEF activity in the presence of V1-41 vesicles. (C) Quantification of GEF activity in the presence and absence of different Ni-NTA membranes. All experiments were normalized to the exchange rate of V1. (D) *In vitro* GEF activity exhibited towards Rab11A mutants Rab11A(Q70L) and Rab11A(S25N). A measurable rate of GEF activity on Rab11A(S25N) was not obtained as the basal state released nucleotide at the same rate as SH3BP5 bound. (E) Quantification of GEF activity on Rab11A WT and Rab11A Q70L. For all panels, error bars show SD (n=3).

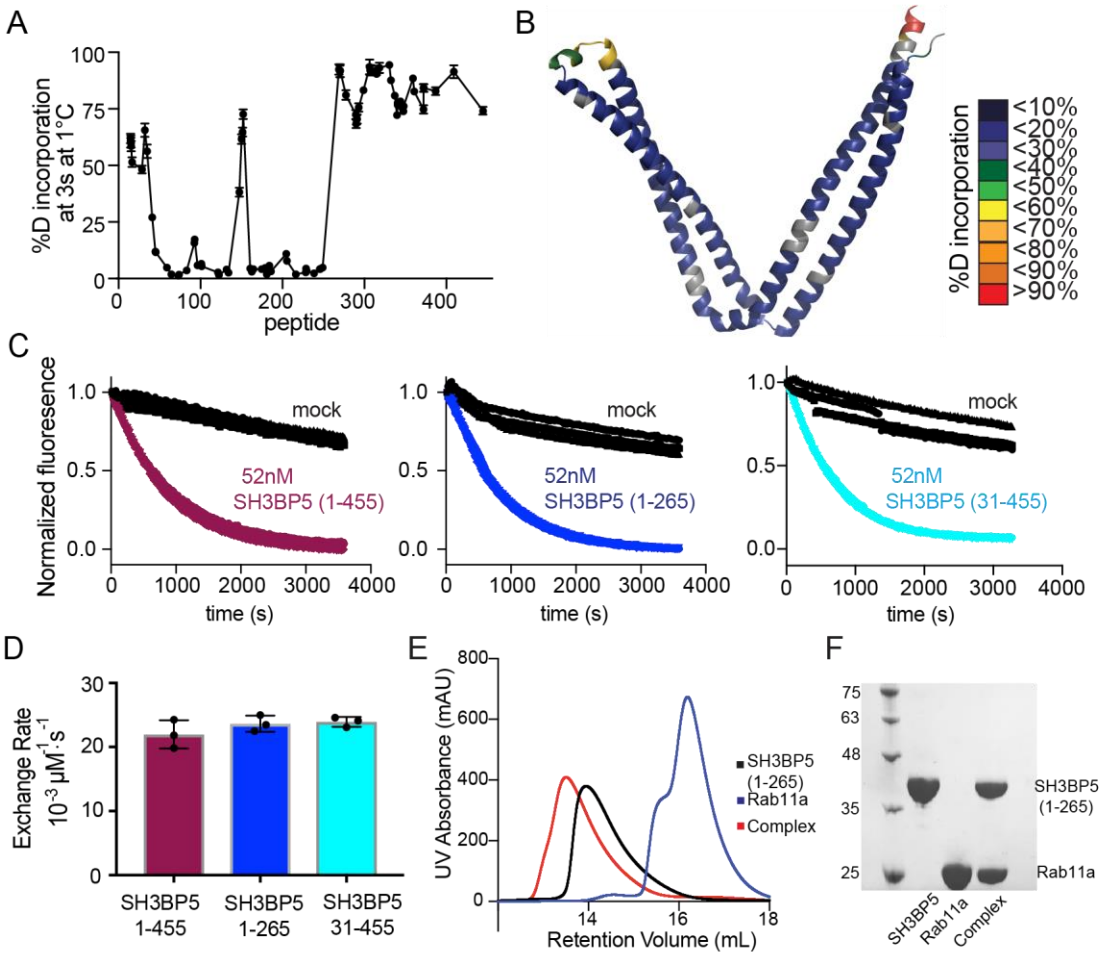

Appendix D. HDX-MS to map the ordered regions of SH3BP5, and GEF activity of SH3BP5 (1-265 vs full length). (A) Hydrogen deuterium exchange levels for full length SH3BP5 (1-455) after 3 seconds of deuterium exposure at 1ºC. Every point represents the central residue of an individual peptide vs the % deuterium incorporation. (B) HDX data from panel A mapped on the structure of SH3BP5. (C) GEF assays of SH3BP5 (1-455), SH3BP5 (31-455), and SH3BP5 (1-265) showed that the crystal construct and the construct used in HDX-MS experiments has the same activity as the full-length construct. (D) Quantification of the GEF data in panel C. For all panels, error bars show SD (n=3). (E) Size Exclusion Chromatography (SEC) trace of the SH3BP5:Rab11A complex. Apo proteins, and proteins mixed at a 1:1 molar ratio were subject to SEC on a Superdex 200 increase 10/300 column. Rab11 and SH3BP5 co-eluted in a new peak, indicating complex formation. (F) An SDS-PAGE gel of each SEC peak is shown (15% gel run at 200V for 45 min and stained with Coomassie Brilliant Blue dye).

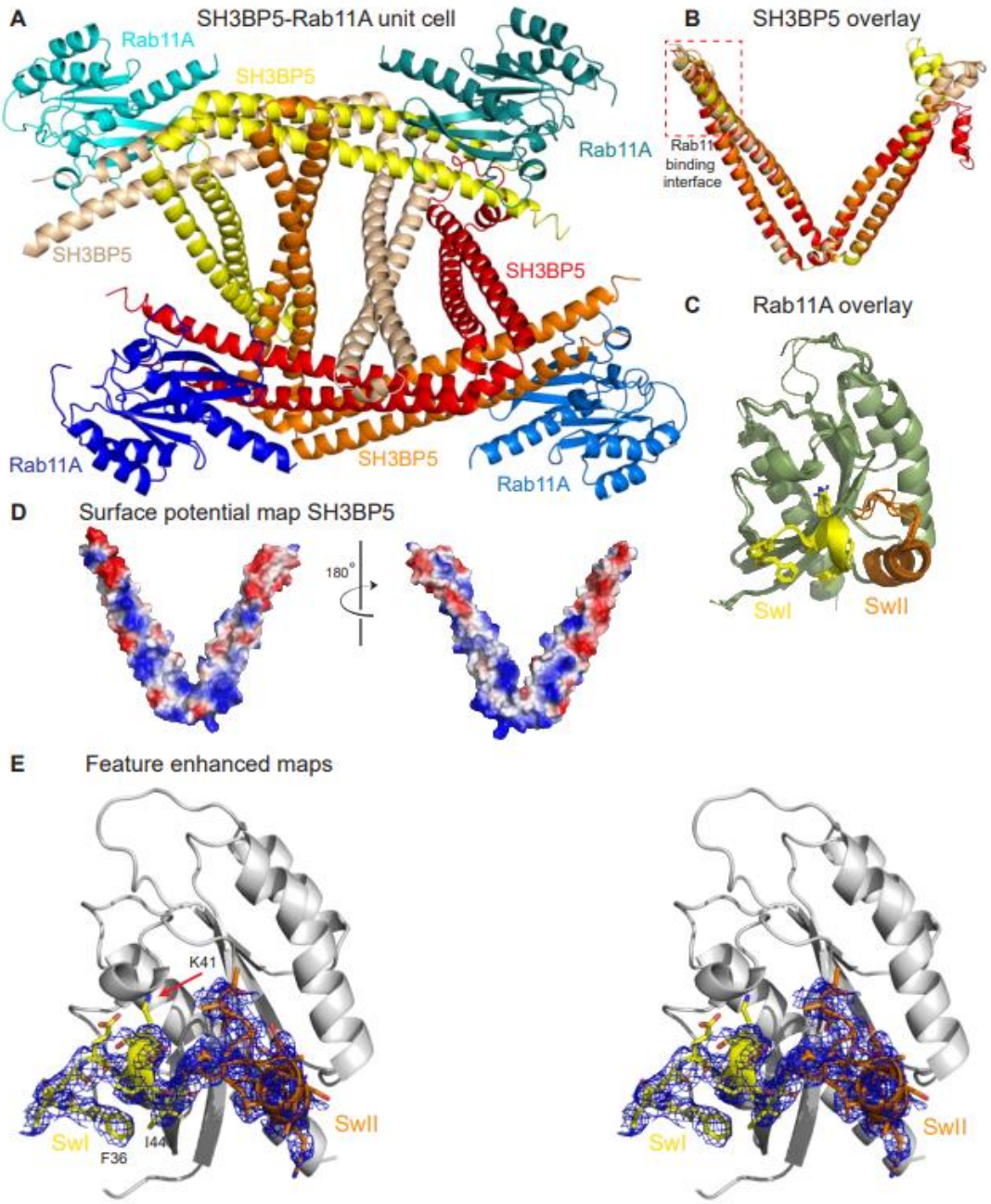

Appendix E. Crystallographic unit cell of SH3BP5 bound to Rab11. (A) The asymmetric unit of SH3BP5-Rab11 is composed of four complexes each of both SH3BP5 and Rab11. The different copies are colored according to the legend. (B) Overlay of the four SH3BP5 copies in the asymmetric unit reveal highly conserved similarity at the Rab11 binding interface, with a large degree of conformational variability at the hinge between helix α2 and helix α3. (C) Overlay of the four Rab11 copies in the asymmetric unit reveal a highly conserved Rab conformation throughout the asymmetric unit. (D) Surface potential map of SH3BP5 generated using APBS(83). (E) Stereo image of the feature enhanced map of switch I and switch II generated in Phenix(91) contoured at 1.0σ (blue mesh). Switch I and II residues are shown as sticks

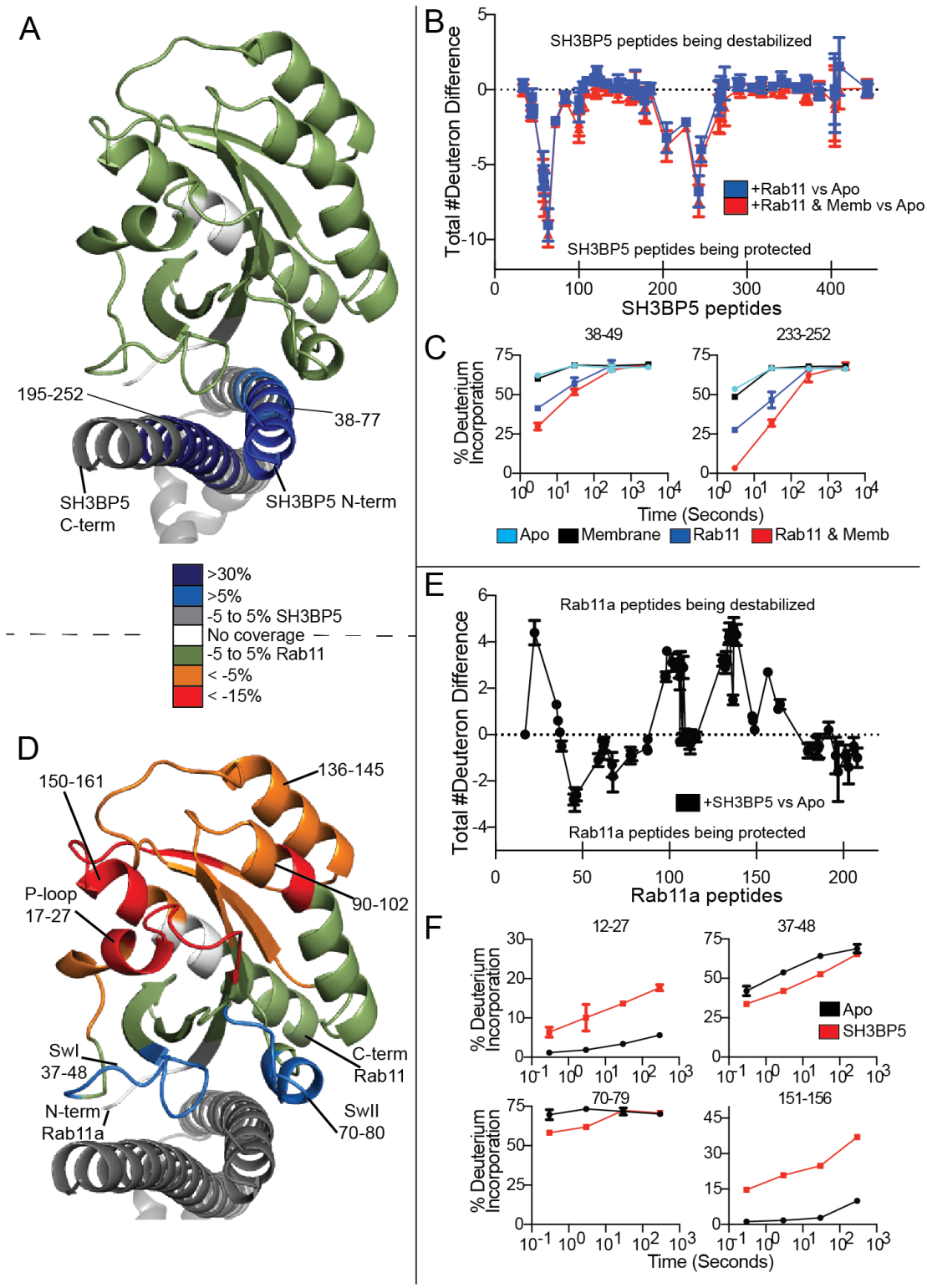

Appendix F. HDX-MS Validates the Binding Interface of Rab11 and SH3BP5, and reveals conformational changes in the nucleotide binding pocket (A) Peptides with significant changes in deuterium incorporation (both >0.5 Da and >5% at any time point) in the presence of SH3BP5 are mapped on the structure of Rab11 bound to SH3BP5. Differences are mapped according to the legend. (B) The number of deuteron difference for all peptides analyzed

over the entire deuterium exchange time course for Rab11A(Q70L) in the presence of SH3BP5 (31-455). Every point represents the central residue of an individual peptide. (C) Selected Rab11A peptides that showed decreases and increases in exchange are shown. The full list of all peptides and their deuterium incorporation is shown in Appendix J-N. (D) Peptides with significant changes in deuterium incorporation (both >0.5 Da and >5% at any time point) in the presence of WT Rab11 are mapped on the structure of SH3BP5 bound to Rab11, according to the legend. (E) The number of deuteron difference for all peptides analyzed over the entire deuterium exchange time course for SH3BP5 (31-455) in the presence of Rab11A (1-211 with a C-terminal His-tag). Experiments were conducted with and without membrane at a final concentration of 0.2mg/ml. (F) Selected SH3BP5 (31-455) peptides displaying decreases in exchange are shown. For all panels, error bars show SD (n=3).

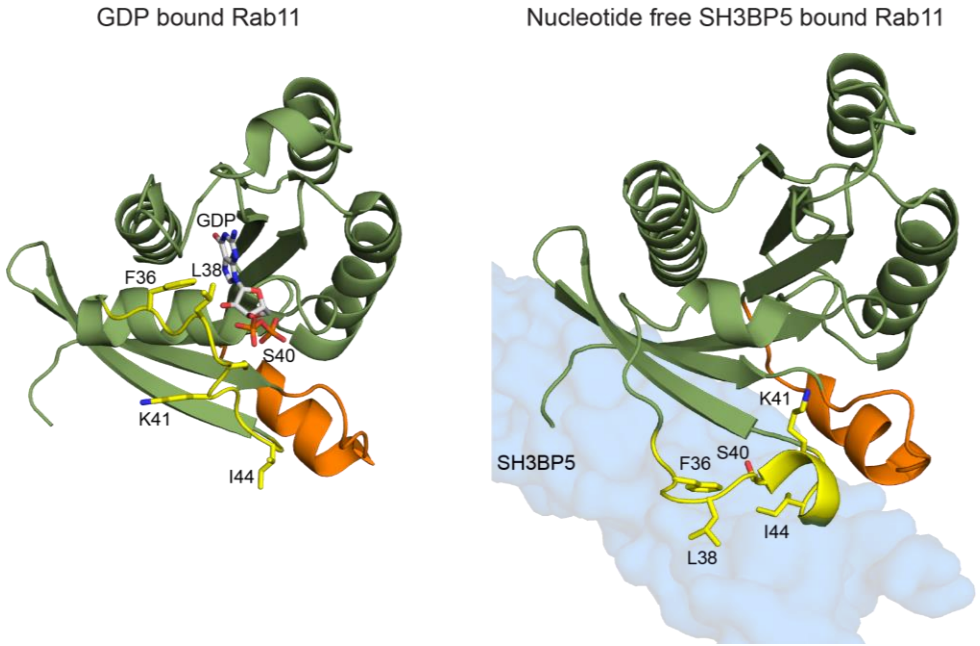

Appendix G. Comparison of GDP bound Rab11 to nucleotide-free SH3BP5 bound Rab11. Switch I is indicated in yellow, with switch II indicated in orange. Switch I residues that are important in SH3BP5 mediated nucleotide exchange are shown as sticks and labeled on the structure. F36 and L38 interact directly with bound nucleotide, and upon SH3BP5 binding these residues interaction with nucleotide is disrupted, allowing for release of bound nucleotide.

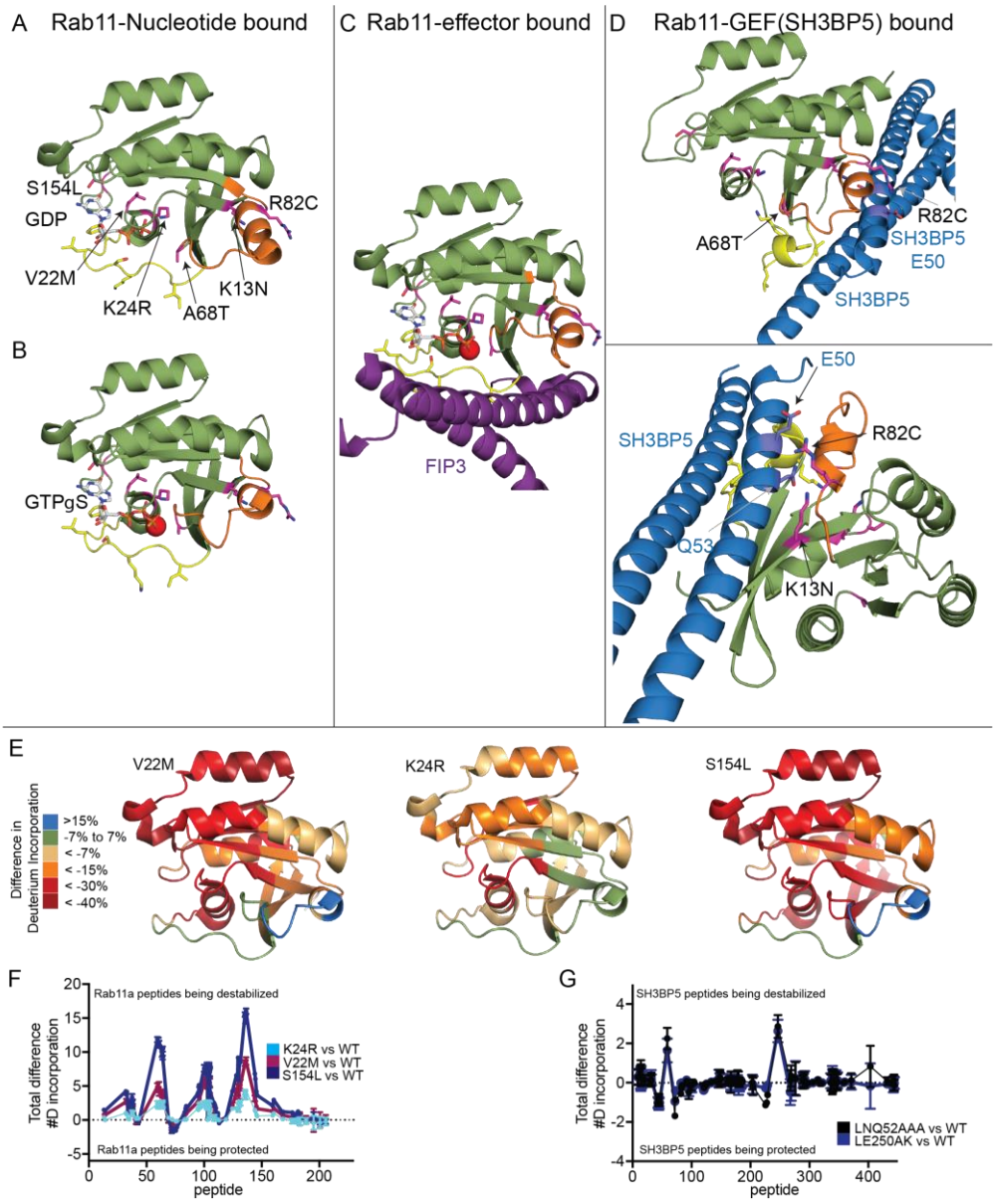

Appendix H. Disease linked mutants of Rab11a and Rab11b mapped on the structures of Rab11 bound to nucleotides, effectors, and GEFs. (A+B) Structure of Rab11 bound to GDP and GTPγS with clinical mutation sites shown in sticks and labeled on the figure. (C) Structure of Rab11 bound to GTPγS and the Rab11 effector FIP3(105). (D) Structure of Rab11 bound to SH3BP5, with two views highlighting interaction of Rab11 mutated residues with contact residues in SH3BP5. (E) HDX-MS experiments comparing WT Rab11 versus V22M, S154L, and K24R. Peptides with significant changes in deuterium incorporation (both >0.5 Da and >5% at any time point) in the mutant are colored on the structure according to the legend. Full HDX experimental data is found in Appendix J-N (F) The number of deuteron difference for all peptides analyzed over the entire deuterium exchange time course for mutant Rab11 vs WT Rab11. (G) The number of deuteron difference for all peptides analyzed over the entire deuterium exchange time course for GEF deficient mutations of SH3BP5 (LNQ52AAA and LE250AK) vs WT Rab11. For all panels, error bars show SD (n=3).

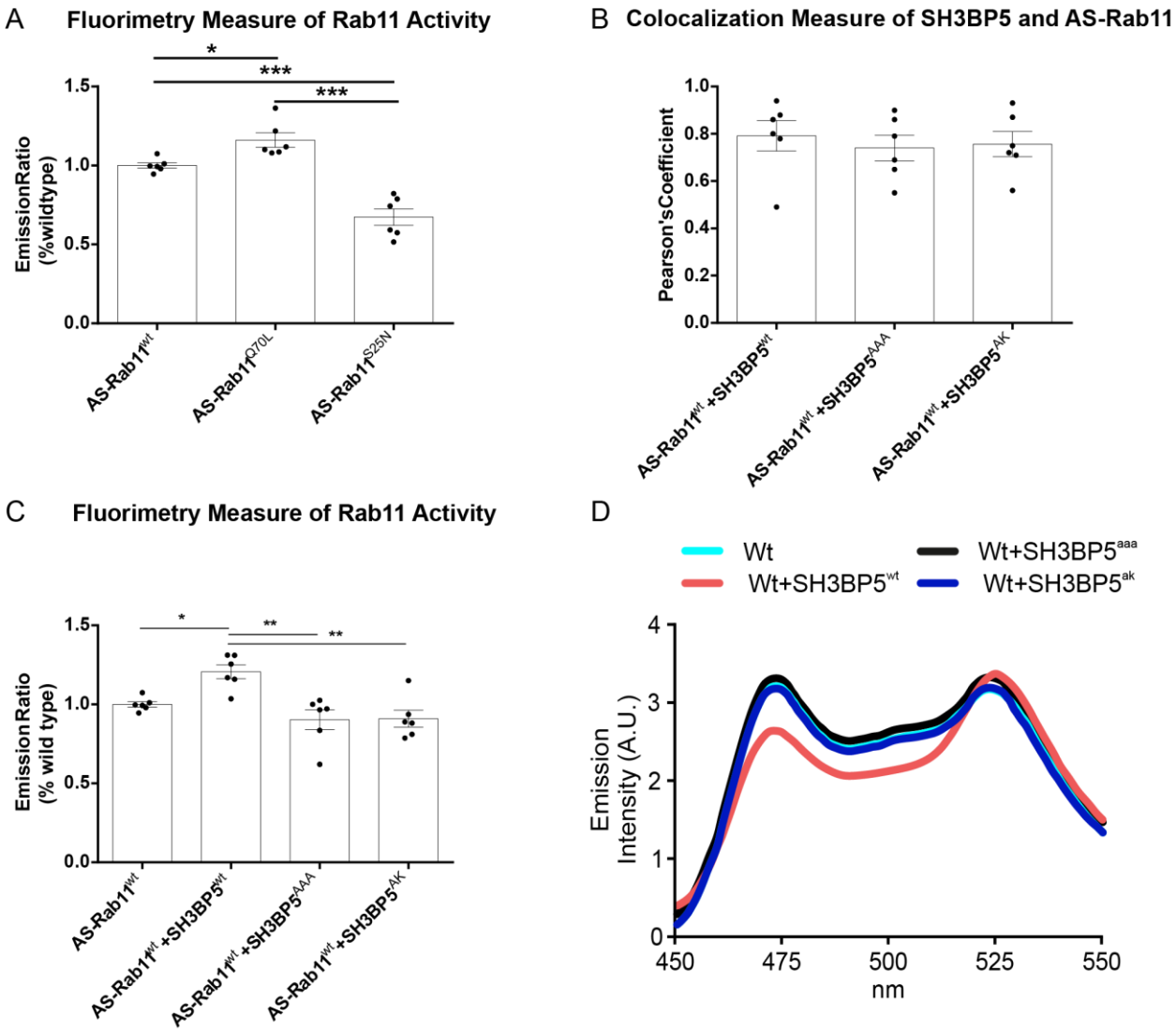

Appendix I. AS-Rab11 FRET experiments using dominant active and negative variants of Rab11 and emission spectrum from cellular experiments of Rab11 activation. (A) Quantification of FRET efficiency of AS-Rab-11wt, constitutively active form (Q70L) or dominant negative (S25N). (B) Quantification of co-localization of SH3BP5 and total AS-Rab11. (C). Quantification of FRET efficiency of AS-Rab-11wt upon overexpression of WT SH3BP5, or expression of LNQ52AAA, LE250AK. For all panels, error bars represent SEM (n=6). Significance determined by one-way ANOVA (*=p<0.05, **=p<0.01, ***=p<0.005). (D) The emission spectrum from excitation at 433 nm for WT AS-Rab11 is shown under either expression of WT-SH3BP5, and GEF deficient SH3BP5 mutant

Appendix J. Peptides used for the Identification of the Intrinsically Disordered Regions in SH3BP5.

S	E	RT	Z	Sequence	Apo 3s at	SD
3	24	7.1	4	AALKRSRSEEPAEILPPARDEE	61.9	2.1
3	25	7.1	4	AALKRSRSEEPAEILPPARDEEE	60.1	2.1
3	26	7.2	5	AALKRSRSEEPAEILPPARDEEEE	58.6	2.3
4	24	7	4	ALKRSRSEEPAEILPPARDEE	60.5	2.7
6	25	6.9	4	KRSRSEEPAEILPPARDEEE	51.5	2.1
25	30	4	1	EEEEEG	48.2	1.7
27	35	8.6	1	EEEGMEQGL	65.6	3.0
31	37	6.8	1	MEQGLEE	56.3	3.0
38	42	4.4	1	EEEVD	27.1	0.9
39	49	9.1	2	EEVDPRIQGEL	11.9	0.9
40	49	8.8	2	EVDPRIQGEL	11.6	0.7
50	66	7.3	4	EKLNQSTDDINRRETEL	4.9	0.4
50	77	10	5	EKLNQSTDDINRRETELEDARQKFRSVL	1.9	0.1
67	77	8.5	3	EDARQKFRSVL	1.3	0.0
69	77	7	3	ARQKFRSVL	1.7	0.2
78	86	7.2	1	VEATVKLDE	3.6	0.4
78	113	12	5	VEATVKLDELVKKIGKAVEDSKPYWEARRVARQAQL	5.8	0.2
87	96	4.8	2	LVKKIGKAVE	15.7	0.6
87	113	8.6	4	LVKKIGKAVEDSKPYWEARRVARQAQL	6.5	0.4
88	96	4.3	2	VKKIGKAVE	17.3	0.5
88	113	8	5	VKKIGKAVEDSKPYWEARRVARQAQL	5.4	0.3
114	127	6.3	2	EAQKATQDFQRATE	2.8	0.1
114	129	9.5	3	EAQKATQDFQRATEVL	1.6	0.1
128	134	4.3	2	VLRAAKE	4.0	0.4
128	138	8.6	2	VLRAAKETISL	2.6	0.1
139	154	7.8	3	AEQRLLEDDKRQFDSA	38.2	2.0
144	154	6.2	2	LEDDKRQFDSA	61.7	2.1
147	154	5.1	2	DKRQFDSA	64.8	2.0
148	154	4.8	2	KRQFDSA	72.6	2.2
155	164	8.6	1	WQEMLNHATQ	4.5	0.8
155	168	9.4	3	WQEMLNHATQRVME	3.1	0.2
159	168	5.3	2	LNHATQRVME	4.1	0.7
169	178	5	2	AEQTKTRSEL	4.2	0.3
169	187	5.3	4	AEQTKTRSELVHKETAARY	4.8	0.3
169	191	6.2	3	AEQTKTRSELVHKETAARYNAAM	1.9	0.3
179	187	4.5	3	VHKETAARY	5.7	0.5
179	191	5.5	2	VHKETAARYNAAM	3.2	0.3
195	212	6.6	4	RQLEKKLKRAINKSKPYF	10.9	1.0
195	214	8.2	5	RQLEKKLKRAINKSKPYFEL	7.8	0.7
213	218	5.2	2	ELKAKY	1.9	0.2
223	232	7.4	2	EQLKKTVDDL	2.8	0.1
223	233	6.7	2	EQLKKTVDDLQ	4.5	1.0
223	234	7.2	3	EQLKKTVDDLQA	3.4	0.1
223	252	12	5	EQLKKTVDDLQAKLTLAKGEYKMALKNLEM	2.3	0.2
237	252	9.9	4	TLAKGEYKMALKNLEM	4.1	0.2
239	252	9.5	3	AKGEYKMALKNLEM	4.3	0.3
244	252	9	2	KMALKNLEM	4.9	0.2
256	280	5.3	5	EIHERRRSSAMGPRGCGVGAEGSST	92.4	2.3
256	282	6	5	EIHERRRSSAMGPRGCGVGAEGSSTSV	91.6	2.6
256	297	8.2	5	EIHERRRSSAMGPRGCGVGAEGSSTSVEDLPGSKPEP	81.1	2.1
257	282	5.9	5	IHERRRSSAMGPRGCGVGAEGSSTSV	91.9	2.9
281	297	9.3	2	SVEDLPGSKPEPDAISV	68.4	1.9
283	294	6.1	2	EDLPGSKPEPDA	72.5	2.0
283	296	7.2	2	EDLPGSKPEPDAIS	70.1	2.0
283	297	8.9	2	EDLPGSKPEPDAISV	70.5	2.0
283	301	8.9	2	EDLPGSKPEPDAISVASEA	75.6	1.9
295	301	6.6	1	ISVASEA	83.2	1.5
302	309	5.7	1	FEDDSCSN	93.6	3.3
302	310	9.7	1	FEDDSCSNF	92.0	2.1
303	310	8.2	1	EDDSCSNF	92.1	2.3
311	316	3.9	1	VSEDDS	92.0	2.2
311	317	4.3	1	VSEDDSE	90.5	0.6
311	318	4.3	1	VSEDDSET	91.2	1.4
311	324	8.9	1	VSEDDSETQSVSSF	93.2	2.3
324	355	13	3	FSSGPTSPSEMPDQFPAVVRPGSLDLPSPVSL	77.6	1.4
325	334	6.8	1	SSGPTSPSEM	94.4	1.5
325	338	10	2	SSGPTSPSEMPDQF	87.7	1.5
325	347	11	2	SSGPTSPSEMPDQFPAVVRPGSL	80.9	1.5
325	353	12	3	SSGPTSPSEMPDQFPAVVRPGSLDLPSPV	72.3	1.4
325	354	12	3	SSGPTSPSEMPDQFPAVVRPGSLDLPSPVS	76.8	1.6
325	355	13	3	SSGPTSPSEMPDQFPAVVRPGSLDLPSPVSL	77.6	1.5
325	357	12	3	SSGPTSPSEMPDQFPAVVRPGSLDLPSPVSLSE	78.0	1.6
335	355	12	2	PDQFPAVVRPGSLDLPSPVSL	75.5	1.5
339	347	7.7	2	PAVVRPGSL	78.3	1.4
339	354	9.9	2	PAVVRPGSLDLPSPVS	74.0	1.5
339	355	12	2	PAVVRPGSLDLPSPVSL	76.2	1.3
356	361	11	1	SEFGMM	88.5	1.6
358	362	14	1	FGMMF	82.7	1.5
362	380	9.4	2	FPVLGPRSECSGASSPECE	74.8	1.8
363	379	7.6	2	PVLGPRSECSGASSPEC	84.2	1.8
363	380	7.5	2	PVLGPRSECSGASSPECE	84.2	1.7
381	391	3.8	2	VERGDRAEGAE	82.9	1.7
381	435	8.3	5	VERGDRAEGAENKTSDKANNNRGLSSSSGSGGSSKS	91.5	2.8
439	448	5.7	2	SKGRDGIIAD	74.2	1.7

Average % Deuterium incorporation: 100.0, 90.0, 80.0, 70.0, 60.0, 50.0, 40.0, 30.0, 20.0, 10.0

Appendix K. Peptides used for the Mapping of the SH3BP5-Rab11 binding interface

				Rab11 peptides	Apo								Complex							
S	E	Z	RT	Sequence	3s at	SD	3s	SD	30s	SD	300s	SD	3s at	SD	3s	SD	30s	SD	300s	SD
12	16	1	10.6	FKVVL	0.2	0.1	0.6	0.1	0.4	0.2	0.9	0.2	0.3	0.1	0.6	0.1	0.5	0.1	0.6	0.1
12	27	3	10.5	FKVVLIGDSGVGKSNL	1.2	0.2	1.9	0.1	3.4	0.1	5.6	0.3	6.4	1.3	10.1	3.4	13.7	0.4	17.7	0.8
28	36	2	8.5	LSRFTRNEF	5.3	0.7	13.3	0.7	25.4	0.7	36.1	0.8	7.4	0.4	17.0	0.2	33.9	0.5	42.9	0.6
28	38	2	10.3	LSRFTRNEFNL	14.1	0.7	21.5	0.6	34.2	0.7	43.8	0.5	13.9	0.6	21.9	0.3	37.2	0.5	47.3	0.4
32	36	2	6.6	TRNEF	13.6	1.6	31.8	1.6	53.5	2.4	62.6	1.7	15.0	0.4	30.2	0.3	56.6	0.4	64.6	2.0
32	38	2	9.9	TRNEFNL	25.1	1.4	37.5	1.4	59.5	1.1	71.7	2.8	23.6	1.1	34.0	0.3	55.1	0.9	69.3	2.4
37	47	2	7.4	NLESKSTIGVE	46.8	1.4	60.5	0.9	68.9	1.2	69.5	0.6	37.2	1.2	46.6	0.3	55.6	0.5	65.2	0.6
37	48	1	10.7	NLESKSTIGVEF	42.0	3.0	53.8	1.6	64.3	1.4	68.9	2.7	33.7	1.1	42.1	1.2	52.7	0.7	65.3	1.5
39	48	1	10.1	ESKSTIGVEF	30.7	2.4	43.5	0.9	55.2	1.3	65.6	0.9	23.5	1.2	32.0	0.4	42.3	0.4	58.5	0.3
48	64	4	9.2	FATRSIQVDGKTIKAQI	11.9	0.9	18.9	0.4	28.3	0.5	33.0	0.9	11.8	0.5	17.7	0.2	25.1	0.6	30.7	0.8
48	70	4	11.3	FATRSIQVDGKTIKAQIWDTAGL	8.3	0.7	13.4	0.3	26.1	0.8	31.4	0.9	8.3	0.4	13.4	0.3	24.3	0.6	29.9	0.9
49	69	3	9.7	ATRSIQVDGKTIKAQIWDTAG	8.5	0.8	13.4	0.3	23.5	0.5	27.9	0.7	9.6	0.3	13.6	0.4	21.9	0.6	27.3	0.6
49	70	3	10.8	ATRSIQVDGKTIKAQIWDTAGL	8.2	0.6	13.1	0.3	25.7	0.7	30.8	0.5	8.3	0.4	13.4	0.3	24.3	0.5	29.9	0.7
49	79	5	10.6	ATRSIQVDGKTIKAQIWDTAGLERYRAITSA	27.7	0.8	31.2	0.3	40.0	0.8	42.7	0.6	24.6	0.6	28.6	0.5	38.5	0.6	42.6	0.8
49	80	5	11.1	ATRSIQVDGKTIKAQIWDTAGLERYRAITSAY	27.8	0.9	32.4	0.3	41.2	0.9	43.4	0.6	24.1	0.8	28.9	0.4	38.9	0.9	43.4	1.1
70	79	2	6.9	LERYRAITSA	69.6	3.3	73.3	0.8	71.7	2.3	70.2	0.4	58.2	1.6	61.9	0.4	72.3	0.4	70.8	0.7
71	80	3	7.6	ERYRAITSAY	65.7	2.0	73.3	0.7	76.8	0.9	75.0	0.9	57.1	0.8	63.5	0.1	74.9	0.9	75.9	0.8
80	88	2	8.7	YYRGAVGAL	12.6	0.7	15.7	0.4	24.4	0.5	29.9	0.4	11.7	0.1	14.5	0.1	20.7	0.5	27.1	0.5
80	89	2	11.0	YYRGAVGALL	10.5	0.8	12.3	0.3	19.0	0.6	23.4	0.2	9.0	0.3	10.9	0.2	15.3	0.3	20.2	0.3
81	88	2	8.0	YRGAVGAL	11.7	0.7	12.4	0.1	15.3	0.3	21.6	0.4	10.9	0.2	12.0	0.2	14.0	0.4	19.6	0.5
89	100	2	10.3	LVYDIAKHLTYE	8.7	0.3	9.6	0.3	17.8	0.9	32.7	0.6	12.4	0.8	17.3	0.3	26.9	0.4	40.2	0.1
89	102	2	10.7	LVYDIAKHLTYENV	7.0	0.4	8.0	0.3	15.5	0.7	31.5	0.7	11.3	0.8	17.0	0.3	26.6	0.6	40.7	0.8
89	108	4	12.6	LVYDIAKHLTYENVERWLKE	4.8	0.2	6.6	0.1	18.7	0.8	31.6	0.5	7.0	0.7	11.6	0.2	23.8	0.6	38.1	1.6
89	111	5	13.4	LVYDIAKHLTYENVERWLKELRD	3.7	0.1	5.4	0.1	16.2	0.6	29.0	0.2	5.8	0.3	9.4	0.2	20.4	0.5	35.1	0.9
89	116	4	12.8	LVYDIAKHLTYENVERWLKELRDHADSN	6.0	0.1	7.7	0.0	18.7	0.9	30.0	0.5	7.7	0.4	11.1	0.2	21.8	0.6	34.6	1.7
90	100	3	9.4	VYDIAKHLTYE	9.4	0.7	10.9	0.5	19.9	1.1	35.7	0.8	13.6	0.9	19.4	0.6	30.2	0.9	44.3	1.1
90	116	5	12.5	VYDIAKHLTYENVERWLKELRDHADSN	6.1	0.2	7.8	0.1	18.5	0.8	29.9	0.6	7.6	0.7	10.8	0.3	21.3	0.6	33.8	1.8
90	117	4	12.7	VYDIAKHLTYENVERWLKELRDHADSNI	6.3	0.1	8.3	0.2	19.4	0.9	30.9	0.4	8.0	0.4	11.7	0.2	22.6	0.5	35.8	1.8
91	119	4	13.5	YDIAKHLTYENVERWLKELRDHADSNIVI	6.4	0.2	8.5	0.1	21.2	0.9	32.3	0.4	8.3	0.3	11.8	0.3	23.7	0.6	37.1	1.3
101	105	2	8.4	NVERW	6.2	1.6	12.9	1.2	49.3	1.8	55.0	2.0	4.1	1.2	9.9	0.3	42.5	1.0	54.8	0.9
101	108	2	8.9	NVERWLKE	4.2	2.9	6.6	0.8	23.6	0.3	30.1	1.1	2.4	0.5	5.2	0.7	20.3	0.5	33.1	2.7
101	111	4	10.7	NVERWLKELRD	1.9	0.8	2.9	0.3	14.9	1.2	23.1	2.0	0.6	0.4	2.6	0.4	13.8	0.7	24.6	0.4
101	116	4	11.0	NVERWLKELRDHADSN	7.4	0.4	9.4	0.2	19.4	0.9	24.9	1.0	7.0	0.4	8.6	0.3	17.3	1.0	25.7	1.7
101	117	4	11.8	NVERWLKELRDHADSNI	8.8	0.3	11.3	0.2	24.9	1.0	31.0	0.8	8.4	0.4	10.4	0.4	22.3	1.1	31.9	2.3
103	116	4	8.5	ERWLKELRDHADSN	8.4	0.6	9.3	0.5	12.7	0.4	16.1	1.0	8.5	0.5	9.2	0.2	12.1	0.5	17.2	0.9
106	116	2	4.3	LKELRDHADSN	13.1	1.2	13.5	0.4	17.6	0.8	20.7	0.4	12.4	0.3	13.4	0.1	16.4	0.3	20.7	0.9
107	117	3	4.4	KELRDHADSNI	11.9	0.6	12.5	0.7	16.0	0.6	19.5	0.8	11.8	0.5	12.9	0.5	15.7	0.4	19.9	0.7
109	116	2	3.4	LRDHADSN	20.0	1.0	21.5	0.5	27.1	0.8	28.9	1.9	19.7	0.8	21.2	0.8	25.8	0.8	29.0	2.0
117	138	4	9.8	IVIMLVGNKSDLRHLRAVPTDE	2.4	0.2	7.3	0.4	15.9	0.6	22.5	0.6	6.6	0.7	13.5	0.4	20.7	0.4	27.8	0.4
118	150	5	10.9	VIMLVGNKSDLRHLRAVPTDEARAFAEKNGLSF	2.7	0.5	7.4	0.4	15.0	0.3	21.1	0.8	5.6	0.7	12.0	0.3	18.6	1.2	27.7	0.6
120	138	4	7.9	MLVGNKSDLRHLRAVPTDE	3.5	0.4	9.8	0.4	20.3	0.5	25.1	0.6	8.4	0.2	17.5	0.6	26.0	0.9	30.0	0.7
121	138	3	7.0	LVGNKSDLRHLRAVPTDE	4.2	0.5	11.1	0.7	22.7	0.7	28.7	0.7	10.4	1.1	20.5	0.4	29.5	0.2	34.4	0.5
121	141	5	6.7	LVGNKSDLRHLRAVPTDEARA	3.4	0.5	8.6	0.5	18.4	0.7	24.2	0.8	7.8	0.5	16.6	0.5	25.8	0.3	32.4	0.9
121	150	5	10.2	LVGNKSDLRHLRAVPTDEARAFAEKNGLSF	3.1	0.4	8.0	0.5	16.7	0.5	22.2	0.7	5.6	0.4	12.4	0.2	20.3	0.5	30.3	1.1
122	141	4	6.2	VGNKSDLRHLRAVPTDEARA	3.7	0.4	9.4	0.5	19.8	0.8	25.8	0.8	9.6	1.8	18.4	0.7	27.3	0.2	34.4	0.9
139	138	3	4.8	RHLRAVPTDE	8.0	1.3	18.2	1.3	32.2	1.0	40.8	0.7	12.6	1.0	27.2	0.8	39.1	0.2	46.3	1.5
139	150	3	9.4	ARAFAEKNGLSF	3.3	0.5	8.7	0.5	16.4	0.3	22.7	0.3	4.0	0.2	10.0	0.1	17.1	0.2	28.5	0.5
140	150	2	9.5	RAFAEKNGLSF	4.1	0.4	9.6	0.6	18.1	0.3	24.8	1.0	4.5	0.6	11.1	0.2	17.9	0.3	30.1	0.7
142	150	1	10.0	FAEKNGLSF	5.5	0.7	13.6	0.9	24.5	0.4	31.8	0.8	6.3	0.4	14.7	0.2	23.9	0.2	34.5	0.2
151	156	1	7.9	IETSAL	1.2	0.1	1.8	0.2	2.8	0.3	10.0	1.2	14.7	0.6	20.8	0.3	24.8	0.6	37.1	0.4
157	162	1	4.2	DSTNVE	11.8	0.6	22.7	1.0	41.3	1.1	56.4	0.1	19.0	1.5	33.1	0.6	49.7	0.4	63.9	0.9
157	164	1	5.0	DSTNVEAA	9.7	0.8	20.7	1.1	41.6	1.1	52.8	2.4	14.2	1.0	28.3	0.5	48.4	1.0	60.6	1.1
170	183	3	8.6	TEIYRIVSQKQMSD	30.8	1.5	35.0	0.4	40.9	0.5	42.3	0.8	29.2	0.8	32.5	0.1	38.4	0.8	42.0	1.6
170	193	4	7.8	TEIYRIVSQKQMSDRRENDMSPSN	35.7	1.2	37.6	0.2	41.3	0.8	40.7	0.9	34.8	0.4	36.5	0.5	40.0	0.4	41.1	0.8
172	193	4	6.9	IYRIVSQKQMSDRRENDMSPSN	41.1	1.1	43.3	0.8	46.4	1.1	46.4	1.0	40.1	1.0	41.8	0.3	45.2	0.5	45.8	0.7
172	216	5	8.5	IYRIVSQKQMSDRRENDMSPSNNVVPIHVPPTTENKPKVQCCQNI	44.0	1.5	47.0	1.1	49.9	1.5	48.7	0.9	42.9	0.8	45.4	1.1	48.1	1.2	48.3	1.2
173	183	3	6.5	YRIVSQKQMSD	41.8	1.5	47.1	1.2	54.4	0.9	55.7	1.2	39.4	1.1	44.2	0.4	52.2	0.3	54.5	0.1
173	193	4	6.2	YRIVSQKQMSDRRENDMSPSN	44.0	1.7	46.2	1.0	49.4	1.2	49.6	1.1	43.4	0.9	45.1	0.3	48.8	0.2	49.1	0.8
173	212	5	7.6	YRIVSQKQMSDRRENDMSPSNNVVPIHVPPTTENKPKVQC	49.7	1.6	51.5	0.3	53.9	0.8	52.8	0.9	48.3	0.5	50.5	0.6	52.8	0.6	52.8	0.8
184	193	2	4.3	RRENDMSPSN	58.4	2.0	59.2	2.3	59.3	1.4	57.8	1.2	57.4	2.1	60.2	1.0	59.9	1.0	58.7	2.0
184	212	5	7.5	RRENDMSPSNNVVPIHVPPTTENKPKVQC	60.1	1.3	62.4	0.2	63.3	0.9	61.8	0.7	58.5	0.8	60.9	0.6	61.9	0.4	60.9	0.2
184	216	5	8.3	RRENDMSPSNNVVPIHVPPTTENKPKVQCCQNI	53.2	1.6	56.5	0.7	58.9	1.1	57.1	1.0	51.2	0.8	54.4	0.8	56.8	0.9	56.3	0.7
194	212	3	7.5	NVVPIHVPPTTENKPKVQC	68.2	2.3	73.2	0.4	74.4	1.0	72.6	0.5	68.2	1.2	72.4	0.4	72.9	0.4	72.0	0.3
194	216	4	8.2	NVVPIHVPPTTENKPKVQCCQNI	60.0	1.6	64.8	0.6	68.4	1.0	66.8	0.6	58.0	1.1	63.1	0.5	66.0	0.5	65.4	0.3

Appendix L. Peptides used for Mapping the interfaces between SH3BP5-Rab11 Complex and membrane

				SH3BP5 peptides	Apo								SH3+MEM							
S	E	RT	Z	Sequence	3s	SD	30s	SD	300s	SD	3000s	SD	3s	SD	30s	SD	300s	SD	3000s	SD
30	37	7.9	1	GMEQGLEE	64.5	1.6	64.3	0.9	62.7	2.4	64.4	0.6	66.2	0.3	65.6	0.8	65.5	0.3	65.7	1.2
30	38	8.2	1	GMEQGLEEE	65.2	1.5	65.6	1.2	63.4	3.8	64.8	1.4	67.7	0.5	66.6	2.0	65.8	1.6	66.8	2.6
38	49	9.5	2	EEEVDPRIQGEL	62.2	0.6	68.5	0.8	66.9	2.1	67.5	1.3	60.1	0.7	68.8	1.0	68.4	1.3	69.1	0.5
39	49	9.3	2	EEVDPRIQGEL	64.6	0.9	71.4	0.8	69.8	2.1	70.5	1.1	62.0	0.7	71.8	0.9	71.1	1.1	71.7	0.5
40	49	9.0	2	EVDPRIQGEL	63.9	1.2	70.8	1.1	69.7	2.3	70.6	0.8	61.6	0.4	71.2	1.2	71.5	0.9	71.8	0.4
43	49	7.9	2	PRIQGEL	71.7	1.3	81.6	2.4	80.5	2.5	78.4	0.1	68.0	0.2	80.8	2.0	80.0	1.1	79.2	2.4
50	65	5.7	3	EKLNQSTDDINRRETE	36.1	2.3	59.5	1.0	59.1	3.8	59.5	1.3	34.8	0.3	60.2	0.2	60.8	0.9	61.0	2.5
50	66	7.6	3	EKLNQSTDDINRRETEL	32.4	1.1	54.6	0.6	56.8	2.7	58.8	1.5	30.4	0.1	54.7	0.5	60.0	0.1	60.1	0.5
50	68	7.5	3	EKLNQSTDDINRRETELED	27.5	1.1	49.9	1.0	55.7	2.2	56.7	1.5	26.7	1.0	50.4	1.3	58.1	2.1	62.0	0.3
50	77	10.3	4	EKLNQSTDDINRRETELEDARQKFRSVL	14.6	0.7	30.9	0.1	43.7	1.0	58.2	1.7	12.4	0.8	30.2	0.6	43.1	1.7	61.7	2.0
67	77	8.8	3	EDARQKFRSVL	1.2	0.3	4.4	0.5	21.9	1.8	59.2	1.1	1.0	0.0	3.8	0.4	21.2	1.8	62.3	0.5
79	88	10.3	2	EATVKLDELV	2.7	1.2	4.8	2.3	15.8	3.0	52.8	1.1	2.4	0.7	4.6	1.8	16.7	5.2	54.5	0.8
87	113	8.7	5	LVKKIGKAVEDSKPYWEARRVARQAQL	9.6	0.5	22.3	0.5	37.9	1.6	61.5	3.1	8.9	0.0	21.5	0.5	40.1	0.4	66.3	1.2
88	113	8.3	5	VKKIGKAVEDSKPYWEARRVARQAQL	8.1	0.6	19.3	0.4	34.2	2.0	59.2	2.4	7.7	0.1	18.6	0.4	37.2	0.4	64.0	0.1
97	113	8.8	4	DSKPYWEARRVARQAQL	1.5	0.3	5.5	0.3	24.8	1.6	62.4	0.5	1.3	0.0	5.6	0.3	27.0	1.6	68.4	0.1
105	113	4.7	2	RRVARQAQL	1.8	0.4	4.8	0.9	26.0	1.3	66.0	1.8	1.7	0.8	5.2	0.6	29.9	0.7	70.7	1.3
114	125	5.8	3	EAQKATQDFQRA	4.3	0.6	17.5	1.6	51.5	1.3	74.2	1.3	4.7	0.1	19.3	1.8	55.3	0.5	75.2	0.8
114	127	6.5	2	EAQKATQDFQRATE	3.6	0.5	18.5	0.6	57.1	1.4	77.0	1.0	3.7	0.0	19.8	1.1	61.1	0.4	78.2	0.4
114	129	9.8	2	EAQKATQDFQRATEVL	2.1	0.4	12.5	0.1	47.2	1.1	70.8	1.5	1.9	0.0	13.1	0.4	49.8	1.4	72.5	1.0
122	129	8.7	2	FQRATEVL	3.9	0.7	16.2	0.6	51.5	0.4	77.8	0.7	3.4	0.1	18.5	1.3	55.2	0.9	79.6	0.5
128	134	4.0	2	VLRAAKE	5.3	1.5	29.2	0.9	69.2	1.1	77.7	3.5	6.2	0.1	30.9	1.6	70.3	1.2	77.1	2.1
130	138	8.0	2	RAAKETISL	25.1	0.7	56.5	0.3	69.7	2.6	72.7	1.3	25.6	0.6	59.0	0.4	72.7	0.2	73.7	0.6
139	143	5.3	1	AEQRL	63.3	2.0	83.6	0.5	82.5	1.5	83.8	2.6	64.6	2.1	84.2	1.5	84.0	0.2	83.0	1.3
139	154	8.0	3	AEQRLLEDDKRQFDSA	53.3	0.9	59.2	0.4	56.8	2.6	58.6	1.8	54.5	0.7	60.2	0.5	59.7	0.1	60.0	0.6
144	154	6.4	2	LEDDKRQFDSA	51.0	1.8	52.0	0.6	50.4	2.7	51.2	0.6	53.7	0.3	52.4	0.9	52.4	0.5	51.8	0.8
147	154	5.3	2	DKRQFDSA	65.7	2.4	68.1	1.0	66.2	2.4	67.4	1.7	68.7	0.1	67.5	1.2	67.8	1.6	67.1	1.1
155	168	9.3	2	WQEMLNHATQRVME	23.8	0.7	56.4	0.6	64.2	2.0	64.5	0.8	24.0	0.5	57.8	0.5	65.3	1.4	66.1	0.5
156	168	7.8	3	QEMLNHATQRVME	22.4	0.8	55.8	0.7	63.8	2.1	64.6	1.0	23.2	0.6	57.6	0.6	66.5	0.1	65.7	0.5
156	178	9.1	4	QEMLNHATQRVMEAEQTKTRSEL	15.0	0.1	49.6	1.3	67.7	1.9	69.9	2.3	14.2	0.0	50.4	0.8	67.8	1.9	69.6	0.8
169	178	5.0	2	AEQTKTRSEL	9.8	0.7	43.0	0.4	66.1	2.5	67.6	1.8	9.5	0.2	43.2	1.2	67.6	1.4	67.4	1.0
169	187	5.5	4	AEQTKTRSELVHKETAARY	3.9	0.6	18.4	0.4	39.5	3.2	47.8	1.4	3.8	0.6	18.8	0.8	41.4	1.2	48.2	1.3
169	191	6.4	4	AEQTKTRSELVHKETAARYNAAM	2.9	0.4	16.3	0.3	38.3	2.1	51.0	1.1	2.7	0.1	16.2	0.3	41.3	0.4	53.5	0.2
170	178	5.0	2	EQTKTRSEL	8.8	0.7	39.0	0.4	63.6	1.9	64.9	1.5	8.5	0.3	39.0	1.1	64.1	1.6	64.1	2.2
179	191	5.7	2	VHKETAARYNAAM	2.7	0.6	12.4	0.6	37.4	0.8	55.3	1.1	2.9	0.0	11.6	0.5	39.1	0.3	58.6	0.4
195	214	8.5	5	RQLEKKLKRAINKSKPYFEL	15.4	1.3	27.8	1.3	37.3	3.3	55.8	3.8	13.8	0.0	26.0	0.8	40.0	1.1	59.1	0.2
223	232	7.7	2	EQLKKTVDDL	1.5	0.4	7.3	0.3	25.2	1.2	56.6	1.3	1.1	0.1	6.9	0.1	27.6	0.3	59.5	0.5
233	252	10.2	3	QAKLTLAKGEYKMALKNLEM	53.7	1.0	66.6	0.2	66.7	1.5	66.3	1.1	48.7	1.3	66.8	0.9	68.0	1.5	68.1	1.7
239	252	9.7	3	AKGEYKMALKNLEM	63.3	0.6	67.4	0.3	66.0	1.8	65.9	0.8	58.6	0.5	67.9	0.5	67.2	1.6	67.7	1.1
253	280	6.2	4	ISDEIHERRRSSAMGPRGCGVGAEGSST	48.1	2.6	49.6	1.0	47.7	2.7	48.9	0.7	51.6	0.5	51.2	1.1	51.0	0.9	49.8	0.8
253	282	6.7	5	ISDEIHERRRSSAMGPRGCGVGAEGSSTSV	50.0	1.5	50.6	0.6	48.3	2.8	50.1	1.4	52.2	0.7	51.5	0.4	51.7	0.2	51.1	0.6
253	294	7.3	5	ISDEIHERRRSSAMGPRGCGVGAEGSSTSVEDLPGSKPEPDA	50.6	1.1	50.8	0.8	49.0	2.0	50.7	1.4	52.1	0.9	51.6	0.6	51.7	0.2	51.7	0.6
256	282	6.2	4	EIHERRRSSAMGPRGCGVGAEGSSTSV	52.0	2.6	53.0	0.6	51.5	2.8	52.6	1.1	54.8	0.7	53.7	0.7	54.2	0.6	53.4	0.4
281	297	9.6	2	SVEDLPGSKPEPDAISV	65.9	0.4	66.6	0.3	65.2	1.6	65.6	1.2	66.8	0.7	67.0	0.8	66.5	1.1	66.9	0.6
283	297	9.2	2	EDLPGSKPEPDAISV	68.0	0.3	68.4	0.4	66.7	2.4	67.7	0.8	69.0	0.4	69.0	0.4	68.4	0.9	69.0	0.5
283	301	9.1	2	EDLPGSKPEPDAISVASEA	71.5	0.5	71.7	0.2	69.9	2.5	71.3	1.1	72.6	0.2	72.5	0.5	71.8	0.9	72.6	0.3
302	310	10.0	2	FEDDSCSNF	38.8	0.5	38.9	1.0	37.7	1.5	37.5	1.3	39.3	1.5	39.6	1.1	38.8	1.5	38.7	0.8
310	324	10.0	2	FVSEDDSETQSVSSF	64.5	0.9	63.5	0.7	63.0	1.5	62.1	1.4	63.6	0.9	63.6	0.8	63.4	1.7	63.1	1.0
311	324	9.2	2	VSEDDSETQSVSSF	65.2	0.9	64.4	0.6	63.2	2.2	63.6	0.6	65.0	0.3	65.1	0.4	64.5	1.5	65.2	0.6
324	338	10.8	2	FSSGPTSPSEMPDQF	63.2	0.4	64.0	0.6	62.6	1.4	63.1	1.4	64.9	1.4	64.6	1.4	64.4	1.0	64.5	0.9
325	357	12.4	3	SSGPTSPSEMPDQFPAVVRPGSLDLPSPVSLSE	66.1	0.3	67.3	0.2	66.4	0.8	67.1	1.2	68.7	0.0	68.2	0.3	68.3	0.2	68.0	0.4
339	354	10.2	2	PAVVRPGSLDLPSPVS	80.4	0.5	80.7	0.1	79.3	1.2	79.7	1.4	81.9	0.2	81.3	0.4	80.9	0.7	81.3	1.1
339	355	11.9	2	PAVVRPGSLDLPSPVSL	76.9	0.3	77.9	0.2	77.0	1.1	77.3	1.5	78.7	0.4	78.2	0.8	78.5	0.6	78.2	0.4
356	361	11.5	1	SEFGMM	71.4	0.3	71.4	0.8	70.0	2.2	69.0	2.3	71.8	1.8	71.8	1.4	70.6	1.6	70.1	0.6
358	362	14.1	1	FGMMF	74.8	0.7	75.9	0.3	75.2	1.0	75.7	1.8	77.0	0.1	76.0	0.6	76.0	0.3	76.1	0.6
359	380	12.1	2	GMMFPVLGPRSECSGASSPECE	51.5	0.2	52.7	0.4	51.6	1.2	51.6	1.4	53.8	1.2	53.9	1.3	53.8	0.6	53.0	0.3
363	379	7.7	2	PVLGPRSECSGASSPEC	67.0	0.5	67.6	0.7	65.6	2.4	67.5	1.3	69.5	0.4	68.8	0.7	68.8	0.1	68.9	0.9
363	380	7.7	2	PVLGPRSECSGASSPECE	65.0	0.6	65.5	0.6	63.6	2.0	65.7	1.5	67.2	0.8	66.7	0.4	66.5	0.0	66.8	0.7
380	391	4.1	3	EVERGDRAEGAE	57.9	1.5	60.0	1.0	59.2	0.5	58.5	2.4	61.0	0.3	59.3	1.8	59.5	1.0	57.4	0.6
381	391	3.9	2	VERGDRAEGAE	58.6	1.7	59.4	0.6	59.0	1.9	58.1	2.4	61.2	0.4	59.8	1.8	59.3	1.1	55.9	2.0
381	427	5.6	5	VERGDRAEGAENKTSDKANNNRGLSSSSGSGGSSKSQSSTSPEGQAL	50.1	2.3	51.9	1.0	49.5	3.0	50.8	1.1	53.3	0.1	52.1	1.0	52.6	0.6	51.3	0.6
381	428	5.7	5	VERGDRAEGAENKTSDKANNNRGLSSSSGSGGSSKSQSSTSPEGQALE	50.5	2.9	52.6	0.8	50.4	2.9	51.7	0.8	54.1	0.1	53.0	1.0	53.5	0.3	52.1	0.5
381	438	9.9	5	VERGDRAEGAENKTSDKANNNRGLSSSSGSGGSSKSQSSTSPEGQALENRMKQLSLQC	42.5	0.6	43.2	0.5	41.6	1.3	41.7	0.9	42.9	1.4	43.4	0.7	42.7	1.4	42.6	1.1
437	448	6.1	2	QCSKGRDGIIAD	59.1	0.9	59.6	0.9	60.1	4.8	59.2	0.4	61.1	0.2	59.8	0.2	60.2	0.9	59.2	0.4
439	448	6.0	2	SKGRDGIIAD	58.8	2.2	60.5	0.2	58.3	2.5	59.4	1.1	61.4	0.5	60.4	1.3	60.3	0.6	59.3	1.0

Relative % Deuterium Incorporation
100.0
90.0
80.0
70.0
60.0
50.0
40.0
30.0
20.0
10.0

					SH3 + MEM + Rab								SH3 + Rab							
S	E	RT	Z	Sequence	3s	SD	30s	SD	300s	SD	3000s	SD	3s	SD	30s	SD	300s	SD	3000s	SD
30	37	7.9	1	GMEQGLEE	64.6	1.4	66.0	0.7	64.4	1.3	65.5	0.8	63.9	0.4	63.5	0.9	65.2	2.7	64.7	1.2
30	38	8.2	1	GMEQGLEEE	65.4	1.8	66.9	1.4	64.8	2.6	66.0	1.5	64.3	1.3	64.0	1.9	65.6	3.5	64.9	1.8
38	49	9.5	2	EEEVDPRIQGEL	29.8	2.3	51.9	2.0	65.5	1.6	68.4	1.4	41.3	0.6	58.6	1.9	68.4	3.4	68.2	0.9
39	49	9.3	2	EEVDPRIQGEL	28.8	2.4	52.9	1.8	68.1	1.4	70.7	1.2	41.4	1.1	60.9	2.6	71.7	4.0	71.7	0.7
40	49	9.0	2	EVDPRIQGEL	30.2	6.7	54.7	2.6	70.1	1.0	75.3	0.6	45.8	2.9	63.0	0.2	73.9	2.1	73.6	0.6
43	49	7.9	2	PRIQGEL	26.7	3.4	55.4	1.7	75.3	1.4	79.6	1.2	42.0	0.9	66.2	3.3	82.7	4.3	78.7	1.9
50	65	5.7	3	EKLNQSTDDINRRETE	8.3	5.4	28.2	2.7	50.1	3.4	59.5	1.2	22.2	0.2	40.9	1.1	55.8	7.3	58.1	3.9
50	66	7.6	3	EKLNQSTDDINRRETEL	9.6	3.4	24.8	1.1	47.0	2.4	57.8	0.4	18.6	0.2	35.8	4.1	55.1	5.0	58.0	2.6
50	68	7.5	3	EKLNQSTDDINRRETELED	7.1	1.7	22.7	1.4	43.9	2.3	58.1	0.6	17.6	1.1	33.9	1.3	54.0	2.4	58.5	2.0
50	77	10.3	4	EKLNQSTDDINRRETELEDARQKFRSVL	4.3	1.2	13.3	0.7	31.2	2.3	53.1	2.4	8.4	0.8	21.0	1.6	38.9	3.3	56.3	1.4
67	77	8.8	3	EDARQKFRSVL	1.1	0.4	2.4	0.4	13.5	1.0	46.6	1.4	1.0	0.3	3.6	0.6	17.3	2.5	51.8	2.1
79	88	10.3	2	EATVKLDELV	2.5	1.2	4.0	1.8	13.5	1.2	49.7	1.1	3.2	1.7	4.8	1.6	15.1	1.3	53.9	0.8
87	113	8.7	5	LVKKIGKAVEDSKPYWEARRVARQAQL	8.1	0.9	17.5	0.1	37.7	1.4	61.4	1.3	9.6	0.3	22.4	0.0	40.7	1.4	63.6	1.3
88	113	8.3	5	VKKIGKAVEDSKPYWEARRVARQAQL	6.8	0.6	15.0	0.4	34.7	0.9	59.9	0.6	8.1	0.3	19.5	0.2	36.9	0.5	62.0	1.5
97	113	8.8	4	DSKPYWEARRVARQAQL	1.7	0.8	5.6	0.5	25.9	0.6	62.3	1.2	1.6	0.4	6.5	0.1	28.2	2.1	66.8	0.7
105	113	4.7	2	RRVARQAQL	2.4	0.1	5.3	0.6	29.9	2.7	70.1	1.7	1.9	0.8	5.4	0.1	27.8	1.8	70.2	1.2
114	125	5.8	3	EAQKATQDFQRA	4.9	0.9	16.0	1.2	57.5	1.7	76.1	0.8	4.9	0.9	17.3	1.7	54.4	3.9	74.4	2.6
114	127	6.5	2	EAQKATQDFQRATE	4.2	0.9	16.9	1.2	62.5	1.8	78.4	0.8	3.9	0.6	19.4	2.0	59.6	3.3	77.0	2.5
114	129	9.8	2	EAQKATQDFQRATEVL	2.5	0.8	12.2	0.8	53.5	1.4	72.6	1.8	2.3	0.4	13.3	1.5	50.1	2.0	72.5	1.1
122	129	8.7	2	FQRATEVL	3.9	1.1	15.8	0.6	58.8	0.7	80.6	1.3	4.0	0.8	18.0	0.7	54.4	1.8	79.0	1.5
128	134	4.0	2	VLRAAKE	7.7	1.4	31.5	1.2	73.7	2.4	78.7	3.2	5.6	0.2	28.0	3.6	70.4	4.7	79.8	2.1
130	138	8.0	2	RAAKETISL	23.3	0.3	58.6	0.2	72.5	1.4	74.0	0.6	24.2	1.1	55.6	2.4	72.7	3.1	73.6	1.7
139	143	5.3	1	AEQRL	58.3	2.1	84.8	1.0	82.9	1.7	84.8	1.1	61.9	1.9	82.4	1.1	85.2	5.8	83.6	2.1
139	154	8.0	3	AEQRLLEDDKRQFDSA	51.4	1.0	60.2	0.8	58.1	1.7	59.4	0.5	52.5	0.9	57.8	0.6	59.1	2.3	59.0	2.1
144	154	6.4	2	LEDDKRQFDSA	52.6	1.1	53.2	0.9	52.2	0.6	53.0	0.8	52.1	0.9	51.2	0.6	51.6	3.8	51.4	2.5
147	154	5.3	2	DKRQFDSA	68.1	1.1	68.5	1.5	67.5	1.3	68.3	1.9	66.7	1.4	65.7	1.1	67.9	5.5	66.5	1.8
155	168	9.3	2	WQEMLNHATQRVME	20.5	0.5	55.1	1.2	65.4	2.0	65.9	1.6	22.4	0.5	55.2	1.7	66.5	3.0	65.8	1.1
156	168	7.8	3	QEMLNHATQRVME	19.4	0.1	54.6	0.5	64.7	1.6	65.3	0.5	21.4	1.2	54.5	1.3	65.5	2.9	64.7	1.6
156	178	9.1	4	QEMLNHATQRVMEAEQTKTRSEL	12.4	0.7	48.2	2.2	69.1	1.4	71.2	1.4	14.1	1.0	47.9	1.2	69.4	2.3	68.5	1.4
169	178	5.0	2	AEQTKTRSEL	8.7	0.7	38.7	0.7	65.8	2.1	68.3	1.9	9.9	0.5	42.0	2.5	67.2	6.0	67.3	2.2
169	187	5.5	4	AEQTKTRSELVHKETAARY	3.3	0.5	15.2	0.6	38.1	2.4	48.2	2.3	3.8	0.3	16.8	1.0	38.4	4.9	47.1	3.6
169	191	6.4	4	AEQTKTRSELVHKETAARYNAAM	2.7	0.6	13.3	0.6	38.5	1.3	52.8	0.9	3.1	0.3	15.5	1.1	38.3	3.3	50.5	3.2
170	178	5.0	2	EQTKTRSEL	8.3	0.3	35.5	0.4	63.4	2.3	65.4	2.5	9.3	0.4	38.7	2.8	65.1	5.8	65.1	3.0
179	191	5.7	2	VHKETAARYNAAM	3.0	0.8	10.2	0.9	37.1	1.7	58.4	2.0	3.0	0.4	12.3	1.2	38.1	2.3	57.3	1.5
195	214	8.5	5	RQLEKKLKRAINKSKPYFEL	9.8	1.3	19.7	0.4	31.7	1.3	50.7	1.4	14.6	0.5	27.0	0.7	40.0	0.9	56.6	2.3
223	232	7.7	2	EQLKKTVDDL	1.4	0.5	5.1	0.6	17.9	0.9	39.3	1.2	1.5	0.5	6.4	0.7	21.0	2.3	48.7	2.9
233	252	10.2	3	QAKLTLAKGEYKMALKNLEM	3.5	1.4	32.1	2.1	62.3	4.3	67.2	2.2	27.6	1.5	45.4	4.2	68.2	3.2	67.4	1.4
239	252	9.7	3	AKGEYKMALKNLEM	18.1	3.9	33.9	2.3	63.2	4.4	66.7	1.9	32.9	1.6	47.1	3.9	67.2	3.6	66.7	1.1
253	280	6.2	4	ISDEIHERRRSSAMGPRGCGVGAEGSST	44.0	0.5	47.2	0.9	48.6	1.8	49.8	1.1	45.2	0.8	45.9	0.2	47.8	4.6	47.8	2.6
253	282	6.7	5	ISDEIHERRRSSAMGPRGCGVGAEGSSTSV	45.5	0.6	48.1	0.4	49.3	0.8	50.8	0.4	46.1	0.6	47.3	0.4	49.0	3.2	48.7	2.8
253	294	7.3	5	ISDEIHERRRSSAMGPRGCGVGAEGSSTSVEDLPGSKPEPDA	48.1	0.7	49.9	0.2	50.1	0.9	52.0	0.5	48.2	0.6	49.1	0.1	51.1	2.1	50.4	2.0
256	282	6.2	4	EIHERRRSSAMGPRGCGVGAEGSSTSV	50.6	1.0	52.4	0.7	52.0	1.2	53.4	0.9	50.6	0.9	50.8	0.0	51.7	4.1	51.2	2.6
281	297	9.6	2	SVEDLPGSKPEPDAISV	65.8	1.1	66.6	1.5	66.5	1.5	66.8	1.2	64.6	0.6	65.1	1.0	67.3	3.2	66.3	1.0
283	297	9.2	2	EDLPGSKPEPDAISV	67.9	1.0	68.6	1.2	68.2	1.3	68.5	1.1	66.6	0.9	67.1	0.9	69.1	3.2	68.3	1.1
283	301	9.1	2	EDLPGSKPEPDAISVASEA	71.6	1.1	72.0	1.3	71.8	1.5	72.1	1.3	70.0	0.7	70.2	1.2	72.4	3.5	71.4	1.3
302	310	10.0	2	FEDDSCSNF	38.2	1.4	38.4	1.8	38.4	0.6	38.7	1.4	36.9	1.2	38.1	0.2	38.5	2.0	38.5	1.7
310	324	10.0	2	FVSEDDSETQSVSSF	63.7	0.7	63.7	2.2	63.4	0.8	63.7	2.2	62.6	1.4	63.5	0.2	65.7	2.7	63.9	1.2
311	324	9.2	2	VSEDDSETQSVSSF	64.3	0.7	64.6	1.4	63.8	1.8	65.1	1.4	63.4	0.6	63.8	0.1	65.8	3.2	64.2	1.3
324	338	10.8	2	FSSGPTSPSEMPDQF	63.5	1.2	63.5	1.5	64.0	0.5	63.9	1.3	61.5	0.9	62.5	0.6	64.4	3.4	63.2	1.0
325	357	12.4	3	SSGPTSPSEMPDQFPAVVRPGSLDLPSPVSLSE	67.5	0.7	67.7	0.6	67.7	0.8	68.3	0.6	65.8	0.3	66.2	0.7	68.4	3.0	67.2	0.8
339	354	10.2	2	PAVVRPGSLDLPSPVS	81.0	0.8	81.4	1.3	81.2	0.2	80.9	1.0	79.8	0.5	79.7	0.5	82.0	3.8	80.1	0.6
339	355	11.9	2	PAVVRPGSLDLPSPVSL	77.8	0.8	78.3	0.9	78.4	0.9	78.7	0.8	76.5	0.2	76.5	1.2	79.2	3.6	77.8	0.8
356	361	11.5	1	SEFGMM	71.9	0.9	72.1	2.1	71.4	1.1	71.2	1.7	70.8	0.5	70.9	1.7	72.2	4.1	71.0	0.5
358	362	14.1	1	FGMMF	75.6	1.6	75.9	0.7	75.6	0.4	76.4	0.5	74.4	1.0	74.6	1.2	76.8	4.2	74.7	1.0
359	380	12.1	2	GMMFPVLGPRSECSGASSPECE	52.3	1.2	52.6	0.8	52.4	0.3	53.4	0.8	50.4	0.3	51.0	1.0	52.4	2.7	51.4	1.1
363	379	7.7	2	PVLGPRSECSGASSPEC	67.3	1.4	68.0	0.7	67.0	0.6	68.4	0.3	65.4	0.7	65.9	0.3	67.4	3.3	67.1	2.9
363	380	7.7	2	PVLGPRSECSGASSPECE	64.9	1.5	65.4	0.5	64.7	0.4	66.0	0.3	63.3	0.6	63.8	0.1	65.1	3.0	65.0	2.8
380	391	4.1	3	EVERGDRAEGAE	58.5	1.5	59.4	1.2	58.3	2.4	58.8	2.3	58.4	1.5	57.0	1.3	58.9	5.3	59.2	0.8
381	391	3.9	2	VERGDRAEGAE	58.8	2.0	58.8	1.9	58.1	2.6	57.6	2.9	57.4	2.8	56.7	2.2	58.5	6.2	58.8	1.3
381	427	5.6	5	VERGDRAEGAENKTSDKANNNRGLSSSSGSGGSSKSQSSTSPEGQAL	51.1	2.0	51.2	1.0	49.8	2.4	51.5	1.2	49.8	1.1	49.3	0.3	49.7	4.8	49.9	3.5
381	428	5.7	5	VERGDRAEGAENKTSDKANNNRGLSSSSGSGGSSKSQSSTSPEGQALE	51.7	1.8	51.9	0.9	50.5	2.5	52.2	1.2	50.4	1.1	49.9	0.2	50.4	4.7	50.5	3.2
381	438	9.9	5	VERGDRAEGAENKTSDKANNNRGLSSSSGSGGSSKSQSSTSPEGQALENRMKQLSLQC	42.3	1.6	42.7	1.8	42.8	0.9	43.1	1.5	41.4	1.3	42.3	0.3	43.3	2.1	43.2	0.9
437	448	6.1	2	QCSKGRDGIIAD	59.8	1.2	59.9	0.6	58.8	1.0	60.5	0.4	59.4	0.5	58.9	0.5	60.3	3.5	59.2	1.5
439	448	6.0	2	SKGRDGIIAD	59.2	1.3	60.3	1.1	59.3	1.2	59.7	1.2	58.5	0.8	57.9	1.3	59.1	4.7	58.7	2.4

Appendix M. Peptides used for Mapping changes in clinically relevant Rab11 mutants

S	E	RT	Z	Rab11 peptides Sequence	WT 3s at	SD	300s	SD	K24R 3s at	SD	300s	SD	S154L 3s at	SD	300s	SD	V22M 3s at	SD	300s	SD
10	16	12.7	2	YLFKVVL	-0.2	0.3	10.2	0.3	-0.4	0.1	18.2	0.3	4.8	2.4	35.6	0.8	2.1	0.7	31.9	1.6
12	16	10.4	1	FKVVL	0.4	0.1	6.7	0.1	0.6	0.2	1.3	0.3	11.1	1.1	36.1	0.9	6.4	0.6	20.1	0.3
28	36	8.2	2	LSRFTRNEF	3.4	0.3	33.4	0.4	5.4	0.3	46.3	0.5	43.2	0.9	54.1	0.2	37.9	0.9	51.9	1.7
28	36	8.2	3	LSRFTRNEF	3.4	0.4	33.5	0.4	5.1	0.7	46.4	0.4	43.1	0.8	53.9	0.2	38.0	1.0	51.7	1.4
28	38	10.1	3	LSRFTRNEFNL	12.0	0.3	40.9	0.3	12.5	0.3	49.3	0.5	44.8	0.6	54.3	0.2	40.5	0.8	52.5	0.5
28	47	9.3	4	LSRFTRNEFNLESKSTIGVE	30.1	0.7	48.4	0.7	32.0	0.4	52.5	0.3	43.4	1.2	53.6	0.2	42.2	0.9	53.1	0.1
28	48	10.9	3	LSRFTRNEFNLESKSTIGVEF	29.5	0.6	49.3	0.2	30.7	0.2	53.0	1.0	40.7	0.9	52.3	0.1	39.2	0.6	53.1	0.6
29	36	7.4	3	SRFTRNEF	4.8	1.1	39.9	1.0	7.4	1.2	52.3	1.7	48.7	0.1	58.5	0.2	47.3	2.2	58.2	0.9
32	36	6.4	2	TRNEF	8.2	1.4	62.0	0.7	12.8	1.3	63.6	1.1	54.6	0.4	62.9	1.3	46.9	1.2	62.4	2.1
32	38	9.6	2	TRNEFNL	21.7	0.6	62.2	0.4	23.6	0.6	62.8	0.3	54.6	0.8	62.6	0.9	49.4	1.1	62.1	0.4
37	45	6.1	2	NLESKSTIG	58.1	1.3	70.7	0.6	61.0	0.8	70.5	1.2	56.3	0.5	69.6	0.4	58.0	1.3	69.8	1.6
37	47	7.1	2	NLESKSTIGVE	53.0	1.3	68.3	0.6	55.6	0.5	68.3	0.7	52.1	0.6	66.1	0.1	53.6	1.2	67.2	1.6
37	48	10.5	2	NLESKSTIGVEF	43.3	1.1	63.1	0.6	45.8	0.2	64.1	0.4	44.6	0.8	60.9	0.3	44.1	0.9	61.4	0.4
39	47	5.7	2	ESKSTIGVE	52.6	1.1	67.5	0.7	55.8	0.3	67.3	0.8	49.1	0.8	65.3	0.6	50.8	1.2	67.3	1.2
39	48	9.8	1	ESKSTIGVEF	38.3	0.5	59.5	0.2	41.0	0.2	60.3	0.2	39.1	0.6	56.6	0.6	38.6	1.2	58.8	0.8
48	71	9.9	3	FATRSIQVDGKTIKAQIWDTAGQE	12.1	0.4	34.3	0.5	13.7	0.3	43.4	0.8	34.7	0.4	65.5	0.4	16.1	1.1	63.2	0.2
48	73	10.0	4	FATRSIQVDGKTIKAQIWDTAGQERY	16.9	0.6	37.1	0.4	18.3	0.1	44.2	0.5	35.2	1.5	66.3	0.6	19.2	0.5	61.9	0.6
48	79	10.1	5	FATRSIQVDGKTIKAQIWDTAGQERYRAITSA	29.1	0.3	45.8	0.4	29.9	0.3	52.2	0.5	39.4	1.1	68.5	0.2	30.9	0.7	64.5	0.2
48	80	10.3	5	FATRSIQVDGKTIKAQIWDTAGQERYRAITSAY	28.6	0.3	46.3	0.5	29.7	0.3	53.0	0.5	40.1	0.8	67.6	0.6	31.3	0.9	63.9	0.3
49	73	9.5	4	ATRSIQVDGKTIKAQIWDTAGQERY	18.0	0.5	38.4	0.3	19.5	0.2	47.1	0.5	38.1	0.6	67.6	0.1	23.8	3.2	62.7	0.6
49	79	9.7	4	ATRSIQVDGKTIKAQIWDTAGQERYRAITSA	30.2	0.3	46.6	0.4	31.0	0.3	53.4	0.4	40.5	0.9	69.1	0.4	32.0	1.3	64.9	0.6
65	73	7.9	2	WDTAGQERY	42.2	0.4	61.3	0.2	45.8	1.7	62.3	0.7	45.7	1.9	60.5	1.2	45.1	1.4	62.0	0.9
65	79	8.5	3	WDTAGQERYRAITSA	56.7	0.2	67.7	0.5	57.1	1.0	68.3	0.5	45.1	1.3	67.6	0.9	50.3	1.3	67.4	0.9
66	79	7.4	3	DTAGQERYRAITSA	63.3	0.3	73.6	0.2	63.8	0.2	73.7	0.6	51.2	0.3	73.1	1.7	56.3	3.5	73.2	1.8
72	79	5.5	2	RYRAITSA	76.4	0.6	80.7	0.6	72.8	0.6	80.7	0.6	53.9	1.1	77.3	0.8	63.2	1.1	80.3	1.9
74	79	4.7	1	RAITSA	79.2	1.8	85.8	1.1	75.8	1.0	85.6	1.4	55.1	1.4	83.7	0.7	64.8	1.8	86.0	1.1
80	86	5.8	2	YYRGAVG	20.7	0.2	46.6	0.6	20.5	0.4	48.3	1.0	25.2	0.8	64.2	0.9	23.2	0.4	58.7	1.5
80	88	8.6	2	YYRGAVGAL	11.8	0.0	27.9	0.3	12.0	0.0	29.4	0.1	15.3	0.2	48.8	0.0	14.4	0.4	41.3	1.3
80	89	10.8	2	YYRGAVGALL	8.5	0.2	20.0	0.3	8.7	0.1	21.1	0.4	11.3	0.5	42.9	0.1	10.5	0.3	34.4	0.5
81	88	7.7	2	YRGAVGAL	10.5	0.2	20.5	0.2	10.6	0.3	22.2	0.1	12.4	0.1	45.6	0.1	12.5	0.5	36.3	1.1
89	100	9.9	2	LVYDIAKHLTYE	8.5	0.2	28.1	0.3	9.7	0.2	43.7	0.3	19.4	0.9	56.2	0.2	25.2	0.8	54.7	0.2
89	102	10.6	2	LVYDIAKHLTYENV	6.8	0.1	25.1	0.3	10.0	0.3	42.5	0.5	17.9	0.7	56.9	0.3	24.1	0.9	57.5	0.2
89	111	13.1	5	LVYDIAKHLTYENVERWLKELRD	3.4	0.1	23.3	0.5	3.9	0.0	34.1	1.4	10.3	0.5	52.8	1.3	13.0	0.4	51.4	0.6
89	116	12.8	5	LVYDIAKHLTYENVERWLKELRDHADSN	5.5	0.0	24.3	0.6	6.0	0.0	32.5	1.5	10.7	0.4	49.6	0.9	13.3	0.5	47.2	0.3
89	117	13.3	4	LVYDIAKHLTYENVERWLKELRDHADSNI	5.8	0.1	26.9	0.6	6.4	0.1	34.5	1.5	10.6	0.5	49.2	0.7	13.2	0.5	48.4	0.6
89	117	13.3	5	LVYDIAKHLTYENVERWLKELRDHADSNI	5.9	0.0	27.1	0.6	6.3	0.1	34.7	1.5	10.6	0.4	49.2	1.0	13.2	0.5	48.5	0.3
90	100	9.2	2	VYDIAKHLTYE	9.1	0.2	30.7	0.5	10.3	0.4	46.3	0.3	21.8	1.0	57.0	0.6	27.7	1.2	56.6	0.1
90	102	9.7	3	VYDIAKHLTYENV	8.3	0.4	28.0	2.3	9.7	0.5	45.3	0.3	19.8	0.6	57.4	0.0	25.8	1.4	57.8	0.1
90	116	12.4	4	VYDIAKHLTYENVERWLKELRDHADSN	5.5	0.1	24.4	1.0	6.1	0.1	32.4	1.4	10.5	0.4	47.9	0.5	13.1	0.6	46.1	0.2
90	116	12.4	5	VYDIAKHLTYENVERWLKELRDHADSN	5.6	0.1	24.5	1.0	6.1	0.1	32.6	1.4	10.5	0.4	48.6	0.8	13.2	0.4	46.2	0.4
90	117	12.7	4	VYDIAKHLTYENVERWLKELRDHADSNI	5.6	0.0	24.6	0.6	6.1	0.0	33.1	1.5	10.9	0.4	49.6	0.4	13.6	0.5	47.8	0.3
91	118	12.8	4	YDIAKHLTYENVERWLKELRDHADSNIV	5.5	0.0	24.4	0.6	6.0	0.1	32.6	1.5	10.7	0.4	49.0	0.5	13.4	0.5	47.3	0.3
91	118	12.8	5	YDIAKHLTYENVERWLKELRDHADSNIV	5.5	0.0	24.3	0.6	6.0	0.0	32.5	1.5	10.7	0.4	49.6	0.9	13.3	0.5	47.2	0.3
91	119	13.4	4	YDIAKHLTYENVERWLKELRDHADSNIVI	5.7	0.1	26.5	0.7	6.2	0.1	33.8	1.4	10.2	0.5	48.1	0.9	13.0	0.5	47.3	0.4
91	119	13.4	5	YDIAKHLTYENVERWLKELRDHADSNIVI	5.8	0.1	26.7	0.6	6.2	0.1	34.1	1.4	10.4	0.5	48.5	1.6	12.9	0.5	47.7	0.3
93	117	12.0	5	IAKHLTYENVERWLKELRDHADSNI	5.2	0.1	25.2	1.2	5.4	0.1	29.4	1.3	8.3	0.2	40.5	0.9	10.0	0.5	40.3	0.1
101	105	8.1	2	NVERW	3.6	0.1	50.7	0.8	3.6	0.4	51.9	0.6	5.6	0.4	56.8	1.0	4.8	0.9	57.2	1.1
101	108	8.7	2	NVERWLKE	1.2	0.1	24.0	0.5	1.5	0.2	26.5	0.5	2.3	0.2	43.2	0.2	2.1	0.5	41.1	0.3
101	116	10.8	4	NVERWLKELRDHADSN	6.6	0.0	20.6	1.0	6.6	0.1	22.8	0.9	6.7	0.1	38.6	0.3	7.2	0.2	33.6	0.2
101	117	11.6	4	NVERWLKELRDHADSNI	7.5	0.1	25.9	1.3	7.4	0.2	28.0	1.3	7.1	0.1	42.1	0.2	7.9	0.3	38.5	0.3
103	116	8.3	3	ERWLKELRDHADSN	8.0	0.1	13.9	0.7	8.3	0.4	16.0	0.7	7.4	0.2	32.2	0.0	8.3	0.3	27.6	1.7
103	116	8.3	4	ERWLKELRDHADSN	8.1	0.1	13.9	0.3	8.1	0.1	15.9	0.5	7.4	0.4	32.3	0.2	8.4	0.4	27.4	1.8
103	117	9.4	4	ERWLKELRDHADSNI	8.1	0.1	19.6	0.3	8.1	0.2	21.4	0.4	7.1	0.5	34.9	0.1	8.1	0.4	30.8	0.4
106	116	4.6	2	LKELRDHADSN	13.0	0.3	18.9	1.0	12.7	0.2	20.0	1.1	10.5	0.4	32.2	0.1	12.9	0.8	29.0	1.2
107	117	4.6	3	KELRDHADSNI	12.0	0.2	17.7	0.9	11.8	0.3	19.1	1.3	10.0	0.4	30.8	0.5	11.9	0.2	27.8	0.9
109	117	5.2	2	LRDHADSNI	15.5	0.2	32.2	0.8	15.0	0.5	32.2	0.8	11.7	0.6	29.7	0.1	14.9	0.8	31.5	1.1
117	121	12.9	1	IVIML	0.3	0.2	8.5	0.3	0.3	0.1	11.9	0.1	0.4	0.1	21.6	0.2	0.3	0.1	24.1	0.2
118	138	8.9	4	VIMLVGNKSDLRHLRAVPTDE	2.0	0.2	16.7	0.1	3.0	0.2	27.2	0.5	20.7	0.8	36.5	0.3	18.5	0.4	33.1	0.8
118	141	8.5	5	VIMLVGNKSDLRHLRAVPTDEARA	1.7	0.1	16.9	0.6	2.7	0.2	27.7	0.5	20.7	0.6	41.7	0.1	17.1	0.6	38.1	1.3
120	138	7.8	4	MLVGNKSDLRHLRAVPTDE	2.4	0.2	22.8	0.2	4.1	0.9	31.8	0.3	23.9	0.5	40.9	0.2	22.6	0.6	38.5	1.0
121	128	6.4	2	LVGNKSDL	2.5	0.4	4.6	0.5	4.9	0.7	30.4	0.8	28.6	1.1	49.1	1.5	26.4	1.1	45.9	3.9
121	138	6.8	3	LVGNKSDLRHLRAVPTDE	3.4	0.4	26.2	0.3	4.6	0.5	36.3	0.6	27.8	0.7	44.4	0.3	25.6	0.9	42.4	1.7
121	141	6.7	4	LVGNKSDLRHLRAVPTDEARA	2.7	0.2	21.3	0.3	3.6	0.2	34.7	1.0	25.9	0.8	48.6	0.3	21.7	0.7	46.0	1.9
121	141	6.7	5	LVGNKSDLRHLRAVPTDEARA	2.7	0.2	21.1	0.4	3.5	0.1	34.6	0.9	25.8	0.7	48.4	0.3	21.7	0.7	46.0	1.9
121	150	10.1	4	LVGNKSDLRHLRAVPTDEARAFAEKNGLSF	2.1	0.1	18.9	0.2	3.0	0.2	33.2	0.7	23.2	0.7	55.2	0.3	14.8	0.4	52.4	0.2
122	138	6.5	4	VGNKSDLRHLRAVPTDE	3.4	0.3	27.4	0.5	4.9	0.9	37.2	0.9	28.2	0.7	44.5	0.3	25.8	0.9	42.9	1.9
122	141	6.3	4	VGNKSDLRHLRAVPTDEARA	2.9	0.2	22.6	0.3	4.1	0.5	36.2	1.1	26.2	0.7	49.4	0.3	22.8	0.9	47.8	2.2
122	150	10.0	5	VGNKSDLRHLRAVPTDEARAFAEKNGLSF	1.7	0.2	18.3	0.4	2.4	0.2	30.7	0.6	22.1	0.9	54.8	0.9	13.4	0.8	51.9	0.1
122	151	9.8	5	VGNKSDLRHLRAVPTDEARAFAEKNGLSFI	2.3	0.2	19.8	0.2	3.0	0.0	34.8	0.5	24.8	0.8	56.6	0.3	16.1	0.8	54.0	0.8
139	149	6.0	2	ARAFAEKNGLS	2.4	0.3	13.3	0.1	2.5	0.4	29.7	0.9	23.8	1.5	67.8	0.4	6.8	1.2	60.8	2.0
139	150	9.2	3	ARAFAEKNGLSF	2.1	0.2	17.6	0.2	2.4	0.2	30.2	0.4	20.8	0.8	59.5	0.1	5.8	1.0	54.9	0.7
142	149	5.9	2	FAEKNGLS	2.1	0.3	14.3	0.2	3.3	0.2	31.5	0.6	25.2	0.9	65.9	0.2	9.2	0.6	58.9	1.8
142	150	9.7	1	FAEKNGLSF	3.0	0.3	24.8	0.2	3.3	0.3	33.0	0.3	22.3	0.8	57.8	0.1	8.2	0.2	52.4	0.6
142	150	9.7	2	FAEKNGLSF	2.7	0.3	24.5	0.1	3.1	0.2	32.7	0.2	22.2	0.6	57.5	0.1	7.6	1.1	52.0	0.7
157	162	4.2	1	DSTNVE	8.0	0.9	52.5	1.1	11.3	1.2	66.1	1.4	39.3	0.8	73.6	0.6	37.3	1.0	73.0	0.9
157	164	4.9	1	DSTNVEAA	6.3	0.8	49.2	0.8	8.5	0.9	63.3	1.2	31.3	0.6	73.4	1.0	29.4	1.2	71.6	1.8
166	170	7.1	1	QTILT	0.6	0.1	1.4	0.5	0.6	0.2	7.0	0.2	1.9	0.3	38.0	0.4	0.6	0.5	31.0	0.5
166	171	8.0	1	QTILTE	0.8	0.2	3.9	0.5	0.9	0.3	7.3	0.2	1.9	0.3	33.2	0.8	1.2	0.1	24.8	0.8
170	183	8.4	3	TEIYRIVSQKQMSD	27.8	0.3	40.1	1.6	27.0	0.7	39.7	0.6	26.4	0.4	50.9	0.4	25.6	1.0	44.5	0.2
170	193	7.6	4	TEIYRIVSQKQMSDRRENDMSPSN	33.1	0.1	39.4	0.5	32.3	0.7	39.7	0.6	31.9	0.2	46.6	0.4	32.0	0.9	41.6	1.6
171	183	7.6	3	EIYRIVSQKQMSD	29.5	0.3	42.4	0.5	28.4	0.6	42.9	0.4	27.8	0.6	52.8	0.4	27.4	0.5	46.2	1.3
172	183	7.2	3	IYRIVSQKQMSD	32.5	0.4	46.1	0.7	31.5	0.2	46.2	0.7	30.6	0.5	55.3	0.8	30.3	0.8	49.5	2.3
173	183	6.3	3	YRIVSQKQMSD	37.8	0.4	52.8	0.7	36.5	0.4	53.2	1.0	35.3	0.5	60.4	0.0	34.7	0.9	55.4	1.9
173	193	6.2	5	YRIVSQKQMSDRRENDMSPSNNVVPIHVPPTTENKPKVQHHHHHH	40.9	0.3	47.2	0.8	39.9	1.0	47.0	1.4	39.3	0.7	51.6	0.4	39.7	1.1	48.2	2.0
173	217	6.3	5	YRIVSQKQMSDRRENDMSPSNNVVPIHVPPTTENKPKVQHHHHHH	33.9	0.3	38.8	0.7	33.1	0.6	38.5	1.1	32.6	0.5	41.2	0.6	32.6	0.9	38.9	1.9
184	193	4.4	2	RRENDMSPSN	59.9	0.5	60.4	2.1	58.1	1.2	60.3	2.7	59.4	0.5	61.1	0.2	59.7	0.8	61.6	1.3
184	217	5.9	5	RRENDMSPSNNVVPIHVPPTTENKPKVQHHHHHH	36.4	0.3	40.1	0.9	35.4	0.7	39.8	1.3	35.1	0.3	40.7	0.3	35.2	0.6	40.0	1.5
194	217	5.2	4	NVVPIHVPPTTENKPKVQHHHHHH	34.2	0.4	39.5	1.1	33.3	0.4	39.1	1.3	32.6	0.3	39.9	0.1	33.0	0.9	39.5	1.4
194	217	5.2	5	NVVPIHVPPTTENKPKVQHHHHHH	34.4	0.3	39.6	1.0	33.5	0.5	39.3	1.4	32.8	0.5	40.1	0.2	33.1	0.7	39.7	1.4

WT

S	E	RT	Z	Sequence	3s at	SD	300s	SD
12	16	10.3	1	FKVVL	0.6	0.3	0.9	0.1
12	27	10.3	3	FKVVLIGDSGVGKSNL	1.5	0.1	5.1	0.1
17	28	8.9	2	IGDSGVGKSNLL	2.6	0.4	4.7	0.1
150	156	9.7	1	FIETSAL	1.2	0.2	5.0	0.6
151	156	7.9	1	IETSAL	1.5	0.1	5.8	0.3

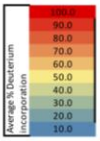

K24R

S	E	RT	Z	Sequence	3s at	SD	300s	SD
12	16	10.2	1	FKVVL	0.8	0.1	1.6	0.4
12	27	10.2	3	FKVVLIGDSGVGRSNL	2.5	0.7	21.8	1.2
17	28	9.1	2	IGDSGVGRSNLL	4.2	0.6	35.6	0.3
150	156	9.7	1	FIETSAL	4.5	0.9	49.1	0.8
151	156	7.9	1	IETSAL	4.2	0.4	45.7	0.7

S154L

S	E	RT	Z	Sequence	3s at	SD	300s	SD
12	16	10.2	1	FKVVL	12.8	0.7	38.2	0.8
12	27	10.2	3	FKVVLIGDSGVGKSNL	28.6	0.4	43.6	0.4
17	28	8.9	2	IGDSGVGKSNLL	43.0	0.4	54.0	0.1
150	156	7.9	1	FIETLAL	16.0	0.4	54.4	0.1
151	156	11.0	1	IETLAL	36.9	1.5	83.4	0.3

V22M

S	E	RT	Z	Sequence	3s at	SD	300s	SD
12	16	10.3	1	FKVVL	7.4	0.9	21.7	0.4
12	27	10.5	3	FKVVLIGDSGMGKSNL	20.0	0.6	32.1	0.4
17	28	9.2	2	IGDSGMGKSNLL	31.0	0.8	42.7	1.5
150	156	9.7	1	FIETSAL	38.7	1.1	71.4	0.8
151	156	7.9	1	IETSAL	42.0	1.1	70.0	1.6

Appendix N. Peptides used for comparing SH3BP5 binding deficient mutations

				SH3BP5 peptides	APO				LNQ52AAA				LE250AK			
S	E	RT	Z	Sequence	3s	SD	300s	SD	3s	SD	300s	SD	3s	SD	300s	SD
3	15	4.1	3	AALKRSRSEEPAE	52.6	3.0	57.9	1.5	51.8	0.9	56.2	1.6	51.7	0.8	57.0	0.8
3	24	7.1	5	AALKRSRSEEPAEILPPARDEE	39.6	2.5	52.0	1.3	38.3	0.4	51.1	1.0	38.8	0.6	51.5	1.4
3	25	7.2	4	AALKRSRSEEPAEILPPARDEEE	38.2	2.5	51.1	1.5	36.8	0.6	50.2	1.2	37.3	0.6	50.6	1.5
3	26	7.1	5	AALKRSRSEEPAEILPPARDEEEE	37.5	2.5	51.0	1.3	36.2	0.5	50.2	1.2	36.5	0.6	50.5	1.5
4	24	7.0	4	ALKRSRSEEPAEILPPARDEE	37.4	2.3	49.6	1.0	35.3	0.6	46.9	1.1	36.5	0.5	50.2	1.4
6	25	7.0	4	KRSRSEEPAEILPPARDEEE	35.1	2.6	49.5	1.1	33.8	0.5	48.6	0.5	34.2	0.5	49.4	1.2
16	25	6.1	2	ILPPARDEEE	45.3	3.0	62.4	3.5	43.9	0.4	61.2	0.5	45.2	0.8	61.8	1.3
25	35	9.0	1	EEEEEGMEQGL	44.5	2.9	55.5	0.9	43.7	0.8	55.1	1.7	43.6	0.7	55.4	0.5
26	35	8.8	1	EEEEGMEQGL	45.1	3.1	55.0	0.9	44.2	0.9	54.6	1.5	43.8	0.9	55.0	0.9
26	37	8.5	1	EEEEGMEQGLEE	41.8	3.2	55.2	0.7	40.9	0.9	54.2	1.2	39.9	0.7	54.6	0.8
27	35	8.7	1	EEEGMEQGL	46.2	2.8	55.5	1.0	45.3	1.3	54.5	1.6	44.8	0.6	55.0	0.7
27	37	9.0	1	EEEGMEQGLEE	44.7	2.9	55.7	0.7	44.0	0.6	55.2	1.5	43.7	0.7	55.5	0.7
38	49	9.2	3	EEEVDPRIQGEL	18.6	2.6	63.6	0.3	27.7	0.5	63.6	0.6	29.8	1.4	64.1	0.4
39	49	9.1	2	EEVDPRIQGEL	20.3	2.8	72.4	0.7	31.3	1.2	71.8	1.1	33.8	1.7	72.0	0.3
39	50	9.2	2	EEVDPRIQGELE	20.2	2.6	69.3	0.9	30.8	1.3	68.8	1.0	32.8	1.7	69.1	0.3
40	**49**	8.8	2	EVDPRIQGEL	21.5	2.7	71.7	0.6	33.1	1.4	71.3	1.3	35.7	1.9	71.4	0.3
40	50	9.1	2	EVDPRIQGELE	20.4	2.9	72.4	0.7	31.5	1.3	71.9	1.0	34.0	1.6	72.1	0.3
43	49	7.7	2	PRIQGEL	22.1	2.5	82.3	1.7	38.5	1.4	81.3	0.9	42.2	1.8	82.9	1.3
67	77	8.5	3	EDARQKFRSVL	1.0	0.1	14.2	0.1	1.0	0.1	32.8	0.9	0.9	0.1	25.3	1.2
69	77	7.0	3	ARQKFRSVL	1.2	0.1	12.1	0.3	1.0	0.1	24.3	0.2	1.1	0.2	17.7	0.7
78	86	7.2	1	VEATVKLDE	1.4	0.4	7.0	0.3	1.4	0.2	14.7	0.8	1.2	0.1	7.3	0.3
78	113	12.5	5	VEATVKLDELVKKIGKAVEDSKPYWEARRVARQAQL	4.2	0.3	25.8	0.2	4.1	0.3	27.7	1.1	4.1	0.1	27.1	1.2
80	86	6.3	1	ATVKLDE	0.9	0.2	6.6	0.6	0.9	0.1	11.7	0.5	1.3	0.2	6.8	0.9
80	87	9.7	2	ATVKLDEL	1.3	0.0	6.8	0.2	1.2	0.1	11.0	0.0	1.1	0.2	7.3	0.0
81	86	5.9	1	TVKLDE	2.2	0.3	7.3	0.7	2.1	0.3	12.4	0.5	2.1	0.2	7.6	0.2
82	86	5.6	1	VKLDE	1.4	0.1	8.2	1.1	2.1	0.3	11.9	0.1	2.2	0.1	7.2	0.2
87	96	4.4	2	LVKKIGKAVE	15.4	1.2	75.5	0.3	14.8	0.3	75.4	1.3	14.7	0.2	75.0	0.1
88	96	3.8	2	VKKIGKAVE	15.7	1.3	74.1	0.0	15.8	0.4	74.0	0.1	15.3	0.2	74.3	0.3
88	113	8.0	5	VKKIGKAVEDSKPYWEARRVARQAQL	4.2	0.3	24.8	0.8	4.1	0.1	25.0	1.2	4.1	0.1	25.7	1.0
97	104	9.6	2	DSKPYWEA	2.6	0.3	15.3	2.2	2.6	0.1	18.1	0.1	2.3	0.3	16.3	0.7
97	113	8.7	4	DSKPYWEARRVARQAQL	0.9	0.1	10.3	0.3	0.9	0.0	10.3	0.0	0.8	0.0	11.5	0.4
114	125	5.7	3	EAQKATQDFQRA	3.4	0.3	28.1	1.1	3.1	0.2	29.8	0.1	3.1	0.2	31.3	0.4
114	127	6.4	2	EAQKATQDFQRATE	2.0	0.3	31.3	1.8	1.9	0.1	32.7	0.4	2.0	0.1	34.8	0.9
114	129	9.6	3	EAQKATQDFQRATEVL	1.0	0.1	25.2	0.5	1.0	0.0	26.9	0.2	0.9	0.1	27.9	0.5
121	129	9.7	2	DFQRATEVL	2.8	0.4	27.6	0.6	2.0	0.1	29.6	0.9	2.1	0.1	30.3	0.5
122	129	8.4	2	FQRATEVL	2.4	0.1	28.8	0.9	2.0	0.0	29.7	0.6	2.0	0.1	30.3	0.7
123	129	7.2	2	QRATEVL	2.0	0.3	31.2	0.9	1.8	0.2	32.3	0.1	1.9	0.2	32.9	1.0
128	138	8.7	2	VLRAAKETISL	2.8	0.5	59.1	0.4	2.6	0.1	59.0	1.0	2.5	0.1	59.8	1.1
130	138	7.8	3	RAAKETISL	2.9	0.6	59.9	0.5	2.7	0.3	59.2	1.3	2.6	0.1	59.7	1.1
139	143	5.2	1	AEQRL	13.9	1.8	84.8	1.2	12.6	0.3	84.5	1.6	12.5	0.5	84.5	0.5
139	154	7.8	4	AEQRLLEDDKRQFDSA	30.9	2.5	59.0	1.5	29.8	0.4	58.2	1.8	29.7	0.4	58.7	1.4
142	154	7.2	3	RLLEDDKRQFDSA	34.9	2.3	53.7	1.8	33.1	0.5	53.0	1.1	34.0	0.6	53.5	1.6
144	154	6.2	2	LEDDKRQFDSA	41.4	2.8	53.0	3.1	40.2	0.4	52.3	0.0	40.9	0.2	52.7	1.3
155	168	9.3	2	WQEMLNHATQRVME	3.0	0.6	61.6	1.4	2.8	0.2	61.3	1.4	2.8	0.2	62.0	0.8
155	178	10.0	5	WQEMLNHATQRVMEAEQTKTRSEL	2.1	0.3	59.6	1.9	2.0	0.1	60.0	1.6	1.9	0.2	59.9	1.4
156	168	7.6	3	QEMLNHATQRVME	3.0	0.6	63.9	1.3	2.7	0.2	63.0	1.1	2.7	0.2	63.6	1.3
156	178	8.9	4	QEMLNHATQRVMEAEQTKTRSEL	2.4	0.4	62.3	1.4	2.0	0.1	61.4	1.8	2.1	0.2	62.8	1.4
159	168	5.3	2	LNHATQRVME	3.9	0.5	62.0	1.8	3.4	0.4	61.9	1.4	3.7	0.1	62.2	0.4
169	178	5.0	2	AEQTKTRSEL	3.0	0.3	58.3	1.9	2.9	0.2	58.3	1.5	3.0	0.2	58.0	1.0
169	187	5.3	4	AEQTKTRSELVHKETAARY	2.0	0.3	30.3	2.2	2.0	0.2	29.7	1.3	2.0	0.2	31.3	1.0
169	191	6.3	3	AEQTKTRSELVHKETAARYNAAM	1.0	0.2	26.1	2.6	0.7	0.2	25.6	0.0	0.9	0.2	27.5	1.1
169	194	7.2	5	AEQTKTRSELVHKETAARYNAAMGRM	0.9	0.2	27.1	1.4	1.0	0.2	26.8	0.1	1.0	0.1	27.5	1.2
170	178	4.9	2	EQTKTRSEL	3.3	0.1	56.7	2.3	3.0	0.2	56.0	2.1	3.1	0.1	56.3	1.3
179	187	4.1	2	VHKETAARY	2.9	0.2	24.8	0.8	2.7	0.3	24.5	0.7	2.5	0.1	26.1	0.4
179	191	5.6	2	VHKETAARYNAAM	1.9	0.2	23.4	0.6	1.8	0.1	23.7	0.5	1.7	0.1	24.8	0.5
179	194	6.5	4	VHKETAARYNAAMGRM	1.8	0.2	27.7	0.9	1.6	0.1	27.4	0.1	1.8	0.2	29.0	1.0
195	212	6.7	4	RQLEKKLKRAINKSKPYF	8.5	0.3	39.3	3.0	8.0	0.2	39.8	0.9	8.8	0.5	39.6	3.1
195	214	8.4	5	RQLEKKLKRAINKSKPYFEL	5.5	0.6	31.5	1.6	5.4	0.2	32.2	2.7	5.6	0.4	32.2	2.0
219	232	11.4	3	YVQLEQLKKTVDDL	0.3	0.1	17.5	0.5	0.4	0.2	26.6	0.1	0.2	0.0	20.4	0.6
223	232	7.4	2	EQLKKTVDDL	0.8	0.0	16.2	0.5	0.8	0.0	28.6	0.1	0.8	0.1	20.0	0.5
226	232	5.7	2	KKTVDDL	1.0	0.1	16.1	1.1	0.8	0.0	28.2	0.1	0.8	0.1	18.7	0.7
253	282	6.6	5	ISDEIHERRRSSAMGPRGCGVGAEGSSTSV	40.4	1.0	47.6	2.0	40.7	0.4	47.1	0.5	42.5	1.0	47.5	1.7
256	282	6.0	5	EIHERRRSSAMGPRGCGVGAEGSSTSV	46.2	0.9	51.3	2.8	46.1	0.1	50.3	0.4	48.3	1.3	50.7	1.2
256	297	8.2	5	EIHERRRSSAMGPRGCGVGAEGSSTSVEDLPGSKPEPDAISV	43.7	1.8	50.2	0.9	43.3	0.3	49.6	1.4	43.3	0.7	49.9	0.9
281	297	9.2	2	SVEDLPGSKPEPDAISV	55.4	3.1	67.1	1.1	54.5	1.1	66.8	1.1	54.3	0.8	67.2	0.5
283	294	6.3	2	EDLPGSKPEPDA	54.9	2.3	66.5	2.2	53.5	0.1	65.7	0.6	55.1	0.4	66.6	1.1
283	297	8.9	2	EDLPGSKPEPDAISV	57.4	2.7	68.7	0.8	56.6	1.0	68.3	1.0	56.3	0.8	68.7	0.6
283	301	8.8	2	EDLPGSKPEPDAISVASEA	63.6	2.7	72.6	0.5	62.9	0.8	72.3	1.2	62.5	0.5	72.6	0.5
295	301	6.6	1	ISVASEA	78.2	1.4	80.4	0.8	77.7	0.3	82.3	1.0	78.1	0.6	81.5	1.0
302	310	9.8	1	FEDDSCSNF	31.0	1.3	36.0	0.9	30.7	0.6	36.0	1.1	31.4	0.4	35.9	0.7
311	318	4.3	1	VSEDDSET	56.3	1.1	57.6	0.8	55.7	0.9	57.0	0.5	56.0	0.9	57.3	0.2
311	324	8.9	2	VSEDDSETQSVSSF	61.7	0.6	62.8	0.5	62.3	0.5	62.6	1.2	61.9	1.2	62.9	0.1
319	324	8.1	1	QSVSSF	81.8	0.5	81.9	1.1	82.2	0.4	82.2	0.1	81.9	1.2	82.5	0.7
324	354	11.9	3	FSSGPTSPSEMPDQFPAVVRPGSLDLPSPVS	62.5	2.4	69.4	0.2	62.0	0.9	69.9	0.8	61.3	0.4	69.3	0.5
324	355	12.9	3	FSSGPTSPSEMPDQFPAVVRPGSLDLPSPVSL	60.7	2.0	67.4	0.2	59.8	0.9	67.6	0.8	60.0	0.5	67.4	0.5
325	347	11.3	2	SSGPTSPSEMPDQFPAVVRPGSLDLPSPVS	66.0	2.3	71.3	0.3	65.5	1.1	71.9	0.6	65.1	0.4	71.6	0.9
325	353	12.3	3	SSGPTSPSEMPDQFPAVVRPGSLDLPSPVSL	59.3	1.9	69.4	0.3	58.7	0.9	69.5	0.6	58.5	0.6	70.1	0.8
325	354	11.9	3	SSGPTSPSEMPDQFPAVVRPGSLDLPSPVSLSE	63.3	2.4	70.2	0.0	62.6	1.0	70.6	0.7	62.3	0.5	70.5	0.7
325	355	12.8	3	PDQFPAVVRPGSLDLPSPVSL	62.4	2.1	69.0	0.1	61.6	0.9	69.1	0.7	61.5	0.5	69.1	0.6
325	357	12.2	3	PAVVRPGSL	62.3	1.9	68.1	0.0	61.5	0.8	68.2	0.4	61.4	0.4	68.3	0.4
335	355	12.5	2	PAVVRPGSLDLPSPVSL	66.1	2.8	74.7	0.0	65.3	1.1	74.8	0.6	65.1	0.7	74.6	0.9
339	347	7.9	2	PAVVRPGSLDLPSPVSLSE	78.2	3.0	88.6	0.8	77.7	0.6	87.8	0.5	77.0	0.5	88.3	1.0
339	355	11.7	2	SEFGMM	69.4	2.8	78.9	0.2	68.4	1.1	79.4	0.6	68.2	0.7	79.1	0.7
339	357	11.1	2	FGMMF	68.3	2.9	77.1	0.2	68.1	0.8	77.3	0.1	67.8	0.3	76.8	0.6
356	361	11.2	1	PVLGPRSECSGASSPEC	67.3	2.3	70.4	0.4	66.8	0.9	71.3	0.8	66.4	0.1	71.2	0.8
358	362	14.0	1	EVERGDRAEGAENKTSDKANNNRGLSSSSGSGGSSKSQSSTSPEGQAL	68.1	2.8	73.1	0.1	66.4	1.5	74.2	1.1	66.8	0.8	73.0	0.2
363	379	7.7	2	ENRMKQLSL	47.2	2.5	64.5	1.1	46.8	0.5	63.7	1.0	47.2	0.6	64.3	0.7
380	427	5.5	5	QCSKGRDGIIAD	49.0	0.6	51.6	2.9	48.7	0.4	50.5	0.8	50.5	0.9	50.9	1.3
428	436	8.6	2	SKGRDGIIAD	66.2	2.4	72.6	0.8	65.7	1.1	71.8	1.1	67.1	1.0	73.3	0.3
437	448	5.9	2	QCSKGRDGIIAD	55.3	2.3	62.6	2.1	54.9	2.0	64.3	0.4	56.7	2.0	63.4	0.8
439	448	5.8	2	SKGRDGIIAD	52.5	3.1	61.8	2.1	51.0	0.4	61.9	0.4	52.9	0.8	62.1	0.2

Average % Deuterium incorporation: 100.0, 90.0, 80.0, 70.0, 60.0, 50.0, 40.0, 30.0, 20.0, 10.0

Appendix O. Table of TRAPP subunits and Rab proteins in Yeast and Mammals.

Yeast TRAPP subunit	**Mammalian TRAPP subunit**	**Subunit group**
Bet5p	TRAPPC1	Core
Trs20p	TRAPPC2	Adaptor
TCA17	TRAPPC2L	Adaptor
Bet3p	TRAPPC3	Core
Trs23p	TRAPPC4	Core
Trs31p	TRAPPC5	Core
Trs33p	TRAPPC6a,b	TRAPPI-associated
Trs85p	TRAPPC8	TRAPPIII-specific
Trs120p	TRAPPC9	TRAPP-II specific
Trs130p	TRAPPC10	TRAPP-II specific
N/A	TRAPPC11	mTRAPPIII-specific
N/A	TRAPPC12	mTRAPP
Trs65p	TRAPPC13	Yeast TRAPPII dimer
Yeast Rab	**Mammalian Rab**	
Ypt1	Rab1	
Ypt31/32	Rab11	

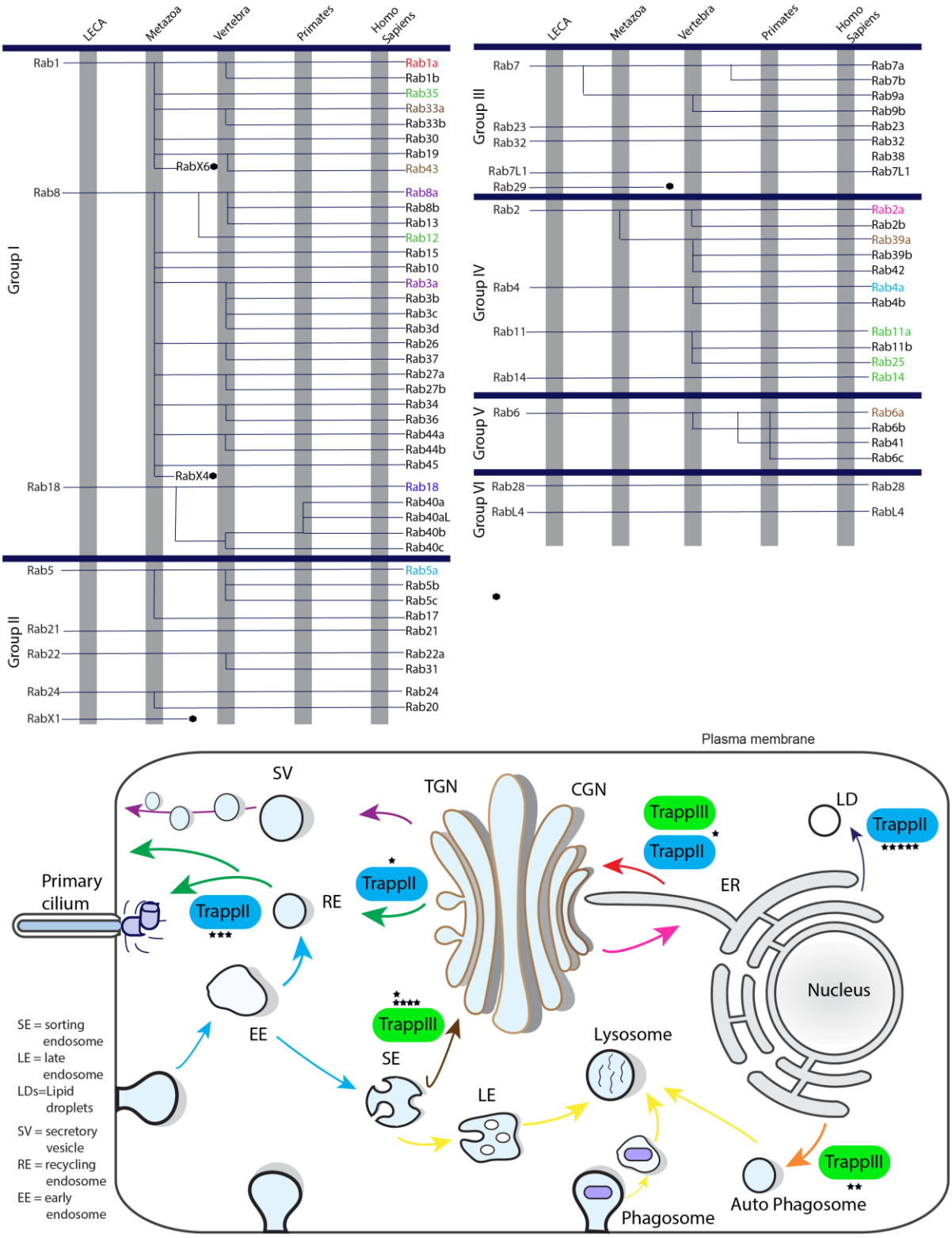

Appendix P. TRAPPII cellular localization and specificity. The location of TRAPPII is noted by stars, depicting the primary research which first showed this subcellular location. *(149), **(150), ***(151), ****(152), *****(144). Figure adapted from Klöpper *et al*(12).

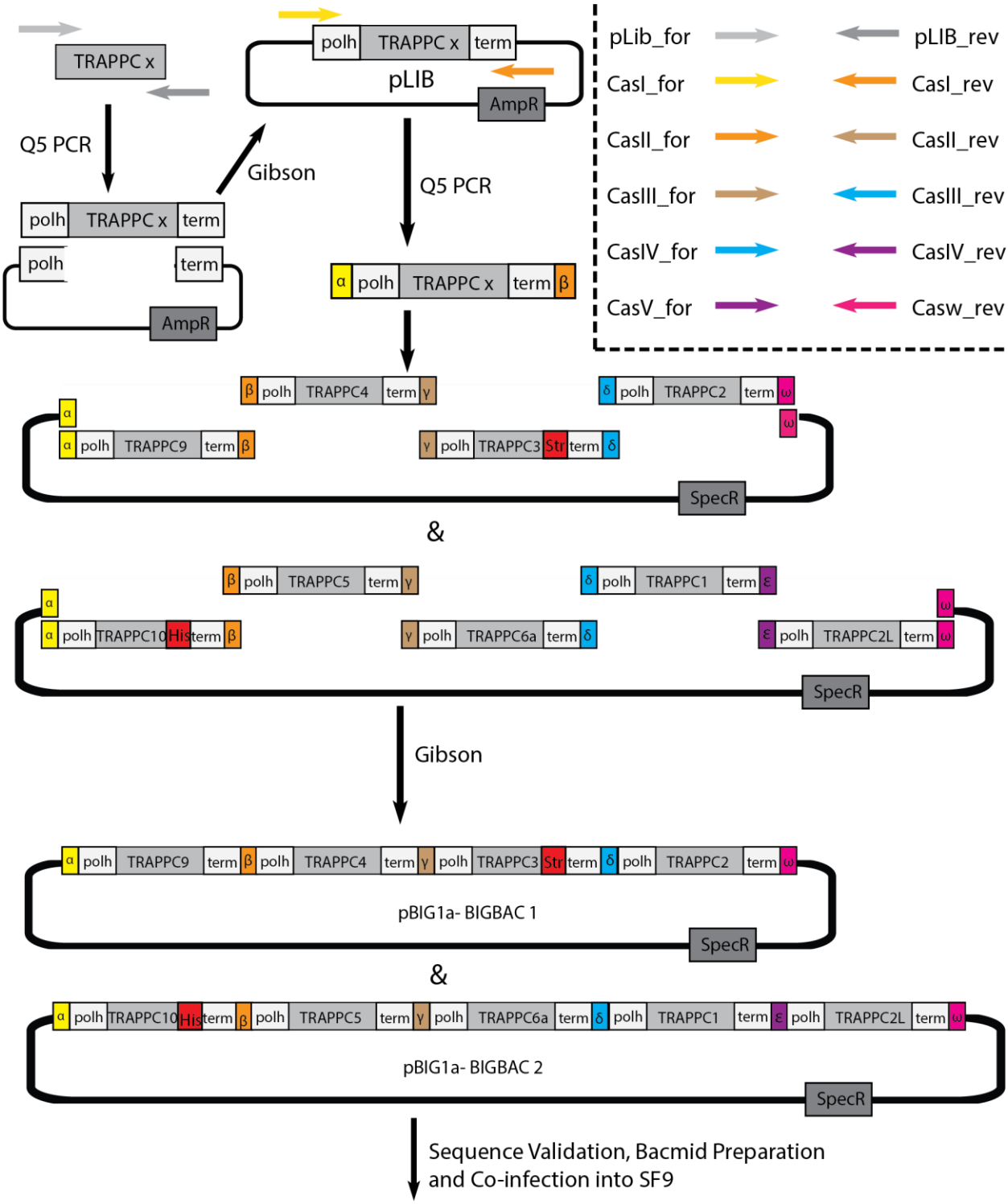

Appendix Q. Schematic depicting the BigBac system used to express TRAPPII. Figure is adapted from F.Weissmann, 2016, PNAS (138)

Appendix R. Membrane enhancement is not altered by C-terminal his tag.
(A) *In vitro* GEF assay of TRAPPII with and without a c-terminal his tag on TRAPPC10, with and without nickelated vesicles (45% PC, 10% PI, 15% PE, 10% PS, 10% PI(4)P, 10% DGS NTA (100nm). Nucleotide exchange was monitored by measuring the fluorescent signal during the TRAPPII (150 nM) catalyzed release of Mant-GDP from 4 μM of Rab11-His6 in the presence of 100 μM GTPγS (C) Bar graph representing the fold enhancement in the presence and absence of membrane with or without the c-terminal his tag on TRAPPC10.

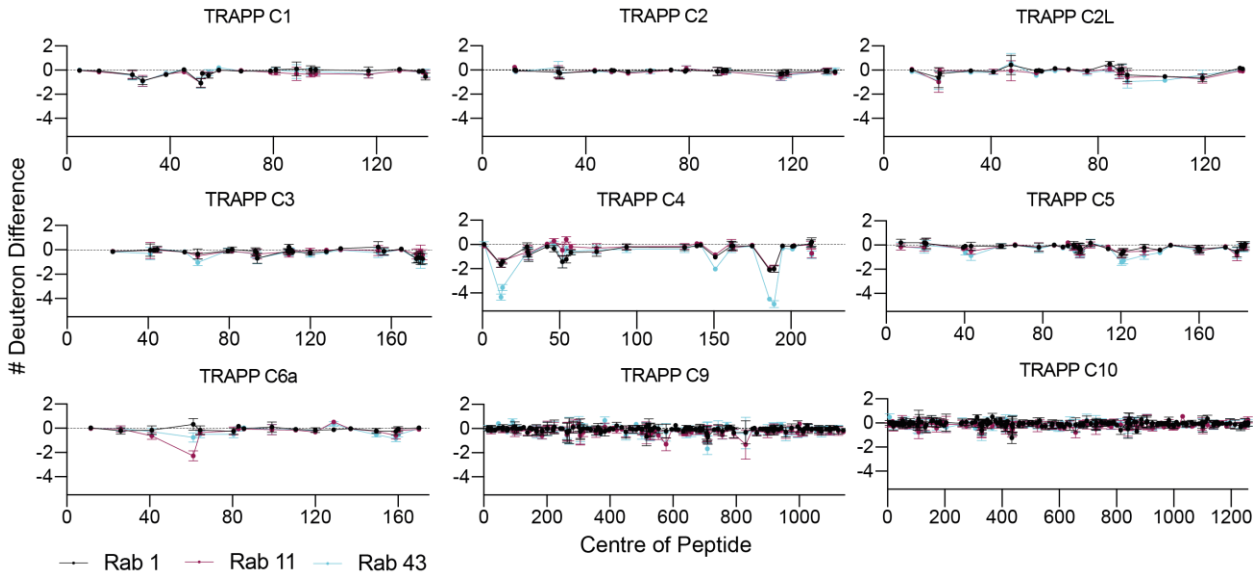

Appendix S. Total number of deuteron difference plots of TRAPPII with and without Rab1, Rab11 or Rab43. This is the total difference across all time points (3s,30s,300s,3000s) between the apo state and the Rab bound state.

Appendix T. Peptides of TRAPPC1, 2, 2L and 3 used for TRAPPII HDX with Rab1, Rab11 and Rab43.

Average % Deuterium incorporation: 100 90 80 70 60 50 40 30 20 10

TRAPPC1

					APO								TRAPP + Rab1								TRAPP + Rab11								TRAPP + Rab43							
S	E	RT	Z	Sequence	3s	SD	30s	SD	300s	SD	3000s	SD	3s	SD	30s	SD	300s	SD	3000s	SD	3s	SD	30s	SD	300s	SD	3000s	SD	3s	SD	30s	SD	300s	SD	3000s	SD
2	8	10.0	2	TVHNLYL	0.7	0.0	0.8	0.1	0.9	0.3	1.2	0.5	0.8	0.1	0.8	0.1	0.8	0.2	0.9	0.1	0.8	0.1	0.8	0.1	0.8	0.0	0.9	0.2	0.8	0.1	0.8	0.2	0.9	0.2	1.6	0.5
9	16	9.5	1	FDRNGVCL	6.2	0.4	12.3	0.7	17.7	0.8	25.7	0.4	6.2	0.4	12.3	1.0	16.8	0.4	25.6	0.3	6.2	0.7	11.5	0.3	16.6	0.7	25.1	0.9	5.6	0.0	11.7	0.3	17.6	0.8	24.8	0.7
17	34	4.9	5	HYSEWHRKKQAGIPKEEE	18.4	0.7	25.3	0.6	31.2	1.0	34.2	0.7	18.6	0.6	23.9	0.5	30.6	0.1	33.4	0.9	17.7	0.2	24.3	0.8	30.3	0.0	34.3	0.3	17.8	0.4	24.6	0.6	29.9	0.8	34.0	0.4
17	42	9.6	5	HYSEWHRKKQAGIPKEEEYKLMYGML	5.5	0.2	8.8	0.3	12.9	0.7	20.1	0.7	5.1	0.1	8.3	0.2	11.9	0.1	18.2	0.4	5.2	0.2	8.3	0.4	12.1	0.3	18.1	0.7	5.3	0.2	8.5	0.3	11.9	0.5	17.7	0.4
35	42	12.5	1	YKLMYGML	1.8	0.2	2.2	0.6	2.1	0.4	10.1	0.2	0.9	0.5	1.0	0.1	1.9	0.4	6.2	0.4	1.0	0.7	1.0	0.2	2.2	0.1	6.5	0.0	1.9	0.8	1.7	1.0	2.0	0.3	6.4	0.8
43	48	10.9	2	FSIRSF	1.7	0.1	6.7	0.7	17.9	0.5	24.6	1.0	2.0	0.4	7.1	0.4	18.6	0.5	24.5	0.2	1.5	0.2	5.6	0.5	18.0	0.7	22.1	0.2	1.8	0.1	7.4	0.3	18.9	0.7	24.0	0.5
43	61	12.8	4	FSIRSFVSKMSPLDMKDGF	5.6	1.0	10.2	0.4	21.8	1.3	34.2	0.7	5.0	0.3	8.9	0.2	18.4	0.1	32.9	0.6	4.7	0.2	9.2	0.2	18.6	0.0	32.7	0.5	4.7	0.1	9.0	0.3	18.7	0.8	32.9	0.7
49	56	7.3	2	VSKMSPLD	15.6	0.4	17.6	0.3	28.1	0.7	44.9	0.3	15.7	0.5	16.9	0.2	25.0	0.4	43.3	0.1	15.1	0.6	16.8	0.4	25.8	0.5	43.5	0.3	16.3	0.1	17.2	0.7	24.3	0.4	43.8	0.5
49	61	10.1	3	VSKMSPLDMKDGF	12.3	0.4	22.4	0.6	32.2	0.9	44.9	1.2	11.9	0.7	21.3	0.4	30.5	0.4	43.9	0.2	11.7	0.6	21.9	0.3	30.5	0.1	43.7	0.6	12.1	0.5	20.7	0.3	31.3	0.1	45.7	0.7
57	61	8.1	1	MKDGF	20.1	1.2	32.9	0.1	50.2	1.4	69.6	0.5	20.4	1.8	33.5	0.9	49.7	0.2	69.5	0.5	19.2	1.4	32.7	0.2	50.7	1.2	69.7	1.1	21.6	0.1	36.2	1.1	52.8	0.5	69.4	0.2
62	73	8.9	3	LAFQTSRYKLHY	0.9	0.1	1.9	0.1	4.3	0.1	5.3	0.3	0.9	0.2	1.6	0.1	4.0	0.1	5.0	0.1	0.9	0.1	1.9	0.2	4.4	0.1	5.2	0.2	0.8	0.2	1.6	0.2	4.7	0.5	4.9	0.1
74	84	10.3	2	YETPTGIKVVM	1.2	0.3	1.3	0.4	2.3	0.5	10.4	0.5	1.2	0.2	1.4	0.3	3.2	0.5	8.9	0.1	0.9	0.1	1.2	0.2	2.1	0.3	8.7	0.1	1.0	0.2	1.2	0.4	3.0	1.0	8.8	0.1
74	88	11.2	2	YETPTGIKVVMNTDL	2.8	0.5	5.6	0.1	7.1	0.2	11.9	0.3	3.2	1.1	5.3	0.5	7.5	0.3	11.9	0.3	2.5	0.7	5.3	0.8	6.8	0.4	11.4	0.2	2.7	0.5	5.2	0.5	7.7	0.7	11.9	0.3
74	104	14.0	5	YETPTGIKVVMNTDLGVGPIRDVLHHIYSAL	10.1	0.2	15.3	0.4	20.0	0.9	21.1	0.6	10.2	0.4	14.8	0.3	20.3	0.6	21.7	0.5	9.3	0.2	14.3	0.3	20.5	0.7	21.3	0.2	9.3	0.4	14.8	0.3	20.8	0.7	21.2	0.6
85	104	14.0	4	NTDLGVGPIRDVLHHIYSAL	15.1	0.3	22.5	0.7	29.4	0.7	30.7	0.3	15.5	0.6	22.1	0.5	29.7	0.3	30.7	0.1	14.6	0.5	21.9	0.3	28.6	0.0	30.7	0.1	14.7	0.3	22.0	0.3	29.6	0.8	30.6	0.1
89	104	12.8	3	GVGPIRDVLHHIYSAL	11.0	0.3	16.2	0.4	22.1	0.2	23.3	0.6	11.6	0.2	15.6	0.4	22.5	0.5	23.1	0.6	10.6	0.6	15.4	0.5	21.3	0.3	23.0	0.1	10.7	0.4	15.9	0.8	22.2	0.5	22.8	0.5
109	125	11.6	2	VVKNPLCPLGQTVQSEL	17.6	0.5	29.8	0.4	37.9	0.4	53.3	1.2	17.7	0.7	29.2	0.1	38.2	0.8	53.0	0.6	17.0	0.6	29.2	0.6	37.2	0.5	52.4	0.4	16.5	0.5	29.1	0.5	37.9	0.4	52.5	0.9
126	132	5.6	2	FRSRLDS	2.0	0.6	1.9	0.7	2.1	0.3	6.5	0.8	1.8	0.4	2.2	0.6	2.1	0.2	8.0	0.5	1.1	0.2	1.6	0.3	2.0	0.0	7.0	0.5	0.9	0.0	1.5	0.2	2.1	0.2	6.9	0.9
133	140	13.1	2	YVRSLPFF	4.5	0.8	13.1	0.2	21.8	0.2	32.4	0.7	4.0	0.2	12.5	0.4	21.9	1.1	31.4	0.4	3.6	0.7	12.7	1.1	21.6	0.1	31.6	0.4	3.4	0.3	12.5	0.5	21.5	1.0	31.7	0.6
133	145	10.9	3	YVRSLPFFSARAG	30.6	0.8	37.0	0.8	41.5	0.6	47.3	1.1	29.6	0.9	35.9	0.7	39.9	0.7	45.8	0.2	29.8	1.2	36.9	0.5	40.1	0.3	46.3	0.9	29.6	0.8	35.8	1.1	42.1	1.4	46.6	0.3
134	142	12.1	2	VRSLPFFSA	24.3	0.4	33.9	0.3	41.3	0.5	50.3	0.8	24.5	0.6	33.2	0.5	41.1	0.7	49.9	0.3	23.4	0.8	33.1	0.7	40.6	0.3	50.0	0.6	24.2	0.6	33.0	0.6	41.1	0.1	49.7	0.5

TRAPPC2

					APO								TRAPP + Rab1								TRAPP + Rab11								TRAPP + Rab43							
S	E	RT	Z	Sequence	3s	SD	30s	SD	300s	SD	3000s	SD	3s	SD	30s	SD	300s	SD	3000s	SD	3s	SD	30s	SD	300s	SD	3000s	SD	3s	SD	30s	SD	300s	SD	3000s	SD
6	19	10.5	2	YFVIVGHHDNPVFE	0.6	0.0	1.6	0.2	6.1	0.3	7.1	0.3	0.7	0.0	1.6	0.1	6.3	0.2	7.0	0.1	1.5	0.2	3.3	0.2	5.9	0.1	6.7	0.1	0.4	0.1	1.4	0.2	6.1	0.1	6.9	0.0
6	20	11.8	3	YFVIVGHHDNPVFEM	0.7	0.1	1.6	0.1	5.9	0.7	7.7	0.3	0.8	0.3	1.5	0.1	6.5	0.5	6.8	0.2	0.9	0.3	1.5	0.1	6.2	0.0	7.2	0.7	0.7	0.2	1.4	0.1	6.1	0.2	7.1	0.8
7	19	9.7	2	FVIVGHHDNPVFE	0.5	0.1	1.9	0.2	6.4	0.4	7.8	0.0	0.5	0.1	1.5	0.2	6.5	0.2	7.5	0.1	0.4	0.1	1.7	0.2	6.5	0.2	7.4	0.3	0.3	0.2	1.3	0.2	6.1	0.4	7.6	0.8
19	40	8.8	4	EMEFLPAGKAESKDDHRHLNQF	15.7	0.6	22.3	0.4	24.6	1.0	29.1	0.5	15.5	0.6	22.3	0.7	24.4	0.2	28.5	0.5	15.9	0.4	22.0	0.1	24.6	1.3	28.3	0.3	15.8	0.8	23.1	0.6	25.0	0.6	28.8	0.8
20	40	8.5	4	MEFLPAGKAESKDDHRHLNQF	16.3	0.8	22.2	0.2	24.1	1.0	29.3	0.9	16.1	1.2	22.3	0.6	23.8	0.1	28.1	0.3	16.2	0.6	21.8	0.4	24.2	0.4	28.2	0.4	15.8	0.1	22.2	0.6	25.0	0.3	27.7	0.3
41	46	6.5	1	IAHAAL	1.5	0.3	2.0	0.2	3.2	1.4	4.6	1.4	1.7	0.0	2.2	0.4	2.4	1.5	3.4	1.6	2.2	0.6	2.5	0.4	3.9	1.5	2.4	0.1	1.1	0.1	2.0	1.1	2.8	1.2	2.8	0.8
47	53	9.6	1	DLVDENM	1.7	0.3	2.4	0.2	3.4	0.3	12.9	0.7	1.4	0.4	1.9	0.1	4.8	0.8	11.9	0.4	1.9	0.9	1.4	0.2	2.9	0.5	11.1	0.0	1.5	0.1	1.8	0.2	2.8	0.9	10.9	0.8
49	53	6.0	1	VDENM	2.2	0.6	4.0	1.0	7.0	0.4	21.3	0.8	1.9	0.2	3.1	0.5	7.2	0.6	20.9	0.6	2.3	0.4	3.1	1.0	7.0	0.6	20.1	0.7	2.2	0.0	2.2	0.2	6.6	0.2	21.5	0.9
54	59	10.5	1	WLSNNM	40.1	0.7	45.6	1.1	48.6	0.6	55.9	0.9	41.3	1.1	42.3	1.2	46.8	0.9	55.8	1.0	39.3	0.7	41.6	0.7	47.2	0.4	55.6	0.9	37.5	0.9	42.7	0.5	48.9	1.9	55.5	1.4
60	70	10.4	2	YLKTVDKFNEW	5.1	0.2	10.9	0.4	14.7	0.6	20.2	0.7	5.2	0.5	10.8	0.4	14.7	0.1	19.8	0.2	5.1	0.6	10.2	0.1	14.3	0.5	19.7	0.1	4.8	0.4	10.2	0.6	15.1	0.5	19.5	0.5
71	75	11.1	1	FVSAF	2.9	0.4	2.3	0.4	2.2	0.1	2.9	0.4	2.8	0.1	2.1	0.3	3.4	0.7	2.4	0.1	2.7	0.3	2.3	0.5	2.3	0.1	2.4	0.3	2.8	0.2	2.0	0.3	2.2	0.5	2.3	0.2
75	82	7.8	3	FVTAGHMR	1.0	0.4	1.8	0.2	5.8	0.6	15.3	0.7	1.0	0.4	1.7	0.1	5.2	0.2	14.3	0.3	1.4	0.1	2.0	0.6	5.5	0.1	14.2	0.4	1.1	0.1	1.4	0.3	5.5	0.7	14.0	0.1
75	83	9.2	1	FVTAGHMRF	1.5	0.6	2.5	0.5	7.6	0.6	14.4	0.4	2.7	0.1	2.4	0.5	7.4	1.0	13.4	0.4	2.9	0.8	4.7	1.9	7.3	0.8	12.7	0.3	2.4	0.9	3.6	1.0	9.1	1.3	13.1	1.1
84	98	9.5	3	IMLHDIRQEDGIKNF	13.7	0.8	15.4	0.6	20.0	0.8	29.9	0.9	13.4	0.8	15.7	0.5	20.0	0.4	29.1	0.5	13.4	0.9	16.1	0.2	19.7	0.4	28.8	0.2	12.6	0.5	16.2	0.1	20.4	0.6	28.9	0.6
84	102	12.1	4	IMLHDIRQEDGIKNFFTDV	8.0	0.3	10.0	0.3	13.1	0.1	20.8	0.3	8.2	0.2	9.9	0.2	13.1	0.4	20.6	0.5	7.8	0.4	9.8	0.3	12.5	0.1	20.7	0.3	7.6	0.3	9.9	0.5	13.4	0.8	20.4	0.1
87	102	11.6	3	HDIRQEDGIKNFFTDV	8.9	0.1	11.3	0.3	15.1	0.3	24.0	0.5	9.1	0.4	11.1	0.1	15.0	0.2	24.0	0.5	8.6	0.4	11.1	0.3	14.6	0.2	23.9	0.1	8.6	0.5	11.0	0.3	15.4	0.6	23.6	0.1
106	125	11.8	3	YIKFSMNPFYEPNSPIRSSA	8.9	0.1	14.6	0.6	20.0	0.6	23.8	0.2	8.8	0.4	13.7	0.1	20.3	0.2	22.4	0.4	8.5	0.2	13.7	0.3	19.3	1.0	22.0	0.2	8.0	0.3	13.4	0.3	19.7	0.7	21.9	0.5
106	126	12.6	3	YIKFSMNPFYEPNSPIRSSAF	7.6	0.2	12.9	0.4	19.2	1.0	23.1	0.0	7.6	0.4	12.3	0.1	18.8	0.4	22.7	0.5	7.1	0.3	12.2	0.4	18.4	0.2	22.5	0.3	6.9	0.6	11.8	0.0	18.6	0.9	22.1	0.2
110	126	11.9	2	SMNPFYEPNSPIRSSAF	11.4	0.1	19.3	0.6	27.1	0.8	34.4	0.3	11.7	0.4	18.7	0.4	27.1	0.1	33.4	0.8	11.0	0.5	18.6	0.4	26.5	0.0	33.3	0.4	10.5	0.7	17.8	0.3	27.7	0.4	32.6	0.5
126	140	7.6	4	FDRKVQFLGKKHLLS	0.9	0.0	2.6	0.1	7.8	0.3	16.0	0.9	1.0	0.1	2.3	0.1	7.8	0.3	15.6	0.3	0.9	0.1	2.3	0.2	7.8	0.1	15.5	0.4	0.9	0.0	2.4	0.0	8.1	0.5	15.1	0.6
127	140	6.9	3	DRKVQFLGKKHLLS	1.3	0.2	3.0	0.1	8.9	0.4	17.8	1.1	1.1	0.2	2.8	0.1	8.7	0.3	17.5	0.3	1.1	0.1	2.8	0.3	9.1	0.2	17.6	0.5	1.0	0.0	2.8	0.3	8.4	0.4	16.9	0.7
133	140	4.8	1	LGKKHLLS	2.1	0.2	6.2	0.5	16.6	0.7	29.7	1.8	1.5	0.4	5.8	0.5	17.1	0.2	28.0	0.6	1.8	0.7	5.3	0.3	16.0	0.6	27.4	0.2	1.9	1.5	5.4	0.7	17.8	0.7	28.5	0.7

TRAPPC2L

					APO								TRAPP + Rab1								TRAPP + Rab11								TRAPP + Rab43							
S	E	RT	Z	Sequence	3s	SD	30s	SD	300s	SD	3000s	SD	3s	SD	30s	SD	300s	SD	3000s	SD	3s	SD	30s	SD	300s	SD	3000s	SD	3s	SD	30s	SD	300s	SD	3000s	SD
5	16	10.4	2	IAVIAKENYPLY	6.2	0.3	13.3	0.3	14.1	0.4	17.2	0.8	6.4	0.4	12.9	0.2	14.3	0.3	17.1	0.1	6.3	0.4	13.1	0.1	14.6	0.1	17.7	0.5	5.4	0.7	12.5	0.5	14.2	0.3	17.1	0.4
5	36	10.6	4	IAVIAKENYPLYIRSTPTENELKFHYMVHTSL	10.4	0.5	16.9	1.0	21.0	1.3	24.8	0.9	10.1	0.8	15.8	0.3	21.0	0.6	24.1	0.4	9.5	0.5	16.3	0.8	20.7	0.2	23.2	0.7	9.4	0.6	15.7	0.1	21.4	0.4	23.7	0.6
17	25	4.6	2	IRSTPTENE	51.6	0.8	60.4	0.7	71.9	1.1	73.3	0.8	48.3	0.6	58.7	0.4	72.0	0.6	73.1	0.9	50.5	0.6	60.2	0.6	71.4	0.7	74.2	0.7	51.0	0.4	59.3	0.3	71.8	0.8	73.9	0.4
29	36	7.6	1	HYMVHTSL	1.9	0.9	1.0	0.3	2.6	1.0	2.2	0.4	1.0	0.4	1.1	1.1	1.8	0.9	2.9	0.2	1.4	0.9	1.0	0.3	1.3	0.4	2.9	0.7	0.9	0.2	0.9	0.3	0.9	0.9	1.8	0.3
37	45	7.5	1	DVVDEKISA	12.5	0.6	20.8	0.4	25.9	0.7	47.4	1.3	12.7	0.6	20.3	0.3	25.3	0.6	46.1	0.4	12.5	0.5	20.2	0.5	25.5	0.3	46.9	0.6	12.1	0.5	19.7	0.6	25.7	0.4	46.7	0.8
37	58	12.8	4	DVVDEKISAMGKALVDQRELYL	39.7	0.8	49.4	1.4	51.6	1.6	57.2	1.2	40.7	0.7	47.0	0.3	53.7	0.9	58.6	1.1	38.4	1.0	49.0	1.0	51.9	0.7	58.4	0.5	39.5	0.8	47.4	1.0	53.8	0.7	60.0	0.5
54	60	11.6	2	RELYLGL	13.8	0.7	33.5	0.8	42.6	0.5	51.4	0.3	14.4	0.9	32.5	0.3	43.7	0.6	49.8	0.8	11.7	0.8	32.0	0.4	42.0	0.6	51.0	0.7	10.1	0.0	31.4	0.6	43.0	1.1	48.0	0.7
56	60	13.0	1	LYLGL	5.4	0.7	21.7	0.4	26.6	0.6	40.6	0.5	6.5	0.9	21.0	0.8	27.8	0.6	38.8	0.5	5.8	0.8	20.8	0.6	26.1	0.2	39.4	1.3	5.6	1.0	21.2	1.0	26.4	0.3	37.7	1.0
57	61	13.0	1	YLGLL	6.0	0.4	22.0	0.5	27.7	0.3	41.4	0.8	6.5	1.0	21.1	0.9	27.6	0.8	39.4	0.8	6.0	0.4	21.3	0.9	27.4	0.1	39.6	0.8	6.1	0.7	20.8	0.4	27.4	0.6	38.8	1.2
62	66	5.8	1	YPTED	29.4	0.7	41.0	0.4	40.8	0.8	52.3	1.1	32.7	0.9	40.7	0.9	42.5	0.8	52.6	0.2	30.3	1.3	41.2	0.7	42.8	0.3	52.8	1.2	28.2	0.6	40.2	1.0	41.8	1.2	51.9	0.7
67	71	6.7	2	YKVYG	0.4	0.3	1.1	0.2	1.1	0.5	5.6	0.3	0.9	0.2	0.8	0.5	2.3	0.7	7.2	0.2	0.3	0.3	0.8	0.5	1.2	0.3	6.8	0.3	0.6	0.1	0.8	0.6	2.1	0.7	5.9	0.3
72	80	7.5	1	YVTNSKVKF	6.2	1.1	8.9	0.5	11.3	0.3	19.1	0.8	6.5	0.8	9.3	0.3	11.4	0.3	17.7	0.6	6.1	0.8	9.0	0.5	11.3	0.8	17.5	0.8	5.7	0.7	8.5	0.6	10.9	0.5	17.1	0.7
81	88	6.7	1	VMVVDSSN	17.3	0.6	26.4	0.8	35.6	1.0	40.4	0.8	24.3	0.7	26.6	0.9	37.3	0.4	40.2	0.8	18.7	0.8	25.1	0.6	36.7	1.2	41.2	0.2	21.1	0.1	23.5	1.4	36.5	1.2	38.8	0.5
81	95	8.0	2	VMVVDSSNTALRDNE	26.4	1.0	37.6	0.8	48.8	1.2	52.3	0.7	26.7	0.5	37.7	1.1	49.0	0.6	51.8	0.5	25.7	1.0	36.8	0.8	48.7	0.4	51.5	0.6	25.1	0.9	37.4	0.3	50.0	0.4	50.8	1.2
83	95	6.2	2	VVDSSNTALRDNE	31.7	0.8	45.7	1.2	57.3	1.6	60.8	0.8	32.0	1.5	45.8	0.6	58.1	0.6	60.2	0.9	31.3	1.1	44.0	1.0	58.6	0.3	60.4	0.5	32.8	0.4	44.4	0.7	58.7	1.2	60.1	0.8
83	99	8.3	2	VVDSSNTALRDNEIRSM	16.6	1.1	27.8	1.1	41.0	0.7	49.0	1.3	16.4	1.2	27.2	0.9	40.2	0.3	47.8	0.7	16.2	1.0	26.6	0.2	39.9	0.8	47.6	1.0	15.8	0.2	26.3	1.1	40.7	0.5	45.4	1.2
100	110	6.7	2	FRKLHNSYTDV	2.5	0.1	6.9	1.1	11.5	0.5	18.6	0.2	2.3	0.3	6.4	0.2	9.8	0.4	15.0	0.5	2.1	0.1	6.9	0.4	10.7	0.4	13.9	0.4	2.6	0.1	6.1	0.4	9.1	0.3	12.5	1.0
111	127	10.0	2	MCNPFYNPGDRIQSSRA	33.0	1.1	43.3	0.1	48.0	0.7	54.4	0.8	32.9	0.6	42.0	0.4	46.6	0.9	52.5	0.2	33.5	0.9	42.4	0.1	46.3	0.1	50.9	0.7	33.0	0.5	41.7	0.8	49.2	1.0	51.6	0.7
131	135	8.2	1	MVTSM	11.7	0.6	23.1	0.4	36.1	1.1	68.3	1.2	14.4	1.2	23.5	0.8	39.2	1.2	67.5	0.4	12.5	1.3	21.2	0.1	36.6	0.3	66.7	0.5	13.4	1.3	22.3	0.4	37.3	0.7	66.2	1.0
132	136	8.2	1	VTSMM	10.3	1.4	23.6	0.6	35.7	0.8	67.6	0.8	14.8	1.1	22.8	0.9	36.1	0.3	67.2	0.1	10.0	1.2	22.2	0.5	35.5	1.2	67.0	0.4	12.4	0.2	22.9	1.2	37.2	0.8	66.4	1.1

TRAPPC3

					APO								TRAPP + Rab1								TRAPP + Rab11								TRAPP + Rab43							
S	E	RT	Z	Sequence	3s	SD	30s	SD	300s	SD	3000s	SD	3s	SD	30s	SD	300s	SD	3000s	SD	3s	SD	30s	SD	300s	SD	3000s	SD	3s	SD	30s	SD	300s	SD	3000s	SD
19	26	12.6	1	FTLTYGAL	1.8	0.8	2.3	0.3	4.4	0.8	12.5	0.6	1.1	0.6	1.7	0.6	3.8	0.5	11.7	0.9	1.4	0.6	1.3	0.3	3.7	0.0	12.5	0.4	1.3	0.4	1.2	0.1	4.2	0.8	11.9	0.8
27	55	11.9	3	VTQLCKDYENDEDVNKQLDKMGFNIGVRL	2.3	0.4	3.9	0.5	4.4	0.8	9.4	0.3	2.1	0.6	4.1	0.0	4.4	0.5	9.3	0.6	2.6	0.4	3.4	0.1	5.1	1.5	8.8	0.2	2.2	0.2	3.7	0.6	4.6	0.5	8.3	0.3
31	55	11.5	4	CKDYENDEDVNKQLDKMGFNIGVRL	2.1	0.2	2.8	0.1	3.3	0.1	6.6	0.1	1.9	0.2	2.7	0.2	3.4	0.1	6.5	0.2	2.0	0.2	2.8	0.1	3.1	0.0	6.6	0.2	1.9	0.1	2.8	0.1	3.6	0.3	6.3	0.3
34	52	11.4	3	YENDEDVNKQLDKMGFNIG	1.5	0.2	1.7	0.2	2.3	0.2	6.3	0.3	1.4	0.1	1.8	0.1	2.2	0.2	6.4	0.2	1.6	0.4	1.9	0.2	2.1	0.1	6.3	0.0	1.6	0.4	1.7	0.1	2.3	0.0	6.1	0.2
34	55	12.2	4	YENDEDVNKQLDKMGFNIGVRL	0.8	0.3	0.7	0.2	0.8	0.2	3.6	0.3	0.8	0.3	0.8	0.3	1.2	0.3	3.3	0.6	0.7	0.2	0.5	0.2	1.0	0.4	3.5	0.3	0.7	0.1	1.0	0.3	1.3	0.2	3.2	0.4
56	60	12.4	1	IEDFL	5.9	0.8	7.4	1.4	16.2	0.8	24.6	0.5	5.8	0.9	6.4	0.5	14.4	0.2	22.1	0.6	5.1	1.2	7.1	0.9	13.5	1.1	22.5	1.1	8.0	1.0	8.1	1.1	14.2	0.6	19.4	0.5
59	70	5.7	4	FLARSNVGRCHD	25.4	0.7	33.7	0.9	38.5	0.3	42.6	0.3	25.8	2.1	33.1	1.7	37.5	0.4	40.3	1.5	24.7	0.6	32.9	0.8	37.3	0.6	40.5	0.8	22.5	0.2	31.0	0.3	36.2	0.4	40.1	1.7
76	83	9.8	3	DVIAKVAF	15.5	0.2	23.8	0.5	33.9	1.1	49.0	0.7	13.8	0.6	23.0	1.3	34.7	0.7	49.6	1.3	14.3	0.3	22.7	0.6	33.2	0.3	50.2	0.5	12.8	1.0	25.5	1.0	35.4	1.4	47.5	1.0
78	85	8.8	3	IAKVAFKM	0.2	0.2	1.1	0.6	6.5	1.0	24.4	1.3	0.1	0.1	1.1	0.7	6.4	0.9	25.2	0.9	0.2	0.2	0.5	0.4	6.5	0.1	23.4	0.6	0.1	0.1	0.8	0.4	5.6	0.5	23.7	1.1
84	102	12.1	2	KMYLGITPSITNWSPAGDE	12.2	0.2	19.4	0.5	27.2	0.6	37.9	0.7	12.4	0.5	18.7	0.0	27.4	0.3	37.5	0.8	11.8	0.3	18.6	0.5	26.9	0.1	37.5	0.4	11.6	0.8	18.4	0.4	27.5	0.4	37.1	0.4
84	103	13.2	2	KMYLGITPSITNWSPAGDEF	11.1	0.3	17.6	0.3	24.9	0.5	34.5	0.7	11.1	0.4	17.0	0.2	24.7	0.3	33.8	0.6	10.8	0.5	17.1	0.3	24.6	0.2	34.4	0.4	10.7	0.3	16.8	0.1	24.7	0.4	33.6	0.7
84	104	12.8	2	KMYLGITPSITNWSPAGDEFS	11.3	0.4	17.7	0.3	24.2	0.8	34.4	1.2	10.9	1.0	16.5	0.3	23.6	0.4	32.5	0.3	10.4	0.2	16.1	0.2	24.1	0.2	35.0	0.8	10.5	0.5	16.5	0.4	24.5	0.9	32.0	0.7
104	114	12.0	1	SLILENNPLVD	17.3	0.4	18.6	0.6	23.5	0.7	35.0	1.1	17.7	0.2	18.5	0.6	22.8	0.5	34.6	0.7	16.6	0.3	18.5	0.2	22.8	0.7	34.4	0.4	16.9	0.9	17.7	0.7	23.7	0.4	33.8	0.6
104	115	14.2	2	SLILENNPLVDF	15.2	0.2	19.8	0.4	25.4	0.9	34.1	0.7	15.6	1.1	19.3	0.4	25.1	0.1	37.0	0.9	14.2	0.5	18.3	0.5	24.1	1.0	33.9	0.2	13.7	0.9	18.5	0.8	26.4	0.6	32.8	0.3
105	114	11.6	1	LILENNPLVD	16.7	0.7	17.7	1.0	23.2	0.5	35.0	1.0	16.6	0.6	17.2	0.5	22.8	0.6	33.6	1.1	16.6	0.7	17.4	0.9	22.6	0.8	33.6	0.7	16.5	0.5	17.2	0.8	23.4	0.4	33.1	1.2
106	115	13.5	1	ILENNPLVDF	13.8	0.1	20.0	0.5	26.6	0.8	35.5	0.4	14.1	0.5	19.4	0.9	26.8	0.4	35.7	0.5	13.5	0.1	19.2	0.4	26.6	0.6	35.7	0.6	13.3	0.2	18.7	0.2	27.3	1.2	34.8	0.9
108	115	12.5	1	ENNPLVDF	5.2	0.4	12.6	0.6	19.4	0.5	30.3	0.9	5.0	0.7	10.9	0.4	19.1	0.7	28.8	1.1	4.8	0.5	11.4	0.6	19.6	1.2	30.3	1.1	4.9	0.9	12.2	0.3	19.9	0.7	30.6	1.1
115	125	9.7	2	FVELPDNHSSL	13.4	0.7	23.0	1.0	33.3	0.6	40.8	1.0	13.2	0.9	22.0	0.6	33.1	0.2	39.3	0.1	13.4	0.9	22.2	0.4	33.3	1.2	40.4	0.4	12.5	0.5	21.6	0.2	33.1	0.6	38.2	0.4
126	130	8.9	1	IYSNL	2.3	0.6	5.7	0.5	20.3	1.2	28.7	0.9	2.8	1.0	4.1	0.6	19.8	1.0	25.5	1.0	4.9	1.2	9.2	0.7	16.6	0.0	25.5	0.9	3.4	0.1	4.4	1.5	18.7	1.4	23.5	1.1
131	139	10.5	2	LCGVLRGAL	0.7	0.1	1.2	0.5	1.0	0.2	1.1	0.3	1.2	0.1	1.3	0.2	1.4	0.5	1.7	0.4	1.0	0.2	1.1	0.3	0.8	0.3	1.2	0.1	0.7	0.0	0.9	0.1	1.1	0.2	0.9	0.1
145	162	9.6	2	AVEAKFVQDTLKGDGVTE	14.3	0.6	28.5	0.4	43.4	0.3	52.6	1.0	14.7	0.8	27.8	0.5	45.4	0.6	52.3	1.0	13.4	0.7	26.9	0.7	45.5	0.1	52.7	1.0	13.0	0.7	27.9	0.7	44.6	1.0	51.8	0.2
151	162	6.8	1	VQDTLKGDGVTE	15.5	0.5	25.7	0.6	40.6	1.4	53.1	1.4	15.8	0.9	25.3	0.6	40.6	0.1	52.1	0.4	15.3	0.4	25.0	0.5	41.4	0.2	52.0	0.9	14.8	0.5	24.9	0.3	41.3	0.6	51.5	0.6
163	167	8.5	2	IRMRF	0.8	0.5	1.2	0.3	1.5	0.3	2.4	0.0	2.2	0.3	2.1	0.8	1.4	0.3	2.5	0.2	1.1	0.2	1.3	0.2	1.5	0.3	2.1	0.3	1.3	0.1	1.1	0.3	1.3	0.2	2.3	0.5
166	179	7.8	3	RFIRRIEDNLPAGE	35.0	0.6	46.1	0.8	52.3	1.2	54.3	0.7	31.3	1.4	44.6	1.0	51.4	0.5	53.9	0.1	33.9	0.6	46.1	1.3	51.4	0.9	53.3	1.4	30.2	1.1	45.8	0.2	52.3	0.4	52.7	0.9
166	183	8.9	2	RFIRRIEDNLPAGEEENL	36.1	0.6	44.9	1.3	48.0	1.9	51.6	0.4	33.3	1.3	43.7	0.2	48.7	0.5	50.3	1.3	35.6	1.4	44.6	0.6	48.4	0.3	50.7	1.2	32.4	1.8	44.2	1.3	49.0	0.3	49.1	0.9
168	179	7.3	2	IRRIEDNLPAGE	40.1	1.0	50.2	0.4	53.3	1.6	55.4	1.2	36.2	1.4	48.7	1.3	52.7	1.3	54.4	0.4	39.0	1.0	48.9	0.7	53.6	0.0	54.8	1.3	35.9	0.4	49.4	0.3	53.7	0.8	53.8	0.3
168	183	8.8	2	IRRIEDNLPAGEEENL	41.2	0.7	48.0	0.9	50.0	0.4	51.8	1.2	38.3	1.3	47.3	0.8	50.1	0.5	49.9	0.7	40.7	0.8	47.6	1.1	49.8	0.4	49.8	0.7	37.8	1.0	46.6	0.6	50.7	0.3	49.2	0.4

Appendix U. Peptides of TRAPPC4, 5 and 6a used for TRAPPII HDX with Rab1, Rab11 and Rab43.

TRAPPC4

					APO								TRAPP + Rab1								TRAPP + Rab11								TRAPP + Rab43							
S	E	RT	Z	Sequence	3s	SD	30s	SD	300s	SD	3000s	SD	3s	SD	30s	SD	300s	SD	3000s	SD	3s	SD	30s	SD	300s	SD	3000s	SD	3s	SD	30s	SD	300s	SD	3000s	SD
-11	-3	5.0	1	YKKAGSENL	57.8	1.5	57.0	0.4	58.0	0.4	58.8	0.9	58.4	0.3	57.5	0.9	59.1	0.4	58.0	0.8	56.5	0.6	57.2	0.9	58.0	0.9	59.7	0.8	57.0	0.8	57.7	1.2	57.9	1.2	58.9	0.7
-2	4	13.1	1	YFQSAIF	21.3	1.0	29.3	0.3	37.9	1.2	47.1	0.5	21.8	1.0	29.0	0.3	39.0	0.7	45.8	0.7	20.7	0.4	28.4	0.9	38.1	0.4	46.4	0.7	21.3	1.0	29.0	0.4	40.2	2.3	45.9	0.4
5	19	11.7	2	SVYVVNKAGGLIYQL	5.2	0.3	14.3	0.1	23.1	0.8	31.4	0.9	4.4	0.1	11.4	0.2	19.8	0.2	25.8	0.4	4.4	0.3	11.5	0.1	19.6	0.2	25.8	0.3	2.5	0.1	7.7	0.6	12.8	0.5	17.5	0.6
7	19	11.6	2	YVVNKAGGLIYQL	5.0	0.2	14.1	0.3	21.6	0.4	30.2	1.0	3.7	0.6	10.7	0.0	19.5	0.7	24.1	0.3	4.1	0.3	11.6	0.2	19.2	0.4	24.1	0.2	1.9	0.0	7.4	0.2	12.9	1.0	16.6	0.8
20	38	11.8	2	DSYAPRAEAEKTFSYPLDL	31.5	0.6	44.2	0.7	51.9	0.7	57.0	0.7	33.2	0.2	42.9	0.1	51.1	0.9	56.3	0.3	29.5	0.9	42.7	0.5	50.3	0.5	58.0	0.8	32.3	0.6	41.4	0.9	50.9	0.1	55.9	0.1
20	39	13.3	3	DSYAPRAEAEKTFSYPLDLL	26.3	0.2	37.0	0.6	46.9	0.8	57.6	0.7	27.1	0.8	35.8	0.9	46.3	0.7	54.7	0.4	25.6	1.1	35.6	0.8	46.3	0.3	57.3	0.8	25.1	0.8	35.6	0.5	47.0	1.2	55.2	0.6
20	40	14.1	3	DSYAPRAEAEKTFSYPLDLLL	23.6	0.9	33.2	0.6	47.7	0.9	58.2	0.8	23.8	1.4	32.2	0.5	45.9	0.3	55.5	0.0	22.5	0.9	31.7	1.1	46.3	0.7	58.1	0.6	24.2	0.1	31.9	1.2	45.9	0.4	56.0	0.5
40	44	5.6	2	LKLHD	17.4	0.6	35.1	1.4	47.6	1.3	48.1	1.2	18.4	1.1	29.5	0.3	46.4	0.4	48.0	1.0	18.2	1.3	33.1	1.4	48.4	0.5	49.8	1.3	18.4	0.1	32.5	0.9	48.1	0.8	48.5	0.3
40	64	9.8	3	LKLHDERVLVAFGQRDGIRVGHAVL	4.6	0.1	9.2	0.3	15.1	0.5	28.9	1.0	4.0	0.1	7.5	0.2	14.5	0.4	25.7	0.9	4.4	0.4	8.5	0.5	15.2	0.4	27.7	0.7	4.1	0.3	7.4	0.3	14.8	0.5	25.4	0.9
43	50	6.5	1	HDERVLVA	3.1	0.4	4.4	1.3	7.5	1.3	19.5	1.4	3.8	0.6	4.0	0.7	7.1	1.4	14.2	1.1	5.6	0.6	6.1	0.3	8.9	0.9	19.2	0.7	4.4	0.6	5.2	1.4	8.3	0.5	17.2	1.0
45	64	9.8	4	ERVLVAFGQRDGIRVGHAVL	5.2	0.1	9.4	0.3	17.4	0.2	31.8	0.4	4.6	0.3	7.7	0.5	15.3	0.6	29.5	0.6	5.2	0.2	9.4	0.1	17.1	0.8	34.6	0.2	3.9	0.2	7.6	0.0	16.6	1.0	33.8	0.4
51	64	8.5	3	FGQRDGIRVGHAVL	5.2	0.2	7.1	0.4	14.2	0.7	30.6	0.7	5.1	0.1	6.5	0.7	12.1	0.1	28.1	0.5	5.1	0.3	6.9	0.1	13.9	0.4	29.7	0.4	5.0	0.1	6.5	0.3	13.2	0.4	27.9	0.3
65	83	9.2	2	AINGMDVNGRYTADGKEVL	17.7	0.4	29.2	0.6	40.1	0.8	48.7	0.2	17.3	1.1	27.9	0.8	39.1	0.3	48.0	0.4	17.2	1.0	28.2	0.3	40.2	0.4	48.3	0.7	16.2	1.0	28.1	0.6	40.2	0.2	48.7	0.4
84	103	10.5	4	EYLGNPANYPVSIRFGRPRL	10.8	0.4	18.8	0.2	21.5	0.6	35.4	0.4	10.6	0.8	18.3	0.2	21.5	0.3	34.7	0.4	10.2	0.6	18.6	0.3	21.6	0.1	35.0	0.4	8.7	0.4	18.4	0.2	21.8	0.2	35.0	0.9
126	136	8.8	1	SPEQGSSGIEM	24.6	0.6	26.3	0.2	26.5	0.5	28.6	1.5	23.4	0.9	25.9	0.4	26.8	0.3	27.0	0.7	24.4	0.7	25.5	0.2	26.8	0.8	27.6	0.3	23.2	0.7	26.0	0.8	25.9	1.2	26.6	0.8
137	141	4.8	1	LETDT	2.8	1.0	2.9	0.2	8.7	0.7	41.0	0.8	2.6	0.2	3.7	0.5	7.3	0.4	37.6	0.7	3.3	0.8	3.8	1.1	9.3	0.6	41.3	0.1	2.3	0.4	3.2	0.9	8.0	0.9	40.7	0.5
137	146	9.4	3	LETDTFKLHC	0.9	0.0	1.3	0.1	2.3	0.1	11.9	0.7	1.0	0.1	1.5	0.5	2.1	0.2	11.1	0.8	1.2	0.3	1.2	0.1	2.5	0.1	11.9	0.6	1.0	0.0	1.0	0.2	2.5	0.3	11.4	0.2
147	155	11.4	2	YQTLTGIKF	11.1	0.2	13.8	0.4	19.9	0.6	35.7	0.8	10.7	0.5	12.1	0.1	15.5	0.4	27.4	0.6	10.8	0.4	13.0	0.3	15.9	0.1	28.9	0.2	9.2	0.4	11.2	0.2	11.8	0.4	19.7	0.9
156	167	8.3	2	VVLADPRQAGID	29.8	1.0	35.8	0.4	43.4	2.0	47.0	1.0	29.8	1.0	35.4	1.2	42.6	0.7	47.1	0.9	29.2	0.5	36.0	0.6	43.3	0.2	49.1	0.3	28.3	1.1	33.3	0.8	43.3	0.9	47.8	0.6
156	169	10.3	2	VVLADPRQAGIDSL	31.0	0.5	37.4	1.3	50.8	1.2	55.8	0.4	31.0	0.4	37.0	0.5	51.0	0.7	55.0	0.3	30.3	0.5	37.0	0.1	50.0	0.3	55.2	0.3	29.4	0.2	36.9	0.6	51.4	0.3	55.0	0.4
170	180	11.3	3	LRKIYEIYSDF	1.3	0.3	1.3	0.1	1.0	0.2	2.4	0.5	1.2	0.2	1.2	0.5	1.0	0.4	1.5	0.2	1.4	0.6	1.1	0.2	1.5	0.4	1.6	0.2	0.9	0.2	0.9	0.4	1.4	0.4	1.1	0.4
181	191	12.9	2	ALKNPFYSLEM	7.9	0.5	17.2	0.4	35.0	1.1	55.9	0.5	6.0	0.2	11.6	0.3	29.7	0.0	42.9	0.3	6.3	0.8	11.8	0.4	28.2	0.0	44.6	0.1	2.7	0.2	5.9	0.3	18.7	0.4	32.4	0.5
181	197	13.4	3	ALKNPFYSLEMPIRCEL	18.2	0.3	27.9	0.9	38.5	0.7	51.7	0.2	16.8	0.4	25.5	0.4	34.8	0.8	43.7	0.2	16.9	0.5	24.3	0.8	35.0	0.5	44.6	0.5	13.8	0.5	20.4	0.8	28.1	0.3	36.2	0.5
192	197	9.3	2	PIRCEL	56.0	1.1	65.9	0.6	65.8	1.6	68.1	0.4	53.8	2.4	66.0	0.8	66.3	0.4	67.0	0.2	55.1	2.2	66.1	0.2	65.0	0.5	66.5	0.9	49.7	2.4	65.7	1.0	66.8	0.2	66.3	1.1
198	204	9.7	2	FDQNLKL	3.6	0.7	5.3	1.7	7.9	0.2	22.5	0.8	4.7	1.0	5.6	0.5	7.3	1.1	19.0	0.3	4.5	1.3	4.7	0.7	7.6	0.2	19.7	0.3	3.9	0.4	4.3	1.0	6.4	0.5	17.6	0.6
198	206	11.2	2	FDQNLKLAL	0.8	0.1	1.1	0.1	2.4	0.2	14.3	0.7	1.0	0.1	1.1	0.1	2.3	0.1	12.4	0.2	0.8	0.2	1.0	0.1	2.4	0.1	13.3	0.4	0.9	0.1	1.0	0.2	2.4	0.7	11.7	0.6
207	219	7.0	2	EVAEKAGTFGPGS	51.8	0.4	63.3	0.7	63.6	1.0	65.7	1.1	52.9	1.1	63.1	1.0	64.2	0.3	65.0	0.7	51.7	1.2	63.0	0.8	64.2	0.2	65.1	1.0	51.4	0.9	63.3	0.6	65.3	0.5	65.8	0.8
208	219	6.8	2	VAEKAGTFGPGS	57.3	1.8	64.8	0.4	64.0	1.5	65.7	1.0	58.3	1.3	64.9	0.7	64.4	0.1	66.4	0.6	55.1	0.2	63.0	1.7	61.7	0.9	63.9	1.3	54.6	0.3	62.2	0.3	62.7	0.6	62.8	0.6

TRAPPC5

					APO								TRAPP + Rab1								TRAPP + Rab11								TRAPP + Rab43							
S	E	RT	Z	Sequence	3s	SD	30s	SD	300s	SD	3000s	SD	3s	SD	30s	SD	300s	SD	3000s	SD	3s	SD	30s	SD	300s	SD	3000s	SD	3s	SD	30s	SD	300s	SD	3000s	SD
3	12	5.6	3	ARFTRGKSAL	45.6	1.5	51.1	0.8	52.1	0.9	54.3	0.6	47.8	1.0	51.2	1.0	53.3	0.5	53.3	0.4	43.9	0.7	51.0	0.7	52.8	0.3	53.7	0.7	44.1	1.0	51.6	0.9	52.9	1.2	53.4	0.8
13	26	7.6	4	LERALARPRTEVSL	52.1	0.6	59.5	0.5	62.5	1.4	67.2	0.4	53.0	0.6	58.9	1.2	64.0	0.3	67.1	0.7	51.3	1.3	58.9	0.6	62.7	0.5	66.9	0.9	49.7	1.1	58.4	0.6	64.0	0.9	66.4	0.4
13	28	7.2	3	LERALARPRTEVSLSA	51.5	1.0	58.2	0.6	62.3	1.6	66.6	1.0	51.3	1.0	56.8	0.7	62.7	0.8	68.8	0.1	50.5	1.3	57.0	0.3	63.1	0.1	69.0	0.5	49.8	0.8	57.0	0.0	63.2	0.7	68.3	0.4
37	42	3.5	2	VQHCQS	7.9	0.6	21.1	2.0	34.1	0.4	43.3	1.2	7.3	1.0	19.5	0.3	33.4	1.1	41.6	1.1	6.1	0.3	18.5	0.4	31.3	0.2	42.5	2.1	4.7	0.7	18.1	1.4	34.4	0.5	42.4	0.6
37	44	4.2	1	VQHCQSRV	18.9	0.5	34.0	0.6	42.1	0.4	44.8	1.0	16.7	0.5	32.8	0.4	43.4	0.5	45.8	1.4	15.9	0.6	31.2	1.0	42.6	1.3	45.9	0.2	15.3	0.6	26.8	1.0	42.4	0.6	44.8	1.1
37	50	10.5	3	VQHCQSRVFSVAEL	27.1	0.7	42.2	0.4	48.6	0.5	50.4	0.9	27.6	0.8	41.4	1.3	48.5	0.4	50.1	0.3	26.8	0.7	40.4	0.3	47.2	0.3	49.9	0.5	26.2	1.7	37.6	0.5	47.7	1.0	49.5	0.7
55	62	5.4	2	AALGRQVG	5.0	1.0	4.7	1.4	5.1	1.0	8.7	0.3	4.6	0.6	3.8	0.4	4.6	0.1	9.1	0.8	4.1	0.4	4.6	0.3	4.7	0.5	8.5	0.7	3.8	0.4	5.1	0.2	5.4	1.4	8.0	0.5
55	63	5.9	2	AALGRQVGA	2.5	0.4	3.1	0.2	3.3	0.4	14.4	1.4	2.5	0.1	3.2	0.6	2.8	0.3	13.7	1.0	3.0	0.3	2.5	0.1	3.0	0.1	13.6	1.0	3.0	0.3	2.5	0.4	3.0	0.2	14.3	1.4
63	69	9.4	2	ARVLDAL	1.1	0.3	1.7	0.2	10.5	0.9	48.5	0.8	1.0	0.4	1.6	0.2	9.9	0.4	49.0	0.1	0.8	0.0	1.9	0.3	10.7	0.8	49.5	0.2	0.7	0.1	1.6	0.4	10.5	0.6	48.9	1.2
70	86	6.3	4	VAREKGARRETKVLGAL	10.6	0.4	15.4	0.4	23.8	0.8	37.6	1.0	10.7	0.5	15.1	0.5	24.1	0.6	36.4	0.5	10.3	0.4	14.8	0.4	24.3	0.3	37.1	0.8	10.4	0.1	15.2	0.3	23.6	0.3	36.4	0.6
84	88	13.0	1	GALLF	1.9	0.7	1.3	0.4	0.9	0.2	2.2	0.5	1.0	0.2	1.3	0.9	1.1	0.3	2.9	0.4	0.8	0.6	1.3	0.5	0.8	0.0	2.3	0.7	2.0	1.0	2.1	1.1	1.0	0.2	2.2	0.4
87	94	11.5	2	LFVKGAVW	4.0	0.7	8.0	0.2	12.5	0.7	16.0	1.4	3.2	0.4	7.1	0.3	15.3	0.8	12.5	0.7	4.7	0.5	7.6	0.8	13.1	0.7	12.0	0.3	3.8	0.0	7.2	0.8	13.2	0.2	12.1	0.2
87	105	12.0	5	LFVKGAVWKALFGKEADKL	3.4	0.2	8.1	0.3	12.6	0.4	20.1	0.6	3.8	0.2	7.7	0.3	13.0	0.3	19.9	1.0	3.0	0.1	7.6	0.4	12.3	0.2	20.2	0.3	2.9	0.4	7.5	0.1	12.8	0.2	19.5	0.4
87	110	11.8	4	LFVKGAVWKALFGKEADKLEQAND	8.5	0.4	14.2	0.1	20.3	0.3	27.3	0.7	8.9	1.0	13.7	0.5	20.6	0.2	26.0	0.5	8.5	0.2	13.5	0.2	19.6	0.3	27.3	1.3	7.6	0.3	13.3	0.4	20.3	0.3	28.0	0.2
87	111	11.8	4	LFVKGAVWKALFGKEADKLEQANDD	8.2	0.2	13.5	0.2	19.5	0.4	28.5	0.5	8.1	0.6	12.7	0.4	20.1	0.5	27.9	0.3	7.4	0.5	12.8	0.1	18.6	0.6	27.7	0.1	7.1	0.0	12.7	0.2	19.7	0.6	27.3	0.3
88	98	12.2	2	FVKGAVWKALF	0.9	0.3	2.7	0.2	4.4	0.2	5.0	0.1	1.1	0.1	2.1	0.2	4.5	0.5	4.8	0.3	0.7	0.3	3.2	1.1	4.3	0.0	7.1	0.2	0.9	0.4	2.2	0.0	4.3	0.1	4.7	0.0
88	105	11.4	5	FVKGAVWKALFGKEADKL	3.7	0.3	9.2	0.2	14.9	0.5	22.9	0.4	3.9	0.3	8.8	0.3	14.9	0.4	22.6	0.3	3.4	0.4	8.6	0.1	14.3	0.3	23.4	0.8	2.6	0.1	8.7	0.2	14.3	0.2	22.0	0.1
88	110	11.2	3	FVKGAVWKALFGKEADKLEQAND	9.5	0.4	15.8	0.5	22.5	0.6	31.4	0.8	9.4	0.5	15.2	0.4	22.4	0.2	31.1	0.4	9.2	0.3	15.1	0.1	21.7	0.1	31.2	0.5	8.5	0.3	14.6	0.2	22.2	0.2	30.7	0.5
88	111	11.3	3	FVKGAVWKALFGKEADKLEQANDD	8.5	0.3	14.4	0.3	20.7	0.4	29.8	0.6	8.4	0.5	13.7	0.3	21.0	0.7	28.7	0.5	8.1	0.3	13.6	0.1	19.9	0.4	29.4	0.5	7.3	0.2	13.4	0.1	20.6	0.3	28.7	0.3
99	110	4.9	2	GKEADKLEQAND	23.7	0.8	34.9	0.2	45.9	0.9	60.1	0.8	23.6	1.1	36.1	0.3	47.1	0.3	59.5	0.8	26.6	0.7	33.8	1.0	44.6	0.3	59.9	0.3	26.2	1.0	34.7	1.2	46.1	1.0	59.4	0.4
111	116	8.7	2	DARTFY	6.2	0.3	17.7	0.9	22.0	0.8	37.4	0.4	5.8	0.9	15.3	0.6	20.5	0.4	34.4	0.2	5.7	0.2	17.3	0.7	20.8	0.5	36.0	0.1	4.7	0.1	18.1	1.0	21.4	0.8	35.1	0.2
115	126	11.4	2	FYIIEREPLINT	26.7	0.4	36.2	0.7	43.1	0.9	51.3	1.4	27.3	1.3	34.5	0.4	39.2	1.1	48.1	0.6	25.8	1.0	34.5	0.8	39.8	1.0	48.9	0.9	24.0	0.1	33.2	0.7	36.4	0.9	48.2	0.6
116	126	9.9	2	YIIEREPLINT	32.1	1.1	43.7	0.4	51.7	1.3	62.4	1.1	33.1	1.4	41.4	0.3	49.5	0.9	59.1	0.1	31.5	0.7	42.2	0.6	49.0	0.1	59.3	0.3	29.7	1.2	40.6	0.1	45.6	0.2	57.9	0.4
117	126	8.7	2	IIEREPLINT	37.4	0.9	50.1	0.6	59.3	1.2	70.2	1.4	38.3	1.5	48.2	0.7	56.6	0.3	66.4	0.4	36.8	1.2	48.6	0.4	56.9	0.2	66.9	0.8	33.5	1.2	46.9	0.2	53.0	0.8	65.3	0.5
127	137	8.8	1	YISVPKENSTL	52.9	1.0	59.7	0.7	63.4	0.7	65.7	1.3	52.6	1.1	58.6	1.1	63.2	0.2	64.7	0.7	50.7	1.3	58.0	0.8	62.0	0.0	64.8	1.4	48.6	1.2	56.2	1.0	63.0	1.0	63.4	0.8
138	142	8.5	1	NCASF	16.8	0.8	38.2	0.1	51.2	1.5	67.7	1.1	14.7	1.1	32.8	1.2	52.5	1.8	60.6	1.4	14.1	1.8	33.3	0.4	52.0	1.8	61.0	1.1	9.6	1.6	30.5	0.4	53.3	2.4	59.9	0.4
143	148	6.7	1	TAGIVE	1.4	0.1	1.6	0.3	1.3	0.3	1.5	0.2	1.4	0.0	1.3	0.2	1.3	0.2	1.6	0.1	1.7	0.3	1.6	0.2	1.5	0.4	1.4	0.2	1.3	0.2	1.4	0.1	1.4	0.3	1.5	0.2
149	170	8.0	3	AVLTHSGFPAKVTAHWHKGTTL	2.9	0.1	5.5	0.1	8.6	0.4	13.2	0.3	2.8	0.2	5.2	0.3	8.1	0.2	12.8	0.4	2.9	0.1	5.3	0.3	8.2	0.3	12.8	0.4	2.6	0.1	5.1	0.1	8.0	0.2	12.5	0.0
150	170	7.9	3	VLTHSGFPAKVTAHWHKGTTL	2.9	0.1	5.6	0.1	8.7	0.5	13.8	0.6	2.6	0.2	5.2	0.4	7.9	0.3	12.8	0.2	2.9	0.2	5.3	0.3	8.3	0.4	12.7	0.6	2.5	0.0	5.0	0.1	8.0	0.2	12.6	0.3
150	171	8.4	3	VLTHSGFPAKVTAHWHKGTTLM	2.4	0.2	4.7	0.2	8.1	0.4	12.8	0.2	2.3	0.3	4.5	0.1	7.3	0.8	12.4	0.3	2.3	0.4	4.0	0.2	7.1	0.9	12.2	0.5	2.2	0.2	4.3	0.2	7.4	0.5	11.7	0.1
171	176	9.1	1	MIKFEE	13.2	0.9	14.6	0.4	18.6	0.6	38.6	0.6	13.0	0.4	14.3	0.6	18.8	0.7	34.2	0.9	14.1	0.9	14.1	0.4	17.7	0.0	36.0	0.7	12.6	0.2	14.2	0.7	18.5	0.7	34.4	0.9
171	188	9.8	5	MIKFEEAVIARDRALEGR	18.4	0.5	33.5	0.8	49.7	0.8	63.6	0.9	17.8	0.8	31.8	0.0	49.9	0.5	62.2	0.7	17.5	0.9	31.8	0.6	48.7	0.6	62.1	0.8	16.8	0.9	31.6	0.8	50.8	0.7	61.9	0.4
175	188	6.9	4	EEAVIARDRALEGR	20.6	0.9	27.2	0.2	33.4	0.5	40.7	1.1	21.2	0.7	27.6	0.9	33.1	0.8	39.4	0.9	20.8	0.7	26.9	0.8	34.2	0.2	40.0	0.7	20.3	0.3	26.9	0.8	34.0	0.8	38.6	0.7
177	188	5.8	3	AVIARDRALEGR	16.3	0.6	36.2	0.7	53.2	1.0	63.8	1.2	16.8	1.1	35.1	0.7	53.1	0.5	63.1	0.7	15.9	0.8	35.2	0.6	53.5	0.2	63.9	0.1	15.2	0.6	35.3	0.2	53.4	0.8	63.5	0.3
178	188	5.1	3	VIARDRALEGR	19.5	0.5	42.1	0.8	59.3	1.4	64.2	0.8	20.1	1.2	40.6	0.4	59.8	0.1	63.1	1.2	18.4	0.3	40.7	0.5	59.6	0.1	64.6	0.5	18.3	0.9	40.6	0.2	59.2	0.9	64.0	0.8
179	188	4.7	3	IARDRALEGR	21.4	1.1	45.1	0.8	58.5	1.1	60.3	0.8	22.6	0.4	43.7	0.7	58.9	0.3	60.9	1.0	19.9	0.4	44.5	1.1	58.8	0.9	60.3	0.8	20.1	1.0	43.7	0.2	59.9	0.6	60.8	0.9

TRAPPC6a

					APO								TRAPP + Rab1								TRAPP + Rab11								TRAPP + Rab43							
S	E	RT	Z	Sequence	3s	SD	30s	SD	300s	SD	3000s	SD	3s	SD	30s	SD	300s	SD	3000s	SD	3s	SD	30s	SD	300s	SD	3000s	SD	3s	SD	30s	SD	300s	SD	3000s	SD
9	14	8.5	2	FLHTEM	0.4	0.3	0.5	0.2	0.7	0.5	0.9	0.5	0.7	0.2	1.1	0.3	0.9	0.8	0.6	0.4	0.3	0.1	0.4	0.4	0.6	0.3	0.6	0.2	0.7	0.2	0.5	0.4	0.6	0.5	0.4	0.0
19	33	9.5	2	WAHDPDPGPGVSAGL	43.7	0.5	44.2	0.6	44.4	0.7	44.8	0.6	43.0	0.8	43.9	0.9	43.8	0.2	44.2	0.7	43.8	0.8	44.2	0.6	43.8	0.5	44.9	0.7	43.9	0.0	44.3	0.2	45.0	1.1	43.7	0.3
34	48	6.1	3	RGEEAGATKGQKMSL	57.2	0.8	57.0	0.9	57.0	0.3	58.5	0.5	57.7	0.8	56.5	0.3	57.2	0.7	57.2	0.9	55.0	0.7	55.6	0.1	56.4	0.4	57.8	0.6	56.5	0.3	57.0	0.6	56.9	0.6	57.1	0.5
49	73	12.8	4	SVLEGMGFRVGQALGERLPRETLAF	13.5	0.7	17.8	0.2	20.4	0.3	29.9	0.9	14.2	0.8	17.0	0.9	23.6	0.3	28.3	0.3	11.3	0.3	15.3	0.2	18.5	0.8	26.3	0.3	12.8	0.1	17.4	0.3	20.3	0.8	27.7	0.2
56	73	10.7	4	FRVGQALGERLPRETLAF	20.9	0.4	25.6	0.1	26.3	0.9	34.4	0.5	20.8	1.2	25.6	0.2	26.7	0.5	33.2	0.5	21.1	0.4	25.2	0.5	25.9	0.3	32.8	0.3	19.7	0.8	25.4	0.7	26.6	0.4	32.1	0.2
74	87	13.9	3	REELDVLKFLCKDL	0.8	0.5	5.2	0.4	13.0	0.5	31.1	0.9	0.7	0.3	5.0	0.0	12.1	0.9	30.3	0.4	0.9	0.2	4.4	0.7	13.5	0.5	29.5	1.2	0.7	0.1	4.1	0.3	12.8	1.2	28.5	0.7
78	88	14.1	3	DVLKFLCKDLW	1.4	0.4	1.2	0.2	4.2	0.7	23.3	1.0	1.1	0.3	1.1	0.1	4.0	0.4	25.7	0.5	1.1	0.1	1.1	0.1	4.2	0.1	23.0	0.6	1.1	0.1	1.2	0.7	4.1	0.1	23.1	0.6
83	88	11.1	2	LCKDLW	1.5	0.8	1.7	0.4	5.8	0.6	15.3	0.7	1.4	0.3	1.4	0.2	5.6	0.4	15.0	0.2	1.1	0.0	1.5	0.7	5.1	0.1	15.6	0.4	1.5	0.2	1.9	0.8	7.2	0.7	14.5	0.8
92	106	5.9	3	FQKQMDSLRTNHQGT	21.8	0.5	31.8	0.7	42.8	1.4	48.3	1.0	22.5	1.0	32.6	0.5	43.4	0.7	47.1	0.7	21.4	0.5	31.4	0.7	43.1	0.1	47.9	1.2	21.5	0.1	31.5	0.5	43.1	0.9	47.9	0.7
107	114	10.9	1	YVLQDNSF	0.9	0.2	2.2	0.2	5.8	0.3	13.4	1.0	1.3	0.2	1.5	0.3	5.5	0.2	12.9	0.4	0.9	0.2	1.4	0.3	5.3	0.4	12.5	0.4	1.1	0.0	1.4	0.2	6.1	0.8	12.5	0.7
115	125	13.2	2	PLLLPMASGLQ	10.0	0.5	21.6	0.3	30.7	0.5	34.5	0.9	10.0	0.6	19.9	0.9	30.9	0.5	34.0	0.3	9.4	0.6	19.9	0.7	30.4	0.2	33.2	0.3	10.3	0.3	19.4	0.2	31.3	0.5	33.4	0.6
125	133	10.0	1	QYLEEAPKF	4.7	0.3	15.0	0.3	26.3	0.8	35.2	1.2	4.7	0.4	14.7	0.4	26.1	0.3	33.9	0.5	7.7	0.3	18.8	0.9	26.8	0.9	36.7	0.3	5.7	0.6	14.4	1.2	30.7	1.0	36.6	0.9
134	140	13.0	1	LAFTCGL	0.6	0.1	0.9	0.3	0.9	0.1	2.8	0.4	0.6	0.0	0.4	0.2	0.9	0.2	2.7	0.3	0.5	0.2	0.5	0.1	0.7	0.1	2.5	0.1	0.6	0.1	0.4	0.2	0.6	0.3	3.0	0.1
146	153	11.4	1	YTLGIESV	6.1	0.1	12.8	0.0	19.8	1.0	36.5	1.0	5.4	0.6	12.5	0.4	20.7	1.3	33.0	1.3	5.7	0.1	12.6	0.2	20.4	1.2	32.6	1.2	4.5	0.8	12.0	0.1	18.3	1.0	31.4	1.3
152	166	12.4	2	SVVTASVAALPVCKF	14.1	0.3	22.6	0.4	36.9	1.0	46.4	0.1	12.3	0.6	22.3	0.3	37.3	1.0	46.0	0.4	12.0	0.9	22.1	0.9	37.2	0.5	43.6	0.7	11.4	0.3	22.2	0.2	36.3	0.9	43.1	0.1
154	166	11.5	2	VTASVAALPVCKF	14.4	0.4	25.7	0.1	35.4	0.6	42.9	0.9	14.6	0.9	25.0	0.5	35.8	0.2	42.3	0.3	13.9	0.9	25.0	0.4	35.1	0.2	42.4	0.2	12.3	0.4	24.4	0.3	34.7	0.2	41.5	0.6
167	173	6.4	1	QVVIPKS	32.4	0.5	40.7	0.6	54.1	1.3	60.6	0.8	32.2	1.4	40.2	0.6	54.5	0.9	62.3	0.4	31.6	0.8	40.1	0.4	54.3	0.3	60.0	0.6	29.7	0.5	40.3	0.6	55.1	0.6	62.1	0.4

Appendix V. Peptides of TRAPPC9 for TRAPPII HDX with Rab1, Rab11 and Rab43

TRAPPC9					APO								TRAPP + Rab1								TRAPP + Rab11								TRAPP + Rab43							
S	E	RT	Z	Sequence	3s	SD	30s	SD	300s	SD	3000s	SD	3s	SD	30s	SD	300s	SD	3000s	SD	3s	SD	30s	SD	300s	SD	3000s	SD	3s	SD	30s	SD	300s	SD	3000s	SD
9	16	6.1	1	CAEDHQTL	1.8	0.6	2.0	0.7	6.6	0.5	12.8	0.2	1.3	0.6	2.0	0.7	6.0	0.8	12.4	0.9	2.0	0.3	2.5	0.1	5.2	0.3	12.2	0.2	1.4	0.2	2.3	0.4	5.5	0.7	12.0	0.3
10	16	5.7	1	AEDHQTL	1.1	0.4	1.7	0.2	1.6	0.1	3.5	0.8	1.3	0.5	1.4	0.4	1.7	0.2	2.8	0.6	0.9	0.4	2.0	0.4	1.8	0.3	2.9	0.4	1.7	0.2	1.5	0.2	1.7	0.1	3.1	0.1
10	17	8.5	1	AEDHQTLL	0.3	0.3	0.3	0.4	0.9	0.7	2.7	1.4	0.2	0.2	0.6	0.5	0.3	0.2	3.3	1.4	0.3	0.4	0.7	0.4	0.4	0.6	2.4	0.6	0.2	0.0	0.9	0.2	1.2	1.5	3.3	0.6
17	31	12.3	2	LVVVQPVGIVSEENF	27.0	0.5	36.3	0.1	39.2	0.5	47.5	0.3	27.4	1.4	35.9	0.5	39.3	0.5	47.1	0.3	26.5	1.2	35.8	0.4	38.6	0.1	47.2	0.3	26.2	0.7	36.0	0.5	39.9	0.8	46.9	0.3
18	31	11.6	2	VVVQPVGIVSEENF	30.2	0.5	40.7	0.3	43.8	0.5	52.9	0.3	30.8	1.0	40.3	0.3	44.1	0.6	52.3	0.3	29.8	0.6	40.3	0.2	43.4	0.3	52.6	0.1	29.3	0.8	40.4	0.3	44.5	0.7	52.2	0.1
32	43	8.0	3	FRIYKRICSVSQ	2.4	0.1	10.6	0.0	15.7	0.5	26.6	0.7	2.7	0.3	10.3	0.2	15.5	0.3	25.9	0.7	2.4	0.2	9.9	0.1	15.6	0.1	25.8	0.6	2.3	0.2	10.1	0.2	15.8	0.0	25.6	1.0
44	50	5.0	2	ISVRDSQ	54.3	0.6	56.7	0.9	64.1	0.5	72.2	1.0	54.0	0.9	56.0	0.7	66.9	1.0	71.2	0.9	53.0	0.5	55.1	0.9	66.4	0.5	73.0	0.1	54.8	1.2	59.5	0.3	67.9	0.3	73.5	0.7
54	67	4.9	4	YIRYRHHYPPENNE	14.8	0.4	22.0	0.5	23.4	0.6	27.2	0.6	15.1	1.0	21.6	0.6	24.0	0.2	26.4	0.5	14.2	0.4	21.5	0.9	23.4	0.1	26.9	0.3	14.1	0.4	22.0	0.3	23.9	0.5	26.8	0.0
55	67	4.4	3	IRYRHHYPPENNE	17.6	0.8	25.3	0.5	27.2	0.3	29.5	0.6	18.1	0.8	25.0	0.3	27.8	0.5	29.9	0.9	16.2	0.9	25.0	0.9	27.0	0.7	30.0	0.3	16.3	0.1	24.9	0.2	27.3	0.6	29.6	0.3
68	80	9.2	2	WGDFQTHRKVVGL	1.4	0.5	2.0	0.2	1.8	0.3	7.7	0.4	1.1	0.4	1.7	0.4	1.8	0.2	7.0	0.6	1.0	0.2	1.7	0.1	1.8	0.3	7.2	0.9	1.0	0.1	1.7	0.3	1.8	0.5	5.9	0.2
72	80	5.5	2	QTHRKVVGL	0.8	0.2	0.8	0.0	1.1	0.2	4.1	0.1	0.8	0.1	0.7	0.1	1.1	0.2	4.5	0.3	0.9	0.1	0.8	0.1	1.1	0.1	4.1	0.3	0.8	0.3	0.8	0.2	1.2	0.2	4.3	0.6
72	82	6.5	2	QTHRKVVGLIT	0.8	0.2	0.9	0.2	1.6	0.4	3.5	0.6	0.8	0.2	1.0	0.1	1.1	0.2	3.4	0.2	0.7	0.1	0.8	0.1	1.3	0.2	3.3	0.2	0.7	0.3	1.1	0.1	1.4	0.7	3.2	0.3
87	95	9.5	2	FSAKDWPQT	30.9	0.9	46.4	0.8	62.7	1.6	66.5	0.9	32.6	1.2	46.7	0.9	62.4	0.5	65.5	0.2	30.8	0.6	45.9	1.1	62.2	0.8	66.0	0.7	35.5	1.3	50.1	1.5	64.6	0.3	66.2	0.7
87	110	11.3	5	FSAKDWPQTFEKFHVQKEIYGSTL	11.5	0.2	22.5	0.5	44.5	0.7	52.3	0.6	11.7	0.5	22.2	0.5	45.3	0.4	52.1	0.8	11.1	0.5	21.7	0.4	44.8	0.0	52.0	0.6	10.9	0.6	21.8	0.3	46.7	0.3	51.2	0.1
100	110	7.8	2	HVQKEIYGSTL	16.9	0.6	32.2	0.4	58.4	1.9	63.6	1.1	17.2	1.1	31.9	0.5	59.3	0.9	62.6	0.5	16.7	0.9	31.3	0.5	58.3	0.1	62.5	0.6	16.3	0.1	31.3	0.1	58.4	0.5	61.9	0.3
111	115	6.9	1	YDSRL	3.7	0.4	4.1	1.2	17.1	0.6	42.9	0.9	2.8	0.2	4.9	0.9	17.8	0.4	42.2	0.4	3.3	0.9	4.0	1.3	17.7	0.6	42.4	1.0	4.9	1.3	4.4	0.5	18.3	0.9	41.9	0.9
116	122	12.6	1	FVFGLQG	26.9	0.8	28.7	0.1	38.0	0.9	52.0	0.9	27.3	0.7	28.4	0.5	38.3	0.8	51.8	0.1	26.5	1.3	28.4	0.5	37.9	0.0	51.7	0.2	27.2	0.1	28.6	0.3	38.8	0.8	51.6	0.7
124	130	4.9	2	IVEQPRT	74.8	0.9	78.3	1.1	78.3	1.5	77.7	1.1	76.9	0.9	77.2	0.3	78.9	0.5	78.7	0.6	73.8	0.6	77.7	0.2	77.6	0.9	79.7	0.1	73.5	1.7	78.5	0.4	79.3	0.2	78.9	1.1
135	143	8.5	1	YPNYEDCQT	41.4	0.9	58.6	0.6	66.1	0.7	70.4	0.2	42.3	2.3	57.7	1.3	65.8	1.3	65.9	0.5	41.8	1.3	58.1	0.5	64.4	1.4	67.9	0.8	40.1	0.8	58.9	0.5	66.2	0.7	67.1	0.3
142	150	5.2	2	QTVEKRIED	2.9	0.5	13.0	0.5	32.2	0.7	48.6	1.0	3.0	0.3	12.1	0.2	33.5	0.3	48.5	0.8	2.6	0.1	11.0	0.2	32.1	0.6	48.7	0.3	2.6	0.2	11.5	0.3	32.6	1.0	48.6	0.5
144	150	4.3	2	VEKRIED	1.6	0.3	4.3	0.7	16.2	0.3	35.9	1.1	2.3	1.1	4.5	0.6	17.0	0.5	36.0	0.3	1.3	0.1	4.3	0.9	16.1	0.6	35.5	0.2	1.6	0.1	4.4	0.6	15.8	0.7	35.4	1.2
151	155	10.7	1	FIESL	0.9	0.2	0.7	0.3	1.7	0.9	4.6	0.4	1.2	0.1	0.5	0.2	0.9	0.3	3.3	0.4	1.8	0.9	0.8	0.3	0.8	0.6	5.0	0.4	0.7	0.3	1.5	0.6	1.6	1.1	3.1	0.9
156	178	9.9	6	FIVLESKRLDRATDKSGDKIPLL	17.6	0.4	21.5	0.5	25.7	0.9	31.2	0.2	17.6	0.8	21.4	0.3	25.9	0.3	30.8	0.7	17.4	0.7	21.2	0.4	25.3	0.1	30.7	0.5	17.1	0.9	21.6	0.1	26.2	0.5	30.3	0.4
156	180	10.8	5	FIVLESKRLDRATDKSGDKIPLLCV	15.1	0.3	20.3	0.3	29.2	0.5	33.3	0.8	15.4	0.6	20.1	0.3	29.0	0.2	32.4	0.2	14.8	0.7	20.0	0.2	28.4	0.5	34.1	0.4	14.9	0.8	20.3	0.5	29.5	0.1	31.4	0.4
179	190	10.6	3	CVPFEKKDFVGL	39.6	0.9	46.2	0.6	48.5	1.3	50.6	0.9	40.4	1.0	44.6	0.9	48.1	1.1	49.3	0.6	41.7	1.2	45.5	0.9	47.8	0.6	48.9	0.3	39.0	0.6	45.6	0.6	49.0	0.7	48.2	1.2
181	190	10.0	2	PFEKKDFVGL	38.0	1.2	43.5	0.7	43.2	1.0	43.1	0.1	36.4	1.1	43.4	0.9	42.6	0.2	43.3	0.2	35.8	1.1	39.9	0.2	41.8	0.8	43.1	0.8	35.6	1.3	40.0	0.4	41.9	1.0	42.7	0.4
190	214	6.5	5	LDTDSRHYKKRCQGRMRKHVGDLCL	6.9	0.5	8.8	0.5	10.4	0.5	12.6	0.8	6.9	0.5	8.9	0.8	10.3	0.4	12.4	0.8	6.7	0.1	8.5	0.6	11.3	0.2	12.7	0.8	6.9	0.3	8.9	0.5	10.5	0.5	12.3	1.2
191	214	5.9	5	DTDSRHYKKRCQGRMRKHVGDLCL	3.7	0.2	5.5	0.3	7.0	0.4	8.9	0.5	3.9	0.3	5.5	0.3	7.2	0.3	8.7	0.6	3.4	0.0	5.4	0.3	7.4	0.1	8.9	0.4	3.5	0.0	5.5	0.2	7.1	0.4	8.8	0.5
215	226	10.6	1	QAGMLQDSLVHY	15.7	1.0	17.6	0.5	19.9	0.2	25.5	0.1	15.4	0.8	17.3	0.3	19.3	0.1	25.4	0.4	16.1	0.6	18.3	0.9	19.2	0.6	25.8	0.5	15.7	0.7	18.8	0.8	19.9	0.4	25.0	0.8
215	228	10.6	3	QAGMLQDSLVHYHM	12.8	0.4	14.5	0.2	14.9	0.2	22.0	0.3	12.9	0.2	14.3	0.1	15.3	0.3	21.7	0.4	12.4	0.7	14.4	0.3	14.6	0.0	21.8	0.5	12.2	0.6	14.4	0.1	15.5	0.7	21.5	0.4
215	232	11.7	3	QAGMLQDSLVHYHMSVEL	7.5	0.5	10.5	1.3	15.5	1.1	23.6	0.6	8.0	0.4	10.2	1.0	15.3	0.8	24.4	1.2	7.2	0.1	9.0	0.3	16.2	0.5	25.1	1.0	7.9	1.0	9.3	0.4	16.6	0.6	24.0	0.2
240	246	13.9	1	LWLGAAL	1.2	0.2	1.4	0.2	1.6	0.5	1.0	0.6	1.2	0.1	1.2	0.1	1.4	0.2	1.9	0.4	1.2	0.4	1.3	0.2	1.2	0.7	1.3	0.5	1.2	0.2	1.1	0.3	0.8	0.3	0.9	0.7
247	251	6.7	1	EGLCS	1.5	0.3	2.0	0.5	1.8	0.3	2.3	1.2	2.0	0.5	1.9	1.0	1.6	0.3	1.3	0.2	1.4	0.2	1.8	0.3	2.0	0.1	2.0	0.4	2.0	0.9	1.6	0.5	2.4	0.7	3.1	1.1
252	276	7.7	5	ASVIYHYPGGTGGKSGARRFQGSTL	28.1	1.0	29.1	0.2	29.1	0.4	32.8	1.3	28.1	0.8	28.9	0.9	29.4	0.6	31.7	0.8	27.3	0.6	28.7	0.8	29.1	0.4	31.8	0.9	27.7	0.3	28.3	0.9	29.7	1.1	30.8	0.3
253	276	7.7	4	SVIYHYPGGTGGKSGARRFQGSTL	29.0	1.4	29.3	0.3	29.4	0.6	33.0	1.6	28.4	0.7	29.5	1.4	29.3	0.1	31.9	1.0	28.6	1.0	29.3	0.3	29.4	0.7	32.2	0.8	28.7	0.3	29.5	1.0	30.4	1.0	31.4	0.3
253	289	6.6	4	SVIYHYPGGTGGKSGARRFQGSTLPAEAANRHRPGAQ	33.3	1.2	33.4	0.4	33.7	0.7	35.8	1.2	33.4	0.6	33.4	1.0	33.6	0.4	35.2	0.8	31.1	0.2	33.0	0.1	34.8	0.1	36.6	0.5	33.1	0.9	33.3	0.9	34.3	0.9	34.9	0.6
277	290	3.6	3	PAEAANRHRPGAQE	56.9	1.3	57.6	1.2	57.8	1.2	58.6	1.1	58.8	1.2	56.6	0.9	58.5	0.7	58.0	1.0	56.9	0.4	57.6	2.0	58.4	0.8	59.8	1.0	58.5	1.0	57.6	1.4	57.7	1.3	58.7	0.7
290	322	11.2	3	EVLIDPGALTTNGINPDTSTEIGRAKNCLSPED	51.2	0.5	55.4	0.5	58.9	0.8	59.9	0.2	52.5	0.1	54.8	0.7	58.0	0.7	59.3	0.3	50.8	1.4	55.3	0.7	57.5	0.1	59.8	0.7	50.7	1.6	55.1	0.4	59.6	0.6	58.9	0.4
291	322	11.0	3	VLIDPGALTTNGINPDTSTEIGRAKNCLSPED	51.7	0.7	55.6	0.7	58.9	1.1	60.1	0.5	52.0	1.8	55.2	0.5	59.2	0.2	59.7	0.4	51.2	1.5	55.3	0.2	57.8	0.5	60.0	0.6	50.3	1.7	55.4	0.2	59.7	0.4	59.4	0.3
293	310	9.1	2	IDPGALTTNGINPDTSTE	63.6	0.5	64.5	0.7	60.8	0.8	62.3	0.8	64.2	1.2	65.2	0.5	61.1	0.1	61.6	0.6	64.0	0.5	66.0	1.0	62.3	0.7	61.8	0.6	65.1	0.4	65.8	0.3	62.9	0.9	61.7	0.8
311	322	6.4	2	IGRAKNCLSPED	31.8	1.2	40.5	0.4	51.7	1.0	54.8	1.2	32.1	1.0	40.2	0.8	52.1	0.1	54.5	0.8	31.1	1.0	39.0	0.8	51.6	1.1	53.9	1.2	31.3	0.7	40.8	1.1	52.9	0.8	54.6	0.4
323	333	8.3	2	IIDKYKEAISY	0.9	0.1	0.8	0.1	1.2	0.2	2.6	0.1	0.9	0.1	1.1	0.1	1.6	0.3	2.3	0.1	1.0	0.2	0.9	0.1	1.4	0.2	2.0	0.3	0.9	0.1	0.9	0.2	1.1	0.1	2.6	0.2
334	345	9.4	2	YSKYKNAGVIEL	11.3	0.6	17.6	0.2	25.7	0.7	34.2	0.9	11.3	0.6	17.0	0.8	26.0	0.5	33.7	0.3	11.2	0.5	17.0	0.3	26.0	0.1	33.6	0.5	11.4	0.0	17.3	1.0	26.6	0.5	33.2	0.4
346	366	8.3	3	EACIKAVRVLAIQKRSMEASE	7.7	0.4	14.3	0.2	23.6	0.7	32.3	0.7	7.7	0.6	14.2	0.5	23.7	0.4	31.6	0.6	7.3	0.4	14.0	0.5	23.5	0.3	31.1	0.4	6.8	0.1	14.2	0.0	24.2	0.2	31.1	0.3
357	366	4.4	2	IQKRSMEASE	21.0	1.0	35.8	0.6	52.0	1.2	63.4	1.5	21.8	1.0	35.3	0.4	53.7	0.5	62.8	1.4	20.0	0.6	35.5	1.0	52.0	0.0	64.3	0.6	19.4	0.4	36.0	1.2	52.1	1.0	64.3	0.4
367	373	10.2	1	FLQNAVY	4.9	0.9	18.8	0.6	44.3	0.6	70.3	1.1	6.7	0.7	18.9	1.2	43.5	0.4	67.6	0.5	4.5	0.6	17.8	1.1	42.7	1.4	67.3	0.2	4.0	0.1	15.8	0.4	42.4	0.9	67.5	0.7
368	373	8.0	1	LQNAVY	4.7	0.1	32.9	0.4	59.0	0.7	71.9	0.7	5.6	0.3	30.5	0.7	56.0	0.7	67.5	0.8	4.8	0.4	33.1	0.9	55.5	0.8	68.4	1.1	4.3	0.4	32.1	1.1	53.6	0.7	70.4	0.5
377	391	9.8	4	RQLSEEEKIQRYSIL	20.5	0.2	31.7	0.5	48.1	0.8	59.7	0.6	21.3	1.2	31.9	0.7	46.4	1.2	58.6	0.5	21.6	0.8	32.5	0.9	46.6	0.5	60.4	0.4	21.7	0.4	34.9	0.6	49.0	0.7	59.7	0.3
382	391	9.6	3	EEKIQRYSIL	3.0	0.3	13.9	0.1	34.1	0.8	57.6	0.6	3.3	0.5	13.1	0.8	33.6	0.2	56.6	0.2	3.0	0.1	12.8	0.5	34.1	0.7	56.8	0.5	2.7	0.2	13.2	0.6	34.6	0.3	56.2	0.6
395	400	13.6	1	YELIGF	1.6	0.4	2.5	0.3	9.7	0.0	20.7	0.5	2.3	1.4	2.2	0.2	9.7	0.9	18.4	0.4	1.7	0.5	1.9	0.1	9.1	0.6	17.6	0.1	1.2	0.3	2.5	0.2	8.8	0.4	17.2	0.2
398	406	6.7	3	IGFHRKSAF	0.7	0.2	0.8	0.1	1.0	0.4	1.1	0.2	0.8	0.1	0.7	0.3	1.0	0.2	1.1	0.2	0.7	0.2	0.8	0.2	1.0	0.1	1.1	0.1	0.8	0.2	0.8	0.2	1.2	0.6	1.2	0.0
407	414	5.9	3	FKRVAAMQ	1.6	0.3	1.6	0.2	3.2	0.8	10.0	0.3	1.6	0.1	1.5	0.3	2.6	0.7	10.2	0.2	1.8	0.5	2.0	0.5	3.4	0.4	10.1	0.5	1.5	0.1	1.7	0.1	3.0	0.9	10.4	0.0
415	429	11.2	2	CVAPSIAEPGWRACY	33.2	0.7	49.8	0.4	59.8	0.9	68.5	0.7	34.2	1.1	49.3	0.5	60.3	0.3	69.6	0.5	32.8	0.3	48.9	0.7	59.4	0.1	69.1	0.6	32.3	0.6	49.4	0.1	60.9	0.4	69.7	0.4
434	440	8.3	1	ETLPGYS	3.4	0.2	11.5	0.3	27.0	0.7	32.4	0.5	4.1	0.7	12.6	0.2	28.7	0.3	31.9	0.6	3.1	0.5	11.2	1.0	27.0	0.2	31.5	0.4	3.0	0.2	11.5	0.5	26.8	0.3	31.6	0.6
441	460	9.3	3	LSLDPKDFSRGTHRGWAAVQ	20.9	0.3	30.0	0.4	33.6	1.1	38.7	0.2	21.1	0.8	30.1	0.7	33.3	1.2	37.2	0.8	20.6	1.1	29.6	0.5	33.1	0.4	38.3	0.6	18.9	0.3	29.9	0.8	33.7	0.5	37.3	0.1
461	468	9.9	3	MRLLHELV	0.7	0.4	0.6	0.4	1.0	0.8	0.6	0.2	1.0	0.1	0.5	0.5	0.6	0.3	1.4	0.5	0.3	0.3	0.3	0.5	0.7	0.8	0.9	0.3	0.6	0.2	0.7	0.7	1.0	0.2	0.8	0.7
467	479	8.1	3	LVYASRRMGNPAL	18.4	1.1	22.0	0.5	32.3	1.1	42.0	0.8	17.7	1.0	22.3	1.1	32.7	0.4	41.4	0.3	17.9	0.8	22.4	0.8	32.2	0.5	41.6	0.6	17.5	1.3	22.0	0.6	32.8	0.3	41.4	0.6
480	487	10.2	1	SVRHLSFL	2.9	0.2	1.6	0.4	1.9	0.3	4.7	0.5	2.6	0.3	1.7	0.1	1.7	0.2	3.9	0.1	2.5	0.1	2.0	0.5	1.6	0.1	4.2	0.4	3.8	0.1	3.6	0.2	3.7	0.5	6.0	1.4
488	494	13.2	1	LQTMLDF	5.7	1.3	12.2	0.4	22.0	0.9	43.6	0.7	8.2	1.8	12.2	0.8	21.2	0.5	43.2	0.5	7.9	0.8	12.6	0.3	22.2	0.0	43.3	0.5	5.0	0.1	10.9	0.6	24.7	0.2	43.1	0.7
493	509	10.3	2	DFLSDQEKKDVAQSLEN	5.6	0.2	8.8	0.0	13.6	0.4	28.2	0.2	5.8	0.2	8.7	0.1	13.6	0.3	28.0	0.1	5.4	0.3	8.5	0.2	13.4	0.1	27.6	0.6	5.5	0.3	8.6	0.1	13.5	0.1	27.7	0.8
493	510	11.5	3	DFLSDQEKKDVAQSLENY	5.0	0.3	8.3	0.3	15.4	0.4	36.7	1.0	5.0	0.1	8.2	0.1	15.7	0.8	36.0	0.8	4.9	0.0	7.9	0.3	14.6	0.1	36.1	0.2	4.8	0.0	8.0	0.3	15.3	0.4	34.2	1.2
510	523	10.7	1	YTSKCPGTMEPIAL	25.0	1.2	39.3	0.5	54.1	2.9	60.4	2.8	26.7	1.4	39.2	0.8	49.9	2.3	56.5	2.4	25.3	2.2	38.0	1.5	52.3	2.1	58.6	2.2	24.6	0.2	38.1	1.5	54.1	1.3	59.2	0.8
510	537	13.4	3	YTSKCPGTMEPIALPGGLTLPPVPFTKL	18.5	0.3	30.9	0.5	41.6	0.7	53.4	0.6	21.1	0.7	30.6	0.9	41.3	1.1	52.9	0.1	18.6	0.8	30.1	0.4	40.7	0.1	52.9	0.2	17.8	0.8	30.0	0.4	41.8	0.9	52.6	0.2
510	545	12.1	5	YTSKCPGTMEPIALPGGLTLPPVPFTKLPIVRHVKL	12.6	0.4	22.1	0.1	33.1	0.6	43.2	0.0	13.1	1.1	21.7	0.4	33.0	0.4	42.7	0.7	12.2	0.6	21.6	0.3	32.4	0.2	42.8	0.3	11.7	0.6	21.6	0.2	33.5	1.1	42.4	0.1
511	519	5.6	2	TSKCPGTME	21.3	0.8	44.2	1.3	53.7	2.1	53.2	2.5	21.8	1.1	44.2	0.5	54.1	0.8	54.6	0.7	20.8	0.3	45.2	1.7	54.4	0.3	56.0	1.2	20.8	1.3	43.4	2.1	52.1	1.8	58.1	0.3
511	545	12.0	5	TSKCPGTMEPIALPGGLTLPPVPFTKLPIVRHVKL	12.6	0.5	22.0	0.2	33.6	0.4	43.9	0.4	13.0	1.0	21.9	0.7	33.5	0.2	43.4	0.7	12.2	0.9	21.6	0.4	32.7	0.3	43.6	0.4	11.7	0.3	21.7	0.3	33.8	0.7	43.1	0.2
524	545	11.3	4	PGGLTLPPVPFTKLPIVRHVKL	6.7	0.3	15.5	0.2	26.7	0.2	38.5	0.2	7.1	0.5	15.1	0.2	26.6	0.4	38.1	0.7	6.6	0.3	15.1	0.2	25.9	0.3	38.0	0.5	6.3	0.4	14.9	0.0	26.2	0.4	37.7	0.6
538	545	6.2	2	PIVRHVKL	4.6	0.9	14.5	0.1	29.7	0.6	34.9	0.9	5.1	0.9	16.2	0.1	29.3	1.3	35.1	0.5	4.0	0.4	13.2	0.2	29.0	0.3	34.2	0.3	5.1	0.3	13.1	0.5	29.3	0.5	35.1	0.6
546	561	9.6	5	LNLPASLRPHKMKSLL	22.9	0.6	25.0	0.1	30.9	0.8	41.8	1.4	23.7	0.5	24.8	1.0	30.8	1.2	41.2	0.7	22.3	1.1	23.9	0.5	29.9	0.3	39.9	0.9	22.9	0.9	25.1	0.4	31.3	1.3	39.4	1.3
565	591	9.0	3	VSTKSPFIYSPIIAHNRGEERNKKIDF	36.5	0.7	38.1	0.6	38.1	0.8	39.4	0.4	36.0	1.0	38.4	0.7	38.1	0.3	38.7	0.5	34.0	0.7	36.3	0.4	37.5	0.5	38.7	0.6	35.4	1.1	38.3	0.9	38.9	0.9	38.2	0.7
592	600	9.4	1	QWVQGDVCE	1.1	0.1	1.4	0.1	3.8	0.2	13.2	0.3	1.2	0.1	1.3	0.3	3.5	0.2	13.0	0.4	1.1	0.2	1.3	0.2	3.4	0.0	12.6	0.6	1.2	0.0	1.0	0.0	3.3	0.5	12.6	0.3
604	612	12.4	1	MVYNPMPFE	9.4	0.4	15.7	0.4	23.9	0.3	25.1	0.4	9.5	1.0	15.5	0.3	24.3	1.0	23.8	0.3	9.0	0.3	15.8	0.5	22.9	0.1	25.2	0.3	8.2	0.3	15.8	0.8	24.4	0.6	25.1	0.5
604	613	14.3	1	MVYNPMPFEL	8.6	0.3	12.8	0.6	20.2	0.1	20.9	0.8	10.0	0.5	14.7	0.6	20.7	0.5	21.8	0.6	8.0	0.7	13.6	0.6	19.7	0.4	20.1	1.2	6.9	0.1	13.6	1.2	19.7	0.4	20.3	0.7
614	620	8.6	2	RVENMGL	2.7	0.5	7.8	0.5	28.9	0.6	50.2	1.1	2.5	0.5	7.5	0.6	28.8	0.4	49.1	0.4	2.8	0.2	7.0	0.6	28.4	0.8	48.6	0.5	2.0	0.1	7.6	0.2	29.4	0.3	48.7	0.5
628	636	12.2	1	ESLPAALSL	22.7	1.0	38.3	0.8	46.9	0.4	61.0	1.3	23.7	1.3	37.6	0.3	46.3	0.5	57.7	1.2	22.2	1.1	37.9	0.9	45.1	0.7	57.8	0.8	21.0	0.4	37.5	1.3	46.2	0.3	60.1	1.0
634	642	10.9	1	LSLPAESGL	31.5	0.6	42.0	0.4	43.0	0.7	44.4	0.8	32.2	1.5	41.6	0.1	43.0	0.4	43.8	0.4	30.8	0.7	41.1	0.3	42.0	0.0	43.6	0.2	30.4	1.5	41.0	0.7	45.1	1.2	43.2	0.4
637	642	7.0	1	PAESGL	48.4	1.1	60.3	0.9	62.7	1.1	64.4	1.0	49.3	1.6	61.0	0.8	63.0	0.5	64.5	0.4	47.5	1.4	59.8	0.3	62.7	0.5	63.9	0.8	47.8	1.2	60.8	0.8	63.1	1.2	64.3	0.3
637	647	11.8	1	PAESGLYPVTL	23.9	0.8	32.1	1.0	36.0	1.1	41.8	0.6	25.4	1.3	31.6	0.3	35.9	0.7	40.5	1.2	23.2	0.7	31.3	0.4	35.1	0.6	39.6	1.0	21.9	0.4	31.2	0.5	34.9	1.1	39.4	0.7
643	647	10.3	1	YPVTL	6.0	0.9	14.5	0.4	15.4	0.3	17.0	0.4	6.3	0.1	14.0	0.3	15.9	0.8	17.0	0.6	5.6	1.0	14.0	0.6	14.7	1.1	16.4	0.5	4.1	0.8	14.2	0.8	14.1	0.6	15.9	0.1
648	656	6.2	1	VGVPQTTGT	14.0	0.6	16.9	0.6	27.0	1.4	45.5	1.1	14.1	0.9	16.1	0.6	28.8	0.2	44.8	0.6	12.4	0.5	15.0	0.5	28.7	0.3	44.6	0.5	13.5	0.9	17.0	0.5	28.1	0.5	45.6	1.1
648	667	10.9	3	VGVPQTTGTITVNGYHTTVF	4.8	0.3	6.4	0.2	13.8	0.3	27.3	0.5	5.0	0.1	6.2	0.2	13.6	0.1	27.3	0.4	4.5	0.4	6.1	0.0	13.3	0.2	26.6	0.3	4.4	0.3	6.1	0.2	13.1	0.1	26.7	0.9
668	674	12.8	1	GVFSDCL	2.3	0.3	9.6	0.3	22.7	0.5	31.2	0.3	2.3	0.4	9.0	0.2	22.6	0.2	31.0	0.3	1.7	0.1	9.0	0.4	22.0	0.1	30.8	0.3	1.8	0.2	8.9	0.5	23.0	0.5	30.3	0.2
674	697	12.3	3	LLDNLPGIKTSGSTVEVIPALPRL	13.6	0.2	20.0	0.4	23.4	0.4	28.2	0.1	14.2	0.5	20.0	0.8	23.3	0.3	28.0	0.7	13.5	0.6	19.6	0.2	23.0	0.1	27.8	0.2	13.2	0.4	19.6	0.1	23.8	0.7	27.7	0.6
675	694	11.8	2	LDNLPGIKTSGSTVEVIPAL	16.1	0.3	23.4	0.3	27.3	0.3	31.2	0.1	16.5	0.6	23.1	0.3	27.6	0.6	31.2	0.8	16.0	0.5	23.3	0.1	27.0	0.0	31.7	0.4	15.6	0.5	23.0	0.0	28.0	0.9	30.6	0.3
675	697	11.9	3	LDNLPGIKTSGSTVEVIPALPRL	13.4	0.4	19.8	0.3	23.1	0.4	28.1	0.1	14.0	0.5	19.2	0.2	23.0	0.4	27.8	0.6	13.3	0.5	19.0	0.1	22.5	0.1	27.9	0.2	13.1	0.9	19.2	0.3	23.2	0.5	27.6	0.6
688	694	11.6	1	VEVIPAL	1.8	0.1	2.0	0.3	2.3	0.5	4.3	0.2	1.7	0.1	1.7	0.6	2.4	0.9	2.7	0.6	1.8	0.5	2.0	0.1	1.5	0.2	3.8	0.7	1.3	0.3	2.0	0.3	3.0	0.5	2.7	0.9
688	697	11.8	2	VEVIPALPRL	1.4	0.3	1.7	0.1	2.1	0.5	7.8	0.1	1.6	0.1	1.5	0.3	2.1	0.1	7.7	0.6	1.5	0.2	1.4	0.1	2.0	0.3	7.4	0.2	1.7	0.6	1.8	0.7	1.8	0.4	7.7	0.6
689	697	11.5	2	EVIPALPRL	2.3	0.4	2.7	0.5	3.0	0.7	10.5	0.5	2.1	0.5	2.9	0.7	2.8	0.9	10.4	0.7	2.1	0.1	2.0	0.2	3.8	0.9	9.5	1.0	2.0	0.2	2.6	0.7	3.2	0.9	9.9	1.3
695	717	8.3	4	PRLQISTSLPRSAHSLQPSSGDE	29.2	0.6	33.8	0.6	35.6	0.8	38.5	1.2	28.9	0.8	33.5	0.9	35.6	0.2	37.1	0.4	28.6	1.0	33.3	0.3	35.1	0.5	36.9	0.5	28.7	1.2	33.5	0.3	36.1	0.5	36.6	0.3
698	717	7.5	3	QISTSLPRSAHSLQPSSGDE	39.7	1.3	42.4	0.9	42.9	1.1	46.4	1.3	39.7	1.3	42.1	1.1	42.9	0.1	43.8	1.0	39.9	1.1	41.8	0.7	42.8	0.6	44.4	1.1	40.2	0.1	43.4	0.3	43.7	1.1	43.6	0.9
698	720	8.2	2	QISTSLPRSAHSLQPSSGDEIST	40.1	1.0	41.7	0.0	42.7	0.6	44.9	1.1	39.5	0.6	41.9	0.4	42.5	0.4	42.6	0.4	39.2	1.2	41.1	0.7	42.0	0.8	43.8	1.1	37.9	0.6	38.6	0.5	42.2	0.1	41.9	0.7
698	723	8.1	3	QISTSLPRSAHSLQPSSGDEISTNVS	38.4	0.8	42.6	0.3	45.0	1.3	48.8	0.4	37.4	1.0	41.6	0.4	44.8	0.4	48.0	0.6	38.0	0.9	42.5	0.6	45.1	0.1	47.8	0.5	38.6	0.7	42.3	0.4	46.5	0.3	47.5	0.5
727	734	7.5	1	YNGESQQL	14.5	0.5	18.0	0.3	29.5	0.5	47.2	0.9	14.5	0.3	17.6	0.1	29.5	0.7	46.1	0.3	14.1	0.3	17.6	0.6	29.4	0.4	46.4	0.9	14.0	0.3	17.9	0.4	30.0	0.4	45.6	0.1
735	749	11.7	2	IIKLENIGMEPLEKL	3.3	0.3	11.4	0.2	17.1	0.0	32.5	0.4	3.3	0.3	11.3	0.1	17.3	0.4	32.1	0.8	3.1	0.2	10.9	0.4	17.0	0.5	31.9	0.5	2.9	0.0	11.0	0.3	17.6	0.7	31.8	0.8
735	751	12.3	3	IIKLENIGMEPLEKLEV	8.6	0.6	17.2	0.9	25.0	0.1	37.3	0.6	8.4	0.8	15.8	0.4	27.2	1.1	36.2	0.8	9.8	1.0	16.1	0.7	24.1	0.6	36.8	1.4	9.0	1.1	17.0	1.4	27.1	1.5	36.3	0.2
750	762	6.9	2	EVTSKVLTTKEKL	45.8	1.0	59.1	0.2	62.2	0.7	68.5	0.8	45.7	1.2	58.3	0.9	62.6	0.9	67.2	0.7	44.0	1.2	57.7	0.5	62.2	0.7	67.0	0.6	43.5	1.1	58.1	0.3	62.8	0.5	66.3	0.5
767	775	11.7	1	LSWKLEETL	47.5	0.2	64.3	0.7	70.1	0.6	68.4	1.1	47.2	0.7	62.5	1.5	68.1	0.7	73.2	0.5	44.7	0.3	63.6	1.2	69.6	0.1	71.2	0.4	45.4	1.8	64.7	0.1	70.9	0.9	73.6	0.4
776	787	9.0	2	AQFPLQPGKVAT	8.4	0.4	32.0	0.0	46.9	0.7	64.5	0.7	8.7	1.3	31.1	0.5	46.4	0.2	66.8	0.4	7.7	0.6	30.9	0.3	46.5	0.2	66.9	0.3	7.2	0.6	30.8	0.3	46.8	0.1	66.7	0.4
788	792	12.1	1	FTINI	1.5	1.0	1.6	0.2	3.1	0.7	10.1	0.8	1.0	0.6	2.8	0.2	3.7	1.0	9.3	1.3	1.2	0.5	2.0	1.3	4.3	0.4	8.9	0.5	2.1	0.9	1.3	1.1	3.4	1.1	9.1	0.4
788	798	12.1	3	FTINIKVKLDF	10.4	0.2	20.0	0.8	24.4	1.3	38.5	1.3	9.8	0.8	17.0	1.6	22.6	1.3	40.3	1.4	9.4	0.4	16.0	1.1	23.0	1.1	40.2	1.6	8.9	0.0	15.7	0.8	24.0	1.3	39.9	0.8
806	855	10.2	5	QDLSDDGISVSGFPLSSPFRQVVRPRVEGKPVNPPESNKAGDYSHVKTLE	43.4	0.3	46.4	0.8	47.4	1.0	49.4	0.1	43.5	0.8	45.9	0.2	47.6	0.2	48.8	1.0	42.4	1.4	46.2	0.6	46.5	0.3	48.3	1.1	42.8	2.0	46.4	0.3	48.2	0.6	48.2	0.2
848	855	5.6	2	YSHVKTLE	13.0	0.7	30.5	0.4	40.4	0.7	49.3	0.8	13.8	0.9	29.8	0.6	40.7	0.4	48.6	0.7	12.9	0.7	29.5	0.2	40.5	0.1	49.0	0.4	11.5	0.6	29.6	0.6	40.8	0.6	48.7	0.4
856	860	11.6	1	AVLNF	3.6	0.1	5.0	0.9	4.4	0.8	5.9	1.0	3.7	0.2	4.2	0.3	5.3	0.7	6.6	0.7	3.4	0.6	4.2	1.2	4.9	0.5	7.0	0.5	3.0	0.6	4.1	1.4	4.9	0.3	6.9	0.8
859	872	7.6	2	NFKYSGGPGHTEGY	4.9	0.8	12.7	0.4	17.6	0.9	27.8	0.5	4.6	0.5	12.4	0.8	17.2	0.3	25.6	0.6	4.8	0.8	12.2	0.1	18.1	0.9	25.9	0.8	4.8	0.3	12.7	0.8	18.2	0.8	25.5	0.3
873	880	10.7	2	YRNLSLGL	7.0	0.4	13.2	0.3	16.1	0.3	29.6	0.9	7.3	0.8	13.1	0.2	16.1	0.6	29.1	0.2	6.6	0.6	13.0	0.5	15.7	0.1	29.1	0.5	6.4	0.6	12.6	0.1	16.2	0.3	29.0	0.6
881	889	9.9	1	HVEVEPSVF	2.7	0.6	2.3	0.3	9.8	0.4	29.5	0.9	2.7	0.5	2.3	0.2	9.4	0.1	29.4	1.2	2.4	1.2	2.7	0.5	9.5	0.3	29.5	0.3	1.9	0.2	2.4	1.3	11.9	0.7	28.3	1.1
890	896	8.1	2	FTRVSTL	20.9	0.5	47.2	0.6	69.8	1.4	73.2	0.7	21.7	1.1	46.3	0.9	70.5	0.2	72.1	0.5	21.1	1.1	45.7	0.7	70.1	1.0	72.4	1.0	20.0	0.5	48.0	1.0	71.3	1.1	71.7	0.2
890	908	10.0	4	FTRVSTLPATSTRQCHLLL	18.7	0.5	26.6	0.2	32.5	0.6	39.4	0.7	18.8	1.0	26.3	0.7	32.6	0.3	38.4	0.3	18.3	1.1	26.2	0.2	32.0	0.0	38.2	0.6	17.9	0.6	26.7	0.6	34.1	1.2	38.2	0.3
897	908	9.7	2	PATSTRQCHLLL	18.4	0.7	19.8	0.1	20.9	0.6	30.1	0.5	18.3	0.7	19.6	0.9	20.9	0.0	29.7	0.2	18.3	0.9	20.0	0.5	20.6	0.7	29.4	0.8	18.1	0.3	18.6	0.9	20.3	0.6	28.6	0.7
907	911	13.2	1	LLDVF	1.6	0.2	2.4	0.3	2.2	0.6	4.3	0.8	2.0	0.4	1.9	0.4	2.2	0.6	5.0	0.2	1.4	0.4	2.1	0.4	3.0	0.1	4.3	0.5	1.5	0.0	2.2	0.5	2.4	0.2	5.0	0.7
909	917	7.8	1	DVFNSTEHE	2.6	0.6	8.0	0.2	16.2	0.7	19.0	1.2	2.3	0.5	8.1	0.5	16.1	0.4	19.3	0.2	2.6	0.5	8.2	0.5	16.4	0.0	18.3	0.4	2.1	0.1	8.1	0.4	16.9	0.6	17.9	0.6
909	927	10.0	3	DVFNSTEHELTVSTRSSEA	15.3	0.2	20.8	0.2	26.0	0.4	30.5	0.6	15.4	0.5	20.5	0.4	26.2	0.1	29.7	0.6	15.2	0.7	20.5	0.4	26.0	0.4	30.3	1.3	15.3	0.3	20.8	0.2	27.3	0.7	30.4	0.4
912	927	6.5	2	NSTEHELTVSTRSSEA	23.4	0.6	28.6	0.5	33.3	0.7	38.2	1.2	23.4	0.6	28.2	0.8	33.2	0.4	37.5	0.6	22.8	0.6	28.0	0.4	34.5	0.3	38.1	1.3	23.4	0.2	28.7	0.8	34.1	0.4	38.2	0.5
918	927	5.8	2	LTVSTRSSEA	43.5	0.6	48.6	0.8	51.8	1.2	59.9	0.6	44.9	0.6	48.5	1.1	52.5	0.4	58.4	1.1	42.6	0.9	48.5	0.9	52.6	0.0	58.5	0.6	43.0	0.7	48.2	0.2	53.1	1.2	59.4	0.9
931	938	4.5	2	HAGECQRM	5.4	0.5	17.0	0.9	25.4	1.0	29.0	0.5	5.7	0.9	15.6	0.8	23.3	0.7	30.5	0.4	4.4	0.2	16.2	0.9	23.6	1.1	29.4	0.5	4.4	0.2	16.6	0.9	22.3	1.1	28.8	0.4
939	947	11.3	1	AIQVDKFNF	42.4	0.4	45.5	0.8	52.0	0.2	51.1	1.1	43.6	1.5	46.1	0.7	50.3	1.2	52.4	0.4	42.8	1.4	45.8	0.6	49.6	1.2	51.1	0.7	41.2	0.4	47.0	0.9	53.7	0.9	54.2	0.9
948	968	8.7	3	ESFPESPGEKGQFANPKQLEE	58.0	0.8	58.5	0.7	58.2	0.8	60.2	0.9	57.8	0.8	58.7	0.7	58.5	0.3	58.5	0.5	58.3	0.8	58.4	0.5	57.6	0.7	58.6	0.7	56.5	1.3	58.6	0.3	59.1	0.4	57.6	0.9
969	982	6.1	4	ERREARGLEIHSKL	40.0	0.5	42.7	0.8	42.6	0.9	44.2	0.8	40.5	1.1	42.7	0.8	43.2	0.3	43.5	0.7	38.7	0.9	42.5	0.8	43.2	0.2	44.1	1.0	37.7	0.9	42.7	0.6	43.4	0.6	43.7	0.3
986	1005	10.9	3	WRIPSLKRSGEASVEGLLNQ	31.3	0.2	42.2	0.6	47.1	0.8	52.4	0.6	32.5	0.5	41.9	0.8	47.1	1.2	52.4	0.5	30.7	0.9	41.5	0.5	46.0	0.2	52.9	0.4	30.2	0.8	41.7	0.3	47.7	0.6	51.2	0.6
998	1005	10.0	1	SVEGLLNQ	1.8	0.6	1.6	0.3	1.9	0.3	2.7	0.7	1.3	0.1	1.4	0.1	2.8	1.2	2.0	0.3	2.8	0.2	3.3	0.9	3.1	0.5	5.6	0.9	1.5	0.3	1.8	0.6	1.7	0.0	1.8	0.2
1006	1018	13.8	2	LVLEHLQLAPLQW	11.7	0.3	30.2	0.4	45.4	1.1	56.6	0.7	11.8	1.2	29.4	0.3	44.9	0.5	55.2	1.4	10.6	0.5	28.5	0.4	44.4	0.1	56.2	0.6	10.5	0.6	28.1	0.2	45.6	0.7	55.8	1.3
1012	1018	12.8	2	QLAPLQW	15.0	1.0	22.0	0.4	38.0	0.9	57.2	1.1	15.2	0.5	21.8	0.7	37.2	0.3	55.8	0.2	14.2	0.8	22.1	0.2	37.2	1.1	56.7	1.0	14.2	1.1	22.2	0.4	37.8	0.7	55.5	0.2
1014	1021	13.8	1	APLQWDVL	2.3	0.3	5.8	0.4	27.8	0.5	44.6	0.9	2.5	1.0	6.7	0.7	27.1	1.0	44.6	0.5	2.3	0.7	5.7	0.1	26.5	0.7	44.1	0.6	2.6	0.0	6.0	0.3	27.3	0.5	43.5	0.7
1022	1028	4.9	1	VDGQPCD	18.2	1.1	38.9	0.4	48.6	1.2	59.4	1.4	19.6	0.9	38.5	1.0	49.1	0.7	60.2	1.3	19.3	0.9	39.4	0.2	48.4	1.4	59.8	1.2	16.7	0.3	39.3	0.2	48.8	0.6	60.6	1.2
1022	1030	4.8	2	VDGQPCDRE	33.1	0.9	42.6	0.8	50.1	1.0	56.2	0.7	34.0	0.7	43.3	0.8	51.2	0.7	57.5	1.1	33.1	0.5	44.2	0.9	50.4	0.7	58.7	0.6	33.1	0.1	44.6	0.7	50.1	0.4	58.5	0.5
1022	1033	6.0	1	VDGQPCDREAVA	29.1	1.1	43.5	1.0	52.0	0.8	58.8	1.3	29.0	1.4	43.5	0.4	51.1	0.7	59.7	1.5	27.2	1.5	43.9	0.5	51.9	0.1	61.0	1.1	26.5	0.9	45.4	0.9	51.9	0.8	59.8	0.4
1035	1043	9.2	2	CQVGDPVRL	2.3	0.5	2.4	0.3	5.1	0.5	18.1	1.1	1.8	0.3	2.6	0.4	4.9	0.6	17.0	0.5	1.9	0.3	2.1	0.1	5.3	0.4	17.0	0.4	2.3	0.4	2.3	0.3	4.9	0.7	16.9	0.4
1037	1043	8.6	2	VGDPVRL	2.3	0.1	2.7	0.3	6.5	0.2	21.5	0.7	2.7	0.5	2.7	0.1	6.5	0.4	20.8	0.5	2.4	0.2	2.6	0.1	6.3	1.0	21.1	0.7	2.5	0.1	2.7	0.2	7.2	0.2	20.6	0.4
1044	1060	10.3	4	EVRLTNRSPRSVGPFAL	5.5	0.1	9.4	0.0	18.1	0.5	22.3	0.3	5.6	0.2	9.5	0.2	18.2	0.3	22.0	0.2	5.6	0.2	9.8	0.6	18.1	0.2	22.0	0.3	5.4	0.0	9.3	0.5	18.4	0.3	21.7	0.3
1044	1079	10.2	5	EVRLTNRSPRSVGPFALTVVPFQDHQNGVHNYDLHD	4.7	0.1	9.0	0.1	12.7	0.6	17.5	0.1	4.8	0.3	8.8	0.1	12.9	0.2	17.3	0.3	4.5	0.2	8.7	0.1	12.8	0.0	17.2	0.5	4.5	0.3	8.9	0.1	13.3	0.1	17.0	0.1
1061	1077	9.5	2	TVVPFQDHQNGVHNYDL	7.3	0.2	15.2	0.1	16.3	0.6	21.6	0.3	8.0	0.3	14.8	0.2	16.3	0.7	21.4	0.5	7.1	0.9	14.9	0.3	16.4	0.0	20.6	0.2	7.0	0.1	15.2	0.3	17.5	0.6	20.9	0.1
1061	1079	8.2	4	TVVPFQDHQNGVHNYDLHD	9.3	0.5	15.8	0.1	17.5	0.5	22.6	1.0	8.9	0.7	16.0	0.5	17.5	0.2	21.5	0.4	8.9	0.5	15.5	0.0	17.6	0.4	21.8	0.5	8.6	0.1	15.7	0.7	17.9	0.8	20.9	0.6
1084	1089	7.9	1	VGSSTF	16.4	1.0	25.8	0.2	39.6	1.0	58.6	1.5	17.2	1.0	26.0	1.1	39.4	0.2	56.7	0.6	16.3	0.9	25.5	0.2	39.6	0.6	57.4	0.6	16.8	0.2	27.8	1.2	42.1	0.7	56.8	1.0
1090	1103	10.5	1	YLDAVQPSGQSACL	9.7	0.2	24.2	0.3	35.1	0.7	45.2	0.6	9.9	1.2	23.8	0.7	35.2	0.2	44.3	0.4	9.2	0.4	23.2	0.4	34.8	0.1	44.0	0.7	8.8	0.2	23.3	0.3	35.8	1.0	43.2	0.5
1092	1103	8.5	1	DAVQPSGQSACL	13.2	1.0	31.0	1.0	41.5	0.5	52.6	0.9	14.6	0.4	30.7	0.6	41.6	0.2	52.0	0.2	13.0	1.1	30.6	0.7	41.0	0.3	51.8	0.2	11.6	0.8	30.8	1.1	42.1	0.9	51.6	0.7
1104	1108	13.0	1	GALLF	0.9	0.2	1.3	0.4	1.4	0.9	3.5	0.5	1.0	0.2	0.9	0.1	1.3	0.7	2.9	0.8	1.2	0.7	1.6	0.5	1.5	0.1	2.9	0.4	1.9	0.9	1.0	0.2	1.4	0.4	2.4	0.5
1108	1114	12.9	1	FLYTGDF	0.8	0.4	1.0	0.1	1.9	0.1	9.4	0.2	0.9	0.1	0.9	0.2	1.7	0.3	9.5	0.6	0.7	0.3	0.8	0.1	1.8	0.1	9.7	0.4	0.8	0.1	0.8	0.1	1.9	0.2	9.4	0.7
1110	1114	9.2	1	YTGDF	1.0	0.4	0.7	0.2	1.0	0.4	1.7	0.3	1.2	0.2	0.8	0.2	1.2	0.5	1.6	0.3	0.9	0.3	0.8	0.2	1.2	0.2	1.9	0.1	1.1	0.4	1.0	0.1	1.2	0.3	1.6	0.4
1115	1120	11.0	2	FLHIRF	6.0	0.5	20.8	0.5	33.4	0.8	37.0	0.9	7.8	0.7	21.2	0.4	33.3	0.7	36.8	0.8	6.9	0.9	20.6	0.4	34.0	0.2	37.5	0.9	6.8	1.1	22.2	0.6	33.9	0.3	37.3	0.4
1115	1133	10.1	4	FLHIRFHEDSTSKELPPSW	17.8	0.5	26.3	0.7	28.8	0.5	29.4	0.3	17.6	0.9	26.1	0.2	28.9	0.7	28.9	0.4	17.3	0.9	26.4	0.3	27.9	0.4	29.2	0.7	16.9	0.8	26.4	0.4	29.0	0.2	29.5	1.2
1134	1144	12.5	1	FCLPSVHVCAL	9.8	0.6	17.5	0.2	25.3	0.4	32.5	0.1	10.1	0.9	17.2	0.1	24.8	0.6	31.3	0.2	9.2	0.7	16.7	0.6	24.0	0.0	31.8	0.9	9.4	0.2	17.3	0.4	25.5	0.3	31.3	0.9

Appendix W. Peptides of TRAPPC9 for TRAPPII HDX with Rab1, Rab11 and Rab43

TRAPPC10					APO								TRAPP + Rab1								TRAPP + Rab11								TRAPP + Rab43							
S	E	RT	Z	Sequence	3s	SD	30s	SD	300s	SD	3000s	SD	3s	SD	30s	SD	300s	SD	3000s	SD	3s	SD	30s	SD	300s	SD	3000s	SD	3s	SD	30s	SD	300s	SD	3000s	SD
3	13	11.3	1	ASEEPLPPVIY	47.4	0.9	61.7	0.3	60.9	1.1	61.0	0.7	50.4	0.2	59.8	0.9	60.0	1.2	60.7	1.6	46.1	0.9	61.5	1.2	60.2	0.3	60.7	0.5	45.9	2.9	64.5	0.8	65.1	0.8	63.7	1.8
6	13	11.7	1	EPLPPVIY	8.7	0.6	27.0	0.4	39.1	1.0	59.8	0.9	10.1	0.7	26.3	1.0	38.4	0.7	61.7	1.0	8.2	0.2	26.4	0.3	38.1	0.7	62.2	1.6	7.9	0.2	26.5	0.4	38.6	0.7	62.6	0.5
14	22	6.5	1	TMENKPIVT	21.0	0.4	30.6	0.1	32.2	0.7	33.3	0.2	21.4	0.6	30.4	1.1	32.5	0.6	33.0	0.8	21.4	0.9	29.9	0.8	32.6	0.9	33.5	0.3	21.4	0.8	30.4	0.6	33.2	0.4	33.8	0.5
14	29	9.0	2	TMENKPIVTCAGDQNL	20.2	0.7	31.0	0.6	33.6	0.4	35.4	1.1	21.2	0.9	30.1	0.5	32.5	0.7	34.5	0.6	20.3	0.9	29.9	0.5	33.4	0.2	34.1	0.6	20.3	0.7	30.9	0.5	34.0	0.7	34.0	0.7
15	22	6.1	2	MENKPIVT	12.6	0.5	23.5	0.9	25.9	0.3	27.0	0.3	14.0	0.9	23.2	0.4	26.2	0.9	26.6	0.6	12.8	1.0	23.4	1.1	28.4	0.8	27.1	0.4	12.7	0.7	23.0	0.1	26.1	0.4	26.4	0.3
23	29	6.7	1	CAGDQNL	37.0	1.0	54.3	0.9	60.4	0.9	63.9	1.0	37.5	1.9	54.4	0.3	60.7	0.6	62.9	0.3	35.7	1.2	53.2	0.7	60.8	0.8	63.4	1.1	35.5	1.0	53.9	0.6	61.6	0.8	62.7	0.9
30	37	11.8	1	FTSVYPTL	7.5	1.0	21.8	1.0	33.2	1.2	52.0	0.8	7.6	1.0	20.9	1.2	32.4	0.8	52.1	0.1	6.8	0.5	21.1	0.7	31.8	1.1	52.6	0.4	6.4	0.1	21.7	0.9	32.8	0.7	51.5	0.7
38	47	7.5	2	SQQLPREPME	10.1	0.9	28.8	1.2	58.4	1.4	74.3	1.2	9.8	1.1	28.8	0.5	58.3	0.2	73.2	0.4	9.8	0.3	27.9	0.8	58.7	0.7	73.3	1.1	9.4	0.6	28.4	0.3	58.7	0.3	72.9	0.4
48	58	5.8	3	WRRSYGRAPKM	42.1	1.3	48.4	0.8	50.9	0.8	52.5	1.2	43.1	1.4	48.2	1.3	50.5	0.8	52.1	0.6	42.8	1.0	49.5	1.0	52.3	0.3	53.4	0.6	41.3	0.3	48.4	1.1	51.2	0.9	51.5	0.4
48	61	7.6	4	WRRSYGRAPKMIHL	22.6	1.0	28.5	0.0	34.9	1.0	42.7	0.7	22.2	0.3	29.0	1.0	34.5	0.3	41.8	0.8	22.2	0.8	28.7	1.0	35.4	1.0	41.0	0.9	22.1	0.8	29.1	0.6	37.2	1.5	40.2	0.4
49	58	4.7	4	RRSYGRAPKM	44.2	1.5	51.5	0.5	54.8	0.6	55.5	1.3	45.8	1.2	50.8	0.8	56.1	0.8	55.7	0.5	42.5	0.9	51.1	0.4	55.1	0.2	55.5	0.6	43.4	1.2	51.6	0.7	55.1	1.4	55.4	0.8
59	65	9.5	2	IHLESNF	3.6	0.5	12.4	0.6	35.5	1.3	46.3	1.1	3.9	0.3	11.8	0.7	35.6	0.4	44.7	0.3	2.8	0.5	11.8	1.2	36.6	0.2	46.9	0.4	2.0	0.2	12.8	0.5	38.9	1.4	50.1	1.1
66	87	13.3	4	VQFKEELLPKEGNKALLTFPFL	11.2	0.1	17.2	0.2	28.9	0.8	38.4	0.2	11.6	0.5	16.9	0.5	29.1	0.3	38.1	0.4	11.0	0.3	16.7	0.3	28.5	0.2	38.2	0.2	10.7	0.4	16.7	0.1	29.4	0.7	37.8	0.3
69	87	13.1	3	KEELLPKEGNKALLTFPFL	11.3	0.2	18.4	0.6	30.3	0.6	40.1	0.2	11.6	0.5	17.6	0.3	30.1	0.4	39.9	0.4	10.9	0.1	17.8	0.2	29.7	0.2	40.2	0.3	10.8	0.5	17.5	0.5	30.4	0.5	39.6	0.2
73	87	13.6	3	LPKEGNKALLTFPFL	10.8	0.1	17.7	0.7	27.3	1.0	34.8	0.6	11.3	0.7	17.7	0.5	26.4	0.3	36.0	0.2	10.3	0.3	17.3	0.2	27.2	0.2	35.4	0.3	9.8	0.6	17.1	0.1	27.7	0.5	35.8	0.4
82	87	14.6	1	LTFPFL	2.0	0.8	0.8	0.6	3.5	0.7	17.9	1.9	1.3	1.3	2.1	1.0	3.2	0.4	18.2	0.9	1.7	1.0	1.3	0.8	2.4	0.2	17.6	0.6	0.6	0.1	0.5	1.0	2.7	0.9	18.9	0.9
88	94	10.5	1	HIYWTEC	3.2	0.5	13.8	0.2	25.4	0.7	27.5	0.3	3.3	0.4	13.2	0.2	26.0	0.5	27.1	0.9	3.0	0.3	13.4	0.6	25.2	0.0	26.8	0.6	2.4	0.2	13.1	0.3	25.6	0.1	26.8	0.6
88	95	11.2	2	HIYWTECC	12.1	0.1	20.5	0.2	30.6	0.3	32.6	0.6	12.2	0.9	20.1	0.6	30.7	0.5	31.9	0.1	11.8	0.9	20.3	0.2	30.4	0.8	32.1	0.1	12.0	0.5	20.2	0.4	31.4	1.0	31.7	0.6
96	124	13.1	5	DTEVYKATVKDDLTKWQNVLKAHSSVDWL	8.6	0.6	18.4	0.3	25.0	1.0	32.2	0.6	9.2	1.1	17.9	0.7	26.0	0.3	32.5	0.6	8.0	0.4	17.6	0.5	24.0	0.4	32.0	0.2	7.7	0.2	17.9	0.6	25.7	1.2	32.1	0.2
97	115	11.3	4	TEVYKATVKDDLTKWQNVL	6.8	0.1	17.0	0.2	23.1	0.2	29.7	0.7	7.0	1.2	16.6	0.5	22.7	0.4	28.8	0.7	6.5	0.3	16.5	0.3	22.2	0.4	29.2	0.5	6.0	0.6	15.9	0.6	22.4	0.7	29.0	0.2
98	115	11.3	3	EVYKATVKDDLTKWQNVL	5.8	0.2	14.8	0.4	19.9	0.6	26.6	0.3	6.3	0.7	13.8	0.1	20.0	0.4	26.3	0.7	4.9	0.7	13.1	0.8	20.3	0.2	29.7	0.8	4.9	0.6	14.2	0.1	20.3	0.1	26.3	0.5
100	124	12.3	5	YKATVKDDLTKWQNVLKAHSSVDWL	5.7	0.3	9.6	0.1	15.1	0.2	23.9	1.2	5.9	0.2	10.0	0.4	15.3	0.3	23.3	1.4	5.5	0.2	9.4	0.1	14.5	0.1	23.4	0.2	5.3	0.2	9.7	0.3	15.5	0.2	22.9	0.7
116	124	10.2	3	KAHSSVDWL	10.2	0.3	15.3	0.2	17.4	0.2	26.4	0.5	10.5	0.5	15.5	0.2	17.4	0.2	27.0	0.7	9.5	0.9	15.2	0.4	17.3	0.0	26.7	0.7	9.1	0.7	15.7	0.3	17.8	0.3	25.1	0.5
125	141	7.2	4	IVIVENDAKKKNKTNIL	35.0	0.9	33.6	0.6	34.1	1.0	38.7	1.0	33.3	0.7	33.8	0.8	33.8	0.5	38.2	0.5	34.9	1.0	33.4	0.7	34.1	0.0	38.3	1.0	34.3	1.0	34.1	1.1	34.5	0.6	37.4	0.4
125	148	7.5	4	IVIVENDAKKKNKTNILPRTSIVD	33.8	0.9	37.3	0.3	38.5	0.9	42.3	1.2	33.9	0.9	37.2	1.2	38.7	0.1	41.4	0.5	33.7	0.9	37.3	0.4	38.7	0.3	41.4	0.7	33.0	0.3	37.5	0.5	39.7	0.9	40.9	0.2
149	162	5.6	3	KIRNDFCNKQSDRC	22.5	0.6	27.9	0.7	39.0	1.3	45.6	1.0	25.2	1.2	27.8	0.9	39.3	1.2	44.2	0.5	22.2	0.1	27.5	0.9	40.1	0.6	45.4	0.7	22.1	0.4	27.7	1.2	40.6	0.2	46.5	0.9
156	162	3.3	2	NKQSDRC	47.7	0.4	52.1	0.7	61.8	0.7	62.0	1.2	49.2	0.3	54.2	1.2	62.4	1.4	62.5	0.9	46.2	1.1	52.6	0.9	62.3	0.9	64.9	0.8	47.6	0.5	52.7	1.5	62.6	0.8	61.7	1.4
163	182	11.3	3	VVLSDPLKDSSRTQESWNAF	20.7	0.4	33.5	0.8	40.5	0.6	43.3	0.2	21.2	1.3	33.2	0.3	41.0	0.9	43.0	0.5	20.0	0.9	32.9	0.5	39.6	0.1	42.8	0.1	19.7	1.5	33.3	0.2	41.6	1.0	42.5	0.1
180	190	13.1	3	NAFLTKLRTLL	0.4	0.5	1.1	0.7	5.8	0.3	20.9	0.7	1.3	0.2	1.6	0.7	6.4	0.7	20.2	0.7	0.9	0.8	1.5	0.5	5.9	0.6	20.3	0.7	1.4	0.7	1.2	0.8	6.0	1.5	20.7	0.8
180	191	13.8	3	NAFLTKLRTLLL	0.2	0.2	0.0	0.0	3.4	1.0	18.7	1.2	0.1	0.2	0.1	0.1	2.8	1.0	18.9	0.3	0.0	0.0	0.4	0.4	4.5	0.7	18.4	1.1	0.0	0.0	0.5	0.4	4.0	0.7	18.5	0.5
192	204	9.7	3	MSFTKNLGKFEDD	0.3	0.0	1.5	0.2	10.7	0.5	25.7	1.1	0.3	0.1	1.6	0.1	10.4	0.2	24.0	0.1	0.4	0.1	1.4	0.2	10.5	0.1	26.1	1.4	0.3	0.0	1.3	0.1	10.5	0.1	23.9	0.2
192	219	11.6	5	MSFTKNLGKFEDDMRTLREKRTEPGWSF	9.9	0.6	18.0	0.2	31.3	0.3	43.8	0.7	9.8	0.3	17.4	0.3	31.8	1.0	44.1	1.6	9.6	0.7	17.0	0.2	31.4	0.4	44.5	1.5	9.8	0.1	17.1	0.3	31.5	0.4	43.1	0.4
255	260	10.3	2	QYVVNF	56.9	1.0	59.3	0.2	58.8	0.9	60.4	0.1	56.9	1.2	58.9	0.1	58.9	1.0	60.0	0.4	56.2	1.5	59.1	0.4	58.0	0.6	59.6	0.8	54.4	1.7	59.1	0.6	60.0	0.2	59.1	0.6
256	267	10.0	1	YVVNFGAGDGAN	33.1	0.9	41.7	0.5	48.2	1.0	55.7	0.3	33.3	1.2	41.4	0.5	48.6	0.5	55.9	0.6	32.7	1.4	41.6	0.2	48.2	0.2	55.9	0.8	32.8	0.3	41.8	0.1	50.2	1.7	55.1	0.2
272	282	10.7	2	FCQPVKSWNGL	23.4	0.8	36.9	0.5	54.5	1.4	62.9	0.5	24.9	0.7	36.5	0.5	53.9	0.9	63.3	0.4	22.6	0.6	35.4	1.0	53.3	0.4	63.2	0.7	21.8	1.2	36.0	0.8	55.1	1.0	62.9	0.8
291	303	5.4	4	EKRESIQRREATL	3.4	0.1	12.6	0.2	38.2	1.3	59.2	1.4	3.4	0.4	12.2	0.3	38.9	0.6	58.9	1.0	2.9	0.1	12.1	0.3	38.6	0.0	59.7	0.5	2.9	0.1	12.3	0.2	39.0	1.1	59.3	0.3
304	310	12.1	2	LDLRSYL	3.5	0.7	5.6	1.2	6.1	1.0	6.4	0.4	4.9	1.0	5.2	0.2	6.3	0.4	7.1	0.6	3.8	0.8	4.7	0.5	5.2	0.9	7.0	1.1	4.0	1.0	5.5	0.6	5.7	1.1	7.4	0.2
305	310	11.3	2	DLRSYL	2.6	0.7	1.7	0.4	5.5	0.2	8.5	1.0	1.9	0.7	1.9	0.9	7.6	1.2	8.9	0.4	1.8	0.5	1.4	0.1	5.6	1.3	6.8	0.4	0.6	0.2	1.4	0.3	2.2	0.5	3.5	0.9
311	317	8.3	1	FSRQCTL	4.0	0.5	3.5	1.0	10.2	1.1	12.7	0.3	6.9	0.6	8.3	0.5	11.9	1.2	13.2	1.6	3.4	0.9	3.6	0.6	10.1	0.7	11.5	1.2	3.7	0.3	4.3	0.7	10.2	1.1	11.2	1.1
318	341	14.5	4	LLFLQRPWEVAQRALELLHNCVQE	0.2	0.3	4.6	1.2	8.5	0.4	17.2	0.5	0.4	0.7	3.7	0.1	8.4	0.1	17.4	0.8	-0.1	0.6	2.3	0.9	8.1	0.5	17.0	0.5	-0.1	0.6	2.9	0.6	8.4	0.3	16.8	0.4
318	344	14.7	5	LLFLQRPWEVAQRALELLHNCVQELKL	0.6	0.5	3.3	0.4	7.6	0.3	16.9	1.0	0.6	0.3	3.1	0.5	7.5	0.4	16.3	0.9	0.4	0.3	2.5	0.6	7.5	0.1	16.2	0.1	0.3	0.2	2.9	0.3	7.0	0.9	16.6	0.7
319	331	10.7	3	LFLQRPWEVAQRA	1.8	0.3	8.8	0.3	19.5	0.9	36.1	1.4	2.4	0.1	8.6	0.2	19.3	0.5	35.0	1.1	2.1	0.3	7.8	0.1	18.8	0.3	33.9	0.6	2.3	0.5	8.1	0.4	20.1	0.2	33.9	0.6
319	344	14.6	5	LFLQRPWEVAQRALELLHNCVQELKL	0.7	0.1	3.7	0.2	8.4	0.2	16.3	0.5	0.7	0.3	3.4	0.5	8.2	0.2	16.7	0.5	0.3	0.2	3.5	0.4	8.2	0.3	16.6	0.5	0.2	0.3	2.8	0.4	8.0	0.3	16.7	0.6
320	341	14.0	4	FLQRPWEVAQRALELLHNCVQE	1.1	0.6	4.2	0.8	11.0	0.2	18.2	0.5	1.0	0.4	3.9	0.7	9.2	0.6	17.4	0.5	0.2	0.3	3.4	0.2	9.0	0.1	17.6	0.6	-0.3	1.3	3.3	0.4	8.9	0.2	17.6	0.8
334	341	6.9	1	LLHNCVQE	2.0	0.1	2.0	0.2	7.5	0.7	9.7	1.4	1.9	0.2	1.9	0.2	8.7	0.2	9.7	0.5	2.1	0.9	2.6	1.2	7.5	1.0	10.9	0.7	2.5	0.9	2.5	0.2	6.8	1.4	10.0	1.6
345	354	10.5	1	LEVSVPPGAL	20.0	0.4	35.8	0.2	45.1	0.6	58.7	0.3	20.4	1.3	35.0	0.3	45.5	0.9	63.3	0.5	19.1	1.0	35.0	1.1	44.7	0.8	63.5	0.2	17.7	0.7	34.3	0.3	45.0	0.4	61.6	1.4
345	356	10.8	1	LEVSVPPGALDC	16.5	0.9	28.2	0.1	38.6	1.2	52.2	1.1	16.6	1.0	27.6	0.4	37.7	1.5	52.4	2.0	16.0	1.3	28.2	1.1	36.6	1.2	53.9	1.0	15.7	0.1	27.4	1.1	38.5	1.7	56.0	1.4
358	363	13.6	1	VFLSCL	6.7	0.4	6.7	0.4	6.8	0.9	7.7	0.4	7.1	0.6	6.2	0.3	8.2	0.9	7.5	1.3	7.0	1.1	5.8	0.3	7.0	0.1	7.5	0.9	8.1	1.5	6.2	0.7	6.5	0.8	7.0	0.5
363	373	11.9	2	LEVLQRIEGCC	24.6	0.4	28.5	0.7	30.8	0.7	40.8	0.9	25.5	0.5	30.9	0.7	32.8	1.1	41.3	1.0	24.6	1.2	27.9	0.1	29.0	0.2	40.6	0.2	23.7	0.6	27.5	0.9	29.1	0.7	40.1	0.2
374	381	4.4	2	DRAQIDSN	48.4	0.9	69.0	0.9	68.3	0.4	70.3	0.8	51.2	1.1	68.5	0.7	69.2	0.8	70.5	1.1	46.9	0.9	69.3	0.2	70.0	0.0	71.7	0.6	44.8	1.2	69.2	0.9	69.4	1.0	70.0	0.6
382	388	7.8	2	IAHTVGL	9.4	1.1	20.3	0.1	33.1	1.0	48.6	1.3	10.0	0.9	20.5	0.7	32.8	0.4	47.5	0.5	8.9	0.6	20.0	0.7	32.6	0.3	47.6	0.6	8.4	0.5	20.6	0.3	32.6	0.5	46.6	0.7
389	402	11.4	2	WSYATEKLKSLGYL	1.2	0.5	1.1	0.6	1.5	0.4	4.5	0.5	1.9	0.2	1.8	0.7	1.7	0.3	5.2	0.1	1.8	1.0	1.5	0.4	1.3	0.6	4.8	0.0	1.9	0.8	1.5	0.1	2.0	0.4	4.7	0.7
389	405	13.0	2	WSYATEKLKSLGYLCGL	1.0	0.3	1.2	0.2	2.6	0.4	9.0	0.1	1.0	0.2	1.0	0.2	2.6	0.2	9.0	0.1	1.0	0.2	1.1	0.4	2.5	0.0	8.8	0.2	1.1	0.5	1.4	0.9	2.6	0.2	9.0	0.4
392	405	11.7	3	ATEKLKSLGYLCGL	0.7	0.5	1.2	0.5	4.4	1.2	10.8	0.8	0.7	0.1	1.6	0.2	3.1	0.3	10.8	0.2	0.7	0.1	1.4	0.6	3.3	0.8	10.7	0.6	1.3	0.3	0.9	0.2	3.4	0.8	10.6	0.8
395	405	11.6	2	KLKSLGYLCGL	1.6	0.6	1.7	0.8	3.3	0.3	13.1	1.0	1.3	0.7	1.1	0.2	3.5	0.1	12.7	0.3	1.2	0.3	1.3	0.2	4.1	0.8	12.5	0.6	1.5	0.5	1.5	0.1	3.8	0.5	12.6	0.7
406	416	6.9	1	VSEKGPNSEDL	39.9	0.8	46.9	0.5	56.3	1.7	58.5	0.8	40.1	0.9	46.7	1.1	55.0	1.0	57.9	1.2	39.3	1.2	46.1	0.6	56.9	0.0	58.6	1.1	39.3	1.1	46.7	0.9	57.2	1.2	57.1	1.0
406	422	8.5	2	VSEKGPNSEDLNRTVDL	18.2	0.9	28.6	0.5	46.8	0.7	57.6	1.2	18.5	0.9	28.4	0.8	46.5	0.4	55.9	0.4	18.0	0.8	27.8	0.2	46.2	0.9	55.6	0.8	18.1	0.5	28.0	0.6	47.8	0.9	55.0	0.8
406	423	10.4	3	VSEKGPNSEDLNRTVDLL	15.6	0.6	23.9	0.4	40.1	1.5	53.7	0.7	15.1	0.6	23.4	1.0	40.3	0.5	53.2	0.8	14.6	0.8	23.5	0.3	39.8	0.5	53.6	0.6	18.9	0.9	23.1	0.2	40.8	0.4	52.6	0.4
417	422	7.3	2	NRTVDL	3.0	0.2	9.6	0.7	39.8	1.5	69.7	0.9	3.1	0.3	9.1	0.8	43.0	1.3	70.2	0.2	3.2	0.4	8.6	0.7	40.3	0.6	69.2	0.8	3.5	0.9	9.8	0.8	39.6	1.1	68.3	0.2
417	423	9.7	2	NRTVDLL	2.9	1.0	8.1	0.2	30.9	1.1	64.4	0.8	2.7	0.6	10.3	0.6	29.7	0.8	63.5	0.7	2.1	0.4	7.8	1.2	29.8	1.2	63.3	0.8	3.0	1.6	8.4	0.2	30.2	0.6	62.9	0.6
423	448	8.9	3	LAGLGAERPETANTAQSPYKKLKEAL	18.3	1.0	21.8	0.3	30.2	0.9	42.6	0.9	18.2	0.8	22.2	1.0	30.1	0.9	41.6	0.6	17.9	0.7	21.5	0.4	30.0	1.0	41.3	0.3	17.6	0.2	21.6	0.3	31.1	1.1	41.3	0.6
423	453	10.7	3	LAGLGAERPETANTAQSPYKKLKEALSSVEA	17.8	0.5	23.0	0.4	29.9	0.7	39.8	0.6	18.1	1.0	22.5	0.8	29.6	0.5	39.1	0.3	17.8	0.6	22.6	0.4	29.7	0.2	39.1	0.2	17.4	0.3	22.5	0.7	30.5	0.2	38.8	0.3
424	448	8.7	4	AGLGAERPETANTAQSPYKKLKEAL	19.7	0.5	23.2	0.1	29.8	0.3	42.1	1.1	19.0	0.6	22.4	0.6	28.1	0.4	39.4	0.5	19.3	0.8	22.9	0.1	29.5	0.5	41.2	0.3	19.0	0.3	23.1	0.3	30.8	0.6	40.6	0.3
424	453	10.7	3	AGLGAERPETANTAQSPYKKLKEALSSVEA	17.2	0.5	21.6	0.2	27.9	0.8	37.1	0.8	17.5	0.8	21.5	0.5	28.1	0.9	36.4	0.3	16.6	0.8	21.2	0.1	27.6	0.4	36.3	0.1	16.6	0.6	21.6	0.6	28.1	1.2	37.3	0.5
454	464	8.1	3	FEKHYLDLSHA	1.9	0.5	2.6	0.8	1.5	0.1	5.6	0.8	1.2	0.7	1.2	0.2	1.6	0.5	5.2	0.6	1.4	0.8	1.5	0.5	1.5	0.7	5.4	0.7	1.0	0.4	1.2	0.3	1.5	0.5	5.4	0.2
455	468	10.0	4	EKHYLDLSHATIEM	0.6	0.3	1.0	0.4	1.0	0.4	3.9	0.1	0.7	0.2	0.8	0.1	1.4	0.3	4.1	0.2	1.0	0.7	0.7	0.4	1.0	0.8	3.7	0.1	0.3	0.1	0.9	0.1	1.1	0.0	3.7	0.3
469	480	7.9	3	YTSIGRIRSAKF	1.4	0.3	1.9	0.1	7.1	0.5	16.3	1.4	1.6	0.3	2.0	0.2	6.7	0.7	15.9	1.4	1.1	0.1	1.9	0.4	6.9	0.1	15.4	1.4	1.2	0.1	1.8	0.2	6.6	0.2	16.0	0.3
469	484	6.9	4	YTSIGRIRSAKFVGKD	1.1	0.1	1.7	0.2	5.9	0.2	14.5	0.8	1.1	0.2	1.7	0.3	6.2	0.2	14.1	0.2	1.2	0.2	1.4	0.1	5.9	0.1	14.0	0.3	1.1	0.1	1.6	0.2	5.7	0.2	14.1	1.2
489	500	4.4	3	YMRKKAPQKAEI	9.3	0.6	24.2	0.4	35.4	0.3	50.3	1.2	9.8	1.0	23.7	0.3	35.6	0.7	50.0	0.7	8.9	1.0	23.7	0.4	35.3	0.3	50.9	0.5	8.3	0.6	23.7	0.0	35.5	0.4	50.8	1.0
501	513	10.8	2	YLQGALKNYLAEG	5.9	0.2	11.9	0.9	29.6	0.4	55.4	0.2	6.0	0.4	11.6	0.4	29.6	0.8	55.4	0.9	5.5	0.3	11.1	0.3	29.3	0.0	55.6	0.6	5.4	0.2	11.1	0.2	30.1	0.4	55.3	1.0
514	527	8.8	2	WALPITHTRKQLAE	1.9	0.3	5.7	0.2	7.1	0.1	8.6	0.2	1.7	0.1	5.5	0.3	7.2	0.3	8.9	0.4	1.6	0.2	5.3	0.1	7.4	0.1	8.4	0.2	1.6	0.2	5.2	0.5	7.0	0.3	8.7	0.3
514	537	9.5	3	WALPITHTRKQLAECQKHLGQIEN	10.6	0.5	19.0	0.4	23.5	0.7	28.0	0.3	10.7	0.8	19.0	0.4	23.5	0.3	28.0	0.7	10.4	0.9	18.8	0.5	23.4	0.1	27.3	0.9	10.1	0.1	19.0	0.1	23.9	0.4	27.2	0.3
529	537	5.2	1	QKHLGQIEN	27.9	0.3	47.0	0.8	54.6	1.0	54.2	0.4	29.8	0.6	47.0	1.2	54.4	1.5	55.4	0.5	28.1	1.1	46.2	1.0	53.9	0.7	56.4	0.7	25.5	1.4	47.1	1.1	53.8	1.2	56.3	0.7
539	544	7.8	1	LQTSSL	2.4	0.5	2.5	0.8	10.2	0.5	38.7	0.3	3.4	0.9	3.0	0.0	7.4	0.2	33.3	0.1	2.0	0.3	2.6	0.6	7.7	0.1	33.8	0.4	2.2	0.6	4.0	0.4	7.5	0.2	32.4	1.4
545	562	6.5	2	LASDHHLTEEERKHFCQE	6.6	0.4	10.5	0.3	15.5	0.6	24.3	0.5	6.8	0.2	10.4	0.5	15.5	0.2	22.6	0.8	6.5	0.3	10.1	0.3	16.1	0.2	23.1	1.2	6.5	0.1	10.5	0.3	15.8	0.5	23.1	0.9
566	585	9.7	4	FASQPSDSPGHKIVLPMHSF	8.0	0.5	15.0	0.2	24.4	0.7	30.6	0.6	7.9	0.4	14.5	0.8	24.5	0.2	29.8	0.1	7.8	0.7	14.5	0.3	24.1	0.0	29.6	0.5	7.7	0.1	14.5	0.3	25.1	0.7	29.2	0.4
567	585	9.4	4	ASQPSDSPGHKIVLPMHSF	8.0	0.4	12.8	0.2	23.2	0.6	29.9	0.7	8.1	1.0	13.0	0.9	23.0	0.1	28.7	0.5	7.8	0.5	12.6	0.3	22.8	0.6	28.7	0.7	7.5	0.1	12.6	0.8	23.3	0.5	28.0	0.6
567	588	10.6	2	ASQPSDSPGHKIVLPMHSFAQL	7.2	0.1	12.6	0.0	21.0	0.6	26.3	0.6	7.3	0.5	12.5	0.5	21.1	1.1	25.8	0.3	7.0	0.6	12.1	0.1	21.1	1.0	25.8	0.1	6.9	0.2	12.2	0.3	21.2	0.7	25.6	0.1
589	606	10.4	3	RDLHFDPSNAVVHVGGVL	9.9	0.2	20.6	0.2	33.2	0.7	46.9	0.7	10.1	0.4	20.0	0.3	33.1	0.4	46.9	0.7	9.4	0.7	20.0	0.4	31.6	0.2	48.4	0.3	9.2	0.8	19.7	0.2	33.0	0.6	46.3	0.8
598	606	9.3	2	AVVHVGGVL	5.5	0.1	19.9	0.3	32.4	0.5	55.3	0.6	5.3	0.7	19.5	0.8	31.5	0.4	55.4	0.4	5.2	0.6	19.3	0.4	32.1	0.4	55.1	0.7	5.0	0.0	19.2	0.9	31.4	0.3	54.1	0.3
599	606	8.9	2	VVHVGGVL	6.0	0.5	23.7	0.7	39.8	0.9	60.9	0.6	6.5	0.5	23.0	0.4	37.4	0.6	58.7	0.6	5.5	0.6	22.3	0.1	37.2	0.7	58.7	0.9	5.3	0.6	22.6	0.4	38.3	1.2	55.9	1.6
608	612	9.7	1	VEITM	10.9	0.5	11.0	0.4	13.4	0.4	14.0	1.1	10.1	0.6	10.6	0.9	12.0	0.7	13.2	0.0	9.7	0.5	11.8	0.2	11.2	0.7	13.5	0.3	13.5	0.7	12.4	0.6	11.5	0.6	13.3	1.0
613	624	8.8	2	YSQMPVPVHVEQ	5.4	0.5	7.5	0.4	13.7	0.3	25.2	0.8	5.4	0.4	7.3	0.5	13.7	0.7	21.3	0.8	5.2	0.6	7.4	0.4	13.2	0.4	20.8	1.1	5.3	0.4	7.7	0.4	13.6	0.3	20.6	0.5
625	631	10.5	1	IVVNVHF	13.0	0.4	17.1	0.1	30.1	1.0	40.6	0.4	13.4	0.8	16.6	0.2	30.0	0.7	40.1	1.2	13.0	0.9	16.6	0.3	29.2	0.8	39.3	0.4	13.0	0.1	16.8	0.4	29.8	0.4	39.5	0.4
632	644	7.2	2	SIEKNSYRKTAEW	49.6	1.0	51.3	0.3	50.1	1.4	52.1	0.9	50.8	0.3	49.9	1.3	50.0	1.2	50.9	1.1	49.2	0.4	50.7	0.7	50.9	0.2	51.4	0.2	50.2	1.2	50.1	0.9	52.2	0.7	52.0	0.4
645	671	10.7	4	LTKHKTSNGIINFPPETAPFPVSQNSL	38.4	0.6	45.7	0.6	45.8	0.7	47.1	0.4	38.9	1.1	45.1	0.7	46.1	0.4	46.3	0.7	36.7	0.9	45.1	0.3	45.4	0.1	46.1	0.2	36.4	1.1	45.5	0.2	47.4	1.1	46.5	0.2
669	676	12.3	1	NSLPALEL	39.8	0.7	61.8	0.8	67.6	0.9	69.7	1.4	39.6	1.0	61.4	0.8	66.4	1.2	68.9	0.9	38.0	0.7	61.4	0.8	67.6	0.9	66.1	0.3	36.5	1.2	61.2	1.3	66.9	1.8	69.9	0.7
680	689	7.5	1	FERSPSDNSL	49.1	1.5	53.3	0.5	53.9	1.1	55.2	1.3	49.0	1.4	53.5	1.2	52.7	0.2	54.2	0.9	49.3	1.3	53.6	0.6	53.2	0.6	54.6	0.2	47.5	0.1	53.6	0.9	54.1	0.9	53.4	0.3
681	689	6.2	1	ERSPSDNSL	53.6	1.1	57.9	1.2	57.8	0.2	58.6	1.0	53.5	1.3	57.7	1.2	55.9	0.4	58.8	1.0	52.2	1.0	55.8	0.8	59.1	0.6	59.3	2.1	51.6	0.4	57.6	0.4	58.0	1.2	58.9	0.3
690	703	11.5	2	NTTGIICRNVHMLL	43.0	0.8	60.4	0.9	59.9	0.9	64.3	0.7	42.4	0.3	58.7	0.5	63.9	1.3	64.1	1.2	43.1	0.3	61.3	1.1	59.8	0.2	62.6	1.0	41.2	1.4	62.2	1.2	63.3	1.5	63.0	1.0
704	720	10.1	3	RRQESSSSLEMPSGVAL	1.6	0.5	1.5	0.1	1.6	0.1	7.7	0.8	1.5	0.3	1.4	0.1	1.6	0.2	7.6	0.6	1.4	0.1	1.4	0.1	1.6	0.0	7.5	0.3	1.5	0.1	1.4	0.1	1.6	0.1	7.7	0.4
718	739	9.1	3	VALEEGAHVLRCSHVTLEPGAN	22.3	0.1	27.7	0.3	31.7	0.4	40.1	0.7	22.6	1.0	28.0	0.5	31.5	0.6	39.0	0.9	21.5	1.1	27.5	0.4	31.2	0.3	38.9	1.1	22.2	1.1	29.8	1.0	32.1	0.3	38.7	0.5
720	739	8.1	3	LEEGAHVLRCSHVTLEPGAN	14.3	0.5	19.1	0.1	23.4	0.5	31.8	1.4	14.4	1.2	19.5	0.6	23.0	0.2	30.7	0.4	14.1	0.8	19.0	0.3	23.5	0.3	31.2	0.4	13.8	0.2	19.5	0.4	23.6	0.4	30.6	0.3
721	739	7.6	3	EEGAHVLRCSHVTLEPGAN	14.0	0.8	19.0	0.0	23.4	0.7	33.5	1.3	14.6	0.3	19.1	0.6	23.6	0.6	32.8	0.3	13.5	0.8	19.0	0.2	23.8	0.4	32.6	0.4	13.1	0.3	19.0	0.2	24.4	0.8	32.2	0.5
725	739	6.9	3	HVLRCSHVTLEPGAN	9.6	0.4	14.3	0.2	18.1	0.6	29.1	1.2	10.0	0.9	14.4	0.4	18.0	0.2	28.7	0.4	9.5	0.5	14.1	0.2	18.2	0.1	28.7	0.7	9.0	0.3	14.2	0.2	18.2	0.2	28.4	0.6
740	760	10.0	3	QITFRTQAKEPGTYTLRQLCA	13.2	0.1	17.0	0.4	18.4	0.5	23.8	0.2	13.5	0.8	16.6	0.3	18.6	0.5	23.9	0.6	13.2	0.6	16.3	0.6	18.5	0.2	23.5	0.6	13.3	0.4	16.8	0.3	19.0	0.7	24.2	0.3
744	752	3.7	2	RTQAKEPGT	44.9	0.2	50.4	1.0	52.9	1.0	62.7	0.7	46.1	1.0	49.6	0.5	54.2	1.0	62.5	0.3	43.5	0.8	50.0	1.1	52.7	1.1	63.5	0.3	44.1	0.7	50.0	0.1	52.4	1.0	62.6	0.5
756	766	11.1	2	RQLCASVGSVW	2.7	0.1	11.0	0.9	15.4	0.8	21.6	0.5	1.4	1.1	10.6	0.8	16.3	0.3	22.3	0.9	1.7	0.8	11.1	0.6	17.0	0.4	21.7	0.1	1.5	1.0	11.1	0.8	16.8	0.3	22.0	0.1
767	777	12.5	2	FVLPHIYPIVQ	5.2	0.1	19.4	0.4	38.5	0.9	51.5	0.4	5.6	0.9	18.6	0.5	38.1	0.5	51.1	0.6	5.2	0.1	18.5	0.4	37.7	0.0	51.6	0.6	4.6	0.2	19.4	0.7	38.7	0.6	51.1	0.2
767	778	12.9	2	FVLPHIYPIVQY	4.1	0.4	15.6	0.2	33.1	0.9	45.0	0.4	4.8	0.5	15.7	0.4	33.2	0.4	44.5	0.6	4.5	0.4	14.8	0.7	32.0	0.1	44.3	0.1	4.1	0.2	15.6	0.6	32.3	0.6	44.4	0.4
767	780	13.5	2	FVLPHIYPIVQYDV	3.0	0.2	11.3	0.1	24.0	0.5	34.2	0.3	3.0	0.4	11.4	0.4	24.0	0.2	33.4	0.7	3.1	0.4	10.8	0.1	23.5	0.3	33.6	0.6	2.8	0.4	10.9	0.1	24.2	0.4	33.2	0.4
779	787	9.8	1	DVYSQEPQL	35.3	0.7	47.7	0.3	53.2	1.3	62.9	0.9	38.7	0.8	47.2	0.2	51.7	0.9	62.0	0.9	33.9	1.5	47.4	0.4	51.5	0.2	61.4	1.0	33.2	1.0	48.1	0.3	51.6	0.4	60.7	0.8
788	796	9.6	1	HVEPLADSL	37.4	0.9	48.2	0.7	54.4	1.0	54.7	1.1	38.8	1.6	48.2	0.8	54.4	0.9	54.1	0.4	38.8	0.9	47.8	0.4	53.6	0.7	56.7	0.7	36.0	0.4	48.3	0.3	54.8	0.6	53.7	0.9
798	806	8.1	3	AGIPQRVKF	3.8	0.4	12.8	0.7	15.1	0.8	35.9	0.8	4.1	0.7	12.0	0.5	14.7	0.6	33.7	0.5	4.3	0.5	11.8	0.4	15.6	0.2	33.5	0.5	3.9	0.1	13.0	0.9	14.9	0.3	34.4	1.4
807	826	8.6	2	TVTTGHYTIKNGDSLQLSNA	15.7	0.3	19.9	0.2	23.1	0.6	39.1	0.6	15.6	0.6	20.1	0.6	22.6	0.5	36.3	0.5	15.2	0.6	19.9	0.4	23.5	0.9	38.5	0.1	17.5	0.8	20.2	0.3	23.6	0.1	36.7	0.8
831	851	7.9	3	ILCQAESRAVVYSNTREQSSE	39.3	1.3	43.1	0.9	43.9	1.1	56.9	1.3	38.8	1.0	42.7	1.0	43.8	0.6	55.4	1.0	38.7	1.0	42.2	0.6	44.7	0.7	55.5	0.6	38.8	1.0	42.9	0.8	45.3	1.5	54.0	0.3
833	845	6.4	2	CQAESRAVVYSNT	43.1	1.1	46.2	0.6	49.9	1.0	66.4	1.3	43.4	0.8	46.5	1.0	49.4	1.0	66.7	1.1	42.4	1.6	45.2	0.5	50.2	1.0	66.5	0.5	43.8	0.7	46.6	0.6	50.3	0.1	66.3	0.7
833	851	6.0	3	CQAESRAVVYSNTREQSSE	45.2	1.1	49.3	0.9	51.3	1.4	63.6	0.8	45.8	1.3	48.8	0.7	52.3	0.6	63.4	1.0	44.1	1.1	48.6	0.9	52.3	0.1	63.9	0.6	44.6	1.7	48.8	0.7	52.1	0.9	63.0	0.5
836	851	5.4	3	ESRAVVYSNTREQSSE	40.8	0.8	45.1	0.5	48.0	1.4	63.0	0.7	41.4	1.3	44.8	1.0	49.1	0.6	61.7	0.7	40.3	0.5	44.7	0.7	48.4	0.0	62.1	0.2	40.0	0.6	45.0	0.5	49.0	0.7	61.7	0.3
838	851	4.9	2	RAVVYSNTREQSSE	42.8	0.6	46.5	0.4	49.4	1.1	60.2	0.6	43.3	0.7	46.4	0.4	49.7	0.8	59.0	0.8	41.9	0.6	47.1	0.7	48.9	0.9	60.8	0.8	41.2	0.3	47.4	1.3	48.7	1.2	59.7	1.0
840	853	5.4	2	VVYSNTREQSSEAA	50.9	1.3	56.7	1.1	61.4	1.3	68.2	0.9	52.4	1.2	56.3	0.5	64.0	0.5	67.4	0.6	49.6	1.1	56.4	0.5	62.2	0.7	67.9	0.8	47.9	0.7	57.0	0.9	62.8	0.6	67.6	0.3
846	853	3.5	2	REQSSEAA	45.0	0.3	54.2	1.0	63.1	1.3	64.6	0.8	46.1	0.7	52.8	0.9	63.4	0.8	63.4	0.3	44.3	0.3	53.1	0.7	63.0	0.7	63.9	0.7	45.6	0.8	52.7	1.4	62.3	0.4	65.2	1.0
854	873	10.3	2	LRIQSSDKVTSISLPVAPAY	11.5	0.4	20.8	0.2	33.4	0.2	41.9	0.2	11.7	0.8	20.8	0.6	33.7	1.2	41.9	0.8	10.9	0.5	20.5	0.5	33.7	0.3	42.6	0.4	11.3	0.1	20.9	0.5	34.9	0.7	42.1	0.4
865	873	10.9	1	ISLPVAPAY	3.4	0.3	12.6	0.1	28.5	0.4	41.7	0.8	4.0	0.8	11.8	0.2	30.9	0.5	40.8	0.8	3.0	0.4	12.1	0.7	32.3	1.2	40.6	0.4	2.7	0.2	12.8	1.1	31.5	0.8	42.6	0.5
865	878	12.9	2	ISLPVAPAYHVIEF	2.6	0.3	7.8	0.8	16.5	0.5	25.5	0.5	1.8	0.3	6.2	0.3	15.7	0.4	21.7	0.5	2.6	0.2	7.1	0.9	16.0	0.5	23.8	0.7	2.2	0.6	6.2	0.4	16.5	0.5	22.8	0.6
881	895	11.2	1	EVLSLPSAPALGGES	39.1	0.2	43.1	1.0	45.1	0.1	48.1	0.5	39.5	1.1	44.5	1.3	44.9	0.5	49.0	0.3	38.3	0.6	43.7	0.4	44.2	0.6	48.3	0.8	38.8	1.1	44.2	0.5	46.0	0.9	48.0	0.7
881	897	11.8	1	EVLSLPSAPALGGESDM	36.1	0.2	40.8	0.6	41.2	0.7	43.9	0.1	36.1	0.6	40.1	0.4	41.3	0.7	43.7	0.8	35.5	1.0	40.5	0.4	40.8	0.3	43.8	0.6	35.7	1.2	39.9	0.4	42.2	1.3	42.9	0.5
898	916	3.6	4	LGMAEPHRKHKDKQRTGRC	30.2	0.8	30.4	1.0	31.0	0.7	30.6	1.4	31.1	0.7	29.2	0.3	31.7	0.1	30.4	0.5	29.5	0.5	30.2	1.4	31.0	0.9	32.0	0.5	30.7	0.6	30.1	1.1	30.8	1.0	31.4	0.8
900	916	3.2	4	MAEPHRKHKDKQRTGRC	28.9	0.8	29.4	1.2	29.9	1.2	29.4	1.8	30.2	0.6	28.4	0.5	30.8	0.5	29.2	0.2	28.4	1.0	28.9	1.2	29.9	0.8	30.8	1.1	29.5	1.1	28.8	0.8	29.6	0.8	30.4	0.9
917	933	12.2	2	MVTTDHKVSIDCPWSIY	12.5	0.6	21.9	0.5	29.1	0.4	39.2	0.6	12.4	1.0	21.7	0.8	29.1	0.3	39.1	0.2	11.9	0.4	21.3	0.4	28.4	0.3	39.3	0.3	11.5	0.2	21.6	0.6	29.8	0.8	38.4	0.4
917	936	12.4	3	MVTTDHKVSIDCPWSIYSTV	15.0	0.3	27.0	0.2	35.9	0.3	44.4	0.4	15.6	0.5	26.5	0.5	36.1	0.4	43.9	0.5	14.5	0.7	26.3	0.2	35.1	0.2	43.9	0.1	14.2	0.6	26.3	0.5	36.6	1.0	43.6	0.3
937	952	12.4	3	IALTFSVPFRTTHSLL	5.5	0.4	12.2	0.3	21.8	0.4	33.7	0.4	5.7	0.5	11.7	0.3	21.7	0.3	33.3	0.6	5.2	0.4	11.6	0.5	21.3	0.2	33.5	0.1	5.0	0.3	11.5	0.2	21.6	0.4	33.3	0.7
940	952	11.1	3	TFSVPFRTTHSLL	6.5	0.4	11.2	0.3	17.9	0.4	22.3	0.1	6.6	0.8	10.7	0.2	18.0	0.3	22.4	0.1	6.2	0.2	11.0	0.5	17.2	0.1	22.7	0.5	5.8	0.4	11.0	0.4	17.8	0.2	22.6	0.1
953	961	4.3	2	SSGTRKYVQ	8.6	1.1	11.1	0.3	13.9	0.3	22.3	0.4	9.5	1.3	10.5	0.3	15.1	0.7	20.1	0.7	8.8	0.7	10.7	0.3	13.6	1.0	22.9	0.5	9.1	1.1	11.3	0.4	13.4	0.6	22.4	0.1
964	969	5.8	1	VQNLSE	15.4	0.5	18.9	1.0	19.2	0.4	28.5	0.4	15.5	0.4	18.5	1.5	19.4	0.7	27.8	0.6	13.7	0.1	17.3	0.8	17.4	0.4	24.9	0.9	14.9	0.0	18.7	1.0	19.4	0.5	27.6	1.1
971	978	11.0	1	DFQLSDSY	3.5	0.3	9.9	0.6	23.7	0.8	36.5	0.7	3.6	0.2	9.2	0.2	23.9	0.6	37.0	1.1	1.4	0.4	9.1	0.9	23.4	0.1	36.8	0.9	3.4	0.1	9.5	0.1	24.2	0.6	36.5	1.0
971	979	12.7	2	DFQLSDSYL	1.8	0.0	5.1	0.2	17.6	0.4	31.4	0.3	1.8	0.1	5.0	0.3	17.5	0.3	31.1	0.6	1.8	0.3	4.6	0.2	17.2	0.0	30.8	0.9	1.6	0.1	4.6	0.4	17.4	0.9	30.7	0.2
979	988	8.7	1	LVDTGDSTDL	21.8	1.0	29.3	0.9	41.4	0.6	46.0	0.8	22.6	0.8	31.1	0.8	42.1	0.2	45.6	1.3	21.7	0.9	29.6	0.4	42.0	0.4	45.7	1.2	20.9	0.3	30.6	0.9	43.3	1.0	44.2	1.1
980	988	7.6	1	VDTGDSTDL	26.1	1.1	35.2	0.5	50.6	0.5	52.8	1.0	25.9	1.1	35.4	1.1	48.5	0.1	51.9	0.7	25.8	0.7	35.1	0.5	48.8	0.2	51.7	0.9	25.8	0.0	35.2	0.6	50.6	0.6	51.0	0.3
989	1008	10.8	2	QLVPLNTQSQQPIYSKQSVF	12.6	0.2	17.1	0.3	23.0	0.2	31.4	0.5	12.6	0.6	16.7	0.3	22.8	0.7	31.0	0.8	12.4	0.1	16.5	0.3	22.8	0.0	30.0	0.8	12.4	0.4	16.7	0.1	23.1	0.4	30.5	0.7
996	1008	9.6	2	QSQQPIYSKQSVF	5.3	0.4	11.8	0.5	19.2	0.6	35.1	1.1	5.3	0.6	11.4	0.6	19.1	0.4	33.1	0.2	5.0	0.5	11.1	0.4	18.9	0.0	33.2	0.5	5.4	0.4	11.4	0.2	20.0	1.1	33.3	1.1
1009	1013	14.3	1	FVWEL	3.4	0.2	4.4	0.3	4.7	0.9	3.5	0.9	4.2	0.4	4.7	0.5	5.3	0.9	4.2	1.1	3.1	0.2	3.6	0.4	5.0	0.3	3.3	0.2	2.1	0.6	3.1	0.5	4.0	0.4	2.3	0.6
1013	1023	10.5	2	LKWTEEPPPSL	19.7	0.8	35.0	0.2	57.1	0.8	64.2	0.4	20.7	0.9	34.3	0.2	55.7	0.6	63.5	0.6	19.0	0.8	34.0	0.2	55.0	0.1	63.2	0.4	19.9	0.5	34.2	0.4	56.5	0.4	62.9	0.4
1028	1036	8.5	1	SVGFSPASE	29.3	0.7	37.4	0.1	46.4	1.3	59.0	0.8	29.4	1.4	37.4	0.5	46.2	0.3	58.9	0.6	33.3	0.8	39.9	0.9	47.1	0.0	61.0	0.3	28.7	0.6	37.4	0.5	46.8	0.3	58.2	0.6
1040	1049	9.5	1	SISLKPYTYE	23.1	0.6	38.0	0.8	49.6	1.0	64.1	1.0	24.6	0.7	37.1	1.0	49.0	1.1	62.7	1.1	22.4	0.9	36.8	0.1	50.5	0.5	63.4	0.9	21.8	1.0	37.0	0.9	50.8	0.5	62.6	0.8
1040	1050	11.8	1	SISLKPYTYEF	17.5	0.7	29.8	1.0	40.6	0.8	52.0	0.7	18.1	0.8	29.2	0.2	40.8	0.7	50.6	0.5	17.2	0.6	28.9	0.2	39.5	0.3	51.3	0.1	17.0	0.5	29.3	0.4	41.0	0.6	51.2	0.7
1056	1073	13.1	2	FTLYNVKAEIFPPSGMEY	9.6	0.3	16.7	0.3	22.5	0.5	27.9	0.4	10.0	0.0	16.2	0.2	23.1	0.6	27.5	0.2	9.4	0.3	16.0	0.2	22.0	0.0	27.3	0.2	9.5	0.2	16.2	0.1	22.9	0.6	27.2	0.6
1064	1073	11.5	1	EIFPPSGMEY	29.1	1.0	42.2	0.7	47.8	0.3	48.6	0.8	28.4	1.0	41.2	0.2	47.8	0.9	49.0	0.5	28.1	0.9	39.6	0.7	46.6	0.0	49.1	0.9	28.0	0.6	39.9	0.2	48.3	1.2	48.5	0.5
1073	1079	6.7	2	YCRTGSL	7.7	0.6	32.4	0.4	48.8	0.5	57.6	0.9	8.5	0.8	31.5	0.7	49.0	0.5	56.6	0.8	7.4	0.5	31.6	0.8	49.4	0.1	55.8	0.5	6.8	0.7	31.0	0.4	48.9	0.6	56.4	0.2
1086	1092	9.2	1	ITRLSDL	12.5	0.3	24.6	0.4	39.0	1.1	60.5	0.5	12.8	0.9	23.5	0.6	39.3	0.7	59.6	1.2	12.4	0.7	23.7	1.2	39.0	0.3	60.2	0.8	12.6	0.5	24.2	0.9	39.6	0.2	59.0	0.7
1093	1108	9.2	3	LEVDKDEALTESDEHF	24.6	1.3	40.4	1.2	44.8	1.0	46.3	0.4	25.6	1.4	40.5	0.6	45.2	0.4	45.3	1.2	25.5	1.4	40.1	0.6	44.6	0.5	45.4	0.9	22.8	1.4	40.6	0.5	46.8	1.2	44.6	0.6
1093	1112	9.3	2	LEVDKDEALTESDEHFSTKL	19.1	0.6	35.4	0.9	41.1	0.4	44.6	0.4	20.2	0.4	35.1	1.1	40.3	0.6	43.1	0.9	18.3	0.7	34.9	0.7	40.2	0.2	44.0	0.2	18.9	0.8	35.3	0.7	40.7	0.7	42.7	0.3
1109	1114	8.2	2	STKLMY	3.3	0.2	12.4	0.5	19.9	1.0	31.2	0.8	4.0	0.6	12.3	1.1	22.3	1.3	30.0	0.8	4.8	1.1	12.0	0.3	18.3	0.5	31.1	0.3	2.7	0.4	12.9	0.5	18.9	0.8	30.0	0.8
1114	1123	10.7	1	YEVVDNSSNW	16.5	0.7	20.4	0.8	22.8	0.7	37.6	1.4	16.8	0.9	20.4	0.5	27.5	0.6	37.3	1.3	15.9	0.3	19.9	0.9	22.8	0.3	36.9	0.8	16.5	0.1	20.0	0.3	24.5	1.4	36.0	1.0
1133	1147	7.1	3	ISMPVAARATHRVHM	6.8	0.3	20.5	0.4	35.9	1.0	38.9	1.1	6.9	0.8	19.9	0.6	35.9	0.4	38.3	0.6	6.4	0.4	19.7	0.8	36.0	0.1	38.3	0.8	6.2	0.1	19.7	0.1	36.2	0.7	37.8	0.3
1136	1147	4.4	3	PVAARATHRVHM	9.0	0.9	21.2	0.6	34.1	0.2	35.8	0.8	9.1	1.2	20.7	0.3	34.4	1.1	35.4	0.5	7.9	0.4	20.8	0.8	34.4	0.3	36.5	0.5	8.2	0.2	20.9	0.7	34.7	0.8	36.3	0.2
1138	1147	7.1	3	AARATHRVHM	7.7	0.8	19.9	0.5	32.9	0.9	36.1	0.7	7.8	0.5	20.0	1.0	32.6	0.8	35.3	0.9	7.6	0.4	19.6	1.1	32.9	0.1	34.9	0.9	8.4	1.3	20.0	0.5	33.8	0.7	34.3	0.5
1148	1153	13.5	1	EVMPLF	1.3	0.2	1.4	0.4	2.4	0.5	10.8	0.5	1.3	0.1	1.4	0.4	2.0	0.3	10.8	0.6	2.1	1.2	1.5	0.7	2.5	0.7	11.0	0.7	1.7	0.4	1.4	0.1	2.4	0.3	10.8	1.2
1148	1154	13.3	1	EVMPLFA	2.4	0.6	6.8	1.0	14.5	0.5	20.4	0.8	2.5	0.4	6.0	0.3	16.8	0.8	21.1	1.0	3.2	0.6	5.8	0.5	15.2	0.4	20.4	0.4	3.2	0.9	6.2	1.0	14.5	0.5	22.3	1.1
1154	1164	12.4	2	AGYLPLPDVRL	0.9	0.2	1.8	0.3	7.9	0.4	21.5	0.4	0.8	0.2	1.4	0.0	7.5	0.3	20.9	0.4	0.8	0.1	1.5	0.4	8.4	0.3	21.4	0.6	1.0	0.4	1.5	0.1	7.6	0.1	20.8	0.7
1155	1164	12.4	2	GYLPLPDVRL	1.0	0.1	1.7	0.1	9.1	0.1	22.9	0.5	1.1	0.2	1.7	0.1	8.9	0.5	22.6	0.5	1.0	0.1	1.8	0.2	9.2	0.5	23.0	0.2	1.1	0.2	1.5	0.1	8.8	0.5	22.7	1.3
1165	1178	6.3	3	FKYLPHHSAHSSQL	12.9	0.4	13.5	0.1	18.8	0.4	26.9	0.4	12.9	0.2	13.7	0.2	18.9	0.4	26.5	0.4	13.3	0.8	13.7	0.4	18.6	0.2	26.5	0.5	12.7	0.1	13.5	0.4	18.9	0.1	26.4	0.1
1183	1189	11.0	2	WIENDSL	53.5	0.6	56.3	0.6	58.4	0.9	59.7	0.3	53.9	0.7	55.3	0.3	57.8	0.3	59.4	0.9	52.2	1.2	54.4	0.6	58.6	1.0	57.2	0.9	52.5	0.2	55.9	0.3	61.6	0.8	58.0	1.2
1190	1204	6.0	2	SVDKHGDDQPDSSSL	36.2	0.8	35.5	0.7	35.8	0.7	36.8	1.2	36.5	0.9	35.6	0.9	35.8	0.6	36.3	0.8	35.4	0.8	35.3	0.3	36.2	0.2	36.7	0.8	36.4	0.5	35.7	0.7	36.6	0.7	36.1	0.3
1205	1226	7.3	5	KSRGSVHSACSSEHKGLPMPRL	18.4	0.9	22.2	0.3	22.6	0.5	23.6	0.7	18.3	0.6	22.3	0.6	22.6	0.2	23.1	0.4	18.1	0.7	22.1	0.2	22.8	0.0	23.2	0.5	18.0	0.2	22.9	0.8	22.5	0.5	22.7	0.2
1227	1243	9.7	2	QALPAGQVFNSSSGTQV	14.2	0.2	20.3	0.1	33.8	0.6	48.5	1.0	14.2	0.7	19.8	0.3	33.8	0.2	47.2	0.4	13.8	0.6	19.9	0.4	33.7	0.1	47.7	0.6	13.3	0.5	19.8	0.2	35.5	0.3	47.0	0.6
1227	1244	10.8	2	QALPAGQVFNSSSGTQVL	13.2	0.4	18.5	0.3	31.7	0.7	48.1	0.7	13.5	0.4	18.0	0.2	31.4	0.4	46.5	0.7	12.8	0.5	18.0	0.2	31.4	0.2	48.1	0.8	12.4	0.4	17.9	0.4	32.1	0.7	47.4	0.7
1244	1255	9.6	2	LVIPSQDDHVLE	34.7	0.6	35.7	0.4	35.3	0.5	36.9	0.5	34.7	0.8	35.4	0.6	35.4	0.4	35.8	0.5	34.2	1.0	34.9	0.6	34.9	0.2	35.3	0.3	34.4	0.2	35.6	0.2	36.3	0.9	35.1	0.5
1245	1255	8.0	2	VIPSQDDHVLE	42.5	1.3	44.0	0.5	42.9	1.4	45.3	0.7	42.5	1.7	44.2	1.0	43.1	1.1	45.0	0.7	41.2	1.0	43.5	0.7	45.9	1.6	44.8	1.0	42.1	0.6	44.2	1.3	43.9	0.8	44.1	0.8
1255	1265	3.2	2	EVSVTHHHHHH	14.0	0.6	15.6	0.5	14.7	0.4	15.6	1.1	15.0	0.6	14.2	0.2	15.2	0.7	14.8	0.2	14.8	0.7	16.2	1.0	15.4	0.9	16.3	0.9	14.9	1.0	14.8	1.0	14.7	0.4	15.7	0.6
1256	1265	3.1	2	VSVTHHHHHH	11.2	0.4	11.6	0.5	11.8	0.4	11.8	0.8	11.8	0.3	11.4	0.3	12.2	0.4	11.8	0.1	10.9	0.3	11.5	0.4	11.8	0.1	12.4	0.5	11.4	0.5	11.2	0.5	12.0	0.5	12.2	0.4

Appendix X. Alignment of human *trapp* genes with their yeast counterparts. This figure was generated using ESpript 3.0(51). (A) Alignment of TRAPPC4 with Trs23. (B) Alignment of TRAPPC5 with Trs31.